K^-

Investigation of the low-energy kaons hadronic interactions in light nuclei by AMADEUS

Dr. Kristian Piscicchia*

Museo Storico della Fisica e Centro Studi e Ricerche Enrico Fermi

INFN, Laboratori Nazionali di Frascati

on behalf of the AMADEUS collaboration

MESON 2014

13th International Workshop on Meson Production, Properties and Interaction

KRAKÓW, POLAND

29th May - 3rd June 2014

*kristian.piscicchia@lnf.infn.it

AMADEUS & DAΦNE

K^-

DAΦNE

Double ring $e^+ e^-$ collider working in C. M. energy of ϕ, producing ≈ 600 $K^+ K^-$ /s

$\phi \rightarrow K^+ K^-$ (BR = (49.2 ± 0.6)%)

- low momentum Kaons ≈ 127 Mev/c
- back to back $K^+ K^-$ topology

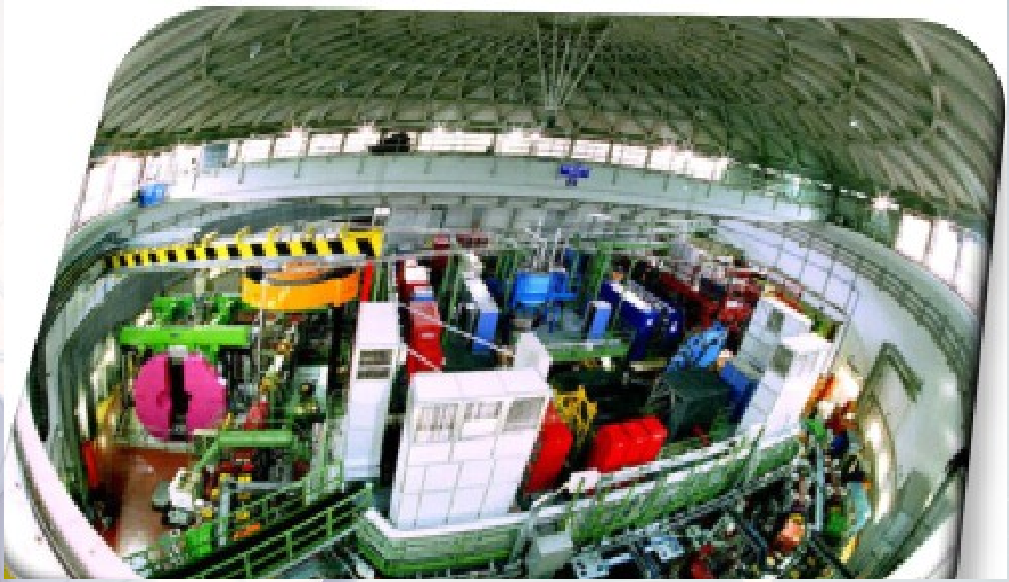

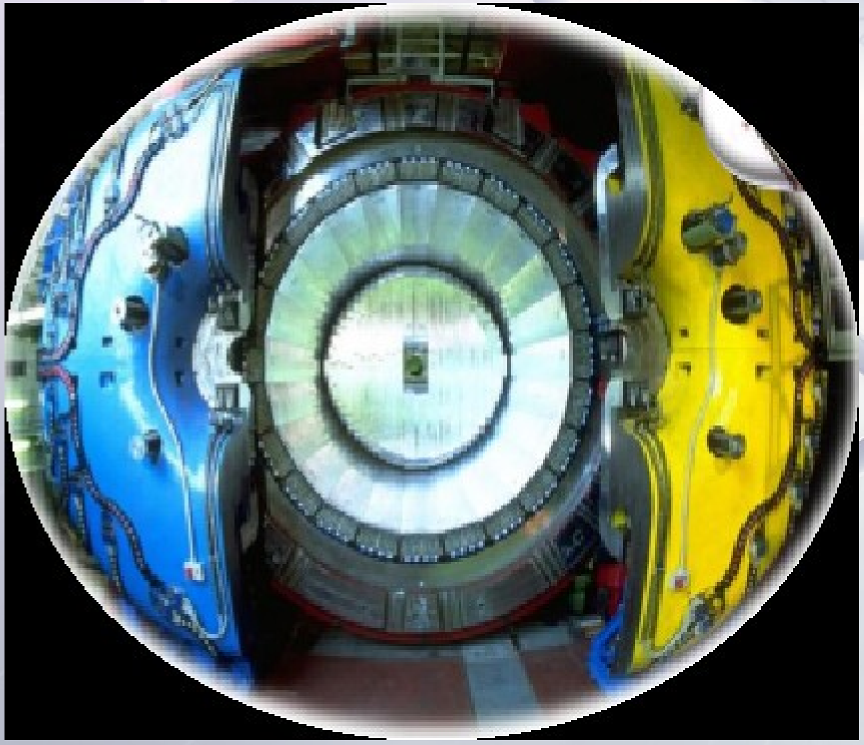

KLOE

- 96% acceptance,
- optimized in the energy range of all charged particles involved
- good performance in detecting photons (and neutrons checked by kloNe group (M. Anelli et al., Nucl Inst. Meth. A 581, 368 (2007)))

Experimental program of AMADEUS

K^-

Unprecedented studies of the low-energy charged kaons interactions in nuclear matter: solid and gaseous targets (d, ^{3}He, ^{4}He, ^{8}Be, ^{12}C …) in order to obtain unique quality information about:

1) **Possible existence of kaonic nuclear clusters (deeply bound kaonic nuclear states)**

⇓

Single & multi – nucleon K^- absorption

2) **Nature of the controversial $\Lambda(1405)$**

Experimental program of AMADEUS

K^-

Unprecedented studies of the low-energy charged kaons interactions in nuclear matter: solid and gaseous targets (d, ^{3}He, ^{4}He, ^{8}Be, ^{12}C …) in order to obtain unique quality information about:

1) **Possible existence of kaonic nuclear clusters (deeply bound kaonic nuclear states)**

Single & multi – nucleon K^- absorption

How deeply can an Antikaon be bound to a nucleus?

Possible bound states:

$K^-pp \rightarrow \Lambda p$

$K^-ppn \rightarrow \Lambda d$

Experimental program of AMADEUS

Unprecedented studies of the low-energy charged kaons interactions in nuclear matter: solid and gaseous targets (d, ^{3}He, ^{4}He, ^{8}Be, ^{12}C …) in order to obtain unique quality information about:

2) Nature of the controversial Λ(1405)

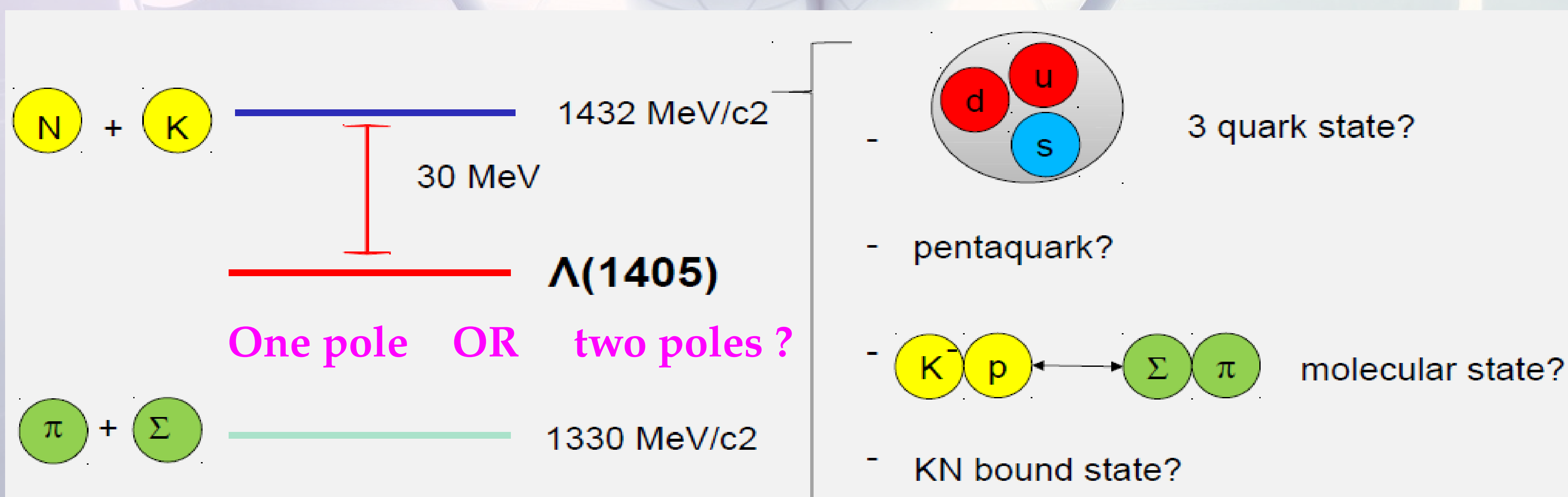

Investigation of K^- absorption on light nuclei

K^-

(H, ^4He, ^9Be, ^{12}C)

AT-REST (K^- absorbed from atomic orbit) or **IN-FLIGHT**

($p_K \sim 100 MeV$)

Reactions:

– Λp from 1NA or 2NA (single or multi-nucleon absorption)

Λd and Λt channels

- K^- 'p' $\rightarrow \Sigma^0\pi^0$
- K^- 'p' $\rightarrow \Sigma^+\pi^-$

'p' , 'n' BOUND nucleons

- K^- 'n' $\rightarrow \Lambda\pi^-$ (direct formation) or …

$K^- N \rightarrow \Sigma^0\pi^- / \Sigma^+\pi^-$; $\Sigma N \rightarrow \Lambda N'$ (internal conversion processes)

R&D for more refined setup: ScFi + SiPM (trigger system) TPC – GEM (inner tracker)

Experimental tests of the trigger prototype for the AMADEUS experiment based on Sci-Fi read by MPPC, Nucl.Instrum.Meth. A671 (2012) 125-128

Performances of a GEM-based TPC prototype for new high-rate particle experiments, Nucl.Instrum.Meth. A617 (2010) 183-185

TWO SAMPLES OF DATA:

K^-

- 2004-2005 KLOE data (Analyzed luminosity of ~2 fb^{-1})

K^- absorbed in KLOE materials (H, ^{4}He, ^{9}Be, ^{12}C)

At-rest + In-flight

- Dedicated 2012 run with pure graphite Carbon target inside KLOE

(~90 pb^{-1}; analyzed 37 pb^{-1}, x1.5 statistics)

K^- ^{12}C absorptions At-rest

Low-energy K^- hadronic interactions studies with KLOE, why?

MC simulations show that :

- ~ 0.1 of K^- stopped in the DC gas (90% He, 10% C_4H_{10})
- ~2% of K^- stopped in the DC wall (750 μm c. f. , 150 μm Al foil).

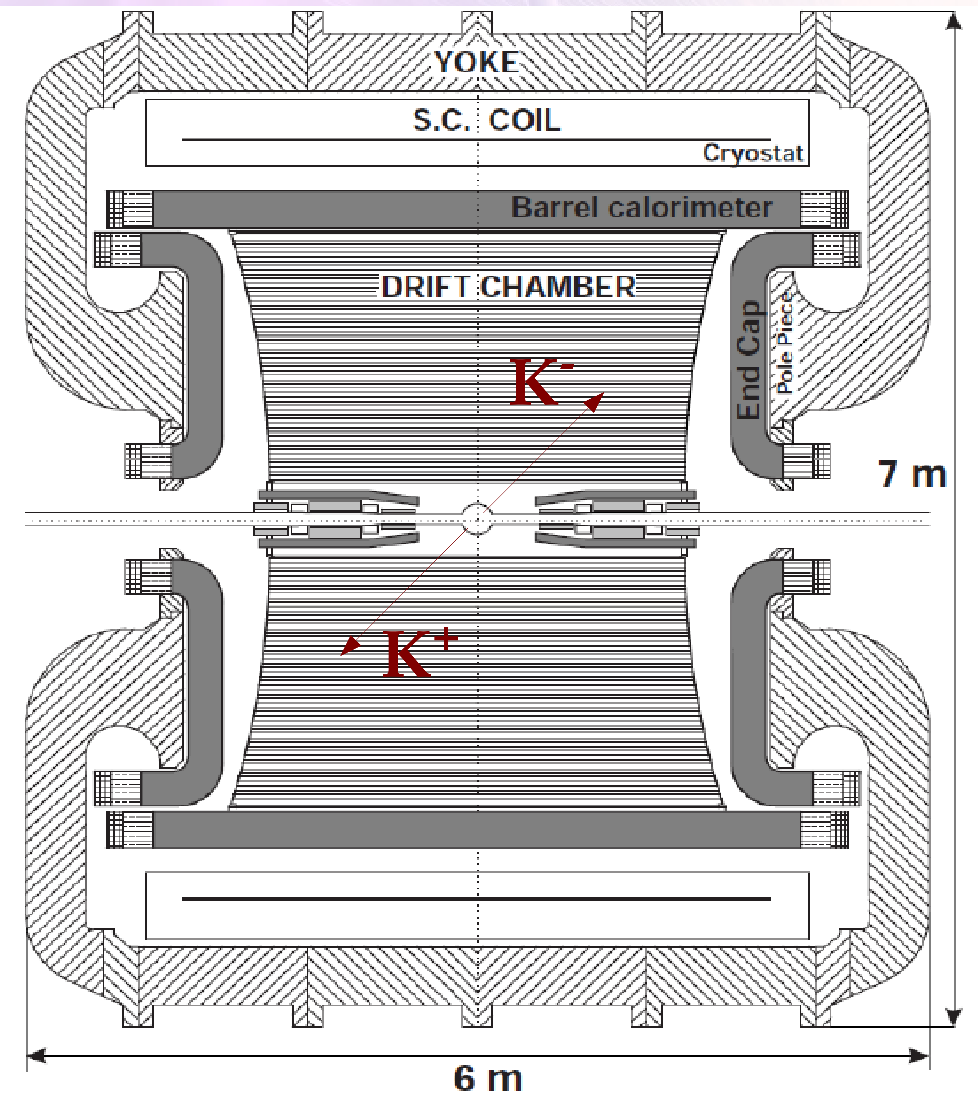

Possibility to use KLOE materials as an active target

Advantage:
excellent resolution ..

$\sigma_{p\Lambda}$ = 0.49±0.01 MeV/c in DC gas

$\sigma_{m\gamma\gamma}$ = 18.3±0.6 MeV/c^2

Disadvantage:
Not dedicated target → different nuclei contamination → complex interpretation .. but → new features .. K^- in flight absorption.

Carbon target inside KLOE

K⁻

Advantages:

- gain in statistics
- K^- absorptions occur in Carbon
- absorptions at-rest.

(~90 pb^{-1}; analyzed 37 pb^{-1}, x1.5 statistics)

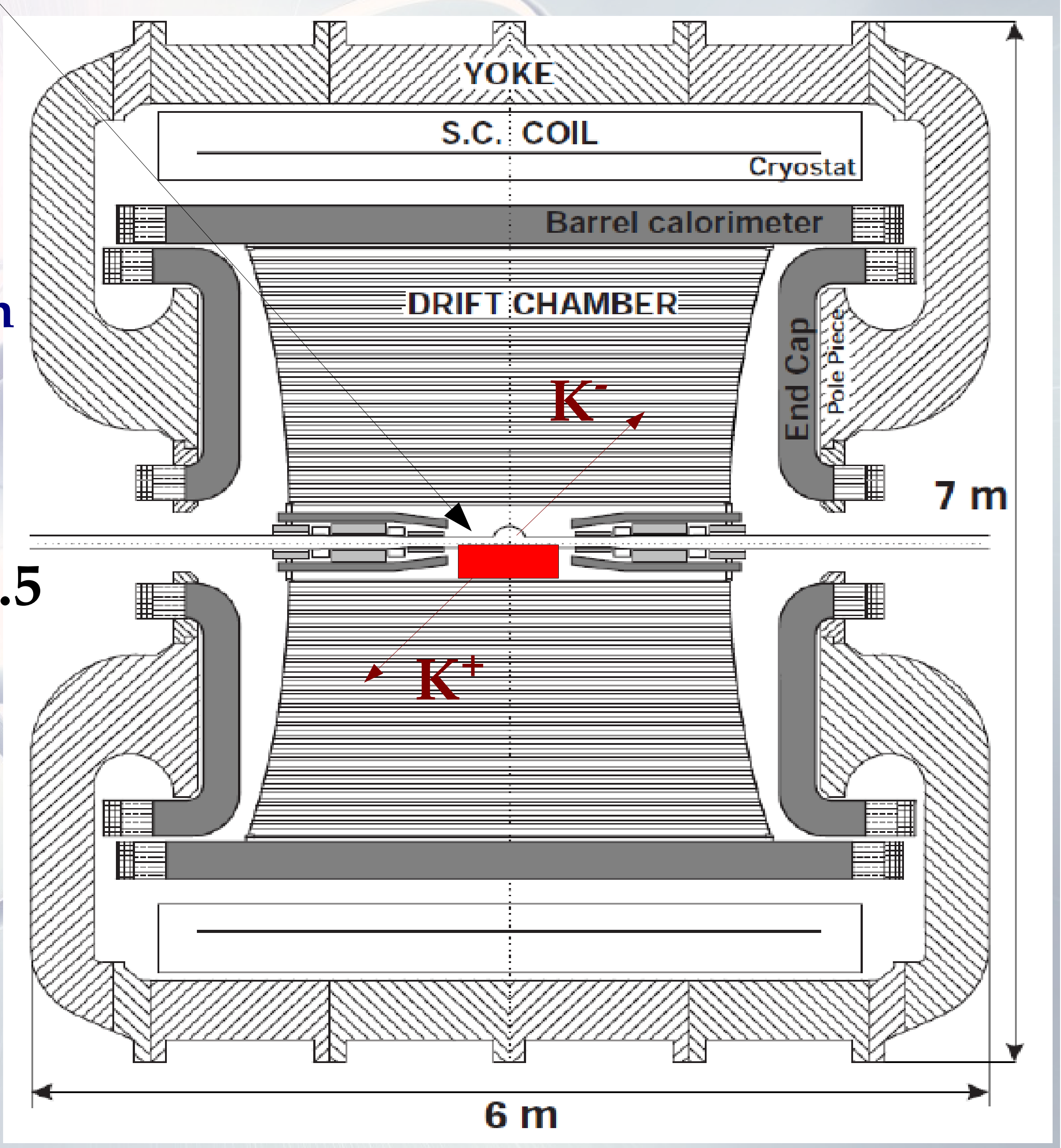

PART 1

kaonic nuclear clusters

Single & multi – nucleon K^- absorption

investigation through

Λp / Λd / Λt

correlation

Λp/Λd/Λt scientific case

K⁻

How deeply can an Antikaon be bound to a nucleus?

Possible bound states: K^-pp – K^-ppn

↘ Λp ↘ Λd

predicted due to the strong $\bar{K}N$ interaction in the I=0 channel. (Wycech (1986) - Akaishi & Yamazaki (2002))

Different theoretical approaches:
- Few-body calculations solving Faddeev equations
- Variational calculations with phenomenological KN potential
- KN effective interactions based on Chiral SU(3) dynamics

K^-pp bound state

	Theoretical prediction	B.E (MeV)	Γ (MeV)
PRC76, 045201 (2002)	T. Yamazaki and Y. Akaishi	48	61
arXiv:0512037v2[nucl-th]	A. N. Ivanov, P. Kienle, J. Marton, E. Widman	118	58
PRC76, 044004 (2007)	N. V. Shevchenko, A. Gal, J. Mares, J. Revai	50~70	~100
PRC76, 035203 (2007)	Y. Ikeda and T. Sato	60~95	45~80
NPA804, 197 (2008)	A. Dote, T. Hyodo, W. Weise	20±3	40~70
PRC80, 045207 (2009)	S. Wycech and A. M. Green	56.5~78	39~60
PRL B712, 132-137 (2012)	Barnea et al.	15.7	41.2

Λp scientific case

K^-

How deeply can an Antikaon be bound to a nucleus?

Possible bound states: K^-pp → Λp

Experimental studies in the Λp decay channel

- pp collisions: DISTO (published), FOPI, HADES (E. Epple → monday afternoon session)
- Absorption experiments:

FINUDA

K- stopped + X -> Λp X'

X = 6Li, 7Li, 9Be

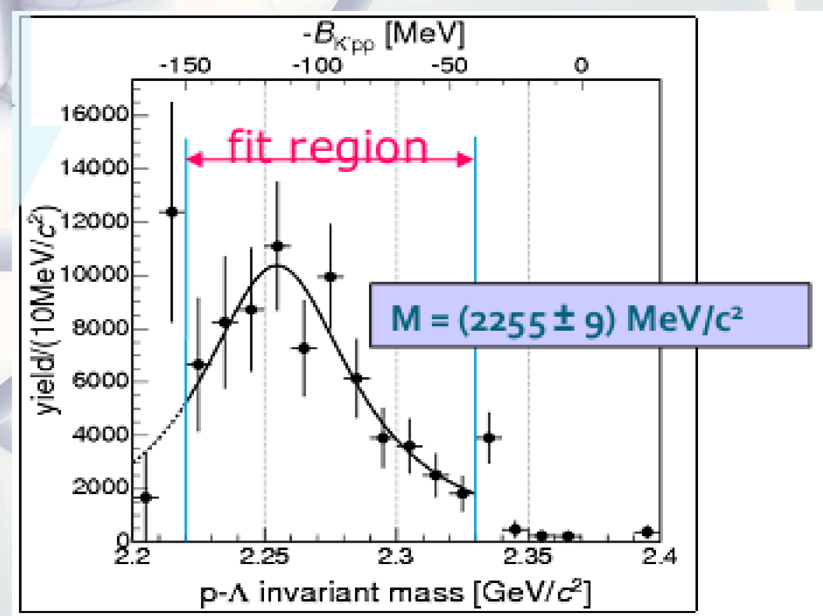

$B = 115^{+6}_{-5}$ (stat) $^{+3}_{-4}$ (sys) MeV

$\Gamma = 67^{+14}_{-11}$ (stat) $^{+2}_{-3}$ (sys) MeV

PRL94 (2005) 212303

Λp scientific case

K⁻

How deeply can an Antikaon be bound to a nucleus?

Possible bound states: K^-pp

→ Λp

Experimental studies in the Λp decay channel

- pp collisions: DISTO (published), FOPI, HADES (E. Epple → monday afternoon session)
- Absorption experiments:

@KEK E-549

K- stopped + 4He -> Λp X

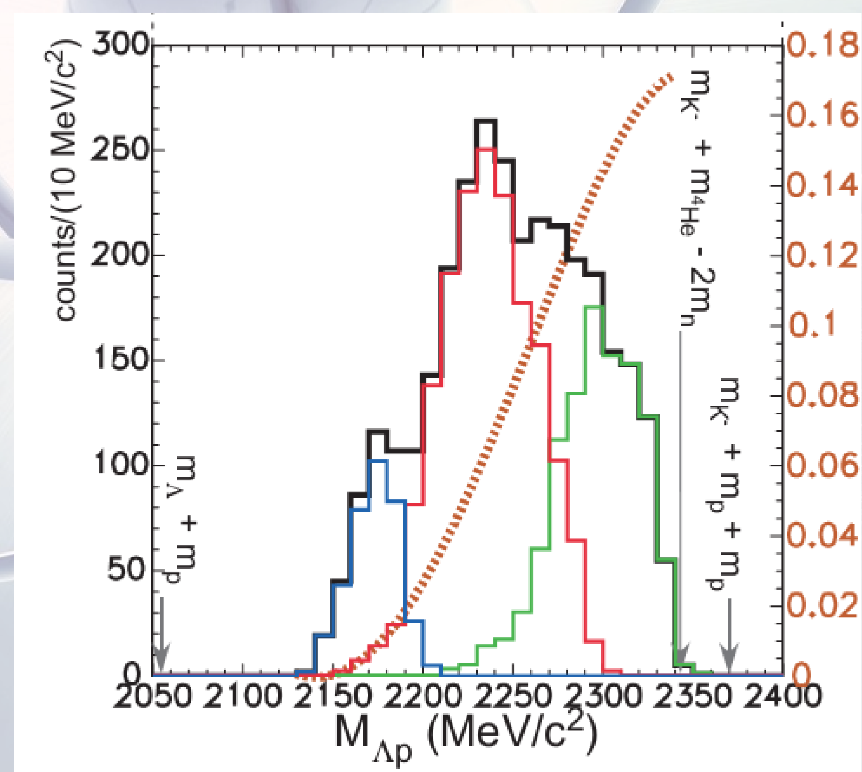

1NA
ΣN/ΛN - DBKS
2NA

Λp scientific case

K⁻

How deeply can an Antikaon be bound to a nucleus?

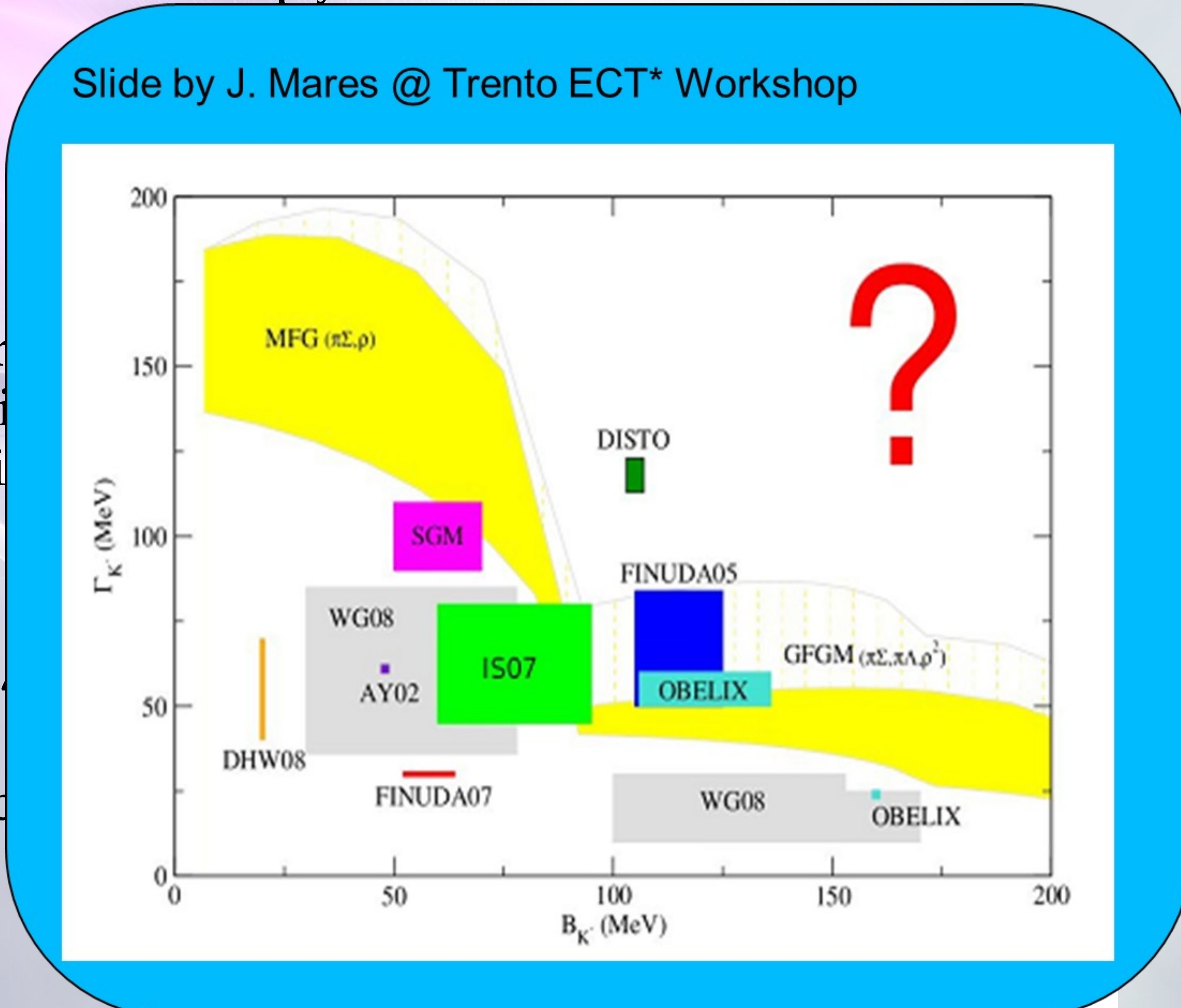

Experimen

- pp collisi … ple)
- Absorpti

@KEK E-5

K- stoppec

NA

N/ΛN - DBKS

NA

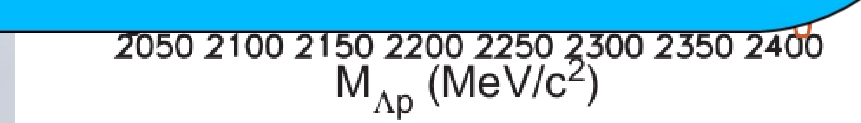

arXiv:0

Λp analysis

K⁻

Analysis of events in the DC gas volume

K- stopped **+ 4He → Λp X**
in-flight abs.

pπ–

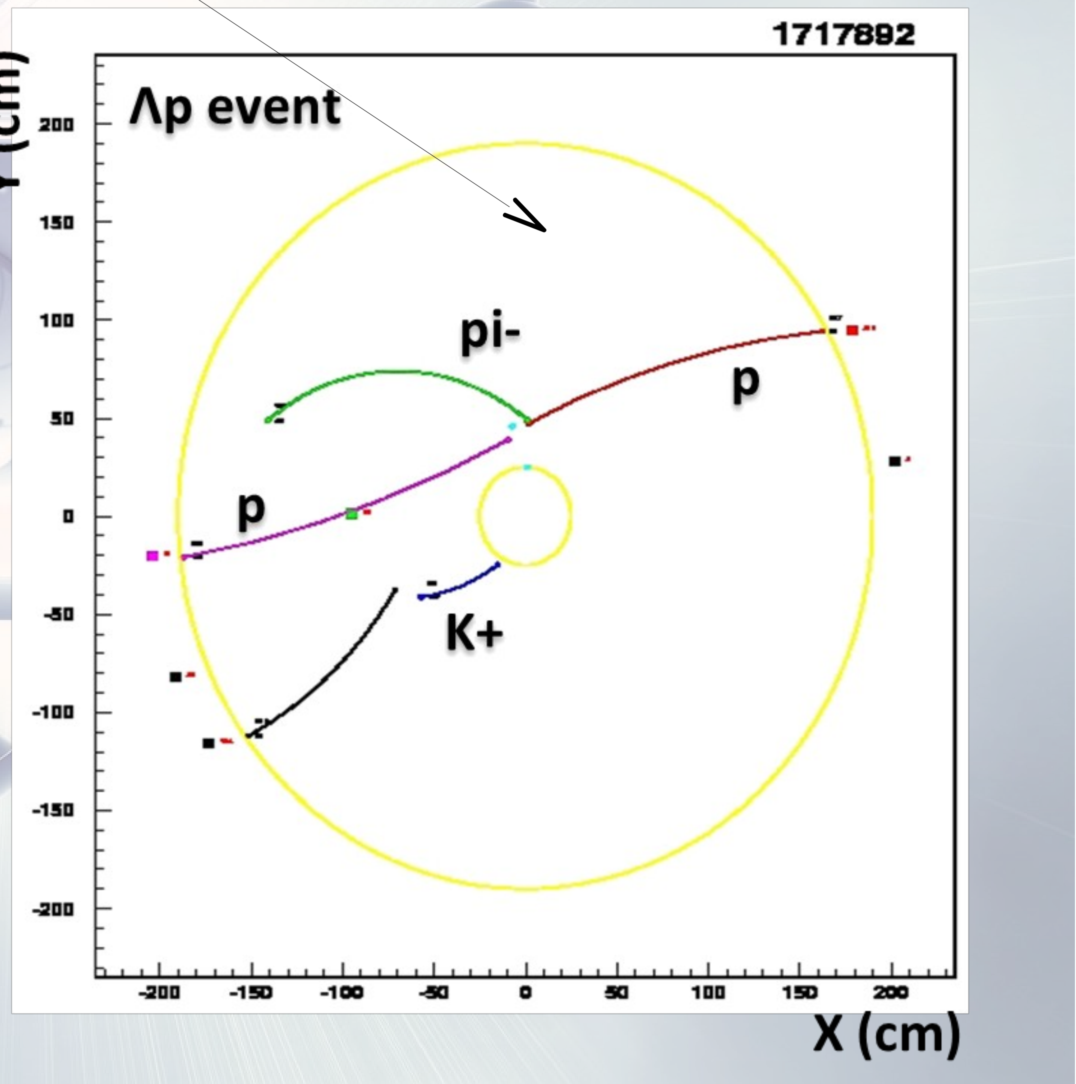

Λp analysis

Resolution study with MC simulation and charged kaons decays:

p_Λ	$0.49 \pm 0.01\ MeV/c$
p_p	$2.63 \pm 0.07\ MeV/c$
$M_{\Lambda p}$	$1.10 \pm 0.03\ MeV/c^2$
r_{vertex}	$0.12 \pm 0.01\ cm$

Acceptance study with phase space **K- + 4He -> Λ p n n** MC simulation

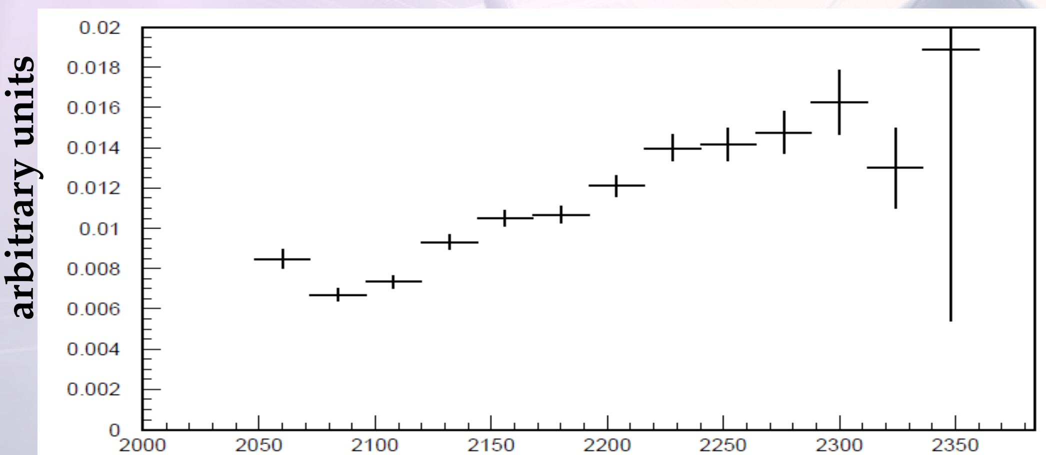

Projection of the acceptance function depending on : (PΛ,Pp,Minv Λp) on the Invariant mass plane

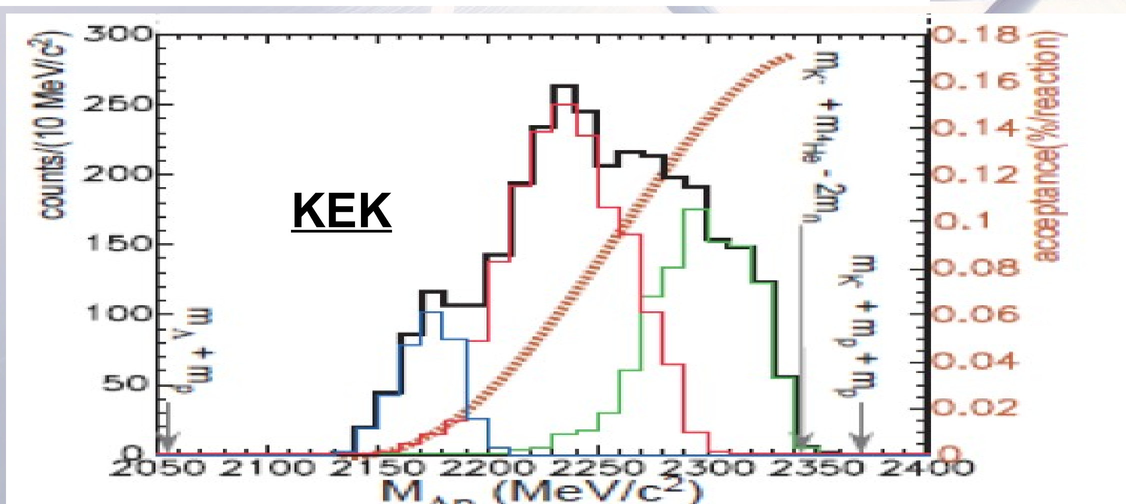

Acceptance allows for quantitative study of all the contributing processes

K^-

- 1NA with Σ/Λ conversion:

K-N → Σπ + **Σp/Λp**

FINAL PRODUCED PARTICLES

- 2NA processes:

K-NN → Λ (Σ0) p

K-NN → Σ0p + **Σp/Λp** conversion in 4He

Pionic 2NA modes: **K-NN → YπN**

- Uncorrelated processes:

Simulation based in «spectator» protons from Λd correlated events in 12C

Λp and Λpπ- samples

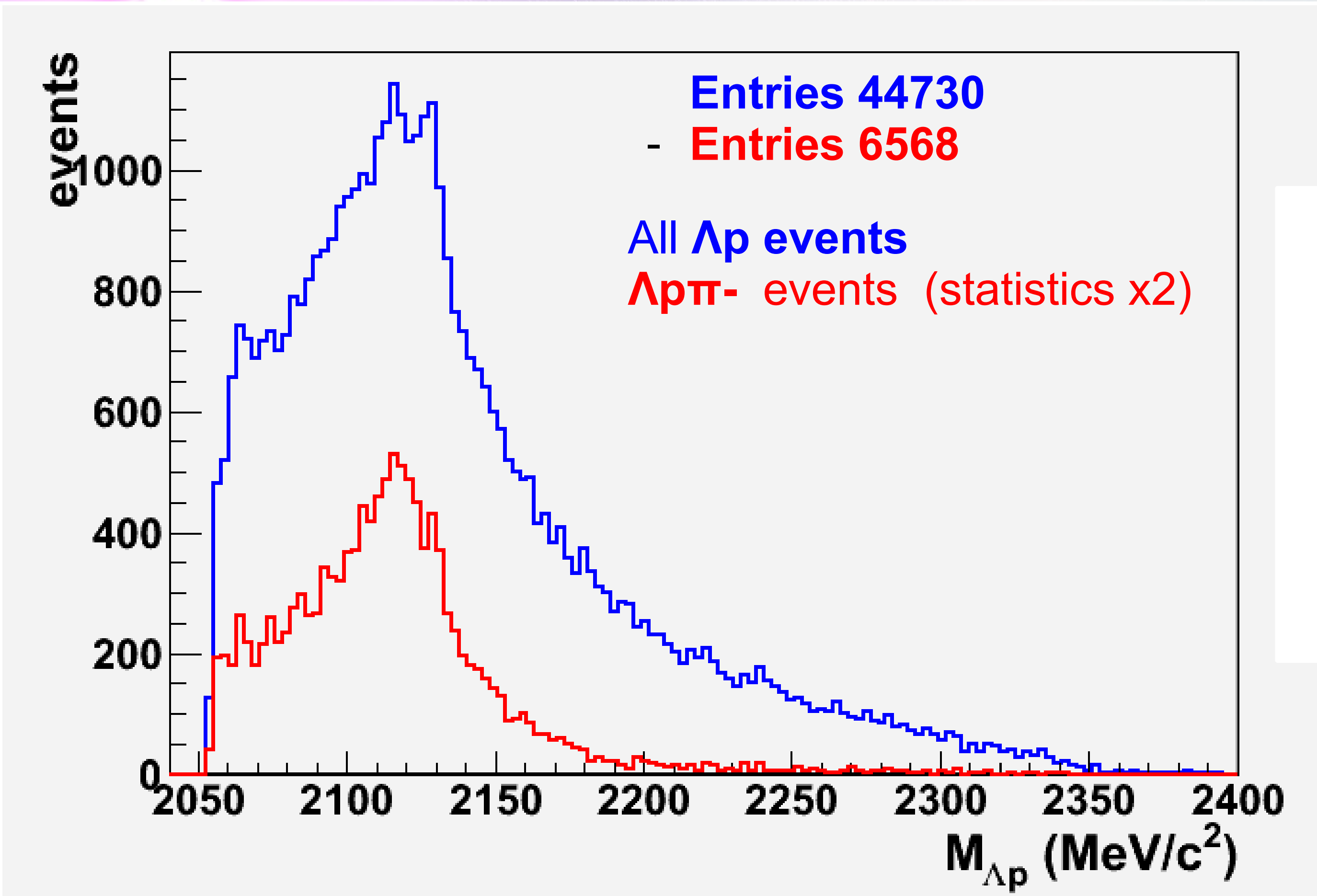

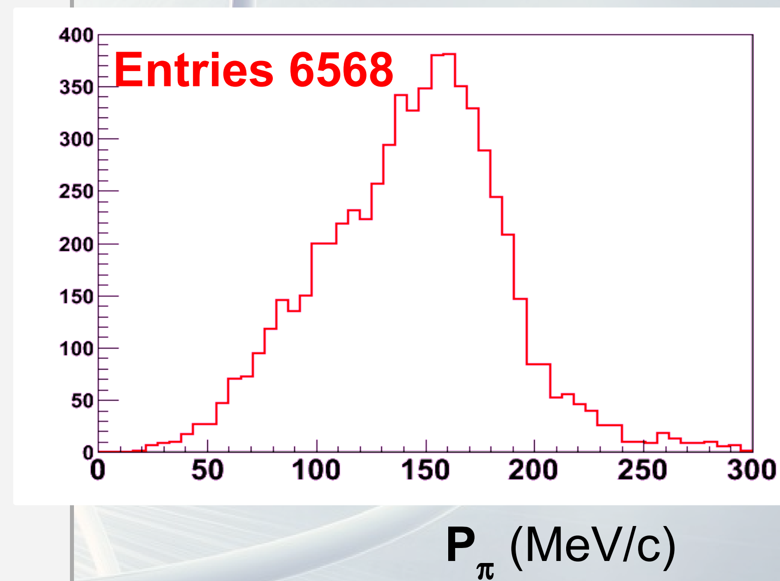

The presence of a pion is the characteristic signal a single nucleon absorption:

Absorption: **K-N → Σπ** + <u>**conversion**</u> process: **Σp/Λp**

detected particles

Λp and Λpπ- samples

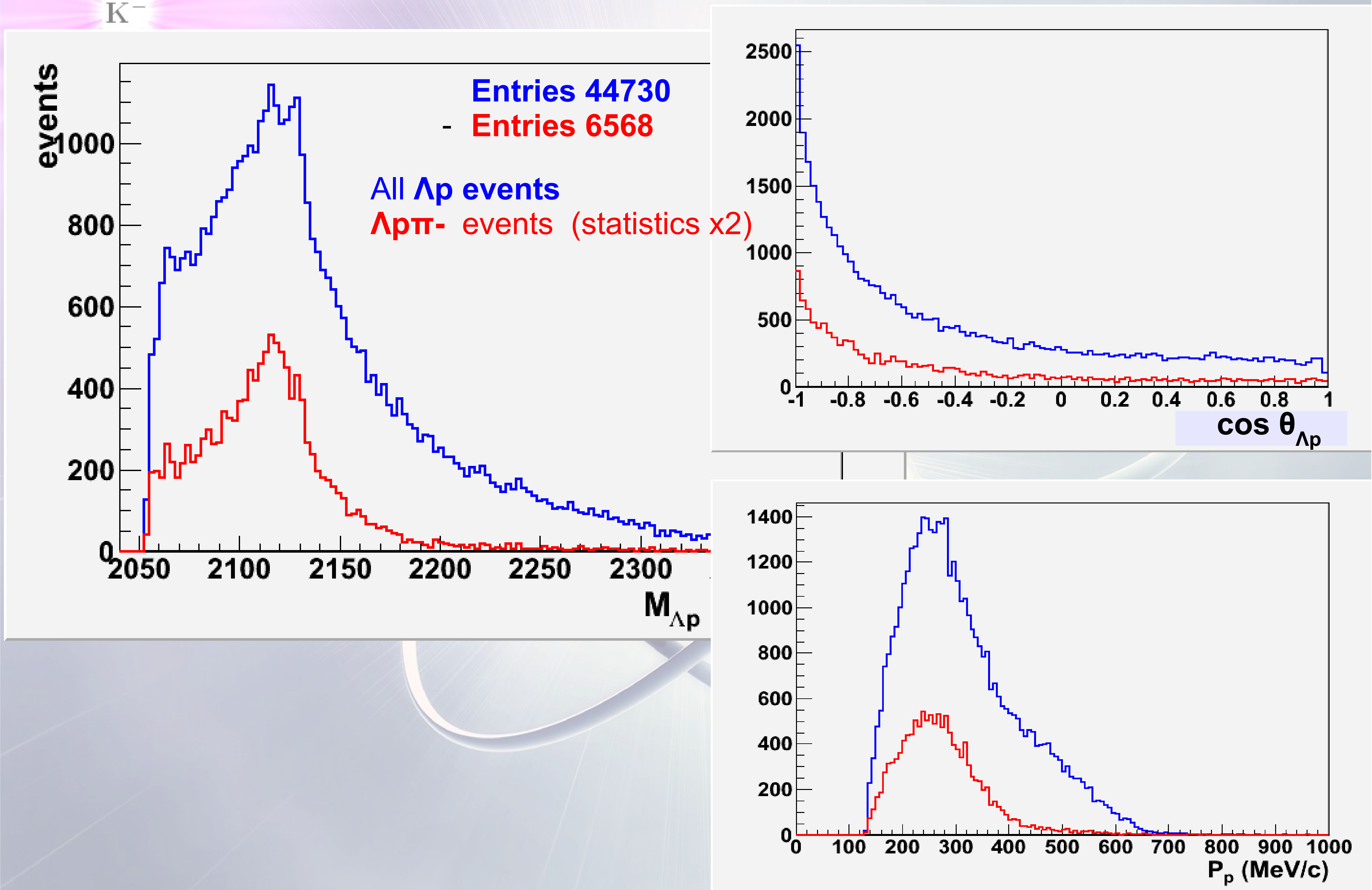

K^-

Λp events, preliminary fit

- 1NA with Σ/Λ conversion:

K-N → Σπ + **Σp/Λp**

FINAL PRODUCED PARTICLES

- 2NA processes:

K-NN → Λ (Σ0) p

K-NN → Σ0p + **Σp/Λp** conversion in 4He

Pionic 2NA modes: **K-NN → YπN**

- Uncorrelated processes:

Simulation based in «spectator» protons from Λd correlated events in 12C

Λp events, preliminary fit

K^-

Fit method: 2D fit
Λp invariant mass
and **cos $\theta_{\Lambda p}$** simultaneously

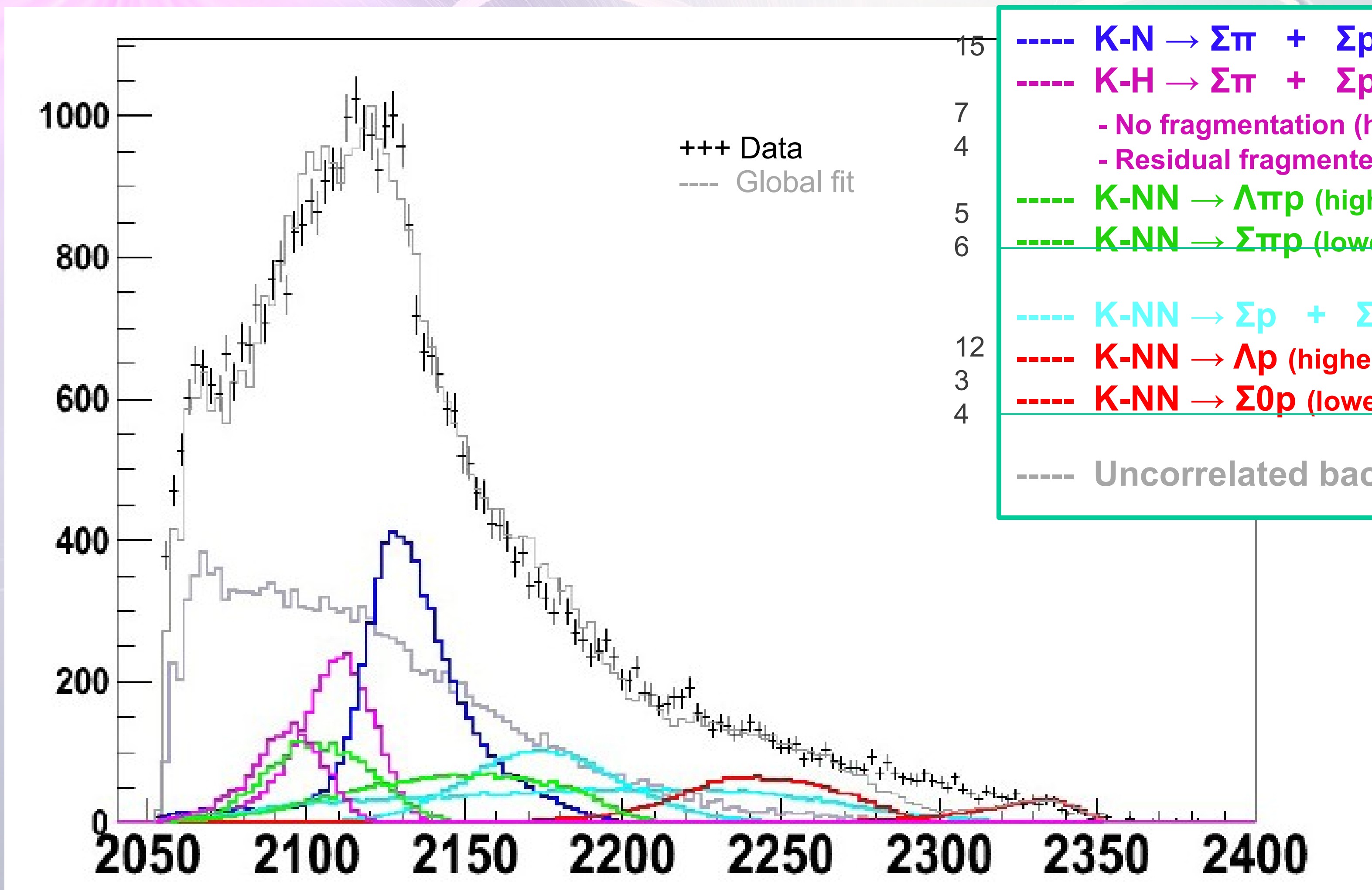

----- K-N → Σπ + Σp/Λp conversion in 4He
----- K-H → Σπ + Σp/Λp conversion in 12C
- No fragmentation (higher mass)
- Residual fragmented (lower mass)
----- K-NN → Λπp (higher mass)
----- K-NN → Σπp (lower mass)

----- K-NN → Σp + Σp/Λp conversion in 4He
----- K-NN → Λp (higher mass)
----- K-NN → Σ0p (lower mass)

----- Uncorrelated background

$M_{\Lambda p}$ (MeV/c^2)

conversion in 12C conversion in 4He

conversion after 1NA

conversion after 2NA: more energetic

Λp events, preliminary fit .. ISSUES

Fit method: 2D fit
Λp invariant mass
and **cos $\theta_{\Lambda p}$** simultaneously

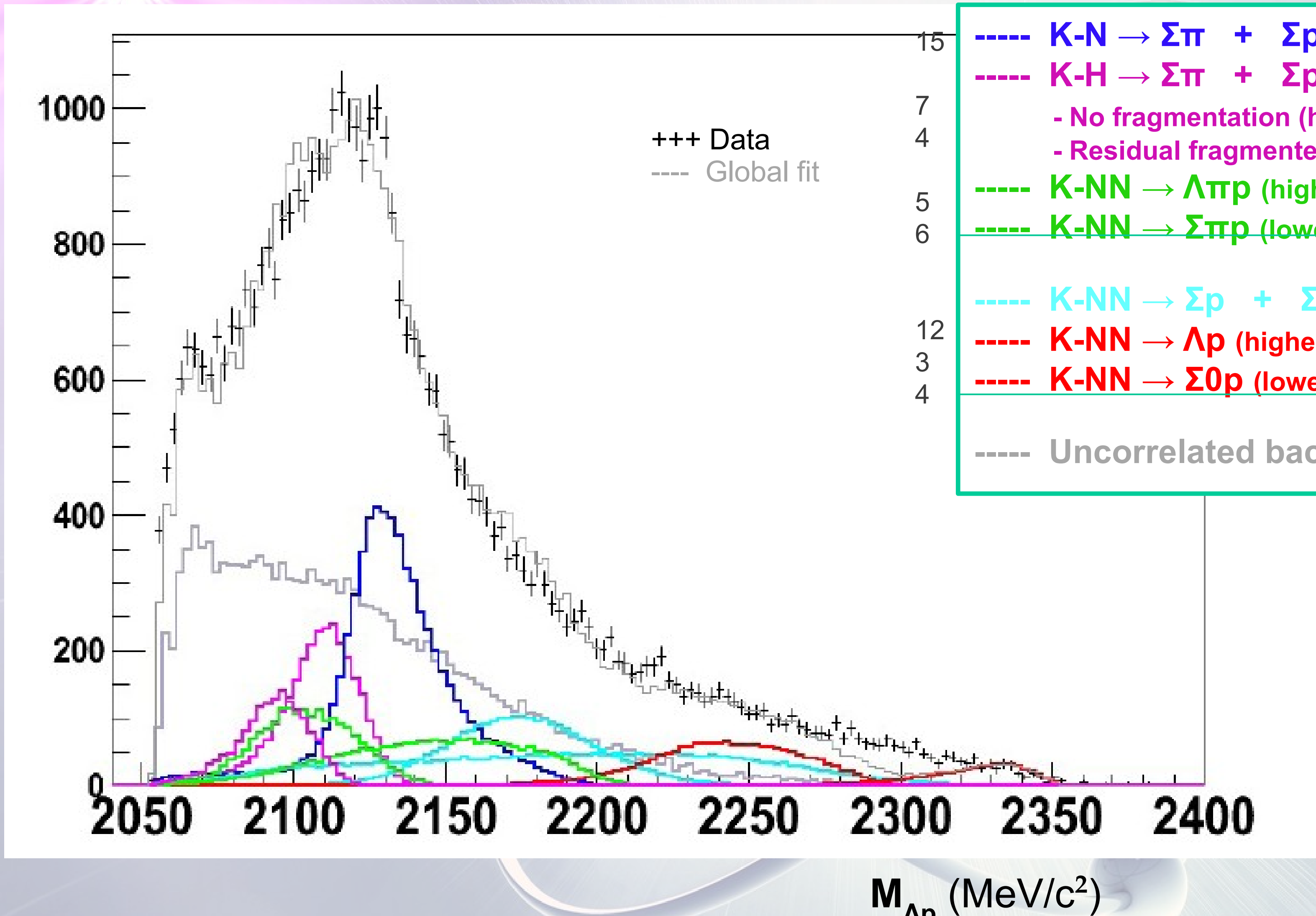

----- K-N → Σπ + Σp/Λp conversion in 4He
----- K-H → Σπ + Σp/Λp conversion in 12C
- No fragmentation (higher mass)
- Residual fragmented (lower mass)

----- K-NN → Λπp (higher mass)
----- K-NN → Σπp (lower mass)

----- K-NN → Σp + Σp/Λp conversion in 4He
----- K-NN → Λp (higher mass)
----- K-NN → Σ0p (lower mass)

----- Uncorrelated background

Is there room for a 2NA pionic mode?

K-NN → YπN

The preliminary fits find «a place» for this processes (~ 5% of Λp events)

Λd search for a K-ppn cluster

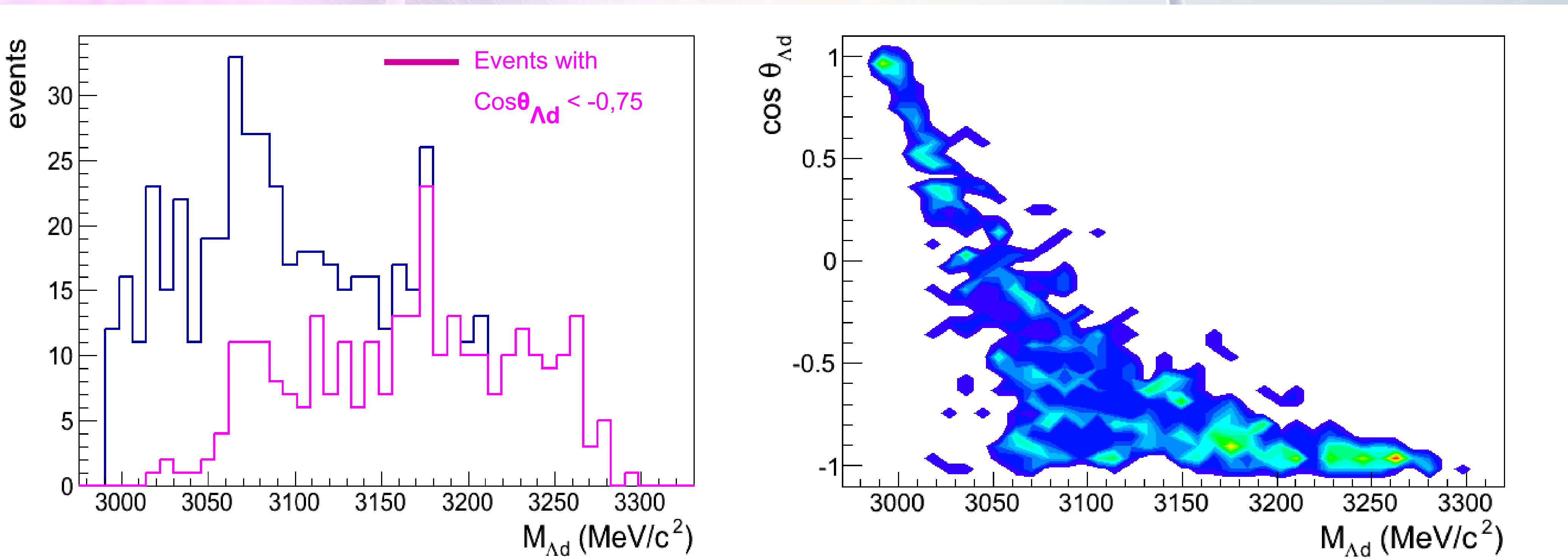

- 572 Lambda-deuteron events in DC gas
- Structures at high Mass correlated with back-to-back events

Λt events

- High energy tritons expected to come from rare 4NA process

- Only observed in bubble chamber experiments 3 events (M. Roosen, J.H. Wickens, Il Nuovo Cimento 66 (1981), 101.) and by FINUDA 40 events adding different materials (Phys.Lett.B669:229-234,2008).

- KLOE statistics in the DC gas: **134 events**

Λt events

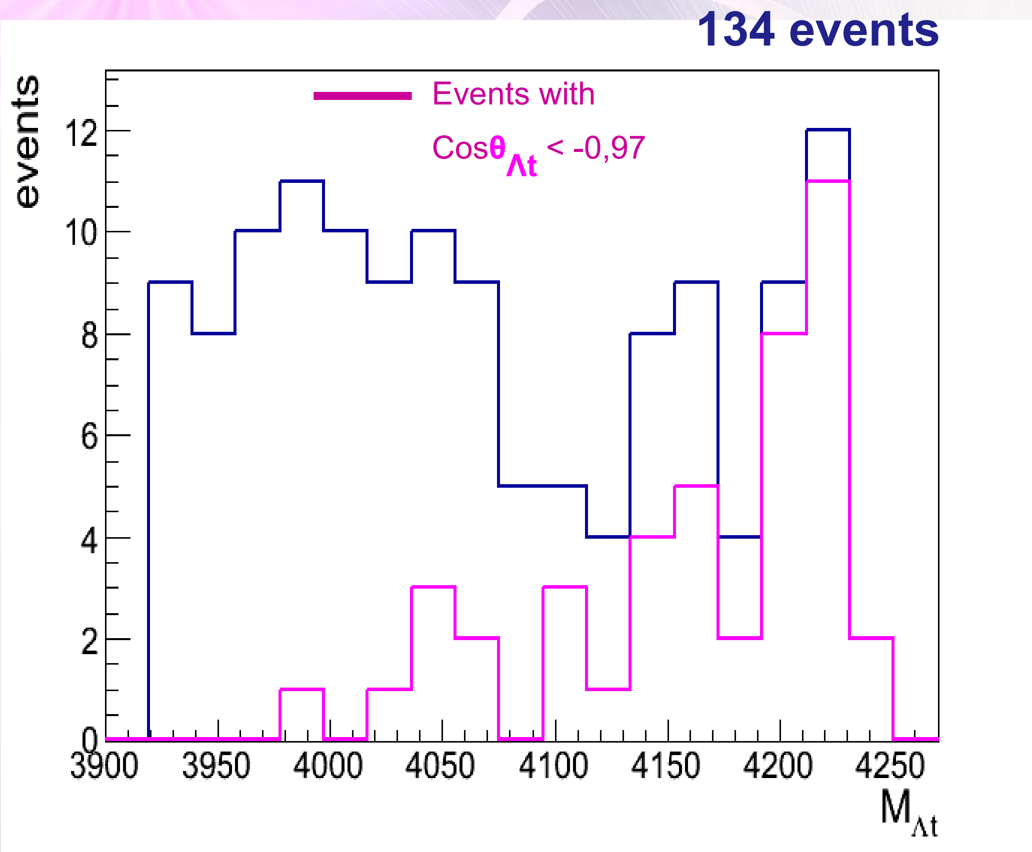

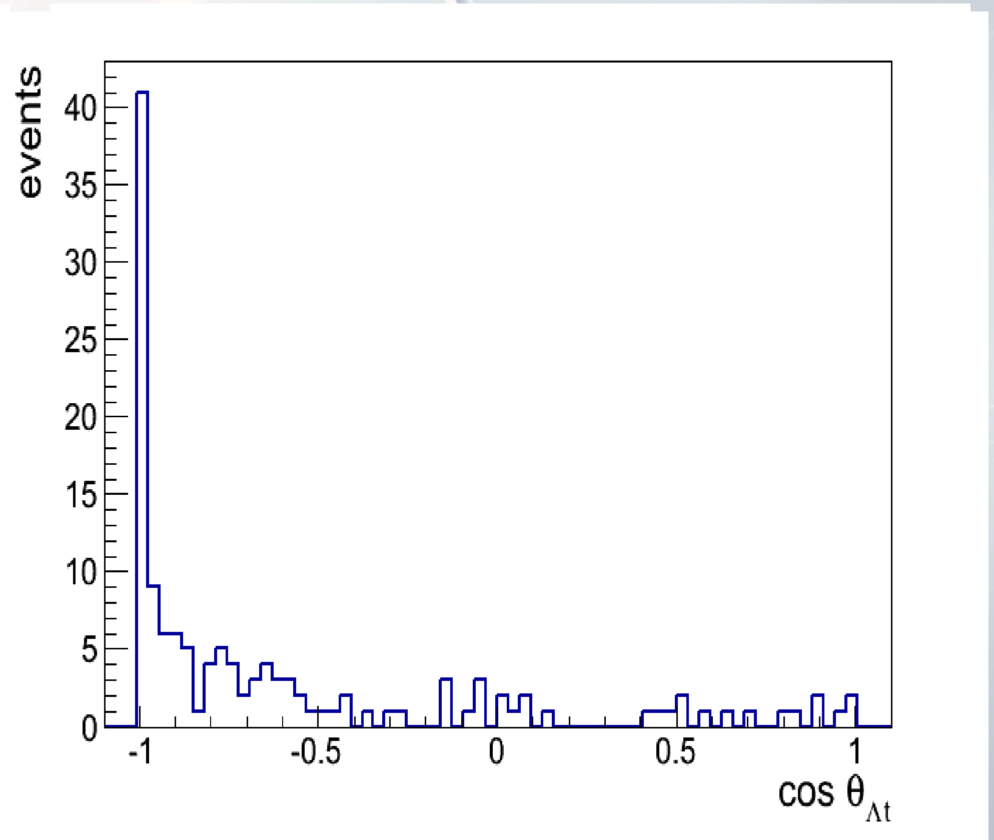

Clear back-to-back enhacement lambda-triton signal

Λt events

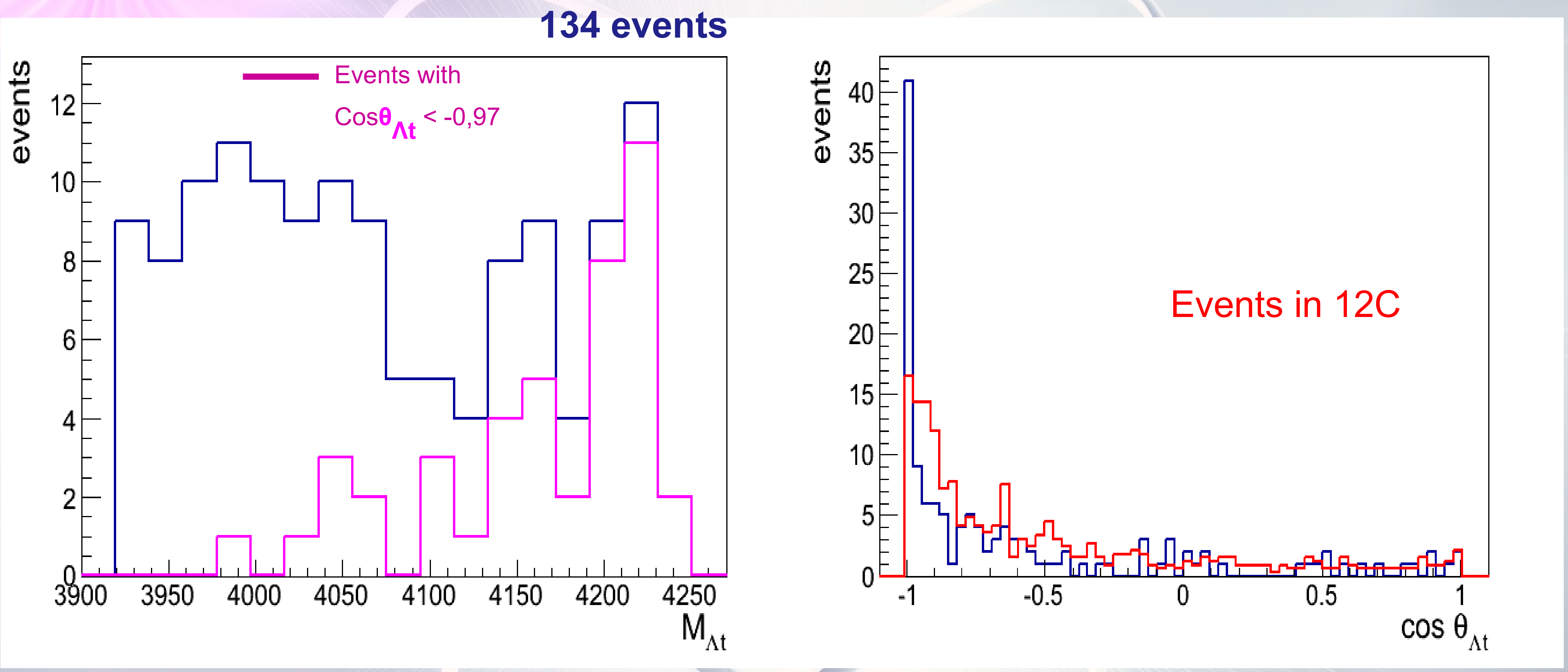

Clear back-to-back enhacement lambda-triton signal

Events in Carbon do not show this feature

K^-

Conclusions PART 1

- K-pp search:

  *The signal from the decay of a K-pp bound state is masked by the Σ/Λ conversion process.
  *No clear peak structure excludes the possibility of a high formation rate and/or narrow width resonance.

- Λd, Λt

  *3- and 4-nucleon absorption processes clearly seen.
  *Additional structures must be investigated. Σ0 contamination? Bound state?

K^-

PART 2

Nature of the $\Lambda(1405)$

investigated through

$\Sigma^0\pi^0$ / $\Sigma^+\pi^-$

correlation

Scientific case of the Λ(1405)

Λ(1405) : mass = $1405.1^{+1.3}_{-1.0}$ MeV, width = 50 ± 2 MeV

I = 0, S = -1 , J^p = 1/2$^-$, Status: ** , strong decay into Σπ**

Its nature has been a puzzle for decades: three quark state, unstable $\bar{K}N$ bound state, penta-quark, two poles??

First experimental evidence:

M. H. Alston, et al., Phys. Rev. Lett. 6 (1961) 698

$K^- p \rightarrow \pi\pi\pi\Sigma$

Λ(1405)

Λ(1116)

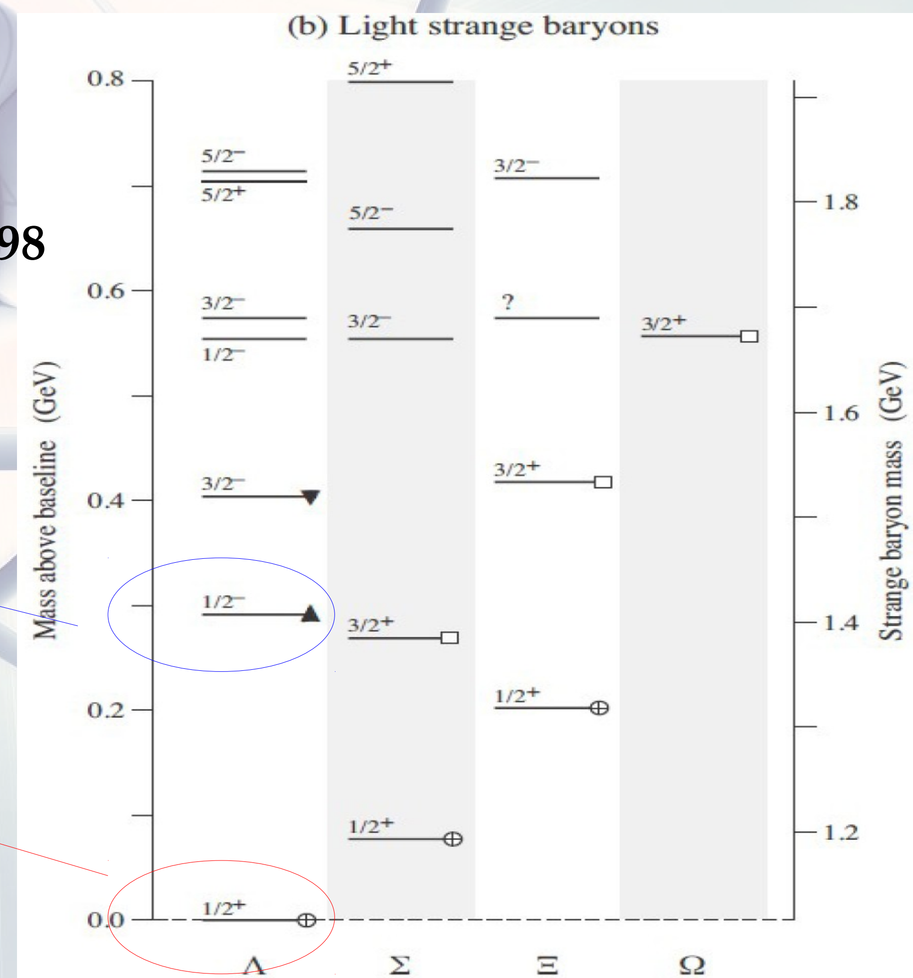

Scientific case of the Λ(1405)

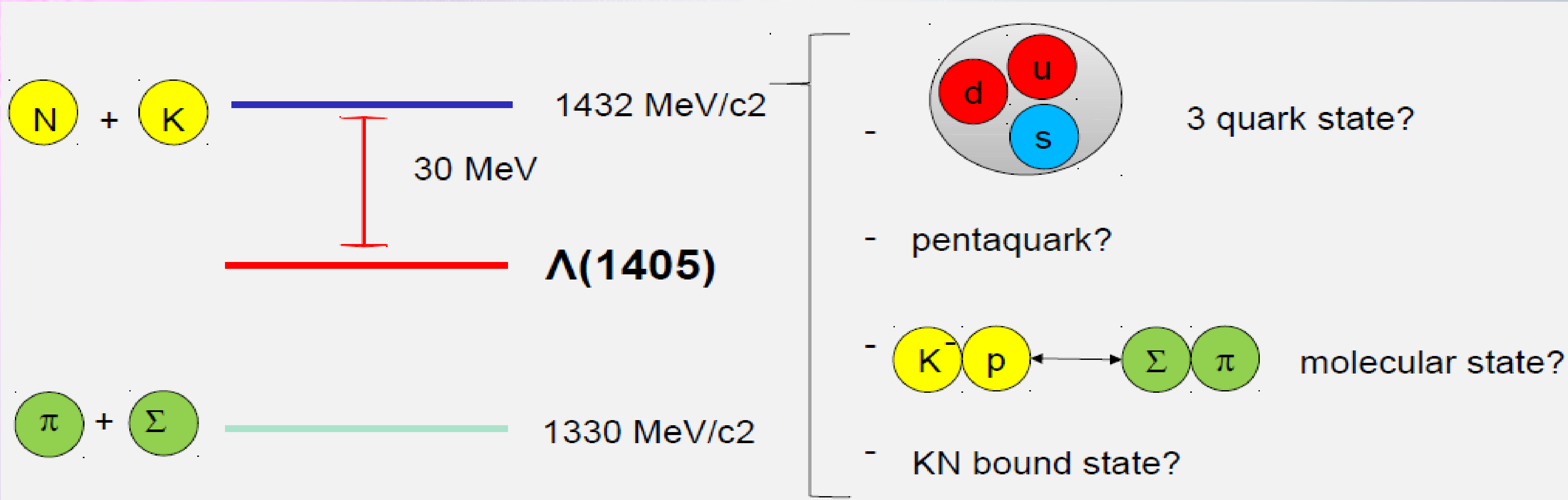

- The **three quark model picture:** Λ(1405) mass??

Similar to the nucleon sector N(1535), the expected mass of the Λ^* is around 1700 MeV.

- **Energy splitting between the Λ(1405) and the Λ(1520) (spin-orbit partner ($J^p = 3/2^-$)) ??.**

R. Dalitz and collaborators first suggested to interpret Λ(1405) as an $\bar{K}N$ quasibound state.

R.H. Dalitz, T.C. Wong and G. Rajasekaran, Phys. Rev. **153** (1967) 1617.

Scientific case of the Λ(1405)

- Chiral unitary models: Λ(1405) is an I = 0 quasibound state emerging from the coupling between the $\bar{K}N$ and the Σπ channels. Two poles in the neighborhood of the Λ(1405):

4) *two poles*: ($z_1 = 1424^{+7}_{-23} - i\,26^{+3}_{-14}$; $z_1 = 1381^{+18}_{-6} - i\,81^{+19}_{-8}$) MeV (Nucl. Phys. A881, 98 (2012))

mainly coupled to $\bar{K}N$ — mainly coupled to Σπ → line-shape depends on production mechanism

- Akaishi-Esmaili-Yamazaki phenomenological potential

Phys. Lett. B 686 (2010) 23-28 Confirmation of single pole ansatz?

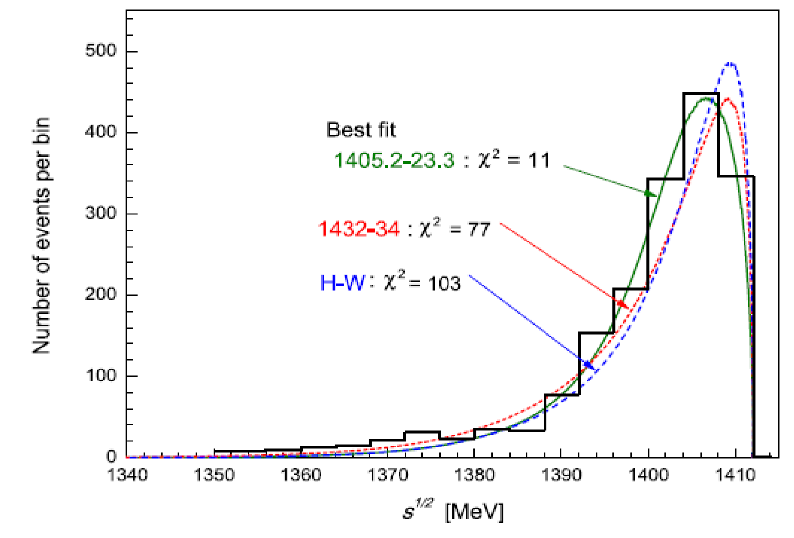

Fig. 6. Detailed differences in $M_{\Sigma\pi}$ spectra among the Hyodo–Weise prediction and the present model predictions.

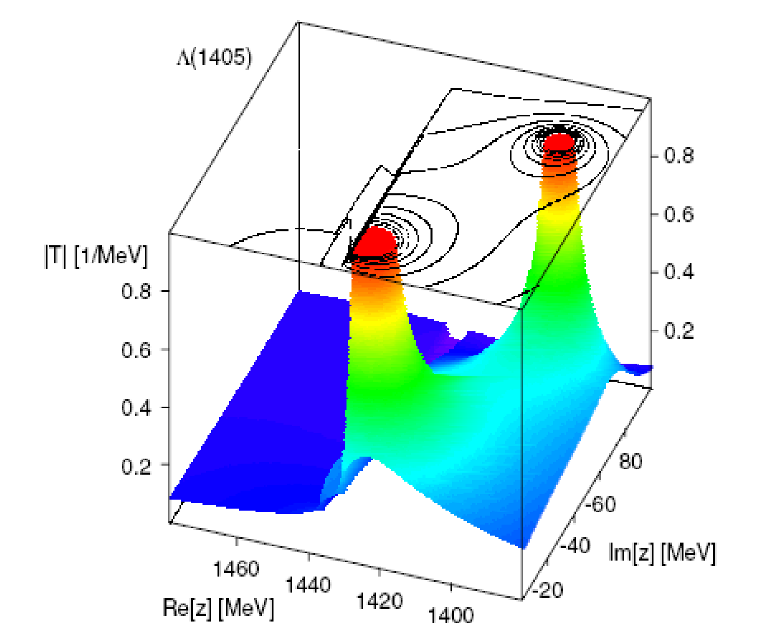

Scientific case of the $\Lambda(1405)$

- Chiral unitary models: $\Lambda(1405)$ is an I = 0 quasibound state emerging from the coupling between the $\bar{K}N$ and the $\Sigma\pi$ channels. Two poles in the neighborhood of the $\Lambda(1405)$:

4) *two poles*: (z ... Phys. A881, 98 (2012))

mainly c... depends on ... mechanism

- Akaishi-E...

Phys. Lett. B6...

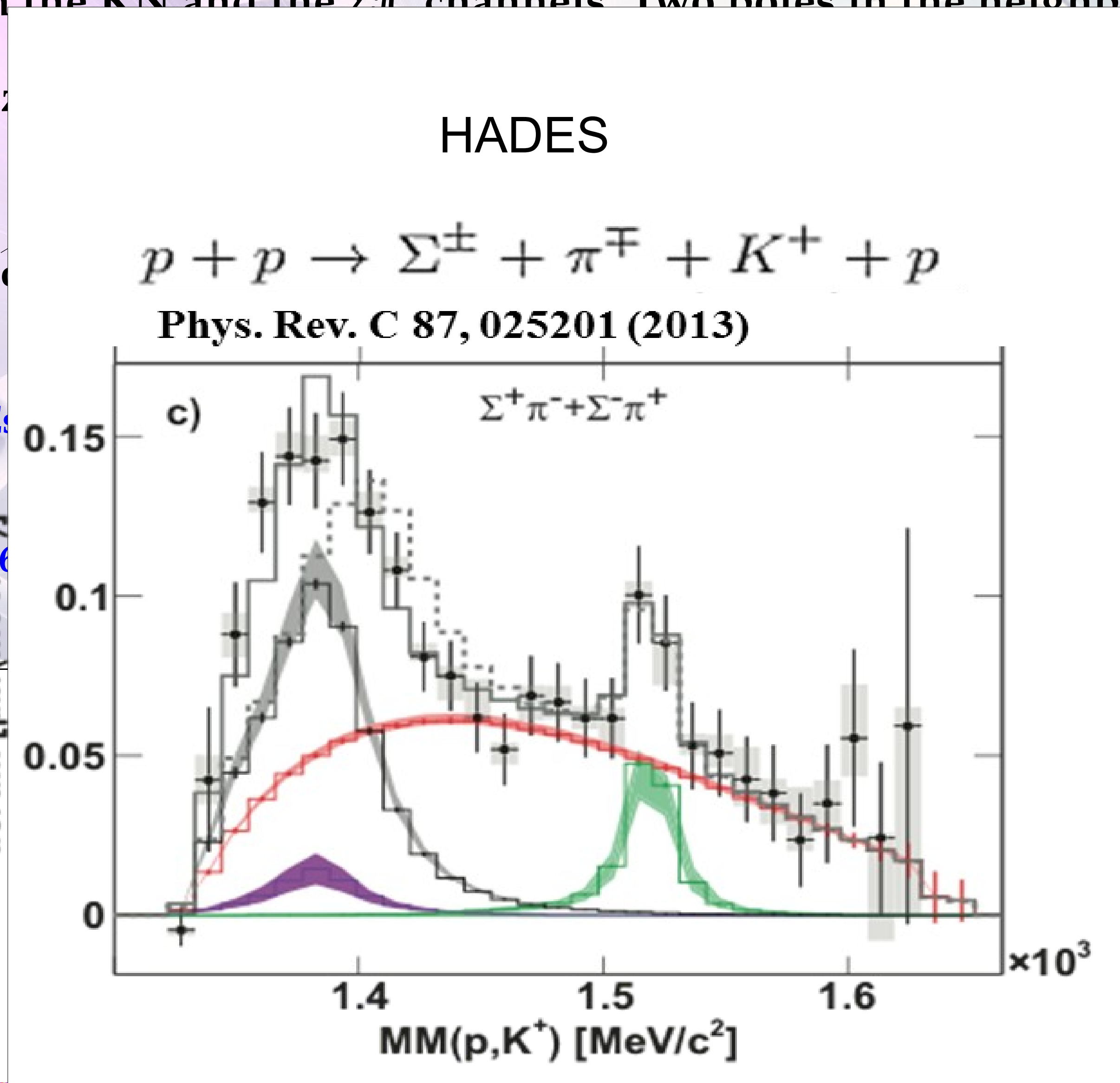

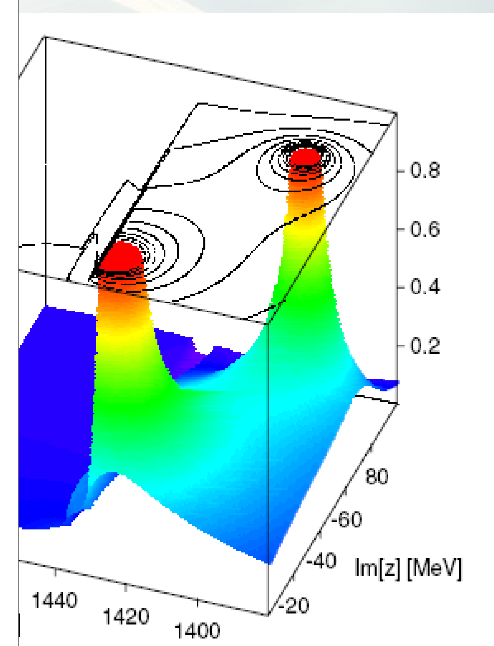

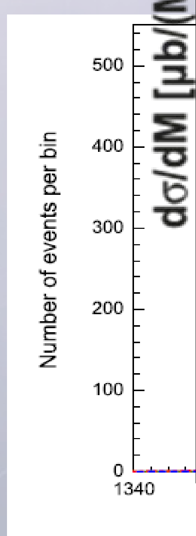

Fig. 6. Detailed differences in $M_{\Sigma\pi}$ spectra among the Hyodo–Weise prediction and the present model predictions.

Scientific case of the Λ(1405)

K^- nuclear absorption experiments .. long history .. BUT

1) $m_{\pi\Sigma}$ spectra CUT AT THE ENERGY LIMIT AT-REST 2) (Σ±π∓) Σ(1385) CONTAMINATION

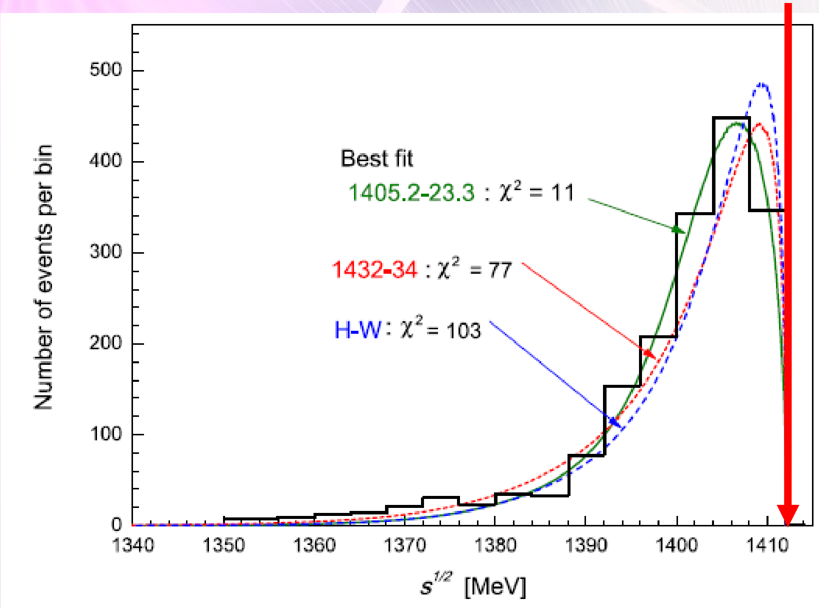

Fig. 6. Detailed differences in $M_{\Sigma\pi}$ spectra among the Hyodo–Weise prediction and the present model predictions.

"A study of K^- ^4He → (Σ±π∓) + ^3H using slow instead of stopping K^- would be very useful in eliminating some of the uncertainties in interpretation"

D. Riley, et al. Phys. Rev. D11 (1975) 3065

Esmaili et el., Phys.Lett. B686 (2010) 23-28

In flight K^- absorption allows to explore the higher mass region

Scientific case of the Λ(1405)

K⁻

Λ(1405) is I = 0

$\Sigma^0\pi^0$ (I =0) golden decay channel

(free from Σ(1385) background I=1)

The $\Sigma^0\pi^0$ spectrum was only observed in 3 experiments … with different line-shapes !

I. Zychor et al., Phys. Lett. B 660 (2008) 167

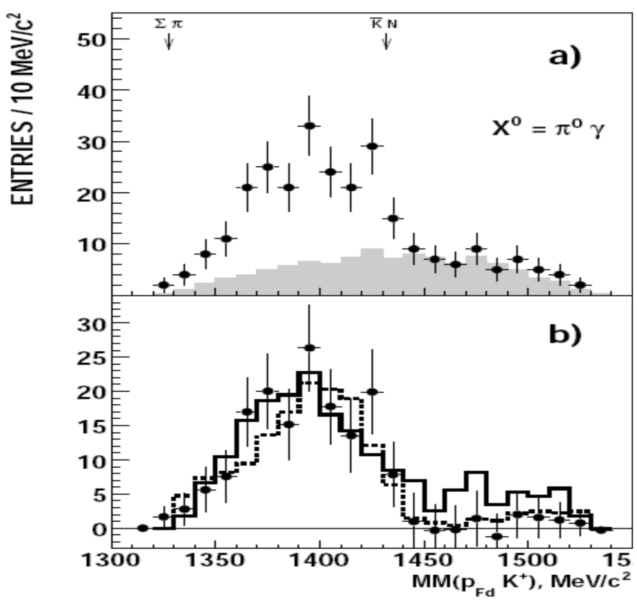

K. Moriya, et al., (Clas Collaboration) Phys. Rev. C 87, 035206 (2013)

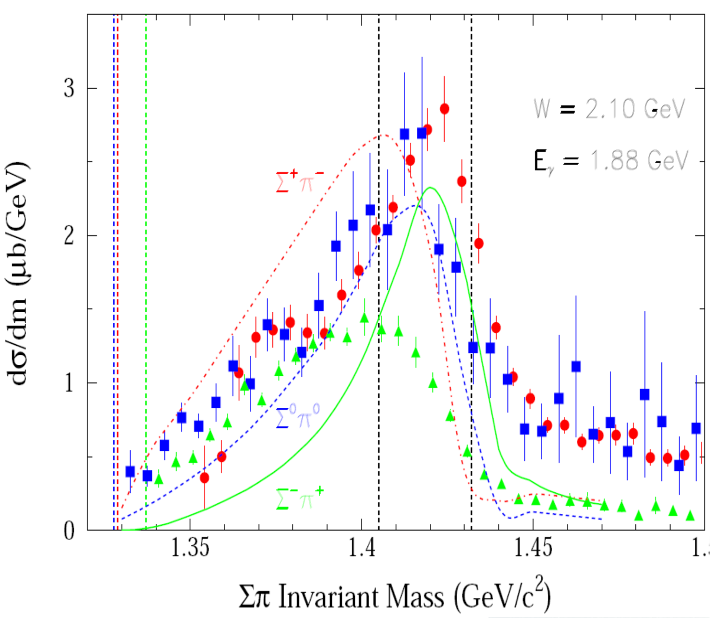

Magas et al. PRL 95, 052301 (2005) 034605 S. Prakhov, et al., Phys. Rev. C70 (2004)

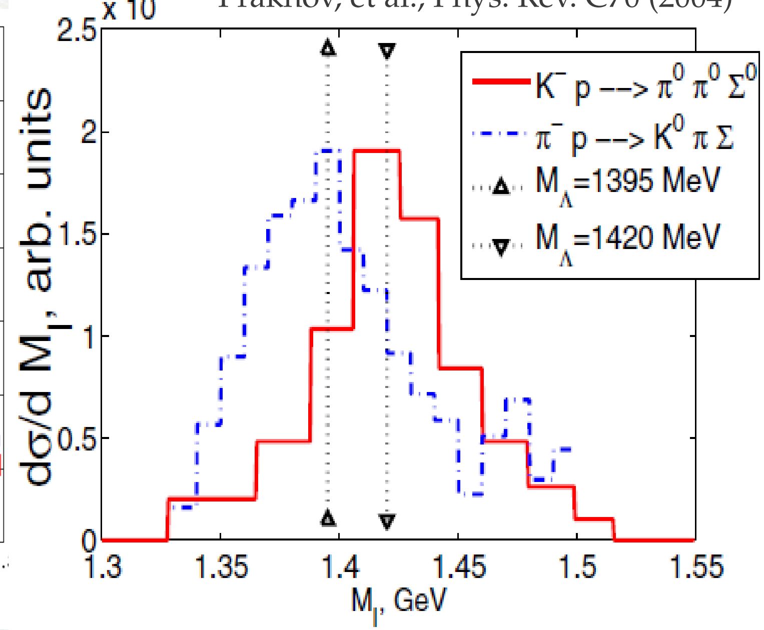

K^-

K^- "p" $\rightarrow\ \Sigma^0\pi^0$

bound proton in ^4He / ^{12}C

$\Sigma^0 \pi^0$ channel

$\Lambda(1405)$ signal searched by K^- interaction with a bound proton in Carbon

$K^- p \rightarrow \Sigma^0 \pi^0$ detected via: $(\Lambda\gamma)$ $(\gamma\gamma)$

Strategy : K^- absorption in the DC entrance wall, mainly ^{12}C with H contamination (epoxy)

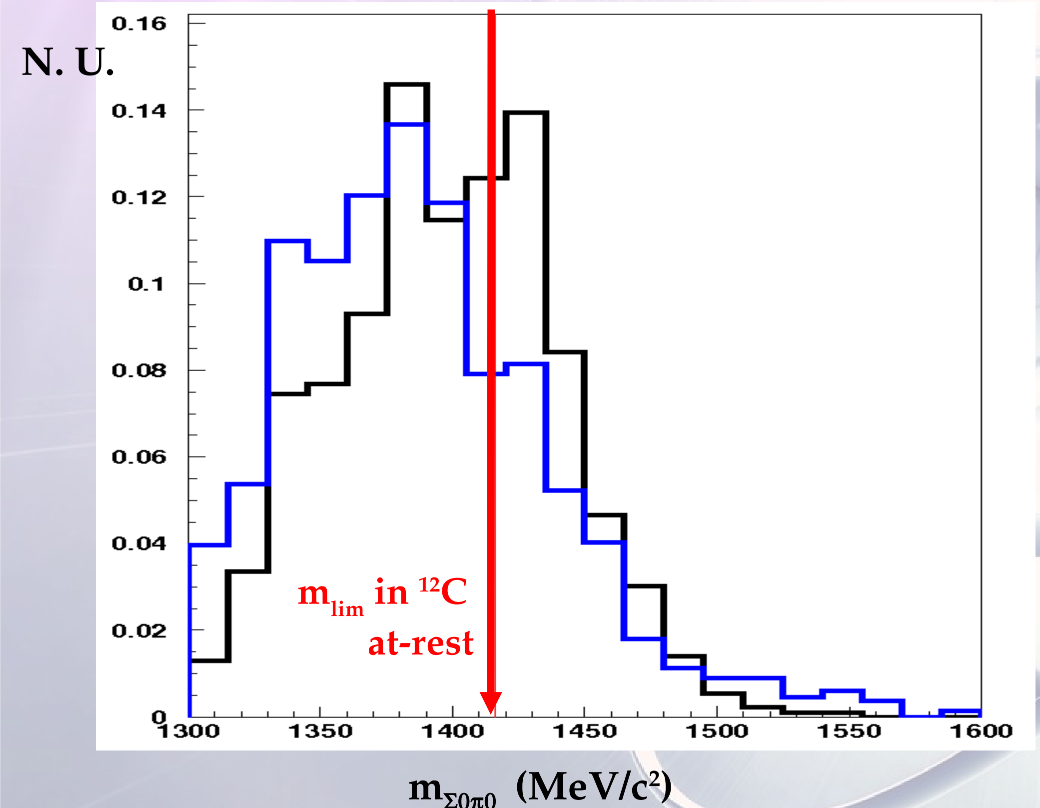

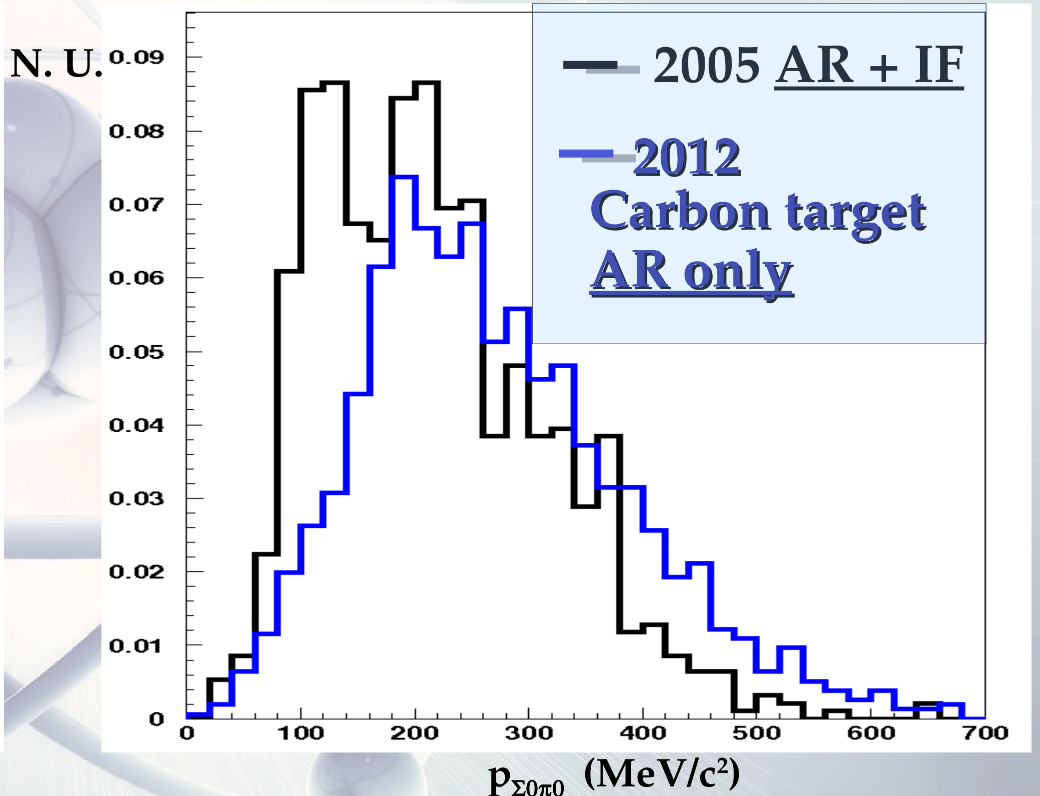

$m_{\pi 0 \Sigma 0}$ resolution $\sigma_m \approx 32$ MeV/c² ; $p_{\pi 0 \Sigma 0}$ resolution: $\sigma_p \approx 20$ MeV/c.

Negligible ($\Lambda \pi^0$ + internal conversion) background = (3±1) % → no I=1 contamination

$\Sigma^0 \pi^0$ channel

K⁻ nuclear absorption experiments .. long history .. BUT

1) $m_{\pi\Sigma}$ spectra always cut at the AT-REST limit

2) ($\Sigma\pm\pi\mp$) spectra suffer $\Sigma(1385)$ contamination

P. J. Carlson, et al. Nucl. Phys. 74 642

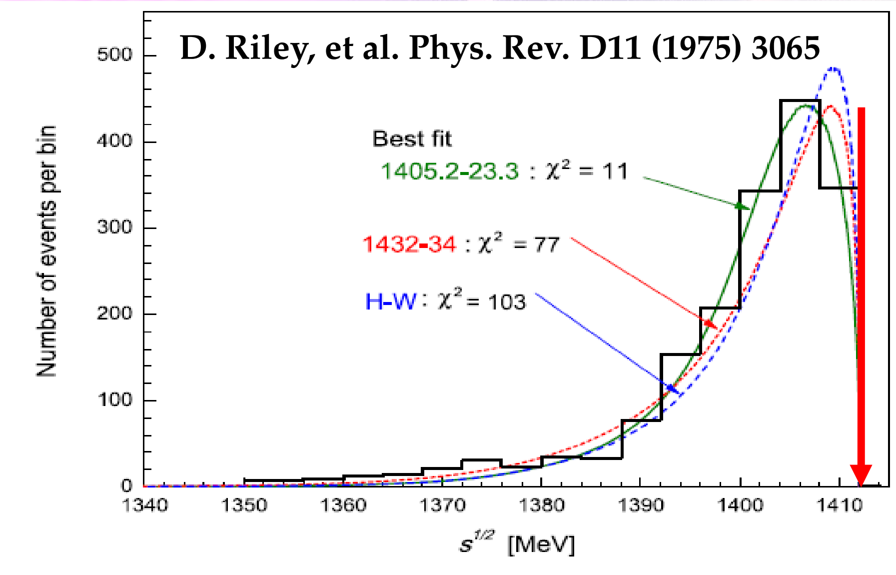

Fig. 6. Detailed differences in $M_{\Sigma\pi}$ spectra among the Hyodo–Weise prediction and the present model predictions.

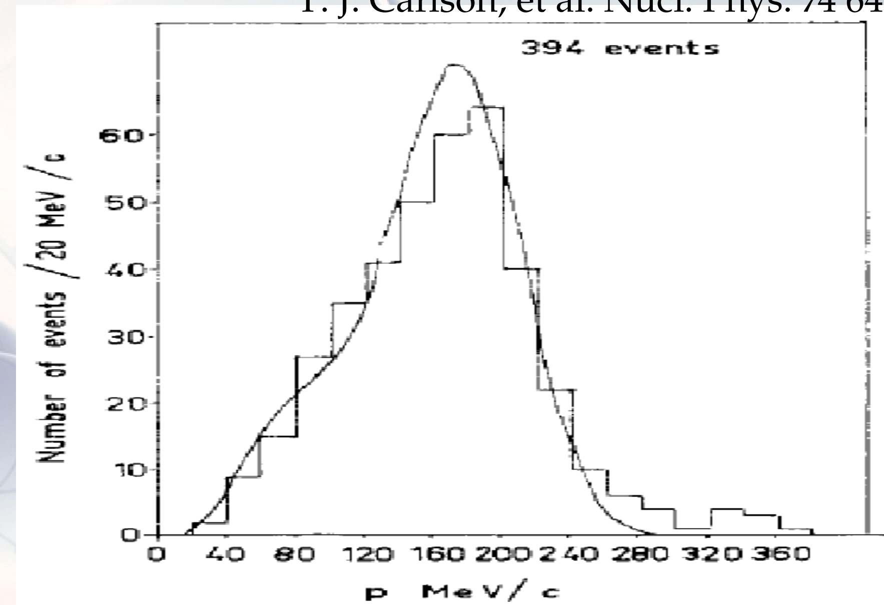

- 2005 AR + IF
- 2012 Carbon target AR only

N. U.

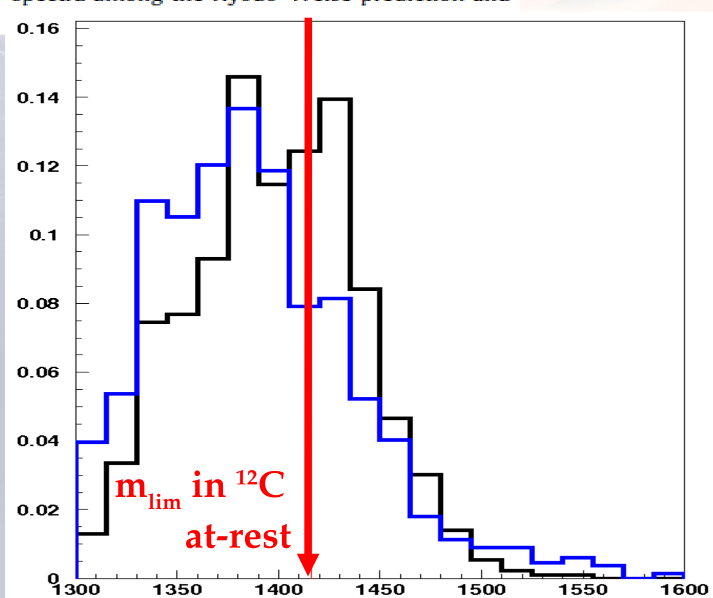

$m_{\Sigma 0\pi 0}$ (MeV/c²)

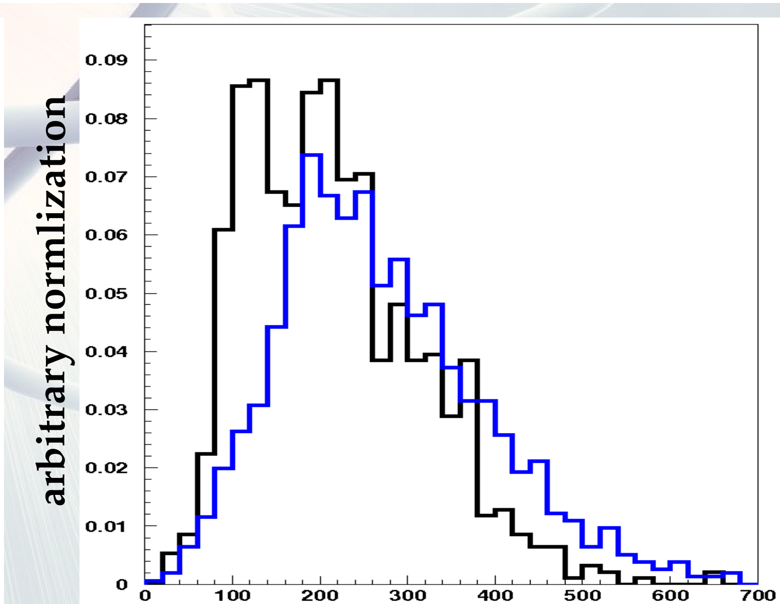

$p_{\Sigma 0\pi 0}$ (MeV/c²)

$\Sigma^0 \pi^0$ channel

K⁻

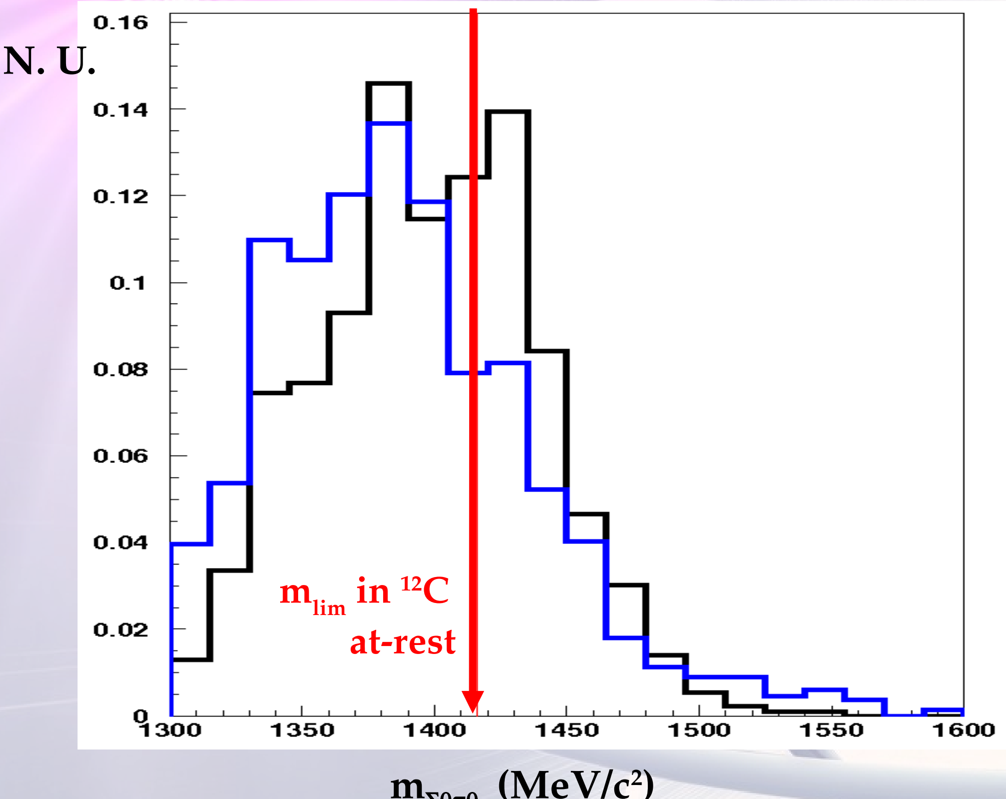

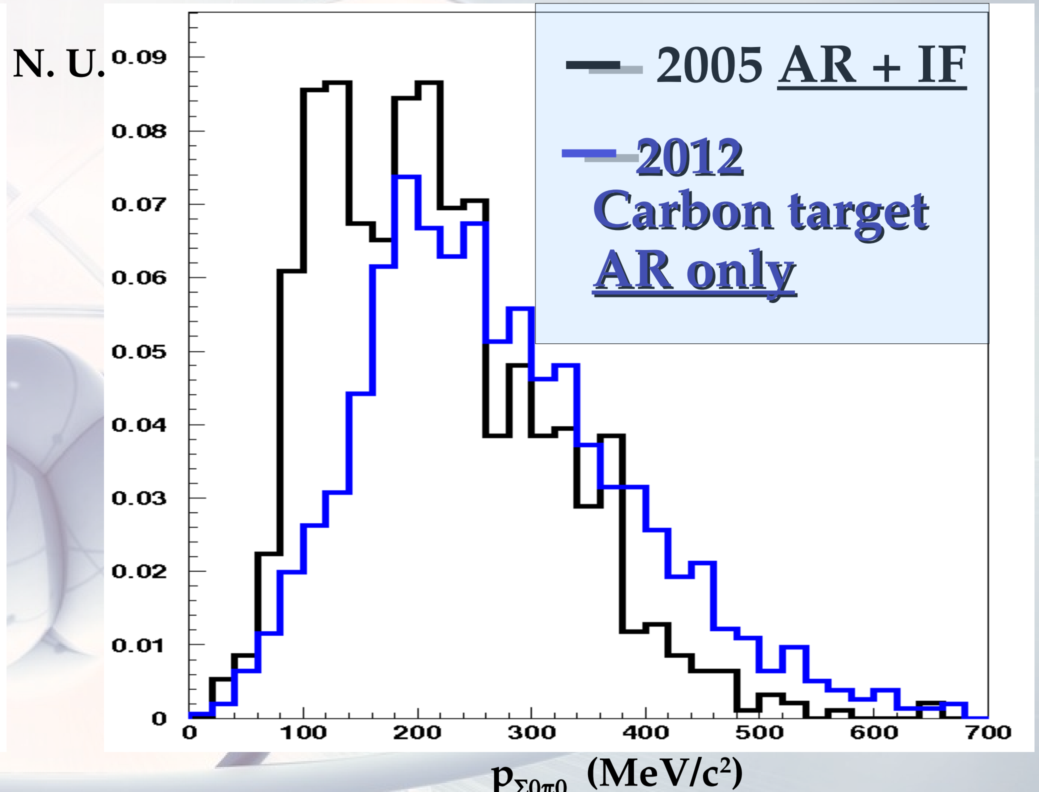

In-flight component …

FIRST EVIDENCE IN K⁻ ABSORPTION MASS SPECTROSCOPY

opens a higher invariant mass region

K^-

K^- "p" $\rightarrow$ $\Sigma^+\pi^-$

bound proton in ^{4}He / ^{12}C

$\Sigma^+\pi^-$ invariant mass spectra

K⁻

$K^- p \rightarrow \Sigma^+\pi^-$ detected via: $(p\pi^0)\,\pi^-$

Possibility to disentangle: Hydrogen, in-flight, at-rest, K^- capture

if resonant production contribution is important a high mass component appears!

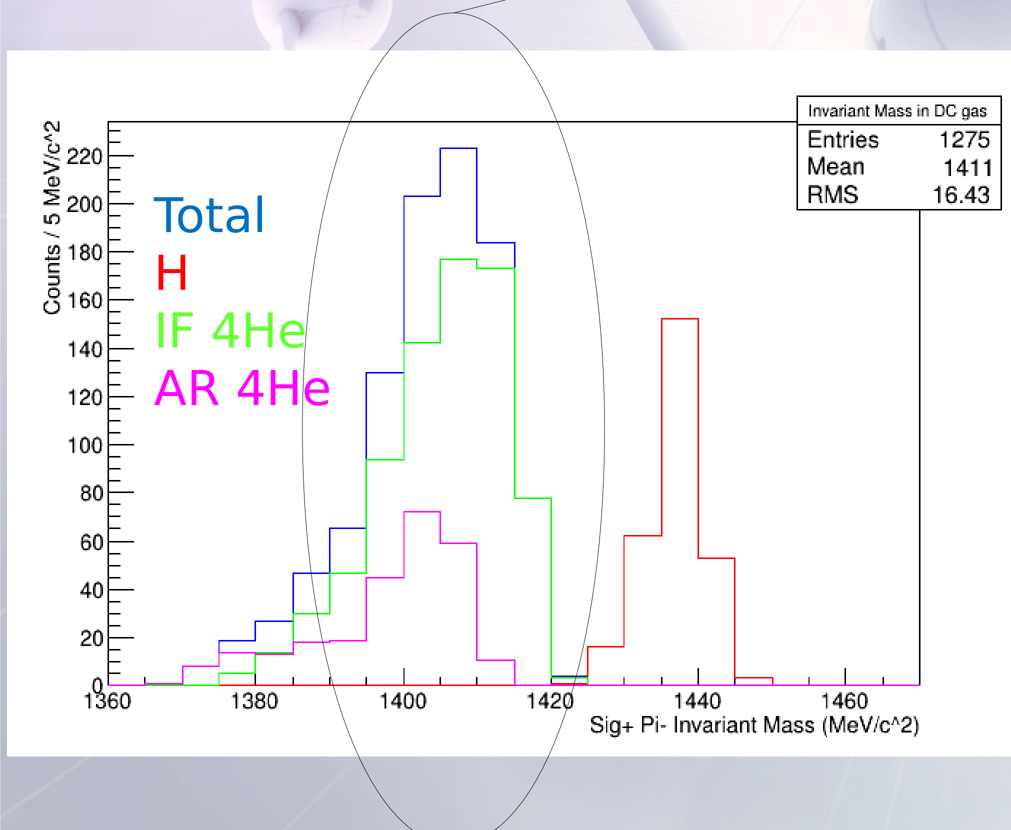

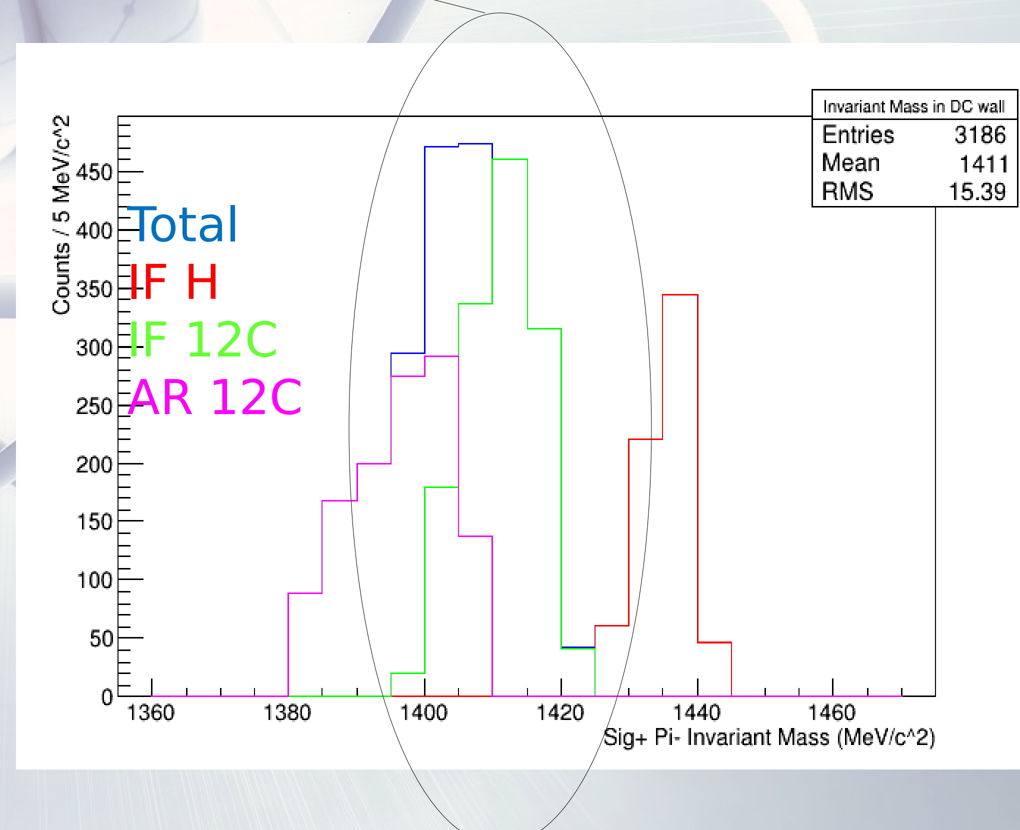

K^-

Resonant VS non-resonant

Another unsolved question ..

$$\mathbf{K^- N \rightarrow (Y^* ?) \rightarrow Y \pi}$$

how much comes from resonance ?

Investigated using:

$\mathbf{K^-}$ **"n"** $\mathbf{\rightarrow \Lambda\pi^-}$ direct formation in ^4He

In collaboration with Prof. S. Wycech

Channel: $K^- \; ^4He \rightarrow \Lambda \, \pi^- \; ^3He$ … the idea

Bubble chamber experiments exhibit two components:

- Low momentum $\Lambda \, \pi^-$ pair → S-wave, I=1, non-resonant transition amplitude.
    - High momentum $\Lambda \, \pi^-$ pair → P-wave resonant formation ?

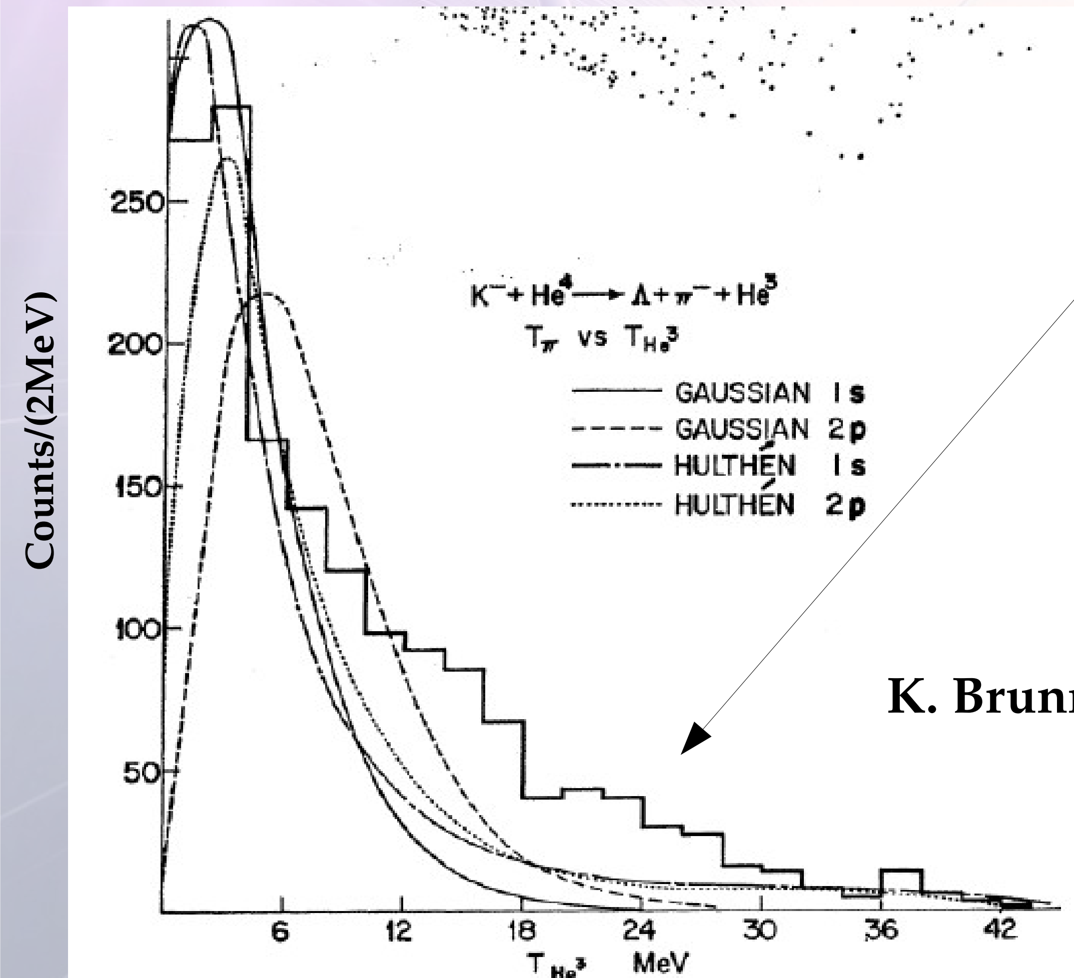

Also exsists in S-state K-mesic atom

as a result of the

three body structure of the system

(K = 1, n=2, ^{3}He = 3)

K. Brunnel et al., Phys.Rev. D2 (1970) 98

Channel: $K^- \ ^4He \rightarrow \Lambda \pi^- \ ^3He$ … <u>the idea</u>

$K^-(s=0)$ $^4He(s=0)$ $n(s=1/2)$ $\Sigma^{*-}(s=3/2) \rightarrow$ **resonance <u>p-wave</u> only**

<u>atomic s-state capture</u>:

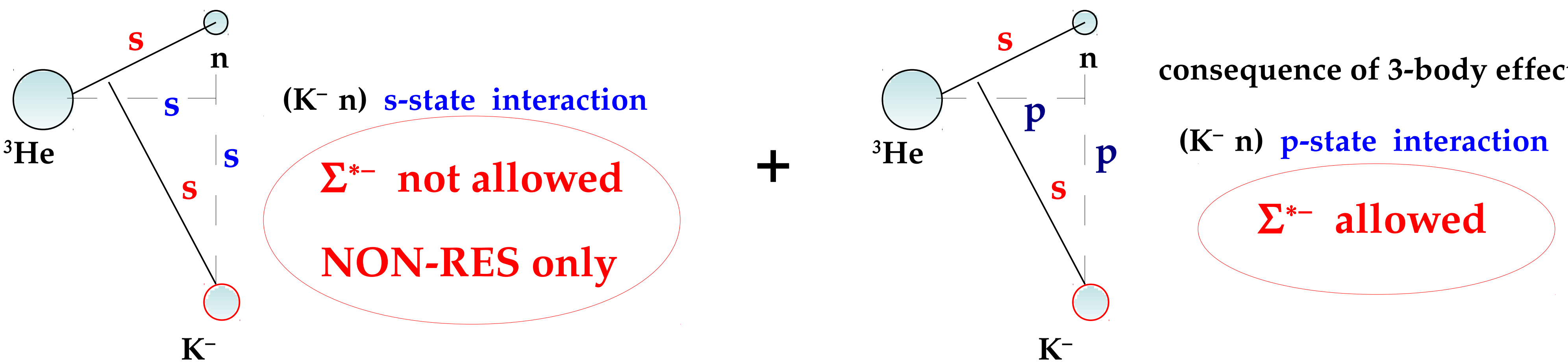

- $(K^- \ ^4He \rightarrow \Lambda \pi^- \ ^3He)$ absorptions from (n s) - atomic states are assumed $\rightarrow$

^4He bubble chamber data (Fetkovich, Riley interpreted by Uretsky, Wienke)

- Coordinates recupling enables for P-wave resonance formation

Channel: $K^- \; {}^4He \rightarrow \Lambda \, \pi^- \; {}^3He$ … the strategy

K^-

- **Fit of the $p_{\Lambda\pi^-}$ observed distribution using calculated distributions :**

$$P_s^{\,s}\,(p_{\Lambda\pi}) = |\Psi_N\,(p_{\Lambda\pi})|^2 \; |f^{\,s}\,(p_{\Lambda\pi})|^2 \; \rho$$ **non-resonant**

$$P_s^{\,p}\,(p_{\Lambda\pi}) = |\Psi_N\,(p_{\Lambda\pi})|^2 \; c^2 \; |2f^{\,\Sigma^*}\,(p_{\Lambda\pi})|^2 \; \rho/3 \; (kp_{\Lambda\pi})^2$$ **resonant**

- **To determine *for the first time* the ratio resonant/non-res.**

↓

$|f^{\,N\text{-}R}_{\;\Lambda\pi}|$ **given the fairly well known** $|f^{\,\Sigma^*}_{\;\Lambda\pi}|$

Channel: $K^- \, {}^4He \rightarrow \Lambda \, \pi^- \, {}^3He$ … calculated reactions

Calculated primary hadronic interactions:

$K^- \, {}^4He \rightarrow \Lambda \, \pi^- \, {}^3He$

- **At-rest :** S-wave non-Res / P-wave $\Sigma(1385)$ Res
- **In-flight :** S-wave non-Res / P-wave $\Sigma(1385)$ Res

$K^- \, {}^4He \rightarrow \Sigma^0 \, \pi^- \, {}^3He$

- **At-rest :** S-wave non-Res / P-wave $\Sigma(1385)$ Res
- **In-flight :** S-wave non-Res / P-wave $\Sigma(1385)$ Res

$K^- \, {}^4He \rightarrow (\Sigma \, \pi)^0 \, {}^3H$

- **At-rest :** S-wave non-Res / S-wave $\Lambda(1405)$ Res / P-wave $\Sigma(1385)$ Res
- **In-flight :** S-wave non-Res / S-wave $\Lambda(1405)$ Res / P-wave $\Sigma(1385)$ Res

$K^- \; ^4He \rightarrow \; \Lambda \pi^- \; ^3He$ preliminary fit

Simultaneous fit ($p_{\Lambda\pi^-}$ - $m_{\Lambda\pi^-}$ - $\theta_{\Lambda\pi^-}$) leaving the ratio At-rest /In-flight and ^{12}C contamination to vary around the estimated values within errors:

Global fit

$\Lambda \pi^-$ At-rest N-R

$\Lambda \pi^-$ At-rest RES

$\Lambda \pi^-$ In-flight N-R

$\Lambda \pi^-$ In-flight RES

$\Lambda \pi^-$ events from $K^- \; ^{12}C$

Σ p/n $\rightarrow$ Λ p/n conversion

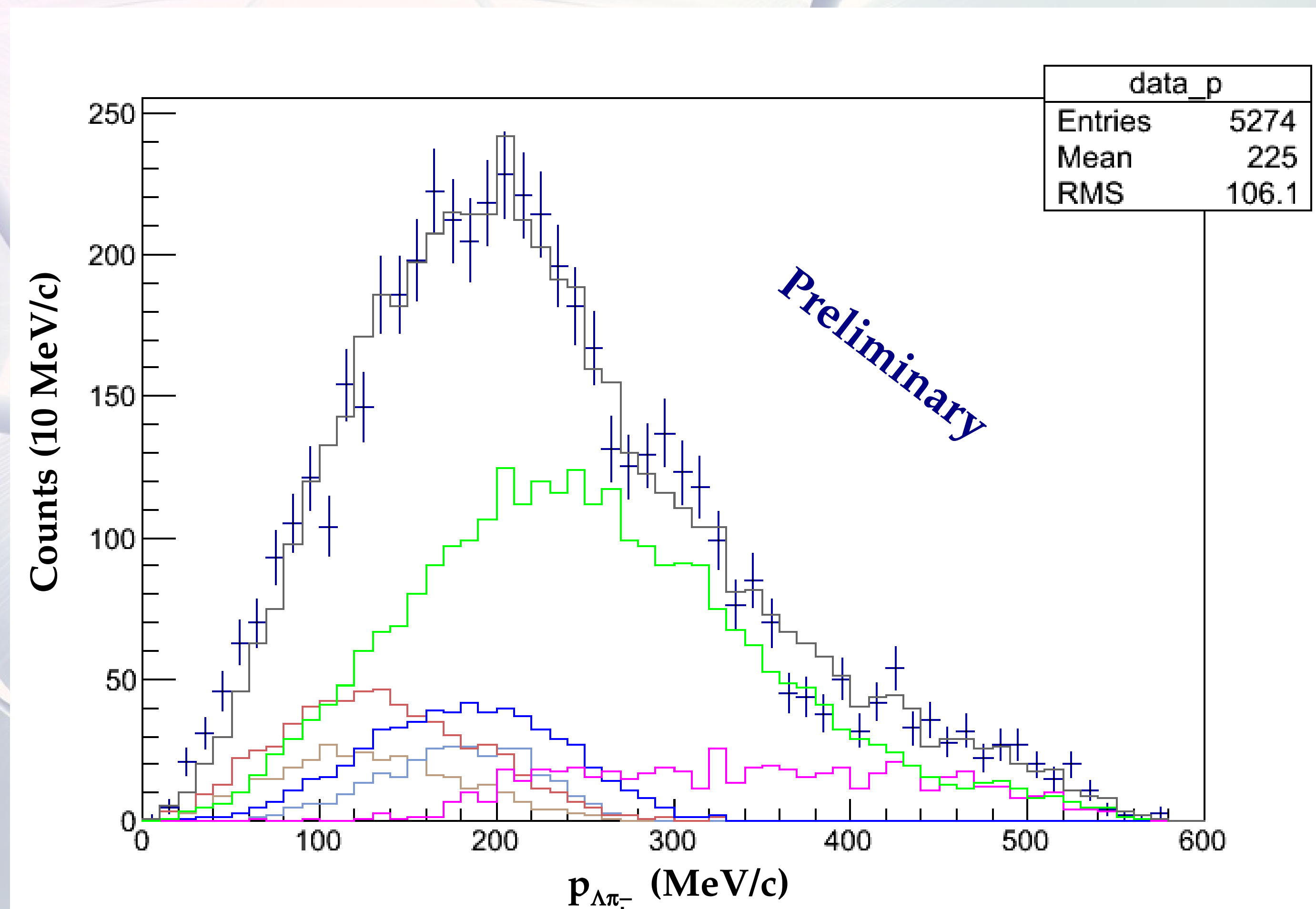

$K^- \ {}^4He \rightarrow \Lambda \pi^- \ {}^3He$ preliminary fit

Simultaneous fit ($p_{\Lambda\pi-}$ - $m_{\Lambda\pi-}$ - $\theta_{\Lambda\pi-}$) leaving the ratio At-rest /In-flight and ^{12}C contamination to vary around the estimated values within errors:

- χ^2/ (ndf – np) = 1.4
- **(At-rest RES)/(At-rest N-R) = 0.9 ± (0.2stat)± (0.4sys)**
- **(In-flight RES)/(In-flight N-R) = 0.9 ± (0.2stat)± (0.4sys)**

Preliminary

- (In-flight) / (At-rest) = 1.9 ± 0.4
- Σ p/n → Λ p/n conversion = (10 ± 1)%
- $\Lambda \pi^-$ events from $K^- \ {}^{12}C$ = (53 ± 2)%

Conclusions PART 2

- $m_{\Sigma\pi}$ spectra show a **high invariant mass component** → associated to in-flight K^- capture
- PRELIMINARY $\Lambda\pi^-$ **first measurement of RES/N-R ratio in nuclear K^- absorption**.

Next steps …

- **Same analysis is ongoing for $\Sigma^0\pi^-$** → extraction of $|f^{N-R}_{\Sigma 0\pi-}(I=1)|$
- Similar description of $\Sigma^+\pi^-$ and $\Sigma^-\pi^+$ production → extraction of $|f^{N-R}_{\Sigma+\pi-}|$ and $|f^{N-R}_{\Sigma-\pi+}|$, a comparison of these could give an estimate of

$|f^{N-R}_{\Sigma+\pi-}(I=0) + f^{N-R}_{\Sigma+\pi-}(I=1)|$ against $|f^{N-R}_{\Sigma+\pi-}(I=0) - f^{N-R}_{\Sigma+\pi-}(I=1)|$

- Branching ratio modifications in different targets (see A. Ohnishi et al., Phys. Rev. C 56 5 (1997) 2767) & **Density dependence of $m_{\Sigma\pi}$ and $p_{\Sigma\pi}$** (see L. R. Staronski, S. Wycech, Nucl. Phys. 13 (1987) 1361 / A. Cieplý, E. Friedman, A. Gal, V. Krejčiřík - Phys.Lett.B698 (2011) 226-230)

Perspectives ..

AMADEUS experiment:

Implementation of dedicated solid targets & cryogenic gaseous targets (H, d, ^{3}He, ^{4}He) inside the KLOE DC.

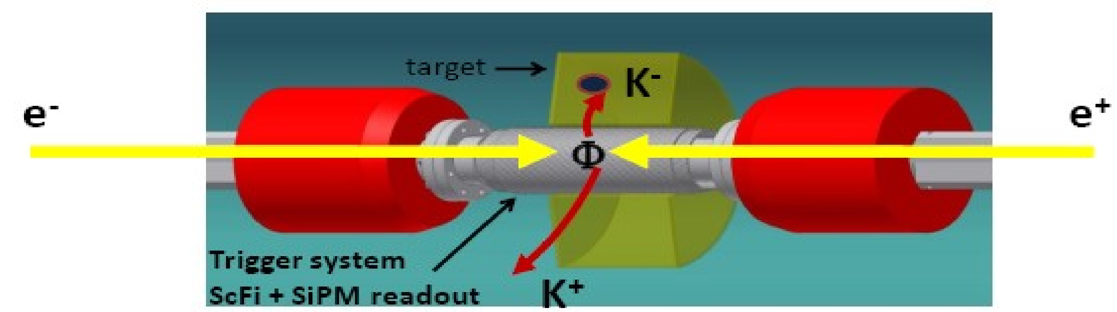

•The AMADEUS setup will be implemented in the 50 cm. gap in KLOE DC around the beam pipe:

•**Target** (A gaseous He target for a first phase of study)

•**Trigger** (1 or 2 layers of ScFi surrounding the interaction point)

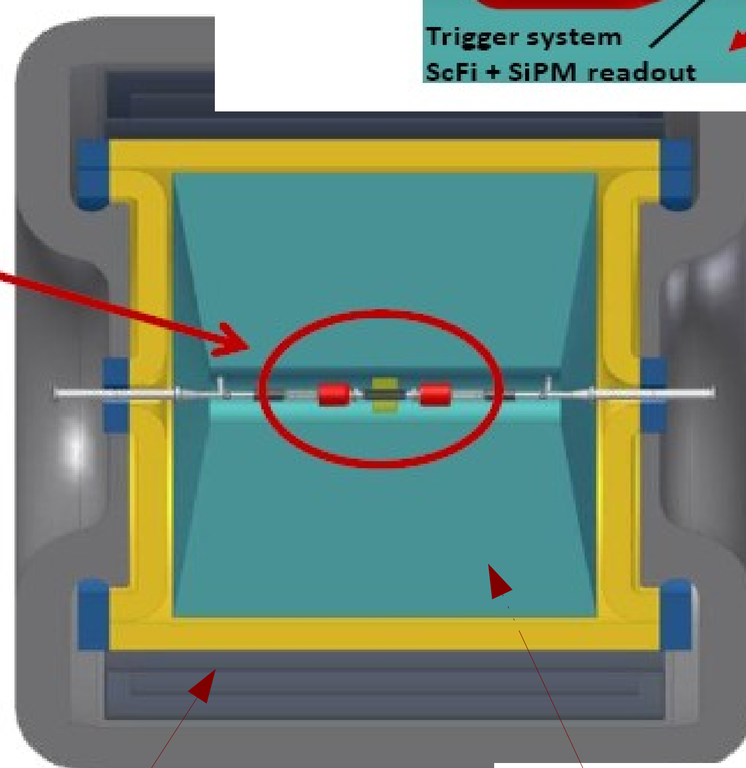

R&D activity is ongoing

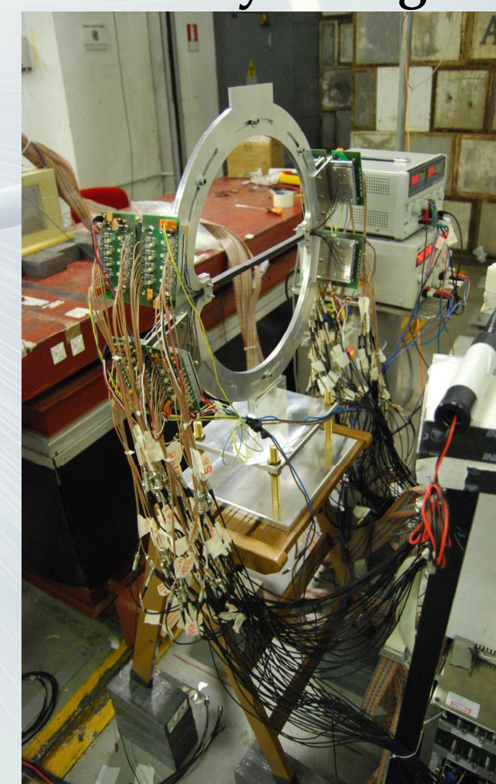

K⁻
Thanks

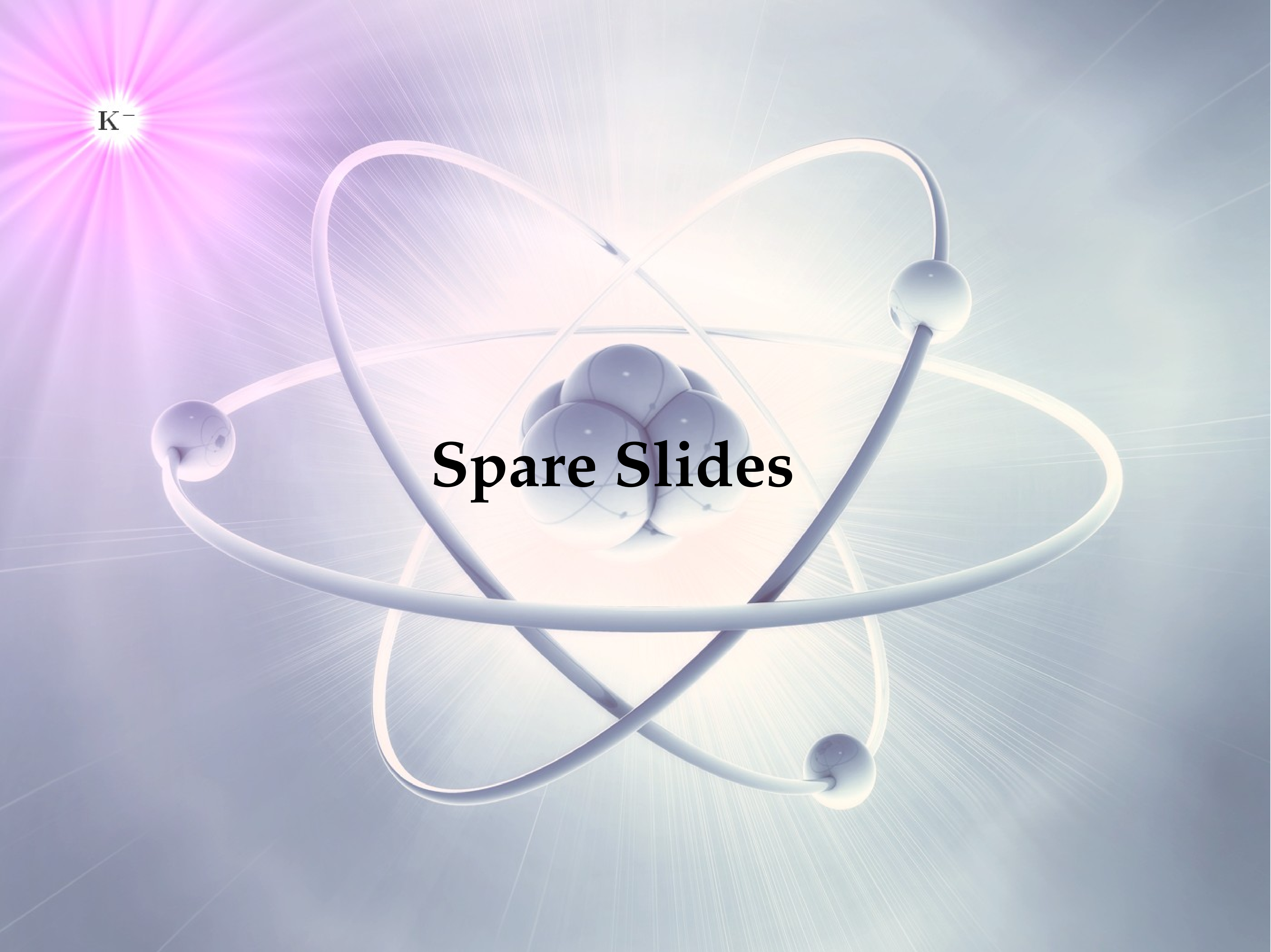

Spare Slides

Experimental program of AMADEUS

K^-

Unprecedented studies of the low-energy charged kaons interactions in nuclear matter: solid and gaseous targets (d, ^{3}He, ^{4}He, ^{8}Be, ^{12}C …) in order to obtain unique quality information about:

1) **Possible existence of kaonic nuclear clusters (deeply bound kaonic nuclear states)**

Single & multi – nucleon K^- absorption

2) **Nature of the controversial $\Lambda(1405)$**

- **Low-energy charged kaon cross sections for momenta lower than 100 MeV/c (still not measured)**

- **Many other processes of interest in the low-energy strangeness QCD sector → implications from particle and nuclear physics to astrophysics (dense baryonic matter in neutron stars)**

Carbon target inside KLOE

K^-

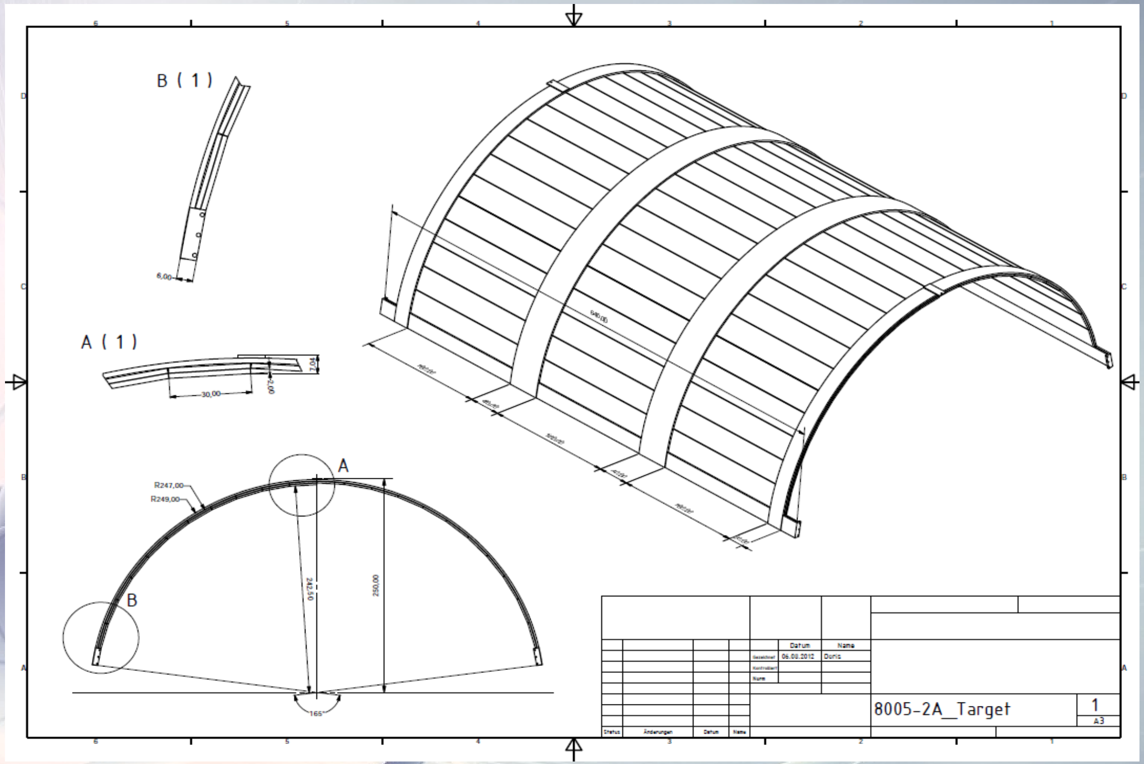

Advantages:

- gain in statistics
- K^- absorptions occur in Carbon
- absorptions at-rest.

- **MC simulation: 26% of K^- stopped in C, 2% of K^- stopped in Al hence aluminium contamination from 19% → 7% !**

- **Thickness optimazied (based on MC simulations) to maximize the number of stopping K^- in the targed, minimizing the charged particles energy loss.**

(~90 pb^{-1}; analyzed 37 pb^{-1}, x1.5 statistics)

p / d / t masses obtained by time of flight

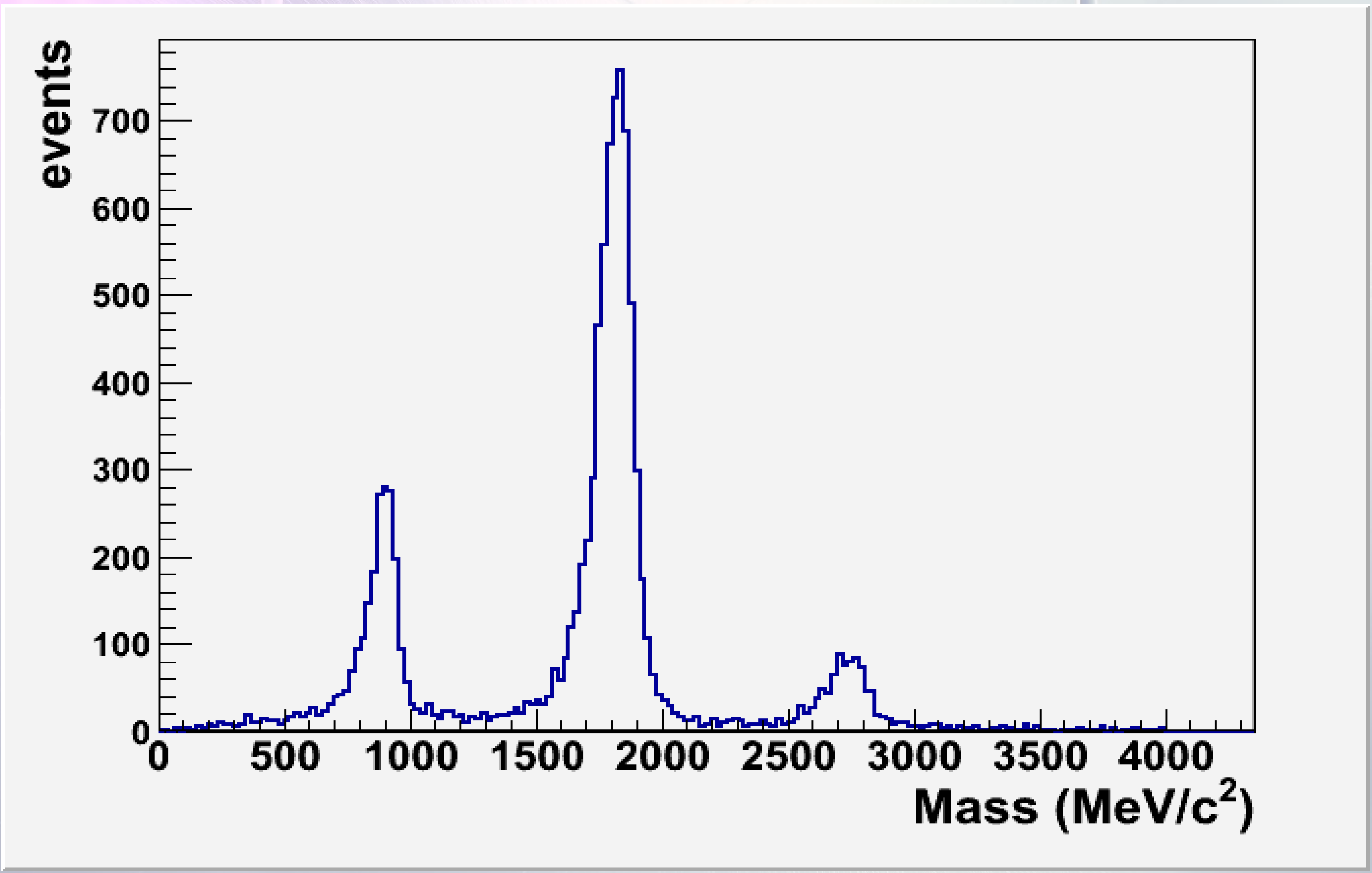

K⁻

$K^- \text{"}p\text{"} \rightarrow \Sigma^0\pi^0$

bound proton in ^4He / ^{12}C

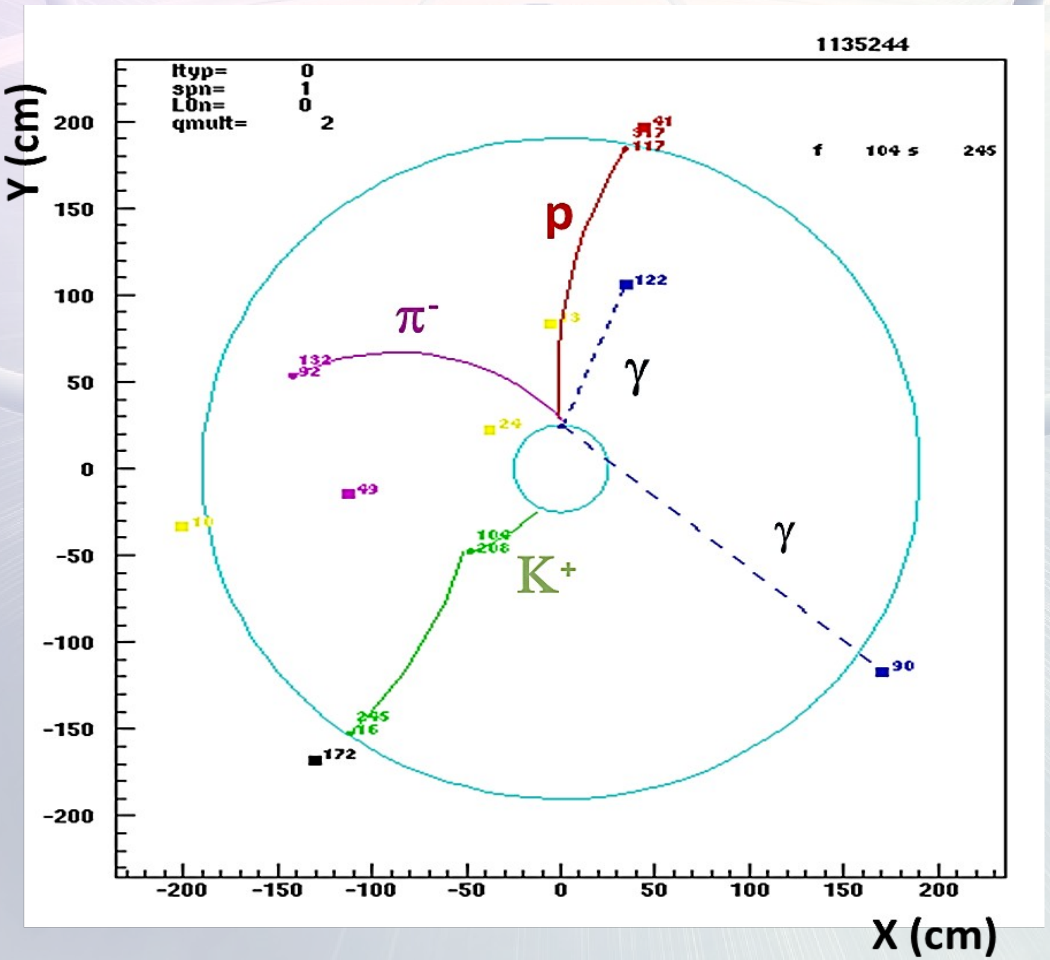

Scientific case of the $\Lambda(1405)$

K^-

The three quark model picture has some difficulties to reproduce the $\Lambda(1405)$. According to its negative parity, one of the quarks has to be excited to the $l = 1$ orbit. Similar to the nucleon sector, where one of the lowest negative parity baryon is the N(1535), the expected mass of the Λ^* is around 1700 MeV (since it contains one strange quark). Another difficulty is the energy splitting observed between the $\Lambda(1405)$ and the $\Lambda(1520)$, if is interpreted as the spin-orbit partner ($J^p = 3/2^-$).

R. Dalitz and collaborators first suggested to interpret $\Lambda(1405)$ as an KN quasibound state.

R.H. Dalitz, T.C. Wong and G. Rajasekaran, Phys. Rev. **153** (1967) 1617.

Scientific case Λ(1405)

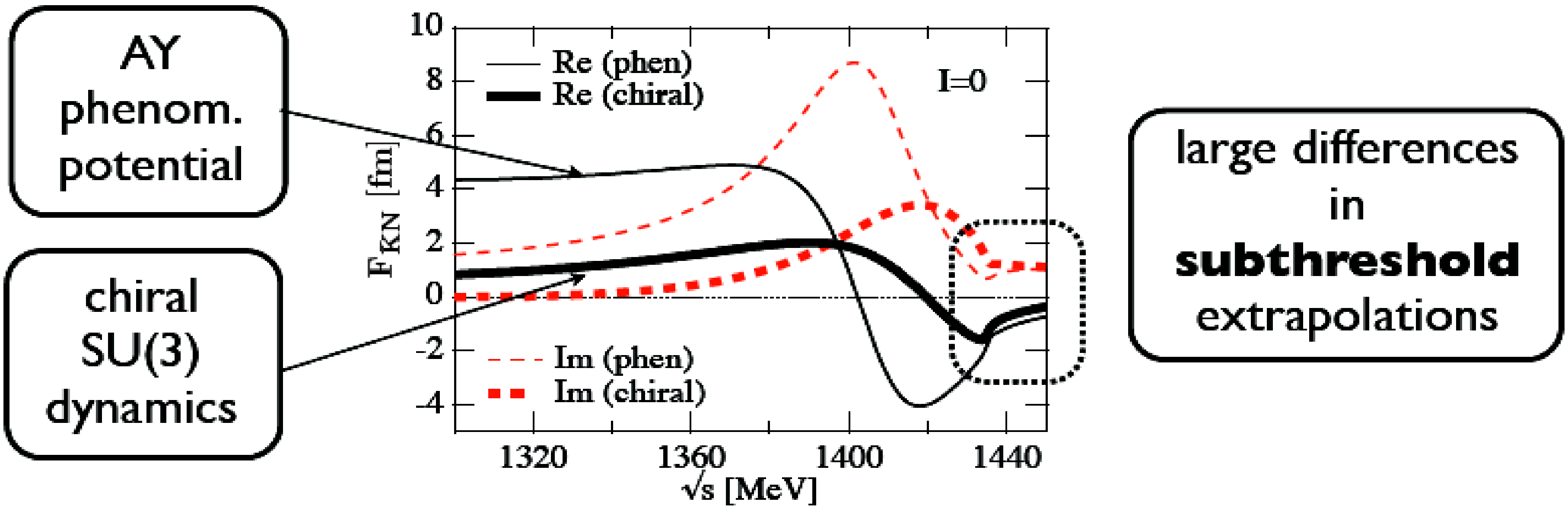

- **Chiral dynamics** predicts significantly **weaker attraction** than AY (local, energy independent) potential in **far-subthreshold** region

TO TEST THE HIGHER POLE:

- production in $\bar{K}N$ reactions (only chance to observe the high mass pole)
- decaying in $\Sigma^0\pi^0$ (free from $\Sigma(1385)$ background I=1)

Distribution shape depends on the decay channel:

$$\frac{d\sigma(\Sigma^-\pi^+)}{dM} \propto \frac{1}{3}\left|T^0\right|^2 + \frac{1}{2}\left|T^1\right|^2 + \frac{2}{\sqrt{6}}Re(T^0T^{1*})$$

$$\frac{d\sigma(\Sigma^+\pi^-)}{dM} \propto \frac{1}{3}\left|T^0\right|^2 + \frac{1}{2}\left|T^1\right|^2 - \frac{2}{\sqrt{6}}Re(T^0T^{1*})$$

$$\frac{d\sigma(\Sigma^0\pi^0)}{dM} \propto \frac{1}{3}\left|T^0\right|^2$$

Scientific case of the $\Lambda(1405)$

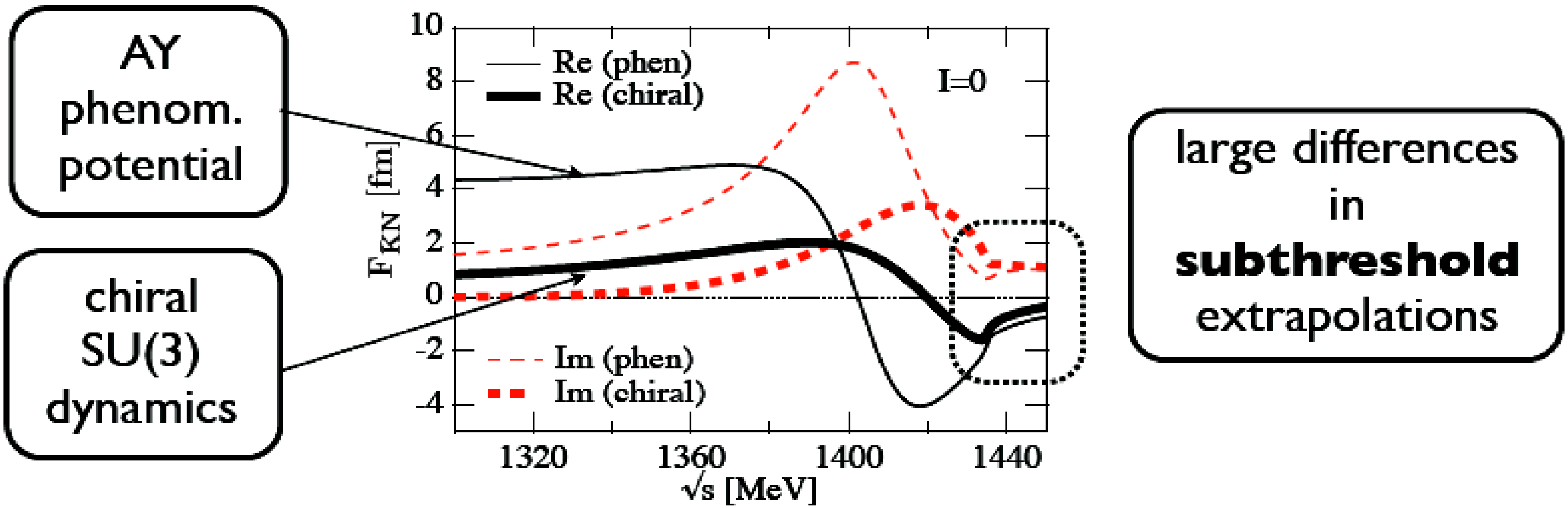

- **Chiral dynamics** predicts significantly **weaker attraction** than AY (local, energy independent) potential in **far-subthreshold** region

TO TEST THE HIGHER POLE:

- production in $\bar{K}N$ reactions (only chance to observe the high mass pole)
- decaying in $\Sigma^0\pi^0$ (free from $\Sigma(1385)$ background I=1)

Scientific case $\Lambda(1405)$

K^- nuclear absorption experiments .. long history .. BUT

K^-

1) $m_{\pi\Sigma}$ spectra CUT AT THE ENERGY LIMIT AT-REST **2) $(\Sigma\pm\pi\mp)$ $\Sigma(1385)$ CONTAMINATION**

P. J. Carlson, et al. Nucl. Phys. 74 642

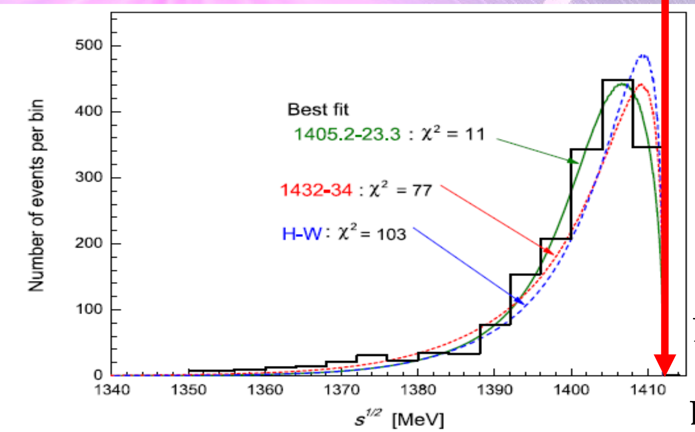

Fig. 6. Detailed differences in $M_{\Sigma\pi}$ spectra among the Hyodo–Weise prediction and the present model predictions.

"A study of K^- $^4He \rightarrow (\Sigma\pm\pi\mp) + {}^3H$ using slow instead of stopping K^- would be very useful in eliminating some of the uncertainties in interpretation"

D. Riley, et al. Phys. Rev. D11 (1975) 3065

Esmaili et el., Phys.Lett. B686 (2010) 23-28

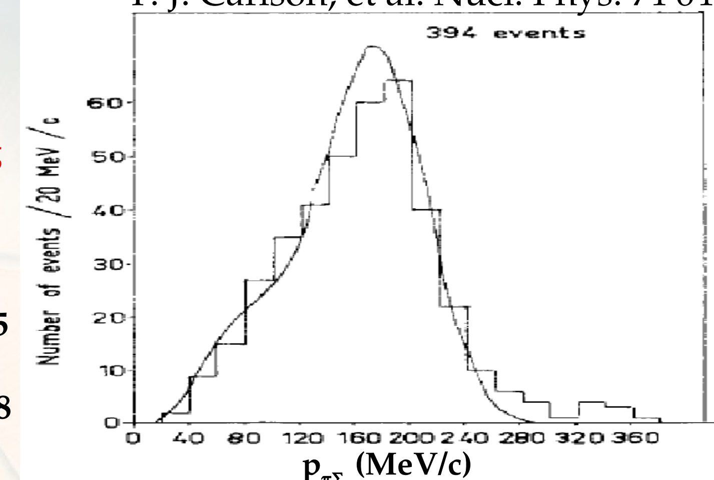

The $\Sigma^0\pi^0$ spectrum was only observed in 3 experiments … with different line-shapes !

I. Zychor et al., Phys. Lett. B 660 (2008) 167

K. Moriya, et al., (Clas Collaboration) Phys. Rev. C 87, 035206 (2013)

Magas et al. PRL 95, 052301 (2005) 034605 S. Prakhov, et al., Phys. Rev. C70 (2004)

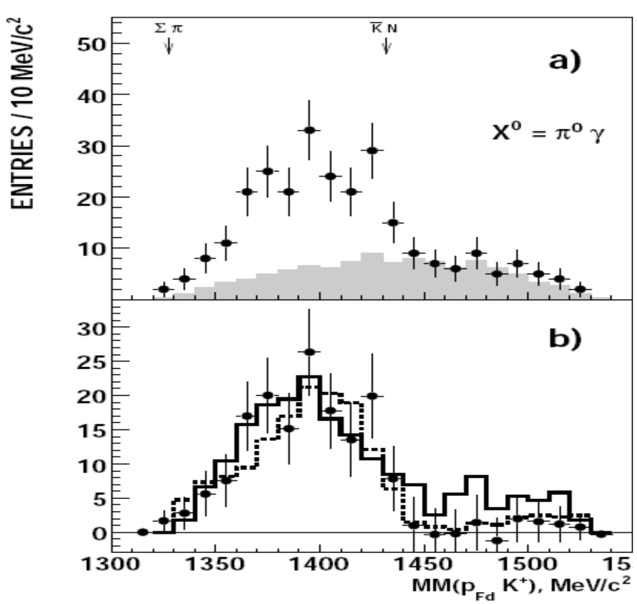

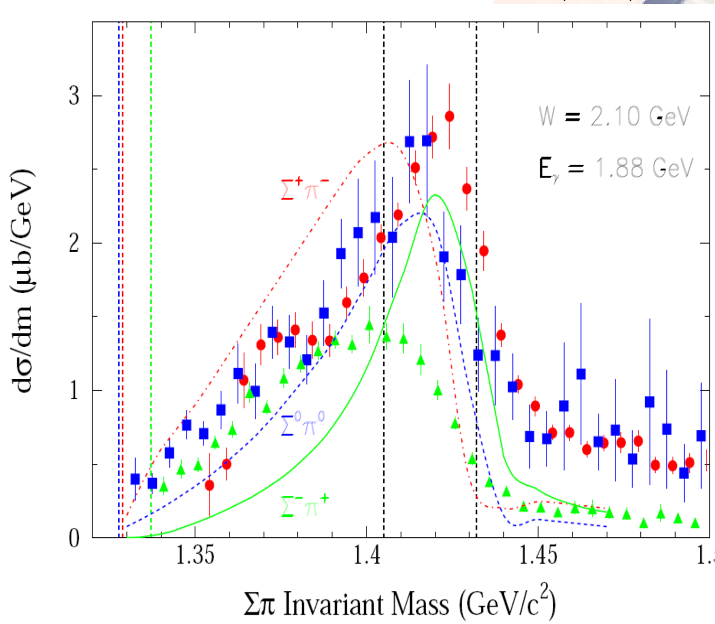

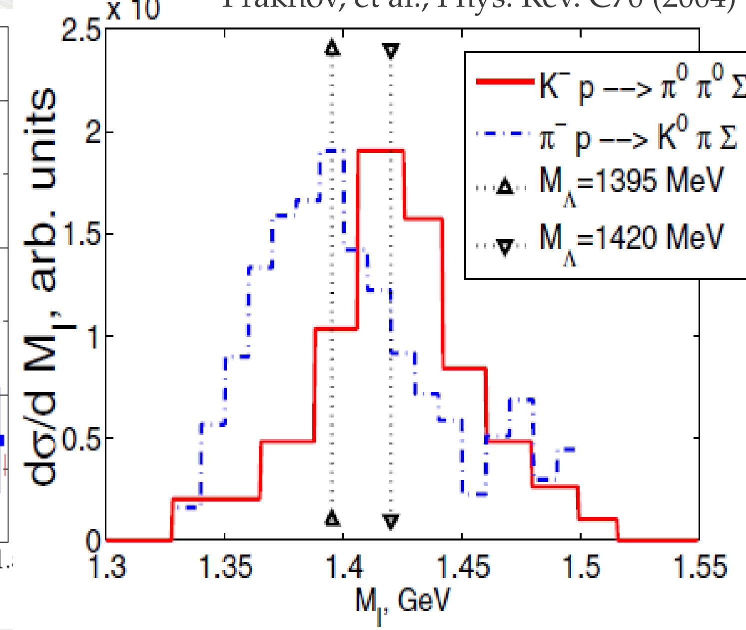

$\Sigma^0 \pi^0$ channel

In-flight component … FIRST EVIDENCE IN K^- ABSORPTION MASS SPECTROSCOPY

opens a higher invariant mass region

$p_{\pi 0}$ resolution: $\sigma_p \approx 12$ MeV/c

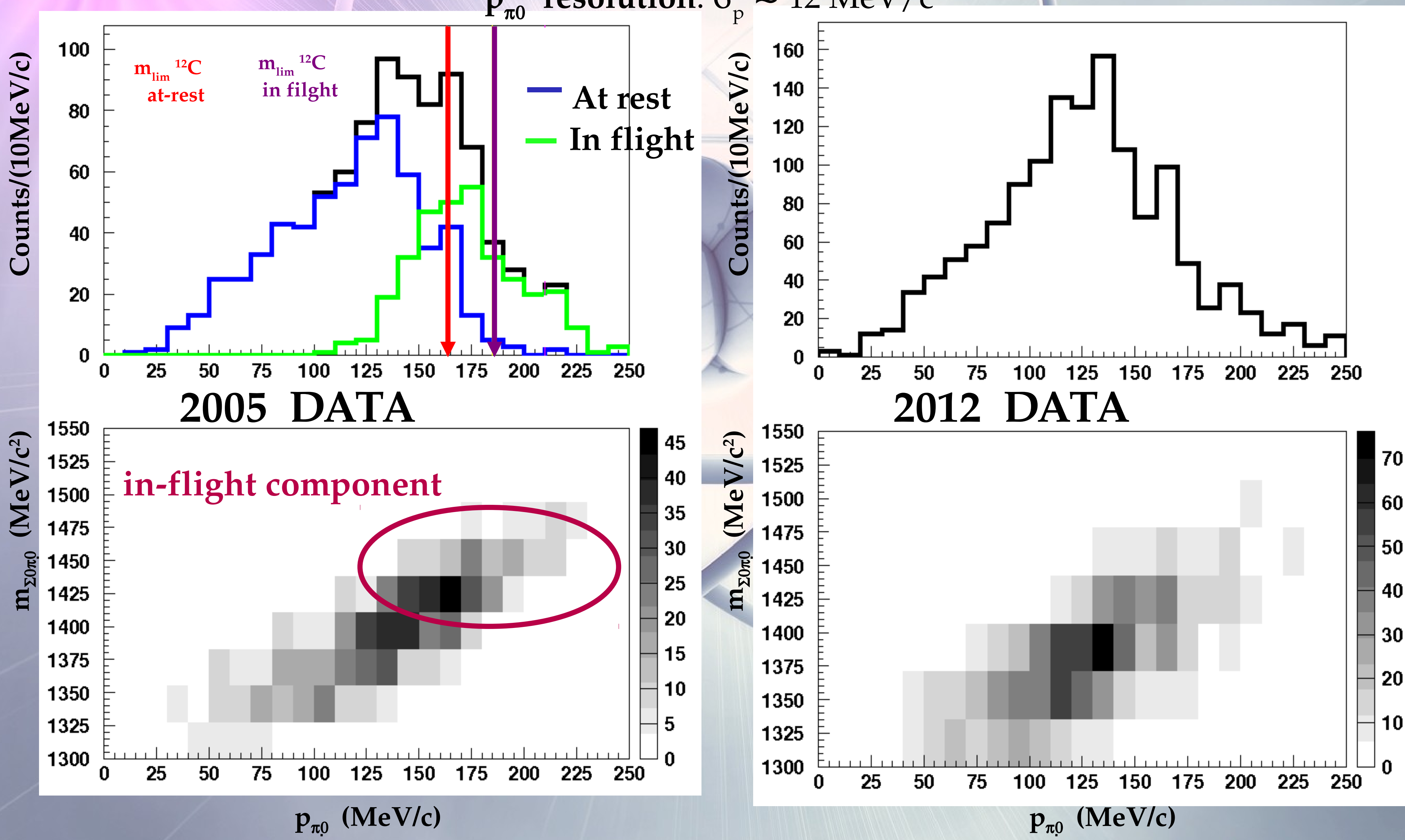

$\Sigma^0 \pi^0$ channel

Acceptance corrected $m_{\pi 0 \Sigma 0}$ spectra, DC wall (left) DC gas (right)

K^-

Acceptance function evaluated in 8 intervals of $p_{\pi 0 \Sigma 0}$ (between 0 and 700 MeV/c) 8 intervals of $\theta_{\pi 0 \Sigma 0}$ (between 0 and 3.15 rad) 30 intervals of $m_{\pi 0 \Sigma 0}$ (between 1300 and 1600 MeV/c^2)

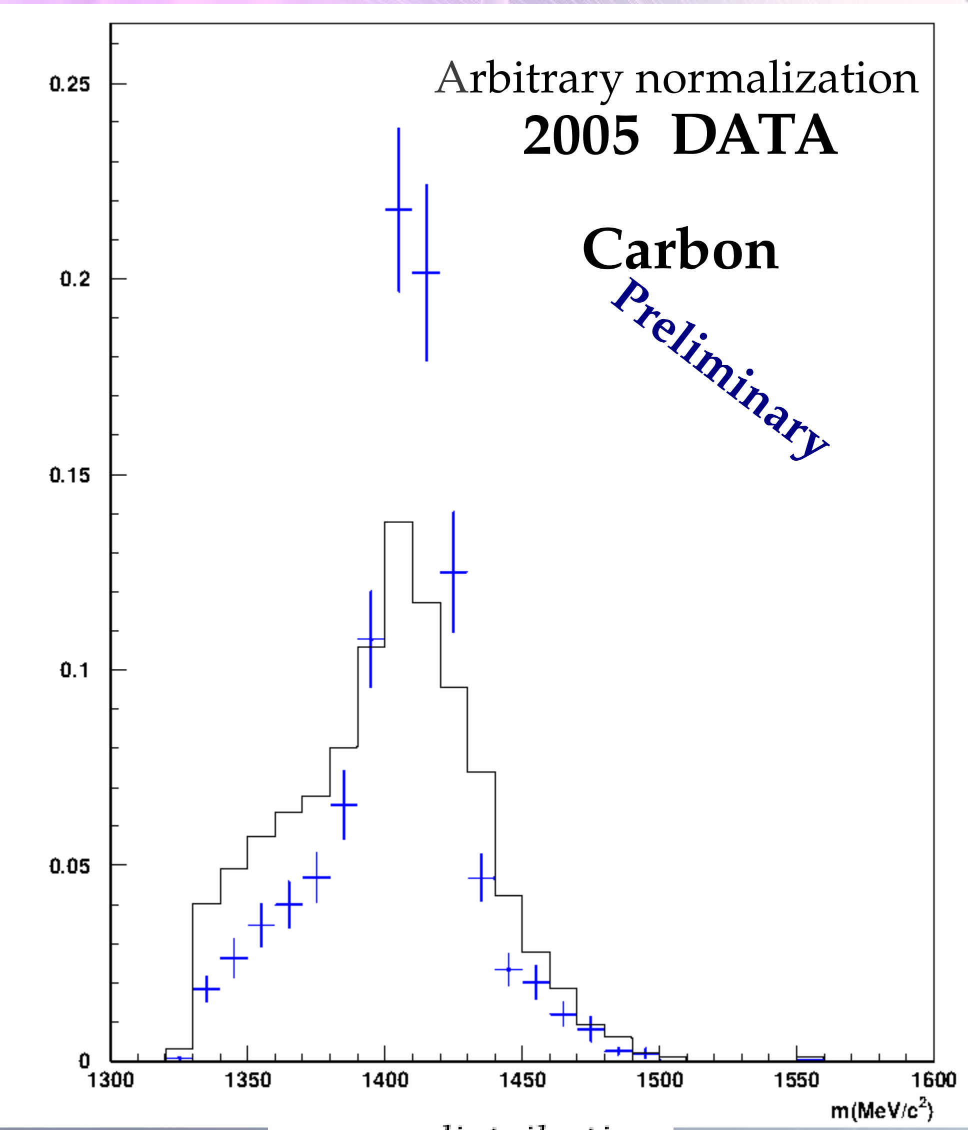

$m_{\Sigma^0 \pi^0}$ *distribution*

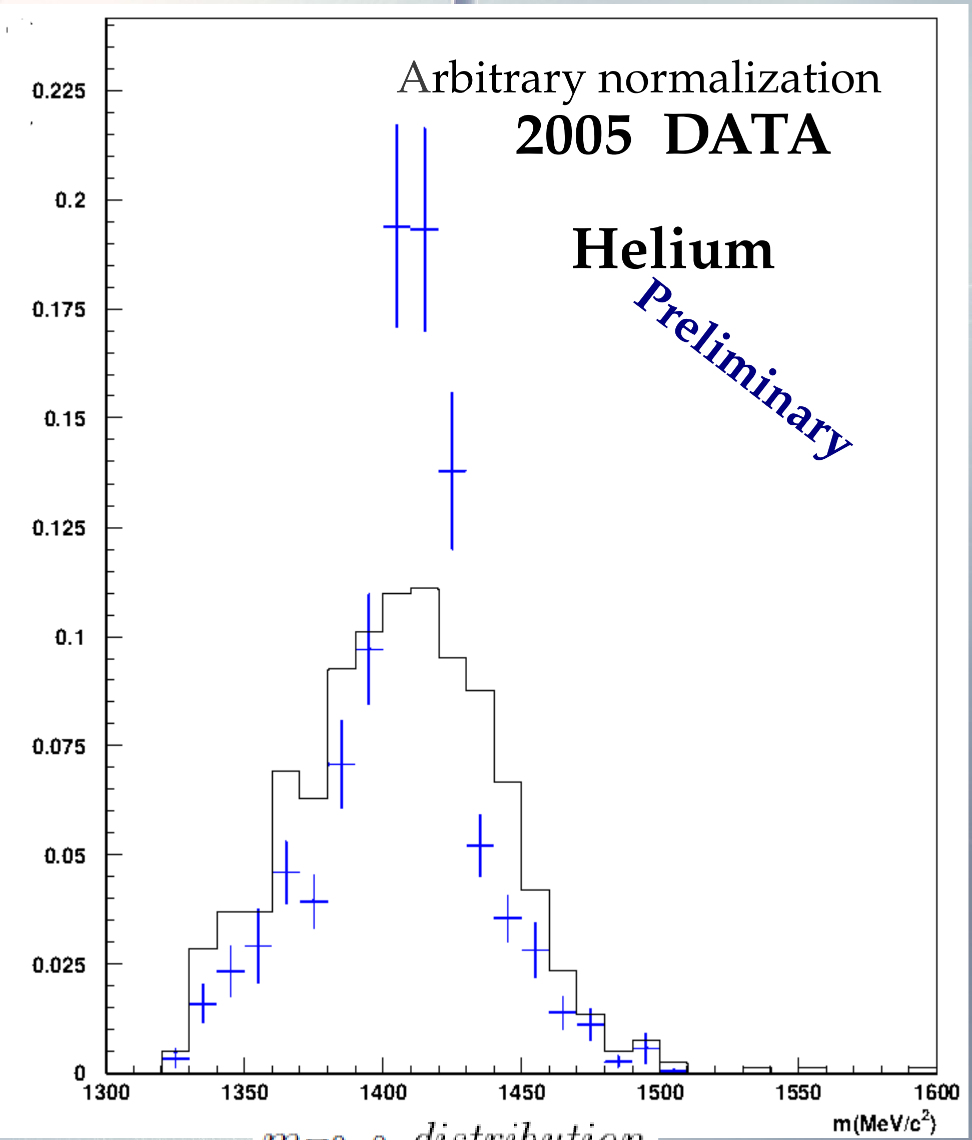

$m_{\Sigma^0 \pi^0}$ *distribution*

HYDROGEN contamination → from $\Sigma^+ \pi^-$

$K^- p \rightarrow \Sigma^+ \pi^-$ detected via: $(p\pi^0)\, \pi^-$

K⁻

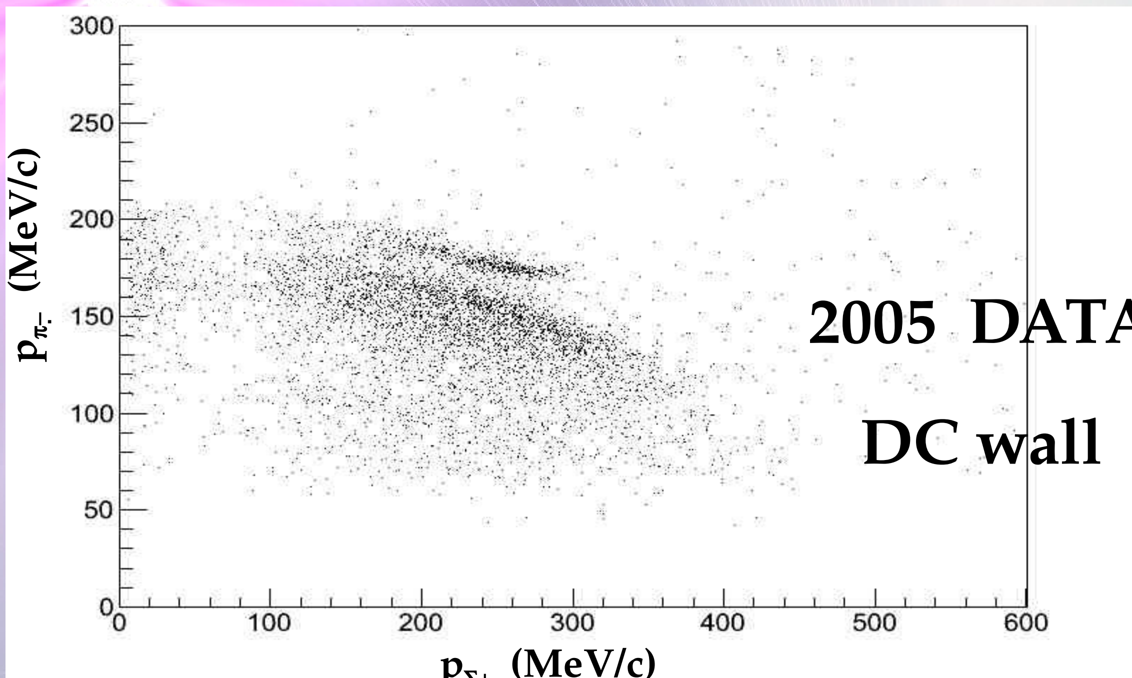

2005 DATA

DC wall

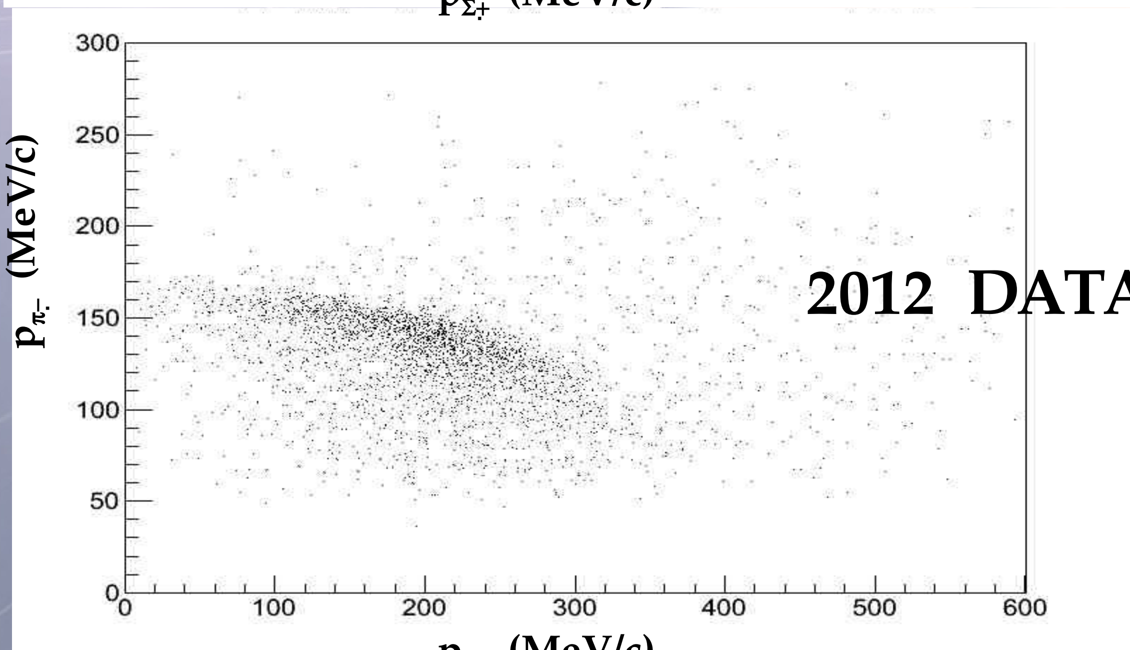

2012 DATA

$K^- H \rightarrow \Sigma\pi$ is peaked at around

1430 MeV !!!

K⁻H interaction probability estimate based on K⁻ interaction AT-REST in hydrocarbons mixture data (Lett. Nuovo Cimento, C 1099 (1972))

order of 1% !!!

NOW

Thanks to the excellent $p_{\pi-}$ resolution

< 1 MeV

...

HYDROGEN contamination → from $\Sigma^+ \pi^-$

$K^- p \rightarrow \Sigma^+ \pi^-$ detected via: $(p\pi^0)\,\pi^-$

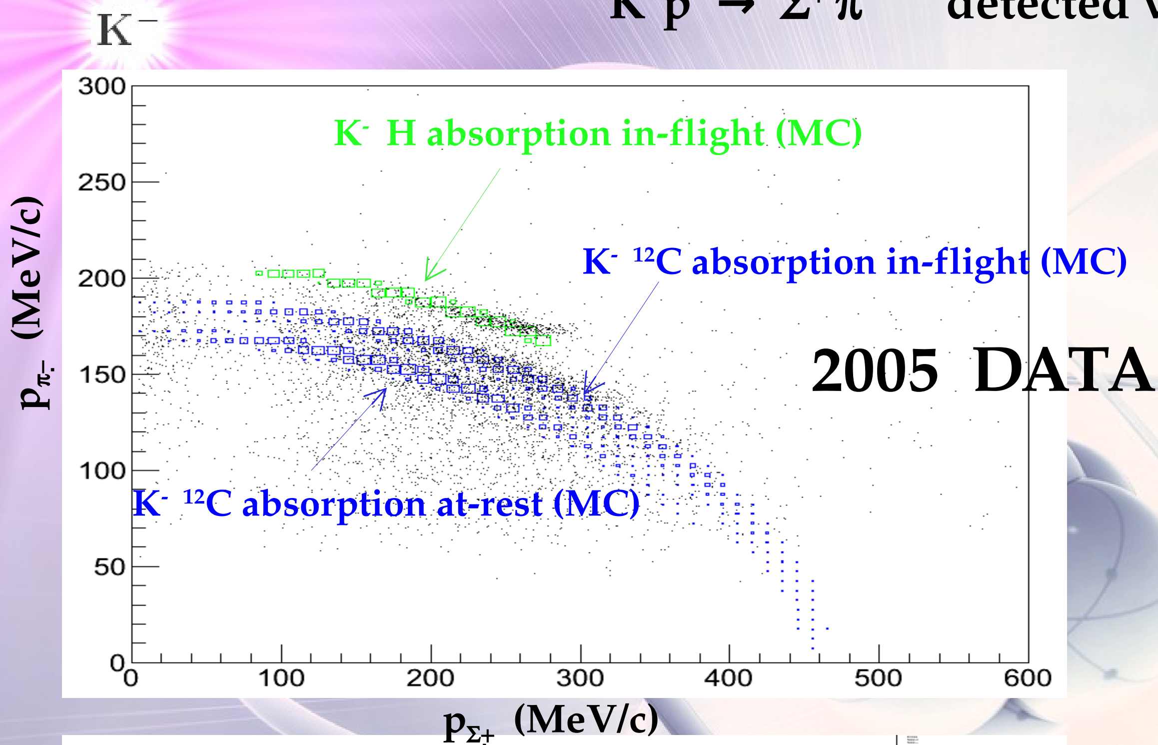

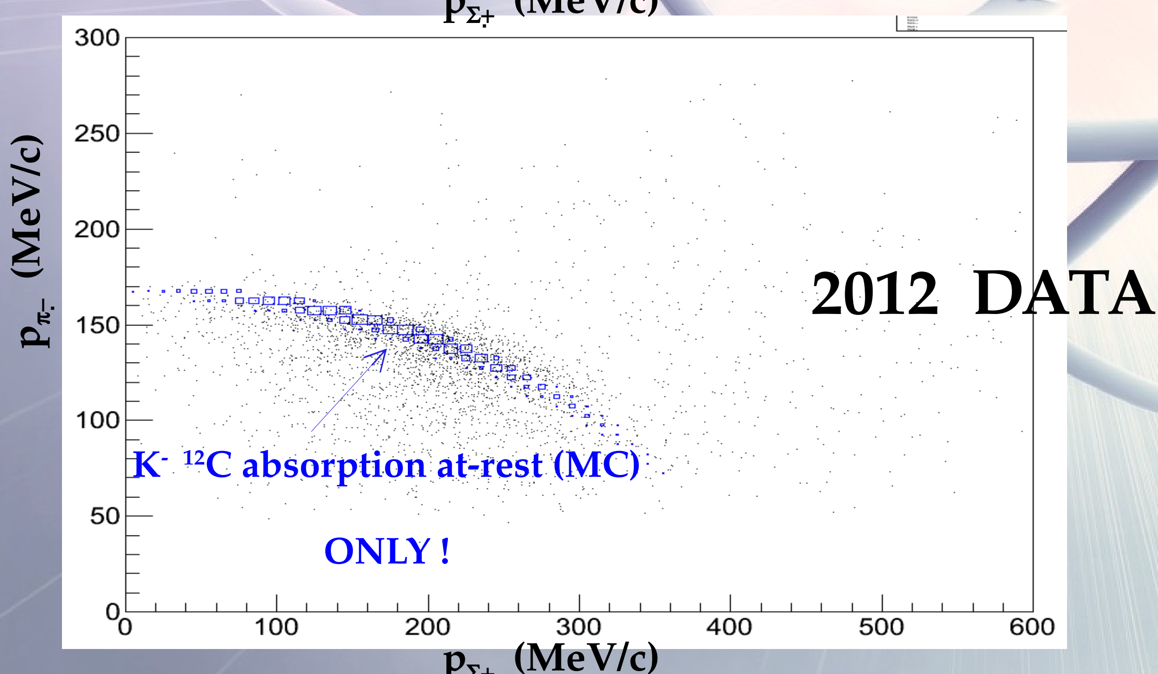

AND

K^- H contribution ~ 20%

… in-flight absorption is extremely different

Σ^0 π^0 channel

Invariant mass spectra with mass hypotesis on Σ^0 and π^0 *non resonant misidentification background subtracted (right)*

$\sigma_m \approx$ *17 MeV/c²* (^{12}C) $\sigma_m \approx$ *15 MeV/c²* (^{4}He)

Similar $m_{\pi0\Sigma0}$ shapes due to the similar kinematical thresholds for ^{4}He and ^{12}C.

2005 DATA

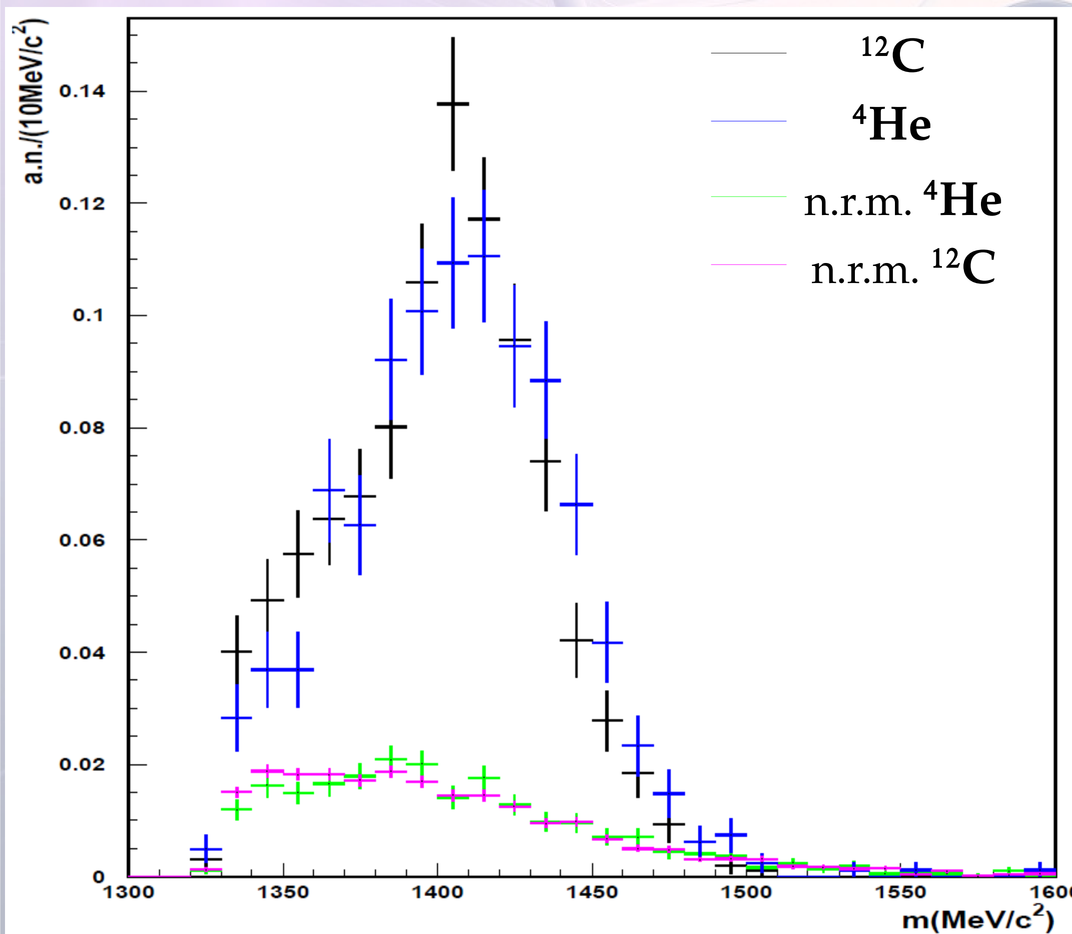

$m_{\Sigma^0\pi^0}$ *spectrum*

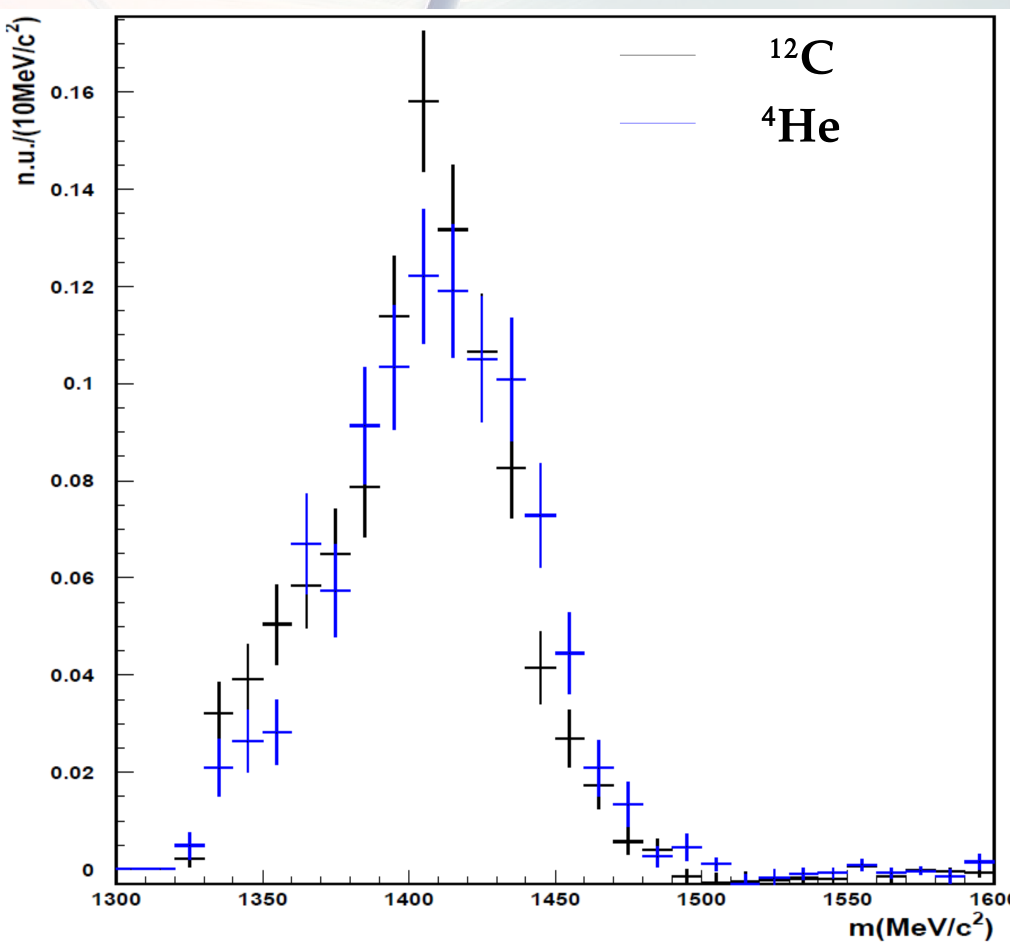

$m_{\Sigma^0\pi^0}$ *spectrum*

Ongoing fit of $\Sigma^0\pi^0$

K^-

8 component fit :

- **Resonant component K^- C at-rest/in-flight. $(M,\Gamma) = (1405 \div 1430\ ,\ 5 \div 52\ )$**
- **Non resonant $\Sigma^0\pi^0$ K^- H production at-rest/in-flight**
- **Non resonant $\Sigma^0\pi^0$ K^- C production at-rest/in-flight**
- **$\Lambda\pi^0$ background (Σ(1385) + I.C.)**
- **non resonant misidentification (*n.r.m.*) background**

Fit of $\Sigma^0\pi^0$ spectrum in C

K^-

χ^2_{min} /ndf ~ 1.7 corresponding to $(M_{min}, \Gamma_{min}) = (1426, 52)$ MeV/c^2

- **Global fit** (red)
- **Resonant component K^- C at-rest** (green)
- **n. r. K^- C at-rest** (blue)
- **n. r. K^- C in-flight** (yellow)
- **n. r. K^- H in-flight** (cyan)
- **$\Lambda^0\pi^0$ background + n. r. m.** (magenta)

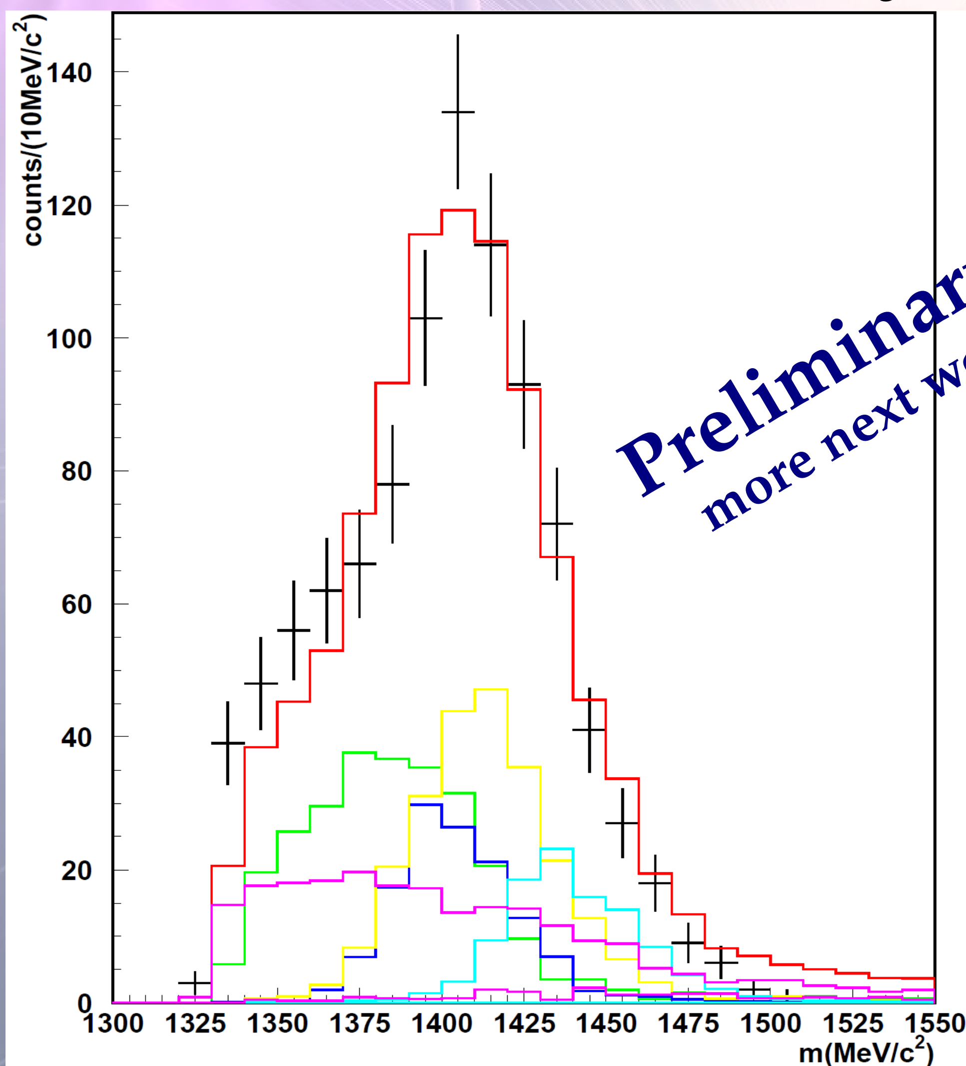

$m_{\Sigma 0\pi 0}$

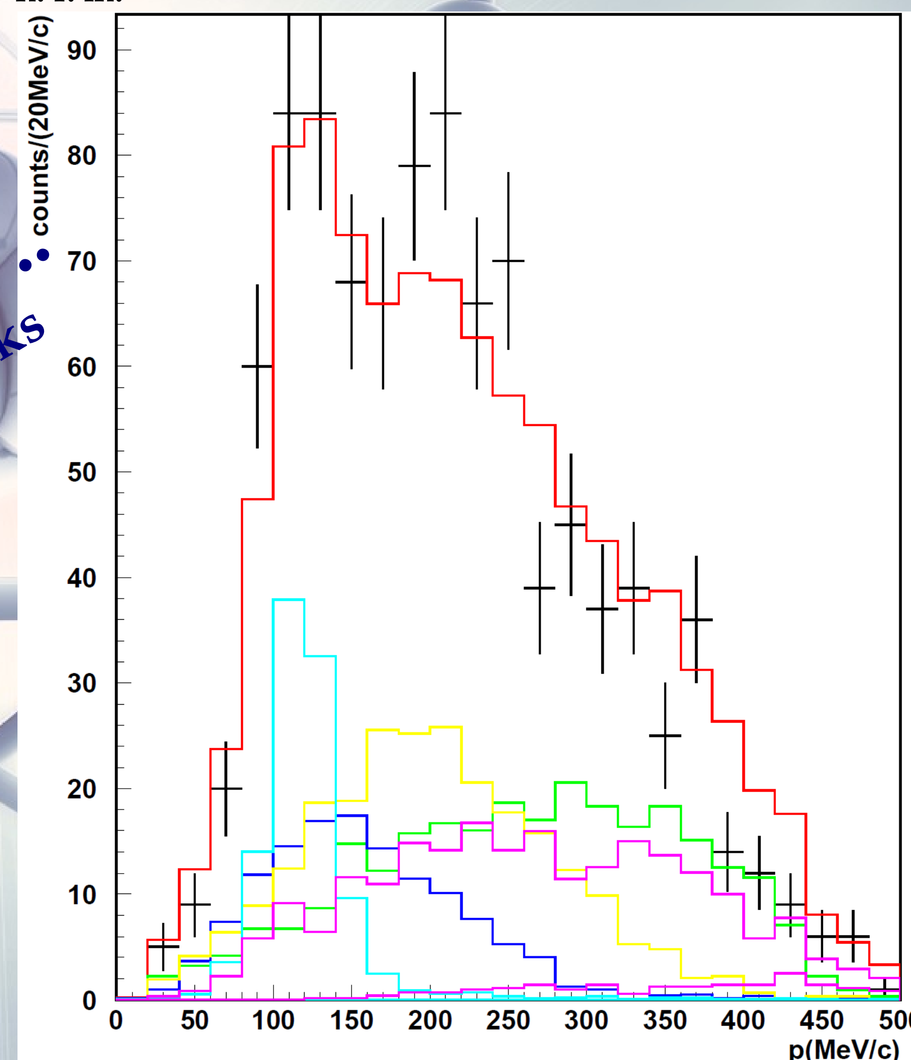

$p_{\Sigma 0\pi 0}$

Issues

Is there room for a 2NA pionic mode?

K-NN → YπN

The preliminary fits find «a place» for this processes (~ 5%) and...

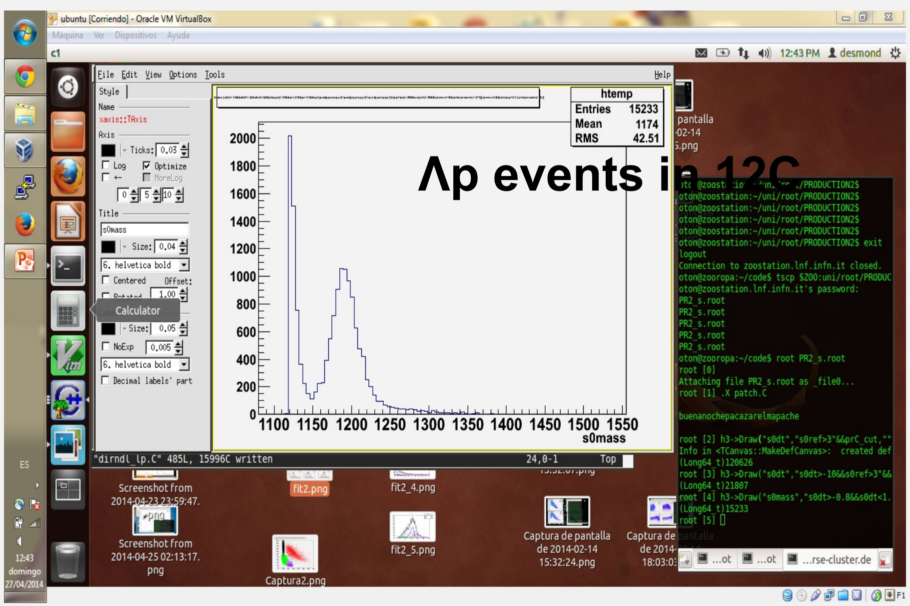

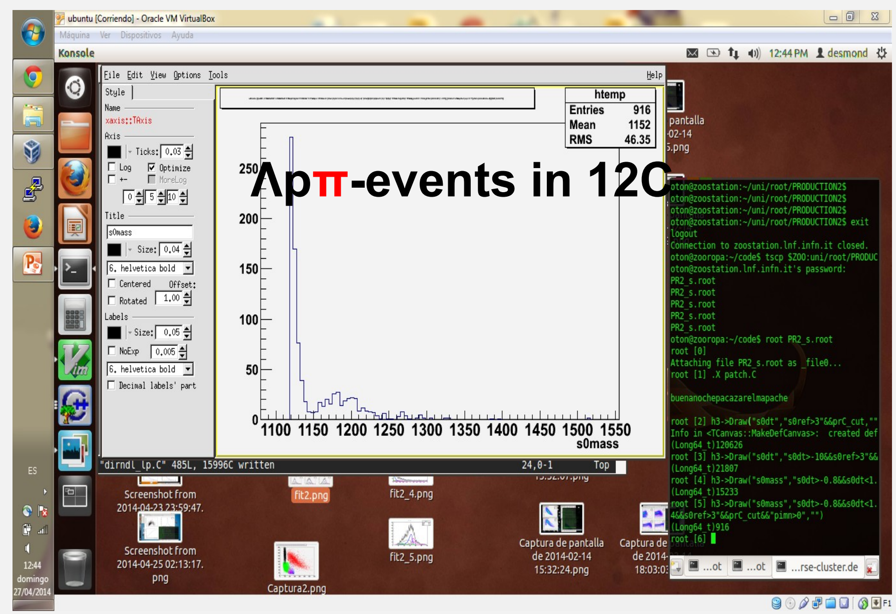

Λγ (MeV/c2)

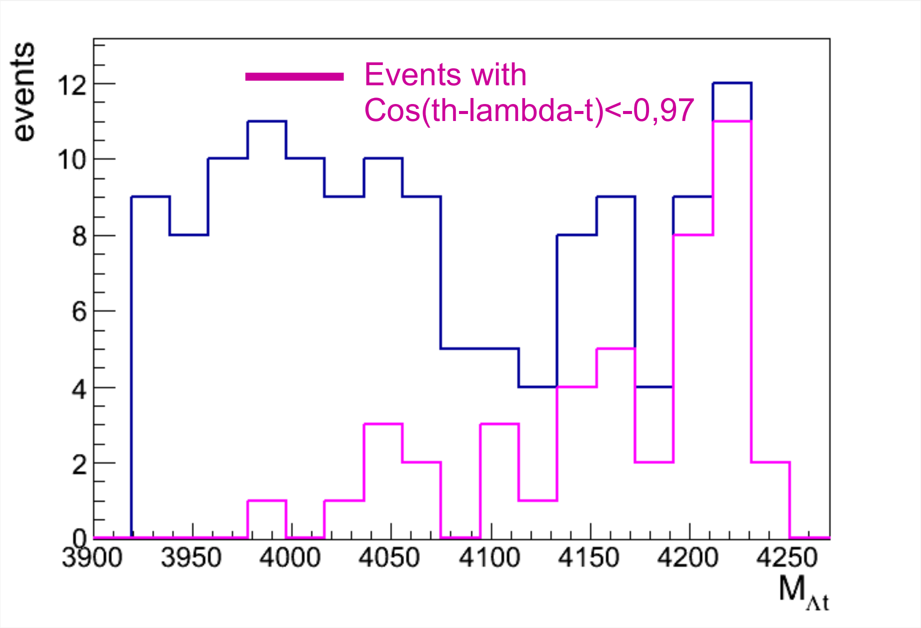

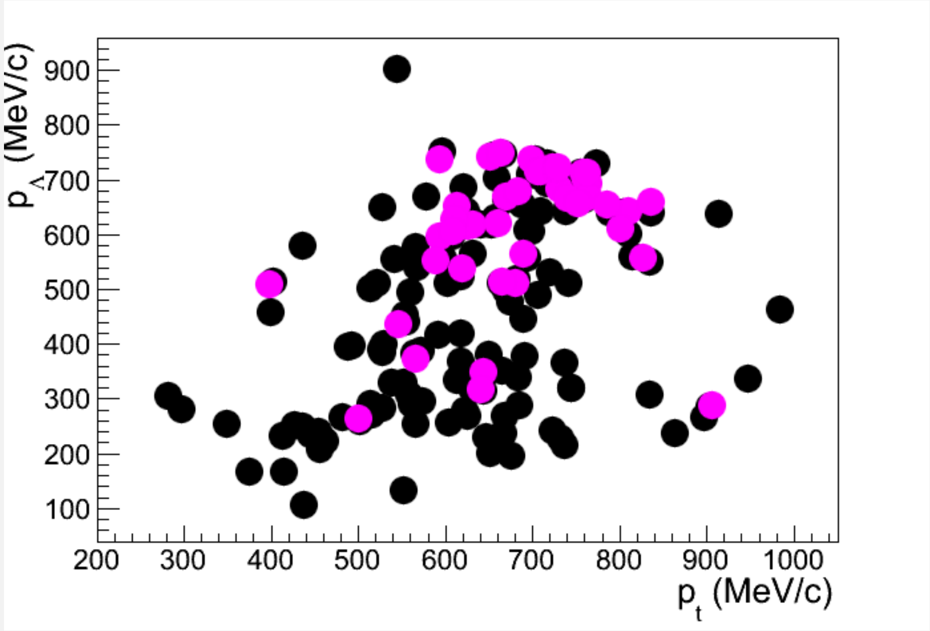

- Clear back-to-back enhacement lambda-triton signal
- Events in Carbon not showing this feature
- 3NA features also seen in the momentum correlations

KLOE: Study of $\Sigma\pi$ in 12C

Use of the calorimeter: Photon detection

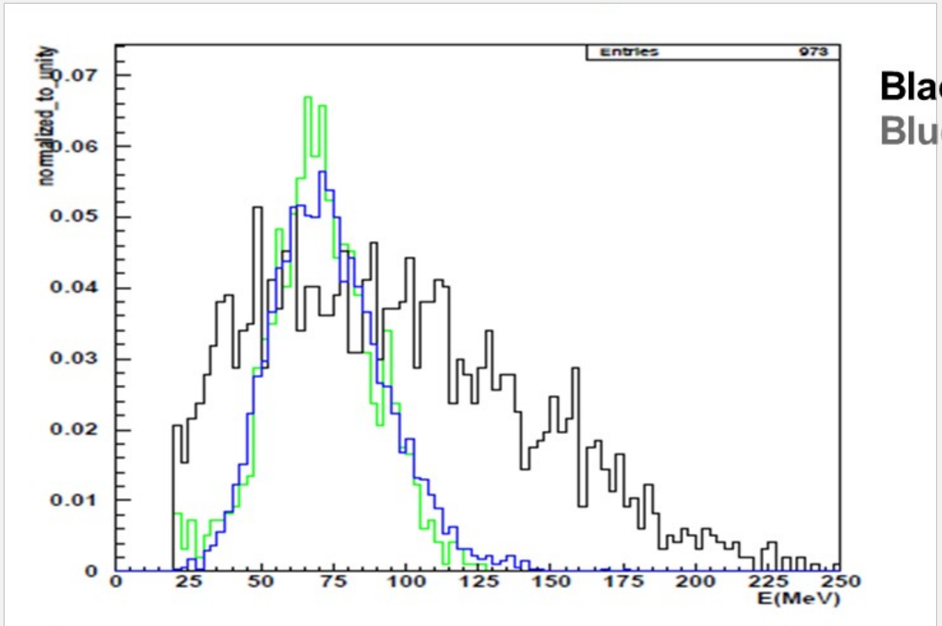

Black -> energy of photons from π^0
Blue -> energy of photons from Σ^0 -> $\Lambda\gamma$

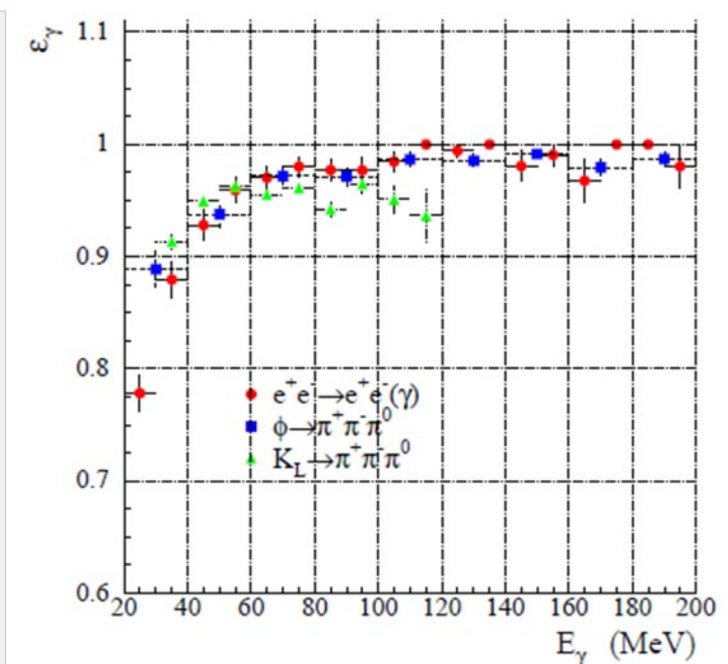

Mass of π0 reconstructed:

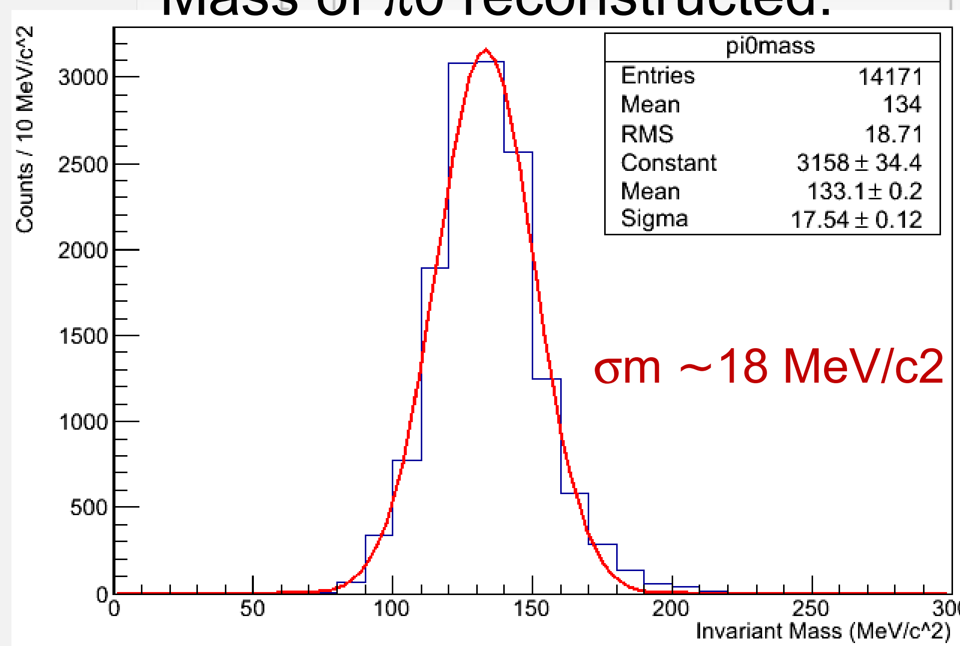

Σ^0 contamination in Λp events

Channel: $K^- \ {}^4He \rightarrow \ \Lambda \pi^- \ {}^3He$ … calculated reactions

Calculated secondary hadronic interactions:

EACH INTERNAL CONVERSION PROCESS:

$$\Sigma \ p/n \rightarrow \Lambda \ p/n$$

was calculated for both P-wave and S-wave produced Σs.

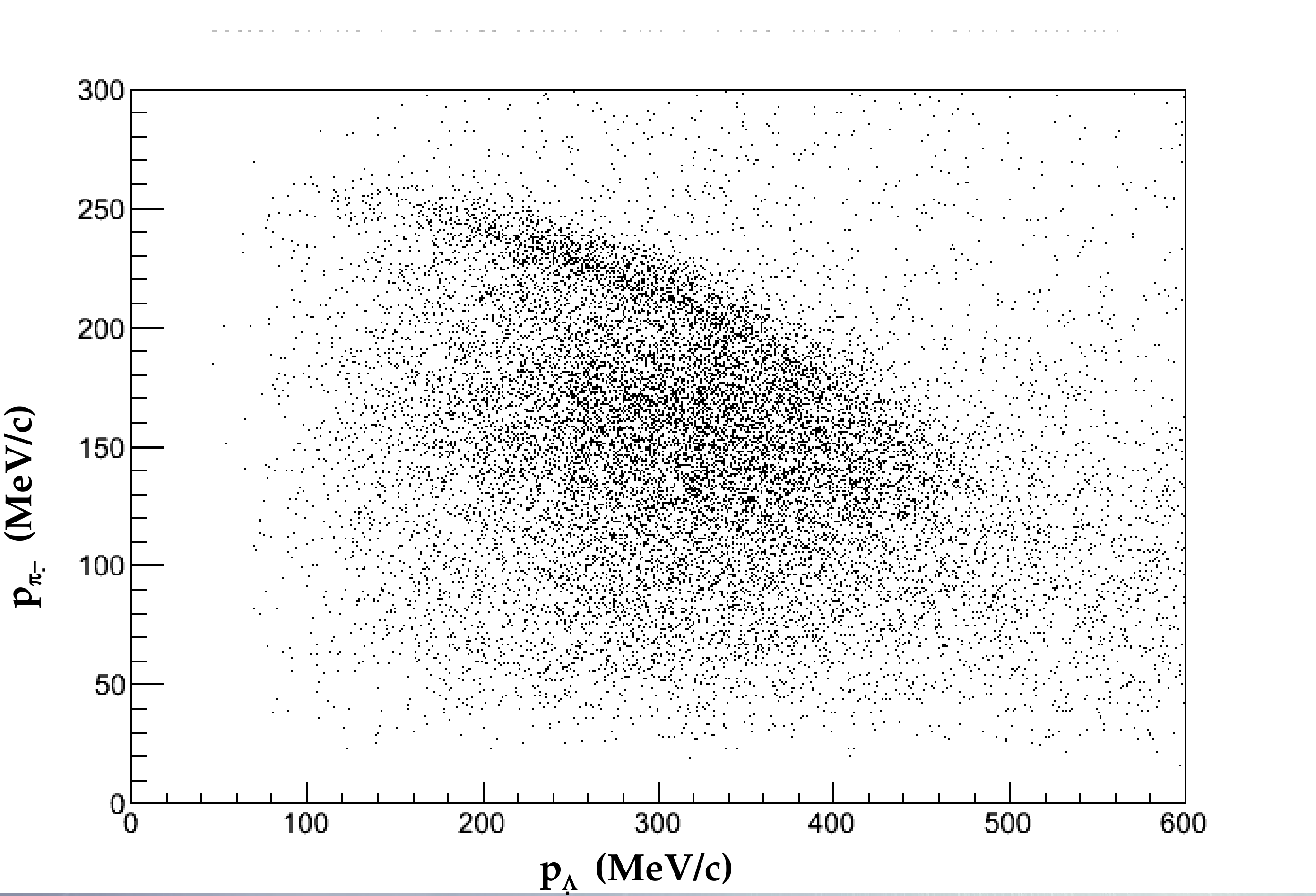

Channel: $K^- \, ^4He \rightarrow \Lambda \pi^- \, ^3He$ … calculated reactions

Calculated secondary hadronic interactions:

EACH INTERNAL CONVERSION PROCESS:

$$\Sigma \, p/n \rightarrow \Lambda \, p/n$$

was calculated for both P-wave and S-wave produced Σs.

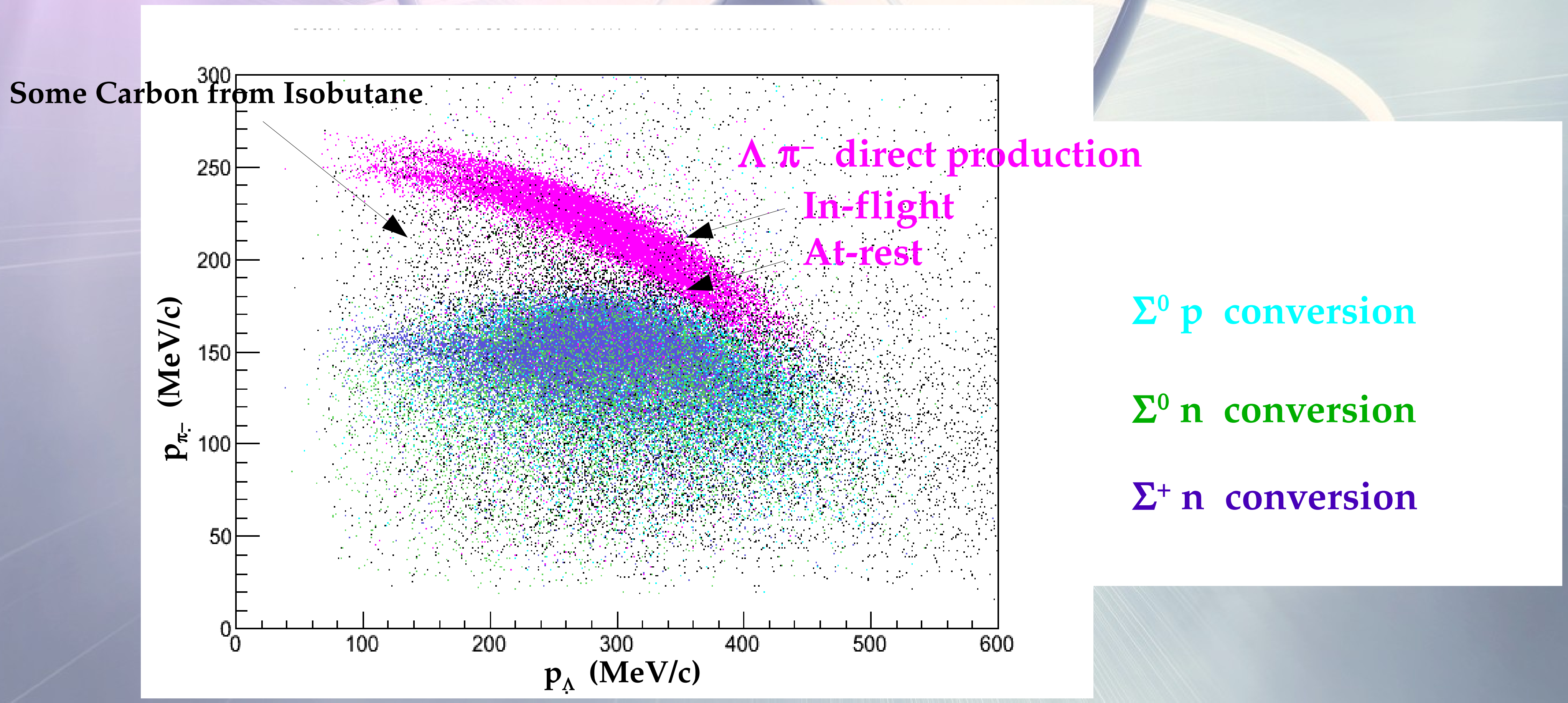

$K^- \; {}^4He \rightarrow \; \Lambda \, \pi^- \; {}^3He$ <u>events selection</u>

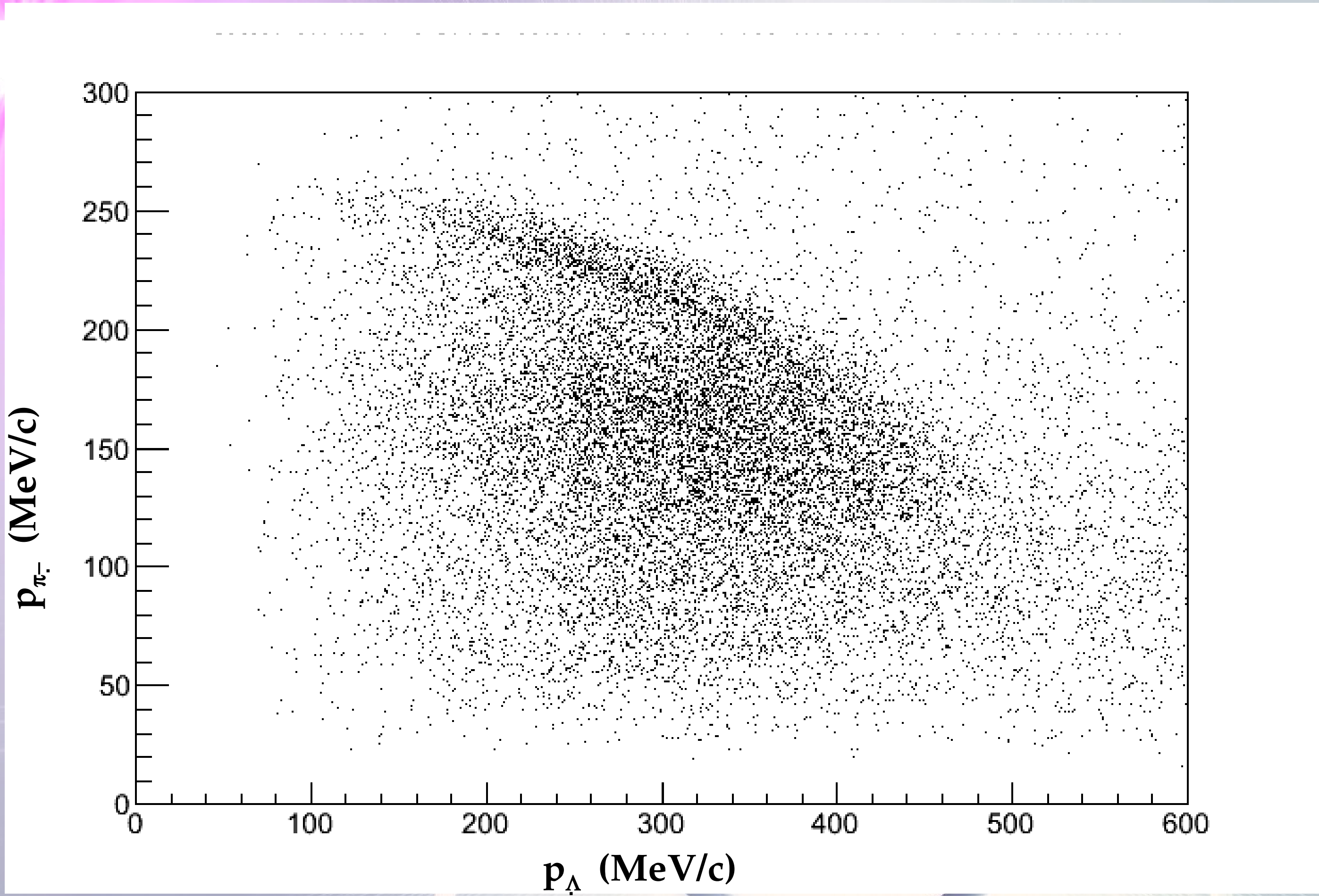

$K^- \, ^4He \rightarrow \Lambda \pi^- \, ^3He$ events selection

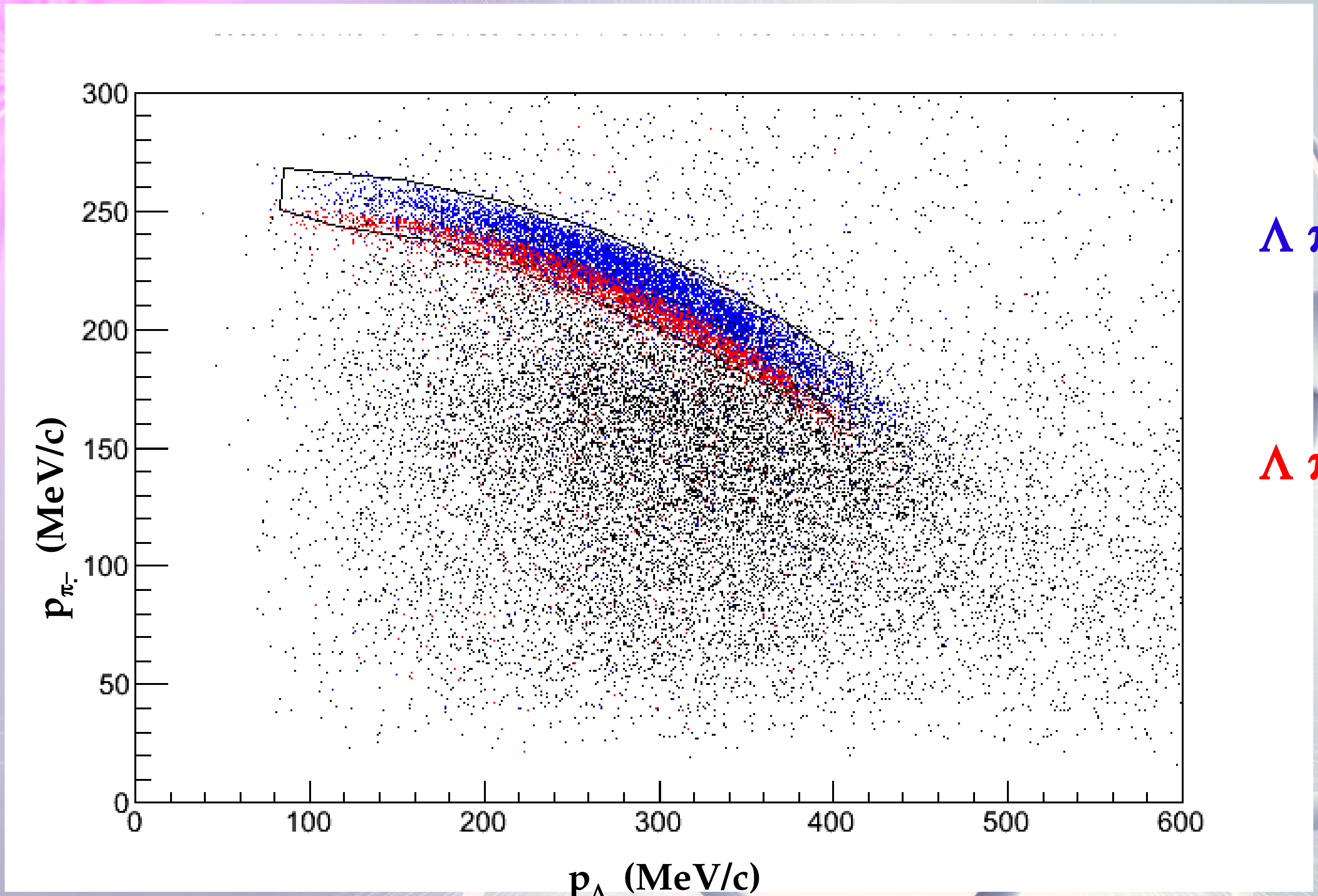

$\Lambda \pi^-$ direct production
In-flight RES + N-R

$\Lambda \pi^-$ direct production
At-rest RES + N-R

- CUT based on MC simulations used to select $\Lambda \pi^-$ direct production events
- At-rest CAN NOT be separated from In-flight → global fit performed
- Background sources: - $\Lambda \pi^-$ events from Σ p/n → Λ p/n conversion
  - $\Lambda \pi^-$ events from $K^- \, ^{12}C$ absorptions in Isobutane

$K^- \ ^4He \rightarrow \Lambda \pi^- \ ^3He$ background

- **Σ p/n → Λ p/n conversion:**

  Each possible conversion channel was simulated

  Σ^0 p / Σ^0 n / Σ^+ n / At-rest / In-flight / from RES and N-R produced Σs

- **$\Lambda \pi^-$ events from K^- ^{12}C absorptions in Isobutane (90% He, 10% C_4H_{10}):**

  K^- ^{12}C DATA in the KLOE DC wall are used

  estimated contribution: $\%(K^{-\,12}C) = 0.44 \pm 0.13$

  $N_{KC}/N_{KHe} = (n_{KC}/n_{KHe}) \cdot (\sigma_{KC}/\sigma_{KHe}) \cdot (BR_{KC}(\Lambda \pi^-)/BR_{KHe}(\Lambda \pi^-))$

  Nuovo Cimento 39 A 338-347 (1977)

  K^- ^{12}C still not calculated:

  - uncertain initial state of K meson $l_K = 1, 2, 3$
  - 4 nucleons in s-orbit , 8 nucleons in p-orbit
  - final state hyperon interactions

$K^- \ ^4He \rightarrow \Lambda \pi^- \ ^3He$ fit

Simultaneous fit ($p_{\Lambda\pi^-}$ - $m_{\Lambda\pi^-}$ - $\theta_{\Lambda\pi^-}$) leaving the ratio At-rest /In-flight and ^{12}C contamination to vary around the estimated values within errors:

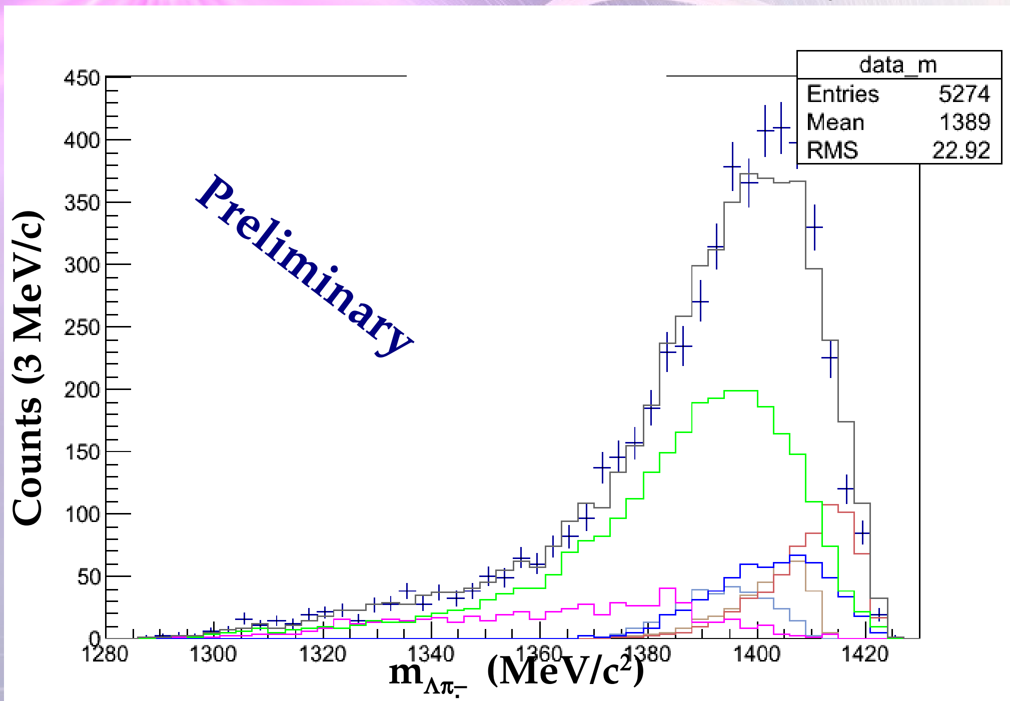

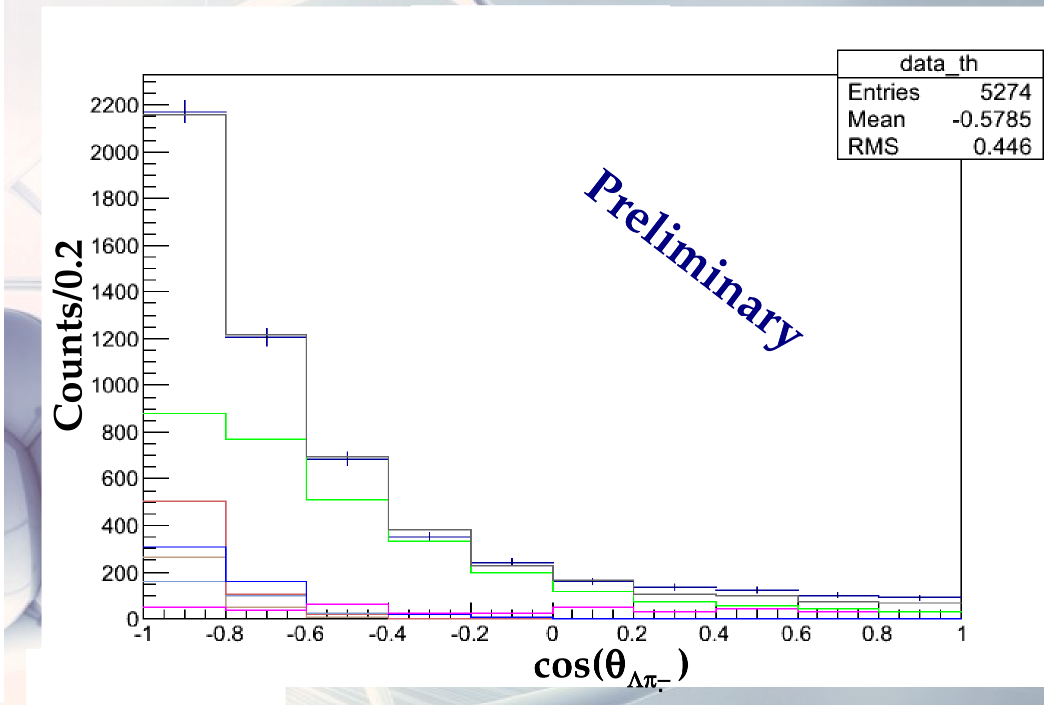

Global fit

$\Lambda \pi^-$ At-rest N-R

$\Lambda \pi^-$ At-rest RES

$\Lambda \pi^-$ In-flight N-R

$\Lambda \pi^-$ In-flight RES

$\Lambda \pi^-$ events from $K^- \ ^{12}C$

Σ p/n $\rightarrow$ Λ p/n conversion

Λ(1116) the signature of K⁻ hadronic interaction

K^-

starting point of the performed analysis reconstruction of the Λ decay vertex: $\Lambda(1116) \rightarrow p\pi^-$ (BR ~ 64 %)

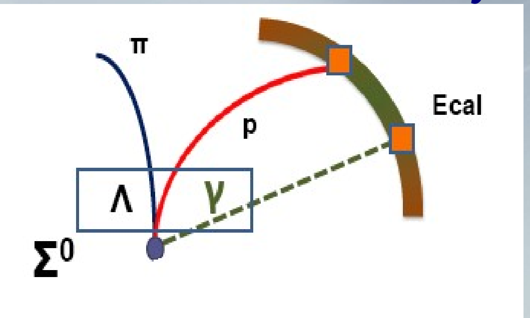

requests:

- vertex with at least two opposite charged particles
- spatial position of vertex inside DC, or in DC entrance wall
- negative tracks with dE/dx < 95 ADC counts.

Positive tracks are requested to have an associated cluster in the calorimeter and the correct *E - p* relation. (KLOE Memo 330 September 2006)

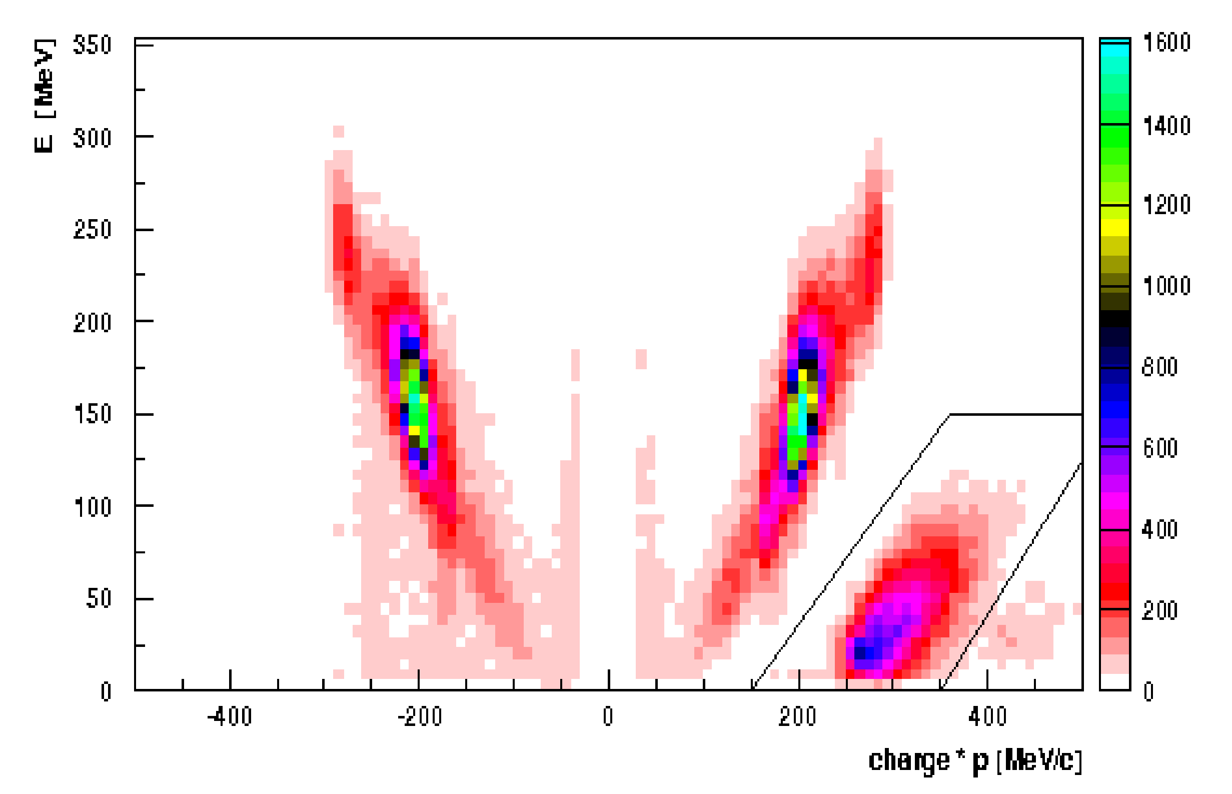

$\Lambda(1116)$ the signature of K^- hadronic interaction

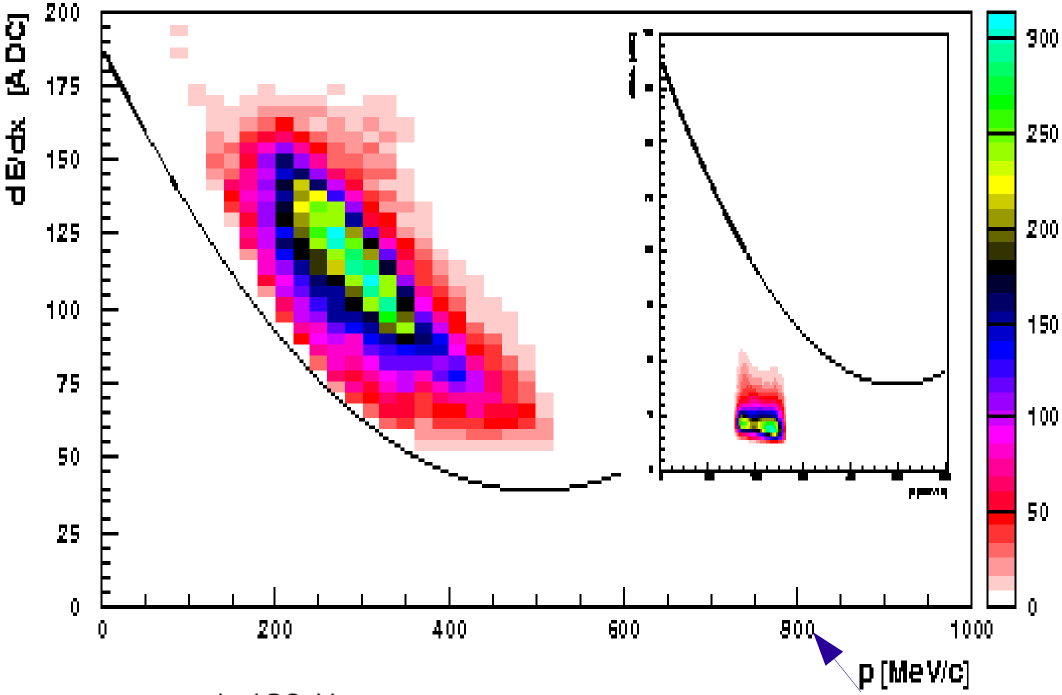

Correction for low momentum positive tracks (due to the kinetic energy threshold of the calorimeter ~ 20 MeV)

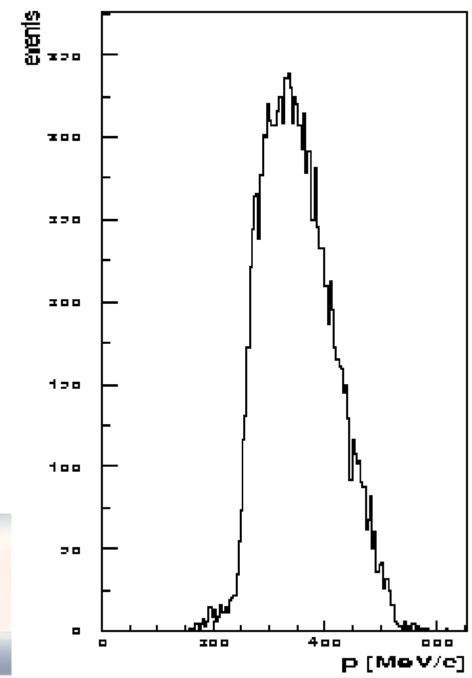

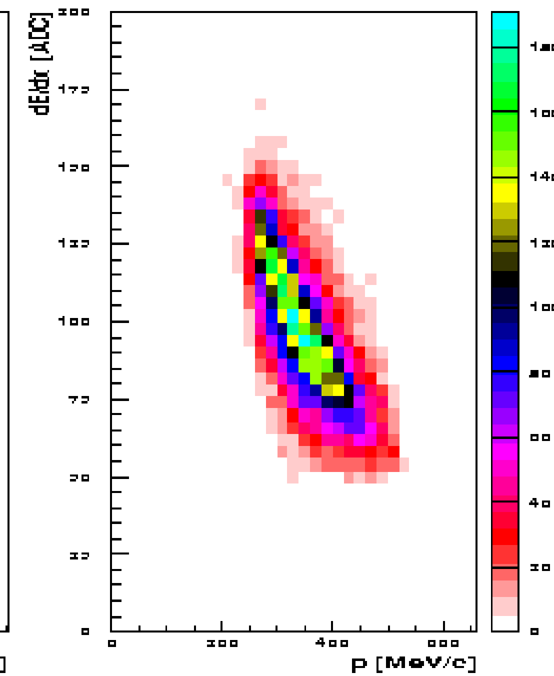

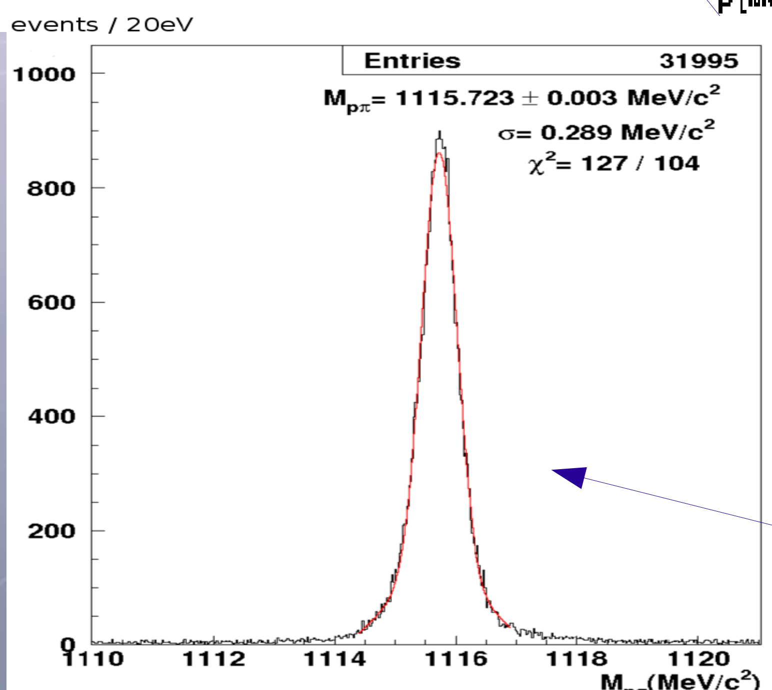

Clear separation with respect to pions (from K^+ two body decay)

Excellent fianal $p\pi^-$ invariant mass spectrum.

K^-

$\Lambda p/\Lambda d/\Lambda t$ and $\Lambda p + \pi^-$ channels

$\Lambda p/\Lambda d/\Lambda t$ and $\Lambda p + \pi^-$ scientific case

K^-

How hadron masses and interactions change in nuclear medium .. approach by means of kaonic nuclear clusters. Deeply Bound Kaonic Nuclear States (ex. K^-pp – K^-ppn) predicted due to the strong $\bar{K}N$ interaction in the I=0 channel.

Wycech (1986) - Akaishi & Yamazaki (2002)

↓

Search for signal of bound states in the Λp channel: candidate to be a K^-pp cluster. Observed (FINUDA, KEK, DISTO) and very debated HADES, L. Fabietti, Status of the ppK- analysis and last words about the Lambda(1405)

↓

interpretation strongly depends on single and multi – nucleon absorption process:

$K^- N \rightarrow \Lambda/\Sigma\ \pi$ single nucleon <u>PIONIC</u>, most probable process

$K^- NN \rightarrow \Lambda/\Sigma\ N$ ($K^- NNN \rightarrow \Lambda/\Sigma\ NN$) multi-nucleon <u>NON-PIONIC</u>, (BR ≈ 20% in ^4He)

Tools for identifying ΛN events

Interaction vertex identified backward extrapolating Λ + N, also using:

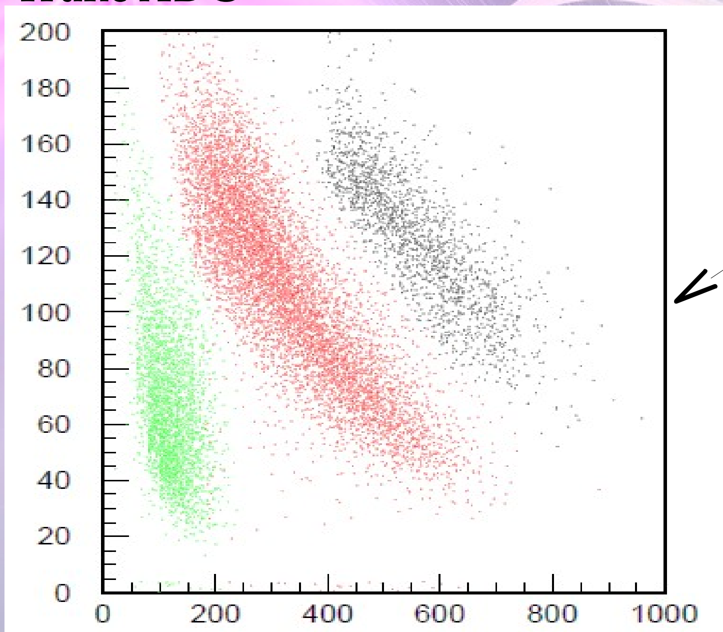

- dE/dx

- EMC:

Time, Energy, Mass by TOF

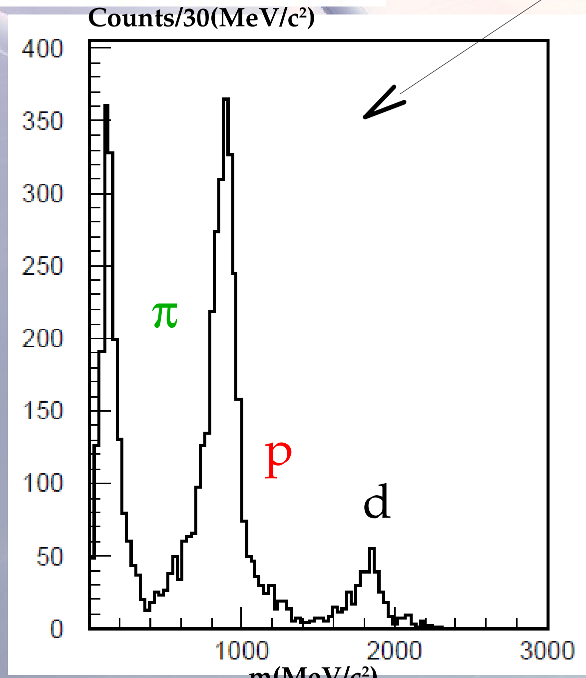

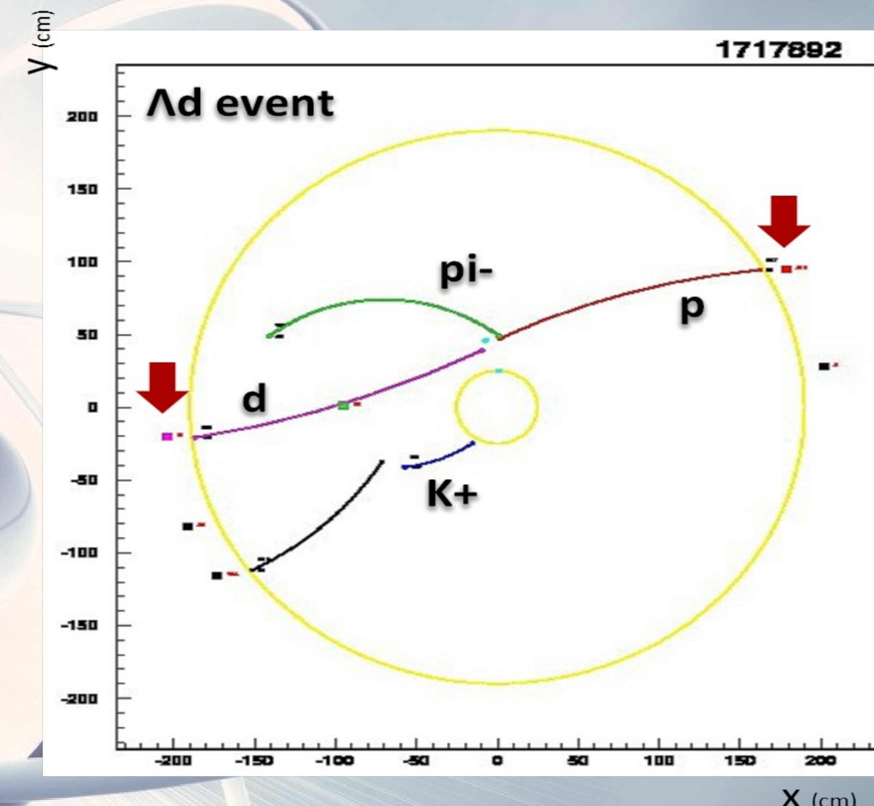

Quality checks using distances:

- Tracked K^- in 12% of events
- Backwards extrapolated K^+ used instead (possible in 95% of events when the K^- is missing)
- Λ decay path

Excellent DC resolution

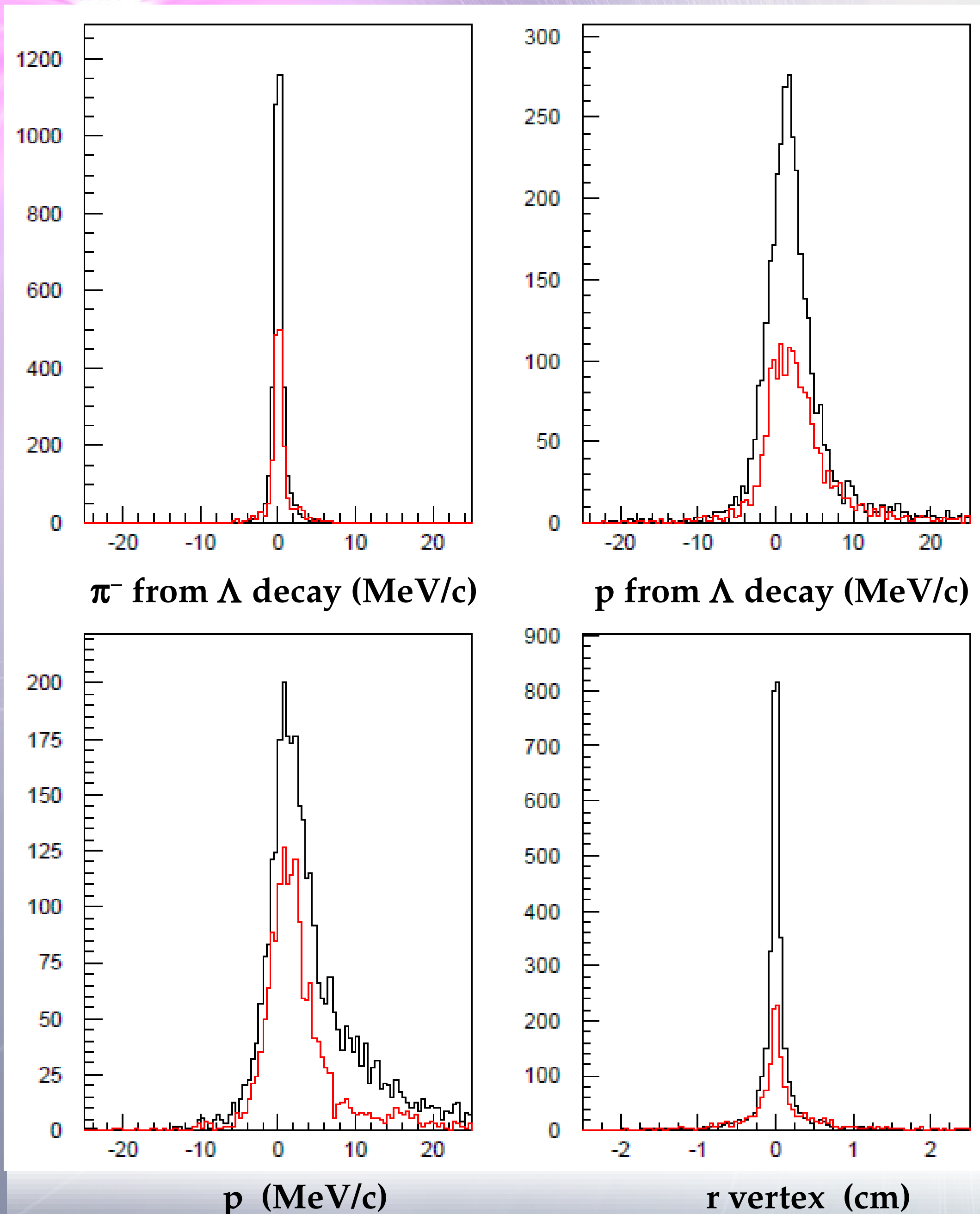

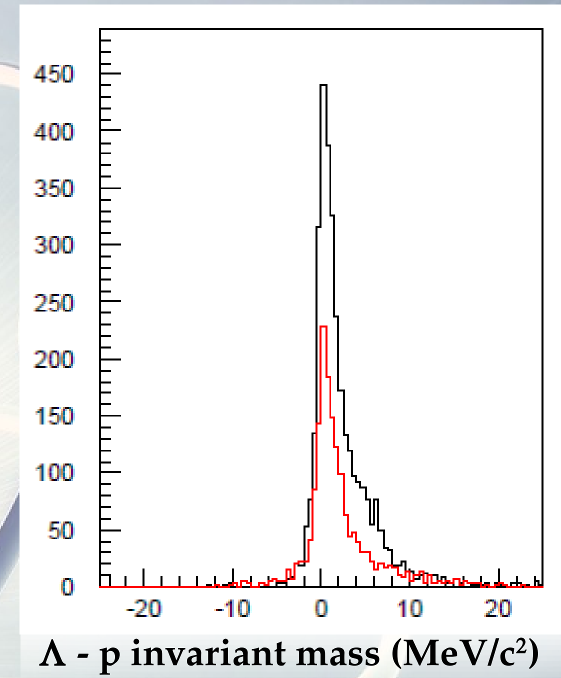

Distributions: MC-Reconstructed

p_Λ	$0.49 \pm 0.01\ MeV/c$	$0.65 \pm 0.02\ MeV/c$
p_p	$2.63 \pm 0.07\ MeV/c$	$2.63 \pm 0.07\ MeV/c$
$M_{\Lambda p}$	$1.10 \pm 0.03\ MeV/c^2$	$1.27 \pm 0.04\ MeV/c^2$
r_{vertex}	$0.12 \pm 0.01\ cm$	$0.16 \pm 0.01\ cm$

Tracks connected by KLOE vtx (left)

Tracks NOT connected by KLOE vtx (right)

Good acceptance ...

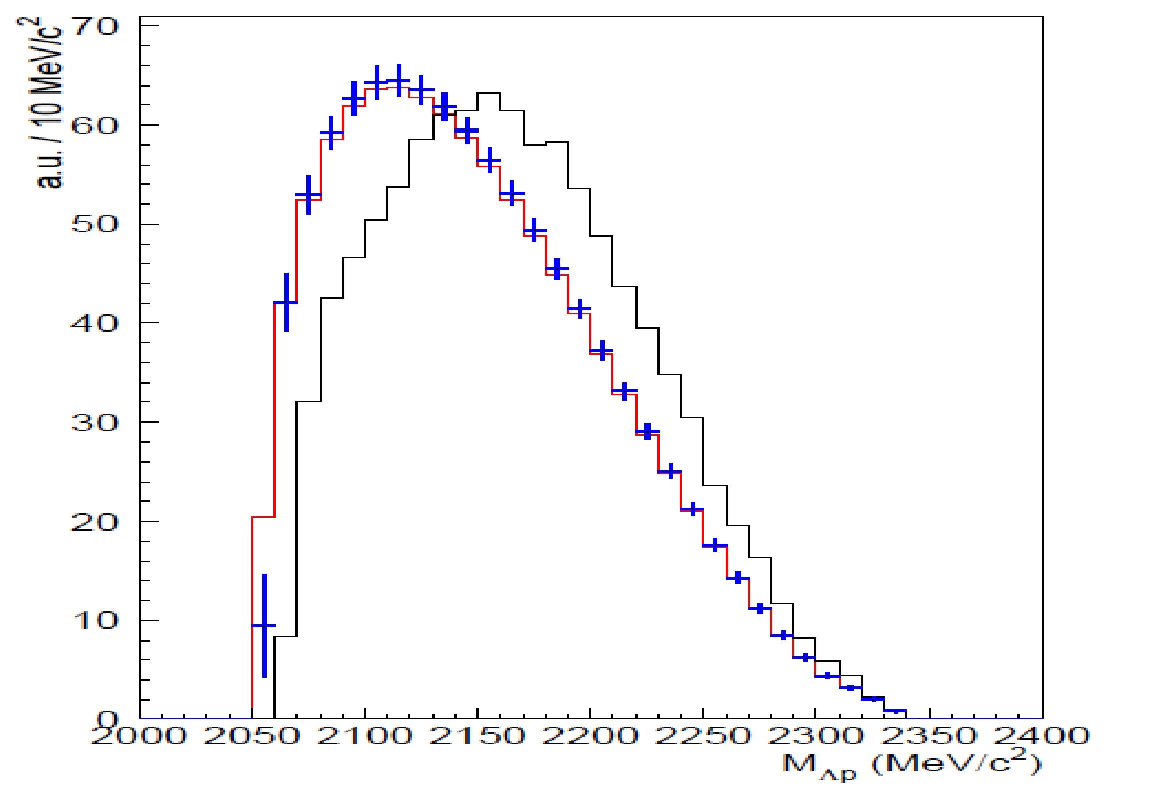

Projection of acceptance function depending on $(P_\Lambda, P_p, m_{\Lambda p})$ on the Invariant mass plane.

True phase space MC
Reconstructed MC
Acc. Corrected MC

Normalization 1:1
(no efficiency evaluation)

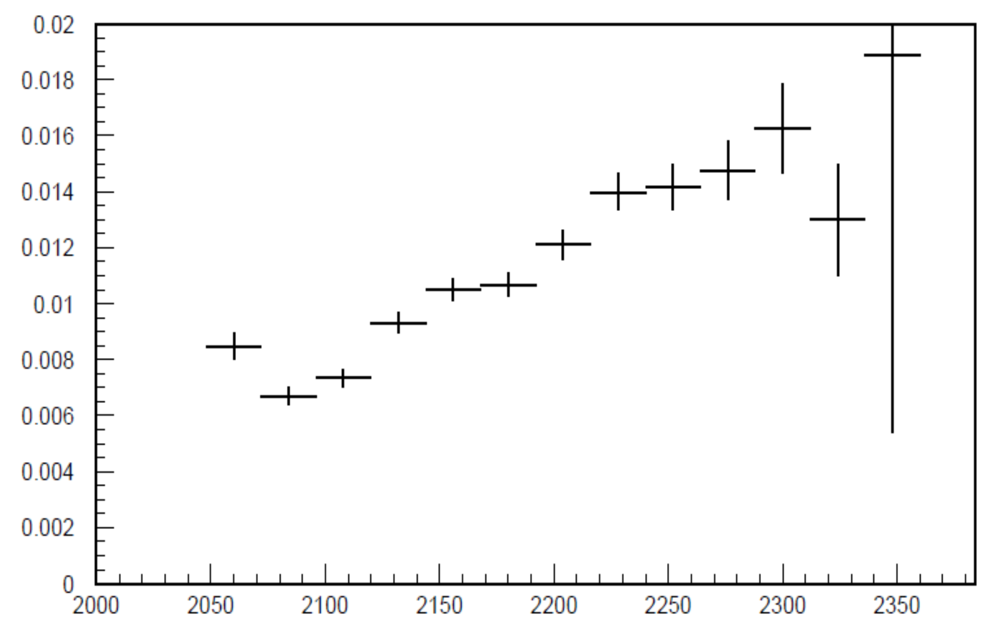

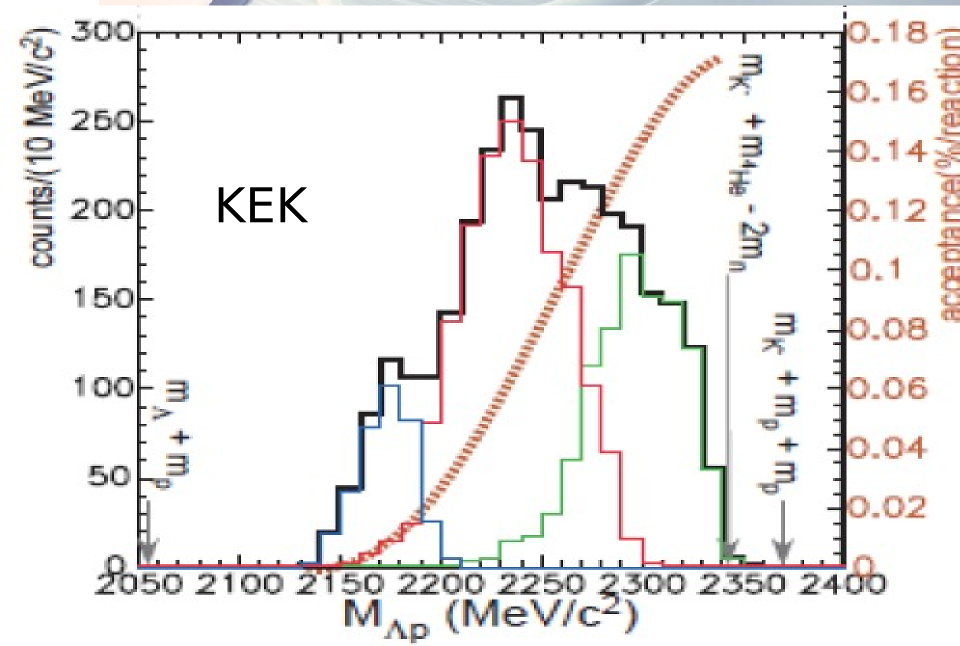

… allows to perfectly disentangle 1N-absorption in Λp correlation study

K^-

K^-pp cluster ??

Background:

1NA: $K^-N \rightarrow \Lambda\pi^-$ (p from residual nucleus)
2NA: $K^-NN \rightarrow \Lambda N$ (pionless)

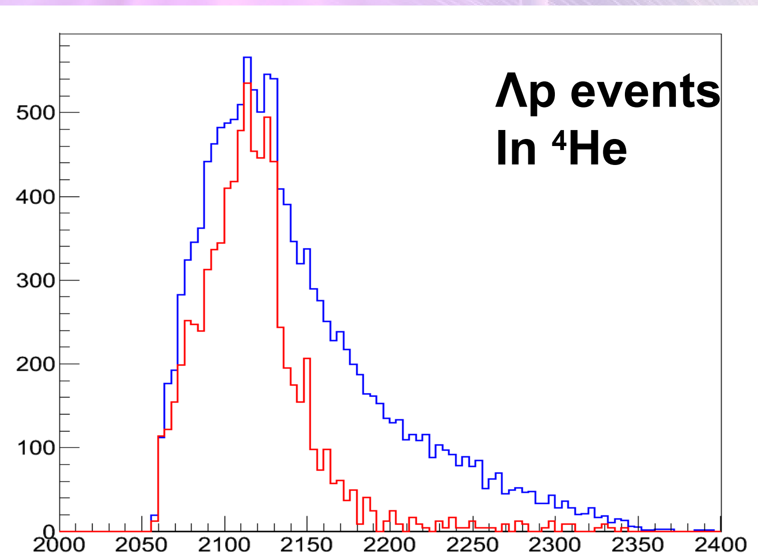

Λ - p invariant mass (MeV/c²)

Λp all events
$\Lambda\pi^-$ (p) events
(arbitrary normalization)

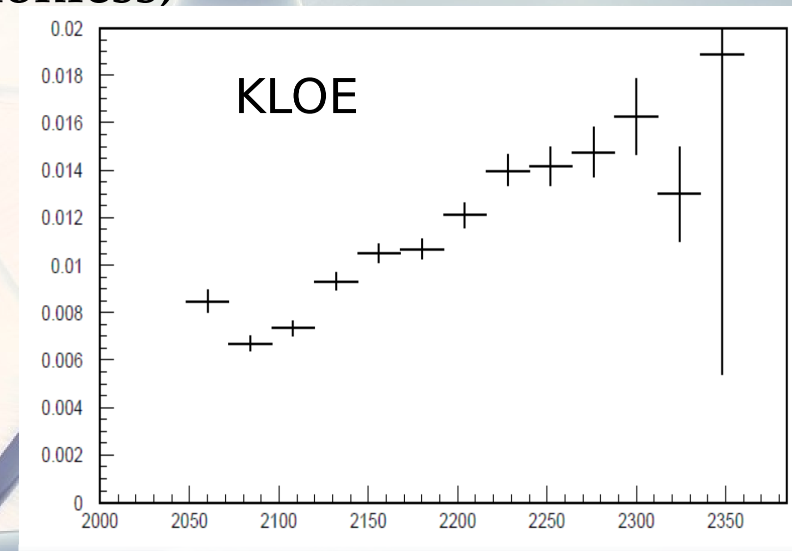

acceptance in Λ - p invariant mass (MeV/c²)
(arbitrary normalization)

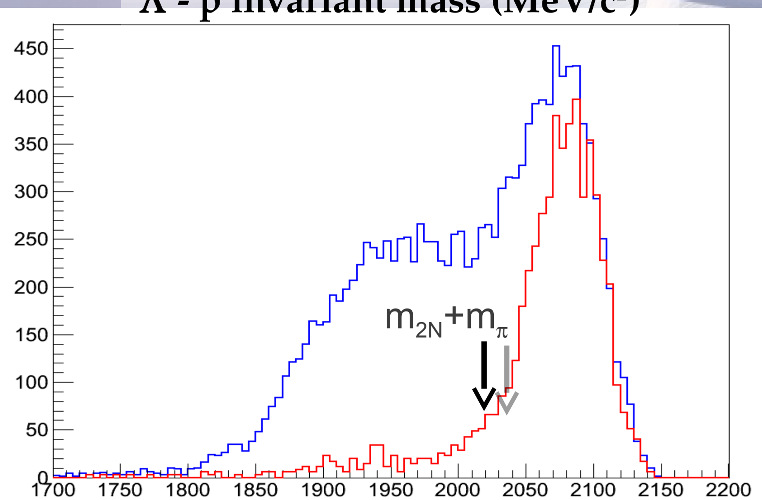

Λ - p missing mass (MeV/c²)

The Λp missing mass for the $\Lambda\pi^-$ (p) events lies exactly in the 2N+π^- masss region

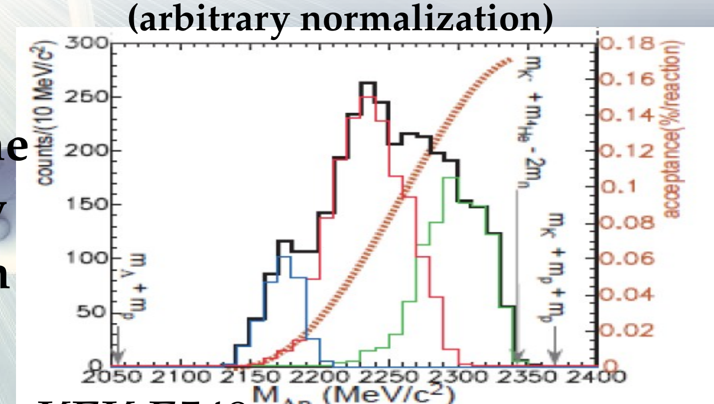

KEK-E549
Mod.Phys.Lett.A23, 2520 (2008)

Λd / Λt analyses

K⁻

Search for signal of bound states in the Λd channel. Candidate to be a K^-ppn cluster. Observed spectra from FINUDA and KEK again showing possible bound states in the high invariant mass region.

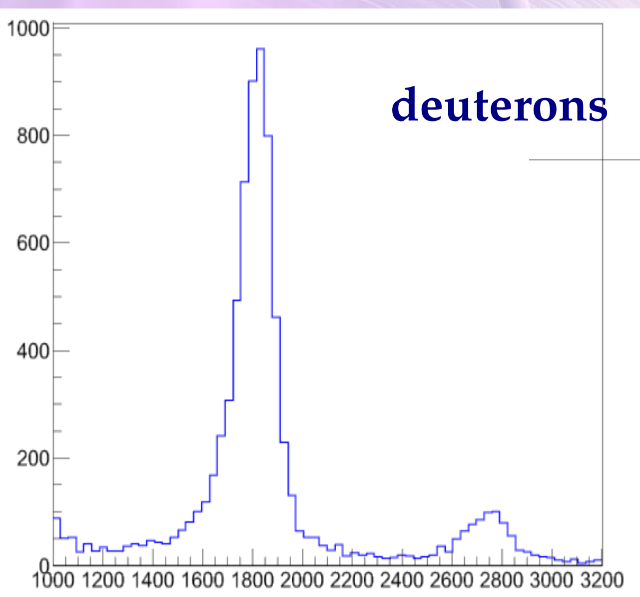

TOF particle mass (MeV/c²)

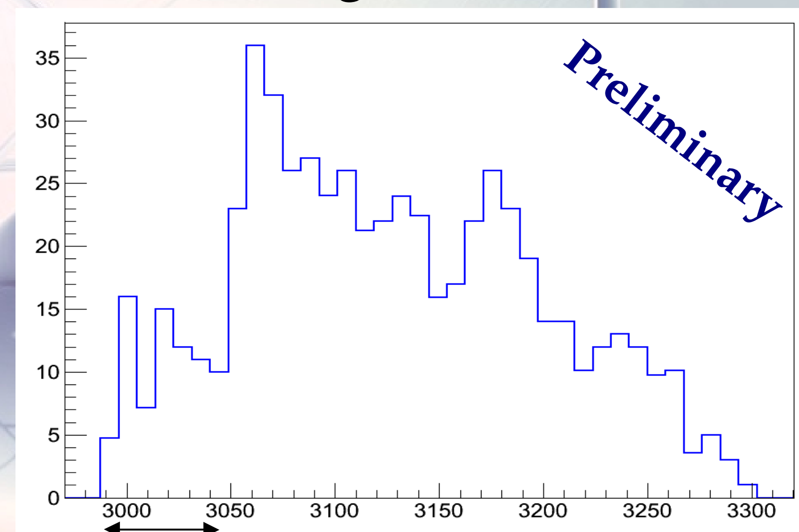

low accept. region

$m_{\Lambda d}$ (MeV/c²)

Λd events
In ^{4}He

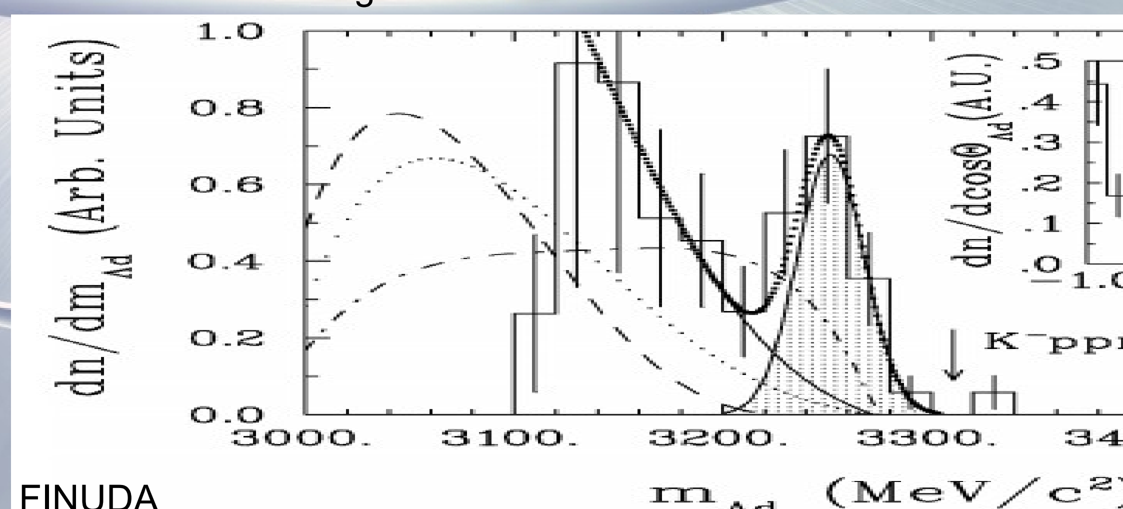

Nucl.Phys.A835, 43 (2010)

Λd / Λt analyses

K^-

Search for signal of bound states in the Λd channel. Candidate to be a K^-ppn cluster. Observed spectra from FINUDA and KEK again showing possible bound states in the high invariant mass region.

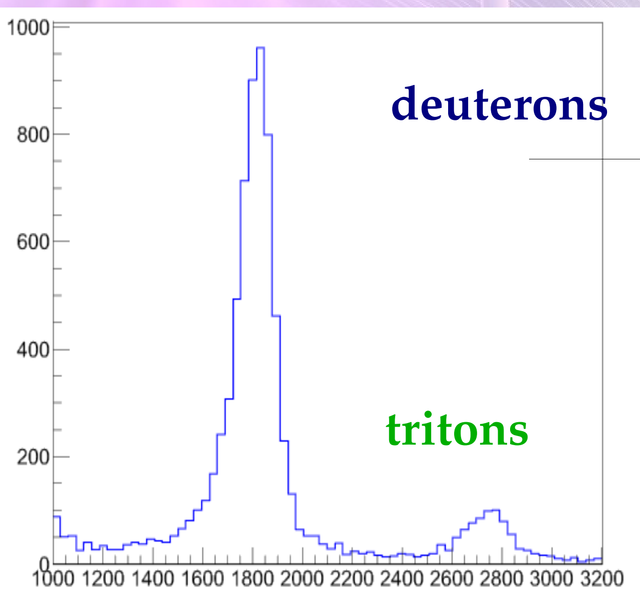

TOF particle mass (MeV/c^2)

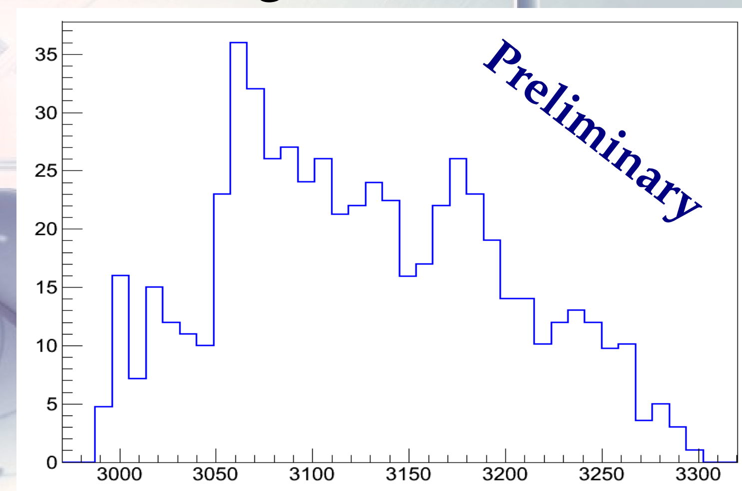

$m_{\Lambda d}$ (MeV/c^2)

Λd events In ^{4}He

Only FINUDA and M. Roosen, J.H. Wickens, Il Nuovo Cimento 66 (1981), 101. (4 events) have shown Λ- t spectra from K^- absorption!

Λt events In ^{4}He

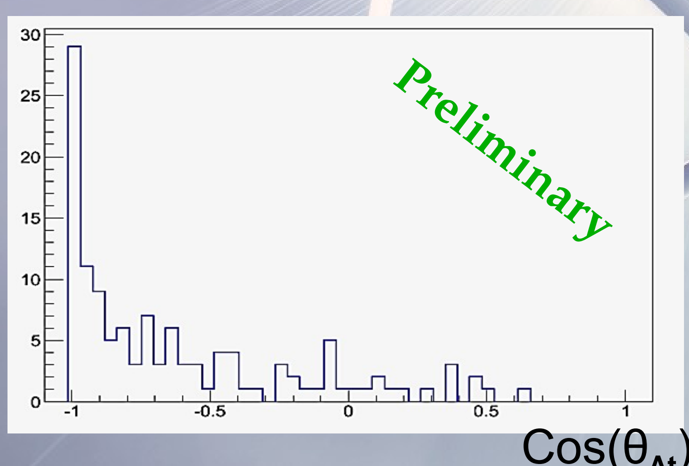

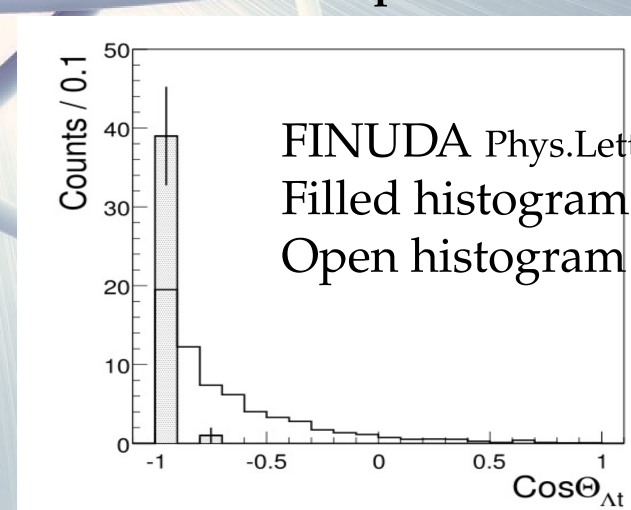

FINUDA Phys.Lett.B 229, 229 (2008)
Filled histogram= data
Open histogram = Phase space simulation

Conclusions $\Lambda p/\Lambda d/\Lambda t$ and $\Lambda p + \pi^-$ analyses

K^-

KLOE excellent acceptance and resolution!

Λp and $\Lambda p + \pi^-$ analyses completed, show important differences revealing the mesonic absorption characteristics.

Good statistics in Λt.

K^-

K^- "p" $\rightarrow \Sigma^0\pi^0 / \Sigma^+\pi^-$ channels

bound proton in ^{12}C

Scientific case Λ(1405)

Λ(1405): (m , Γ) = ($1405.1^{+1.3}_{-1.0}$, 50 ± 2) MeV, I = 0, S = -1 , $J^p = 1/2^-$, Status: **,**

strong decay into Σπ

<u>Its nature is being a puzzle for decades</u>: 1) *three quark state*: expected mass ~ 1700 MeV

2) *penta quark*: more unobserved excited baryons 3) *unstable $\bar{K}N$ bound state*

4) *two poles*: ($z_1 = 1424^{+7}_{-23} - i\, 26^{+3}_{-14}$; $z_1 = 1381^{+18}_{-6} - i\, 81^{+19}_{-8}$) MeV (Nucl. Phys. A881, 98 (2012))

mainly coupled to $\bar{K}N$ — mainly coupled to Σπ → line-shape depends on production mechanism

Line-shape also depends on the decay channel

$$\frac{d\sigma(\Sigma^-\pi^+)}{dM} \propto \frac{1}{3}\left|T^0\right|^2 + \frac{1}{2}\left|T^1\right|^2 + \frac{2}{\sqrt{6}} Re(T^0 T^{1*})$$

$$\frac{d\sigma(\Sigma^+\pi^-)}{dM} \propto \frac{1}{3}\left|T^0\right|^2 + \frac{1}{2}\left|T^1\right|^2 - \frac{2}{\sqrt{6}} Re(T^0 T^{1*})$$

$$\frac{d\sigma(\Sigma^0\pi^0)}{dM} \propto \frac{1}{3}\left|T^0\right|^2$$

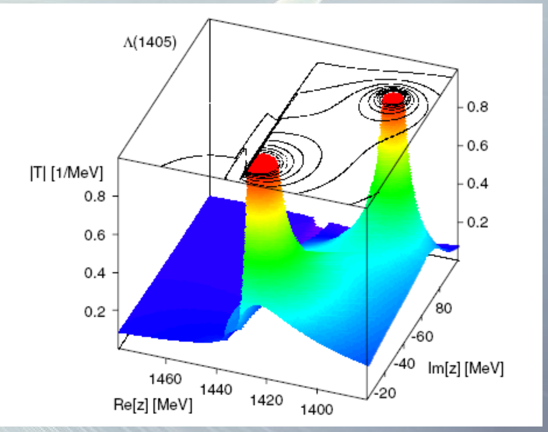

TO TEST THE HIGHER POLE:

production in $\bar{K}N$ reactions (only chance to observe the high mass pole)

decaying in $\Sigma^0\pi^0$ (free from Σ(1385) background)

Complementary to HADES measurement

See L. Fabietti's talk

Scientific case Λ(1405)

K^- nuclear absorption experiments .. long history .. BUT

K^-

1) $m_{\pi\Sigma}$ spectra always cut at the at-rest limit   2) $(\Sigma\pm\pi\mp)$ spectra suffer Σ(1385) contamination

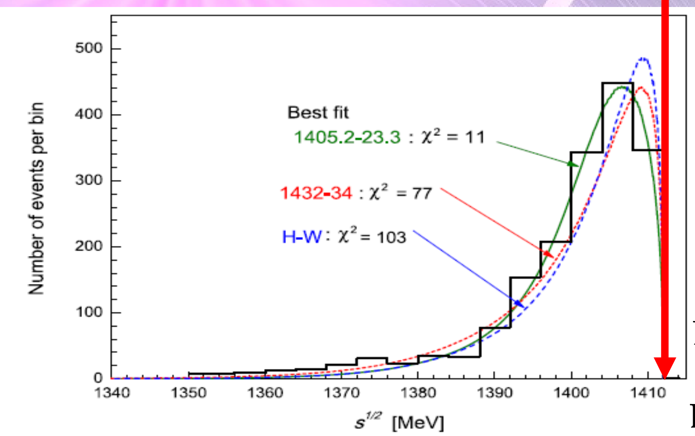

Fig. 6. Detailed differences in $M_{\Sigma\pi}$ spectra among the Hyodo–Weise prediction and the present model predictions.

"A study of K^- $^4He \rightarrow (\Sigma\pm\pi\mp) + {}^3H$ using slow instead of stopping K^- would be very useful in eliminating some of the uncertainties in interpretation"

D. Riley, et al. Phys. Rev. D11 (1975) 3065

Esmaili et el., Phys.Lett. B686 (2010) 23-28

P. J. Carlson, et al. Nucl. Phys. 74 642

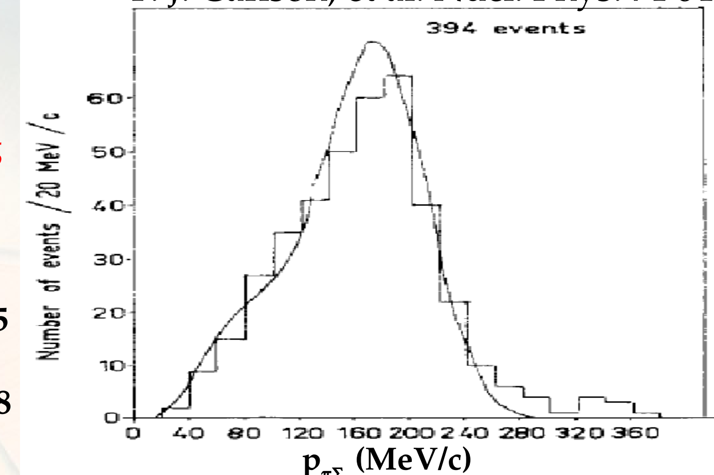

The $\Sigma^0\pi^0$ spectrum was only observed in 3 experiments … with different line-shapes !

I. Zychor et al., Phys. Lett. B 660 (2008) 167

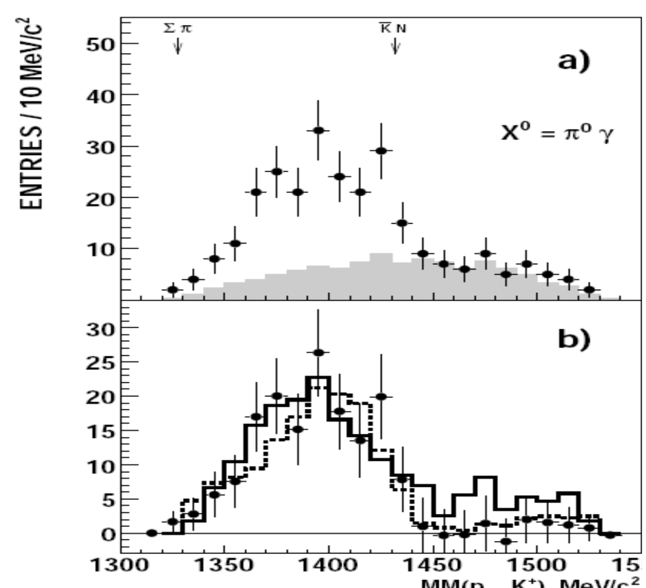

K. Moriya, et al., (Clas Collaboration) Phys. Rev. C 87, 035206 (2013)

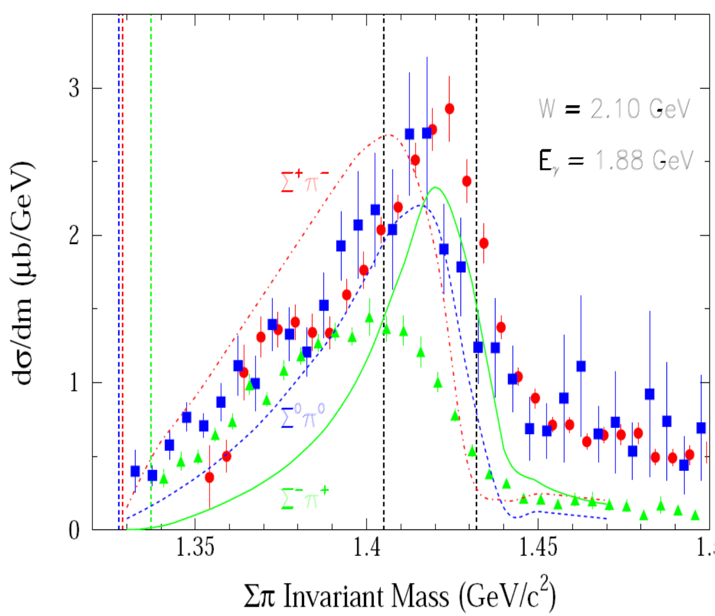

Magas et al. PRL 95, 052301 (2005) 034605 S. Prakhov, et al., Phys. Rev. C70 (2004)

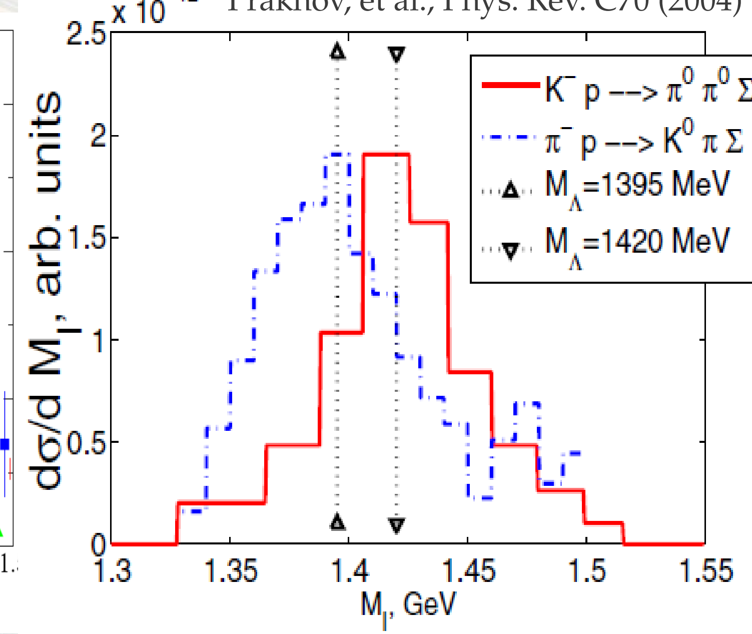

Photon clusters identification

K^-

K^- "p" $\rightarrow \Sigma^0\pi^0 \rightarrow (\Lambda(1116)\,\gamma_3)\,(\gamma_1\gamma_2) \rightarrow (p\pi^-)\,3\gamma$

1) 3 neutral clusters selection ($E_{c1} > 20$ MeV) not from K^+ decay ($K^+ \rightarrow \pi^+\pi^0$)

2) photon clusters selection: $\chi_t^2 = t^2/\sigma_t^2$ where $t = t_i - t_j$

time of flights in light speed hypothesis.

Selects three photon clusters in time from the Λ decay vertex r_Λ

3) photon clusters identification: γ_3 from $\pi^0 \rightarrow \gamma_1\gamma_2$ distinctioncay

$$\chi^2_{\pi\Sigma} = \frac{(m_{\pi^0} - m_{ij})^2}{\sigma^2_{ij}} + \frac{(m_{\Sigma^0} - m_{k\Lambda})^2}{\sigma^2_{k\Lambda}}$$

i,j and *k* represent one of the previously selected candidate photon cluster.

4) Cuts on χ_t^2 and $\chi_{\pi\Sigma}^2$ optimized on MC simulations & splitted clusters rejection

The algorithm has (from true MC information) an efficiency (98±1)% to identify photons and (78±2)% to select the correct triple of neutral clusters.

Photon clusters identification: Σ^0 invariant mass

K^-

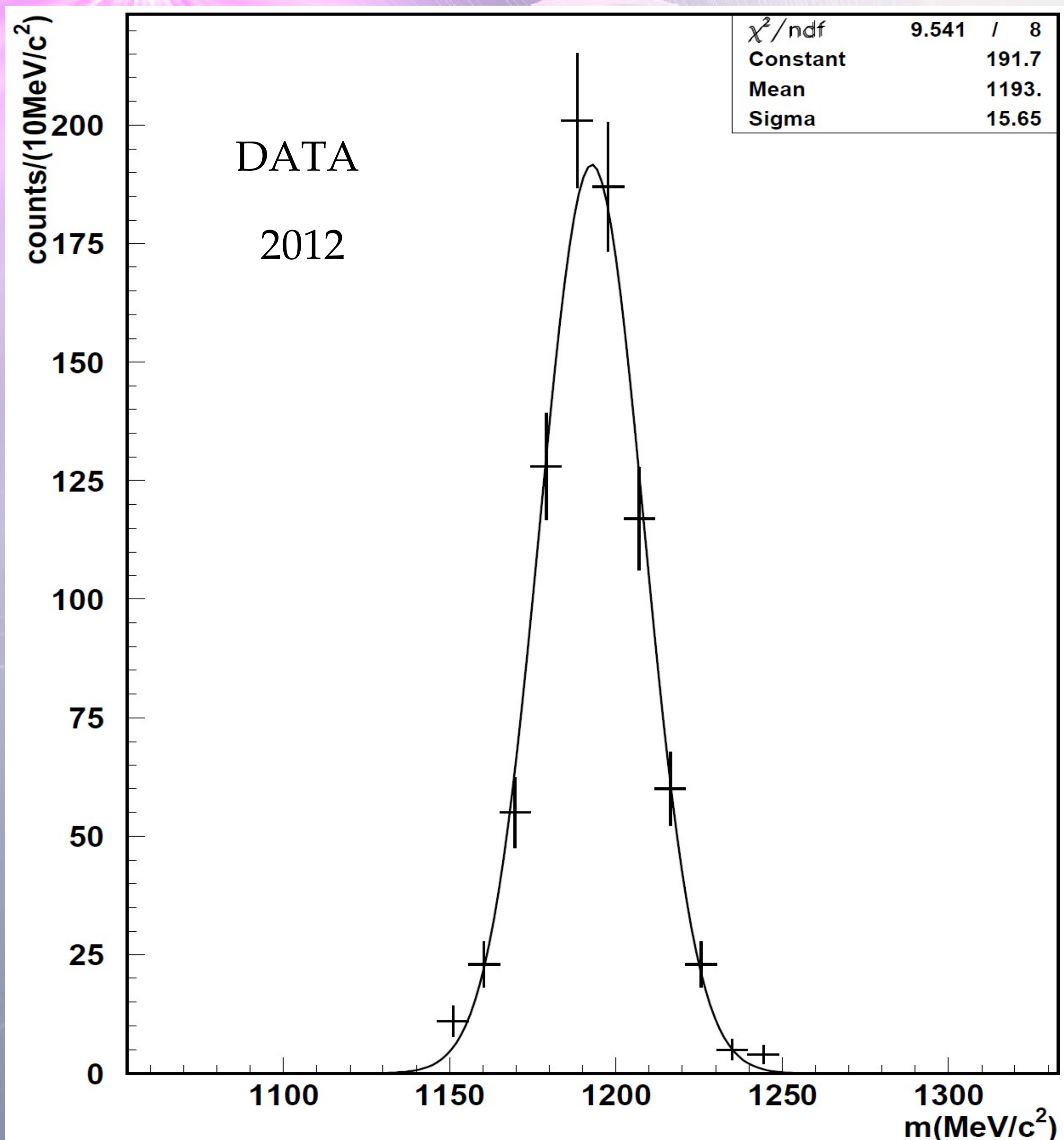

$m_{\Lambda\gamma3}$

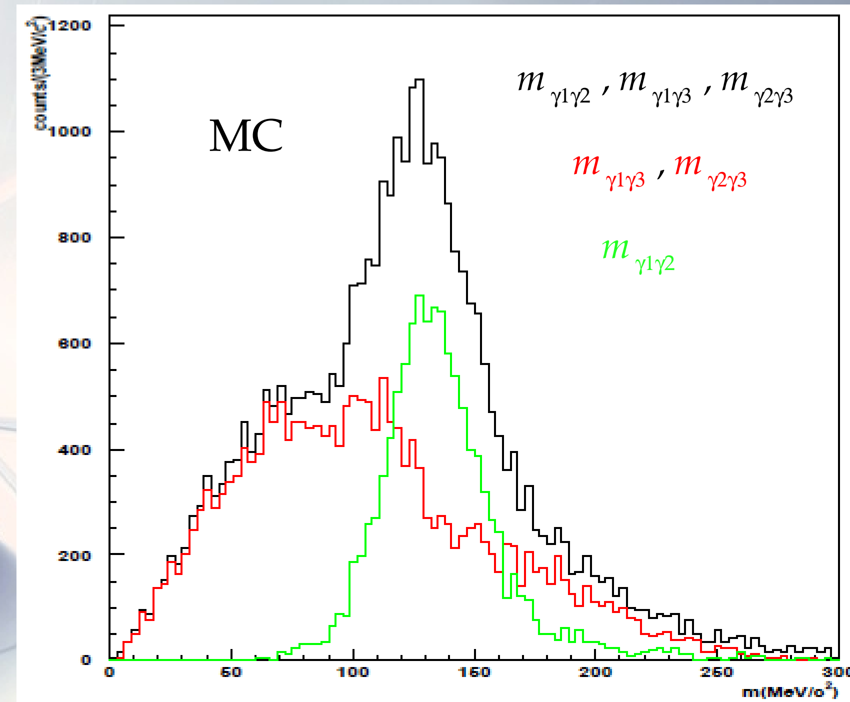

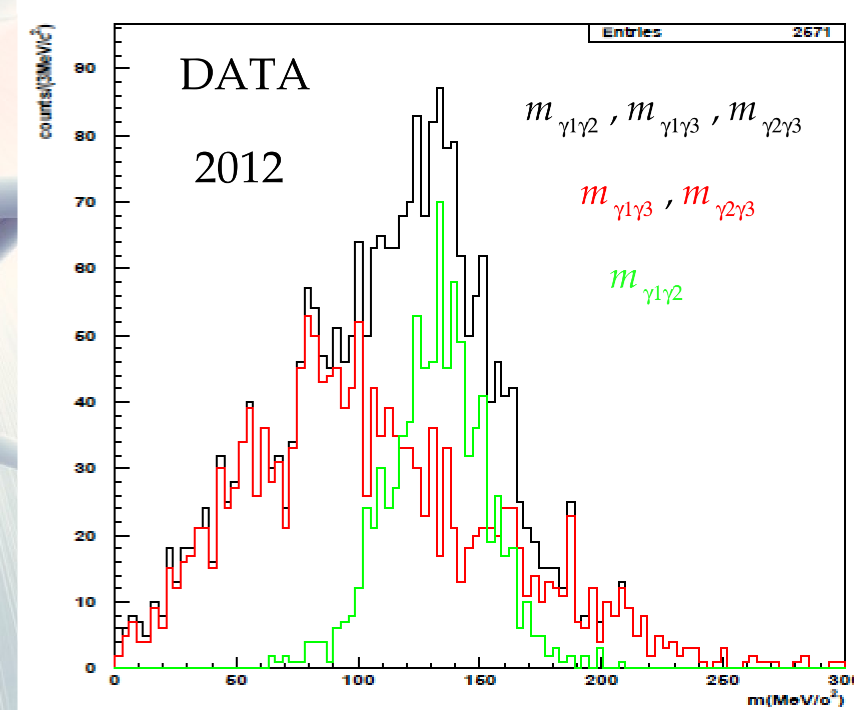

$\Sigma^0 \pi^0$ channel

K^- $\Lambda(1405)$ signal searched by K^- interaction with a bound proton in Carbon

$K^- p \rightarrow \Sigma^0 \pi^0$ detected via: $(\Lambda\gamma)$ $(\gamma\gamma)$

Strategy : K^- absorption in the DC entrance wall, mainly ^{12}C with H contamination (epoxy)

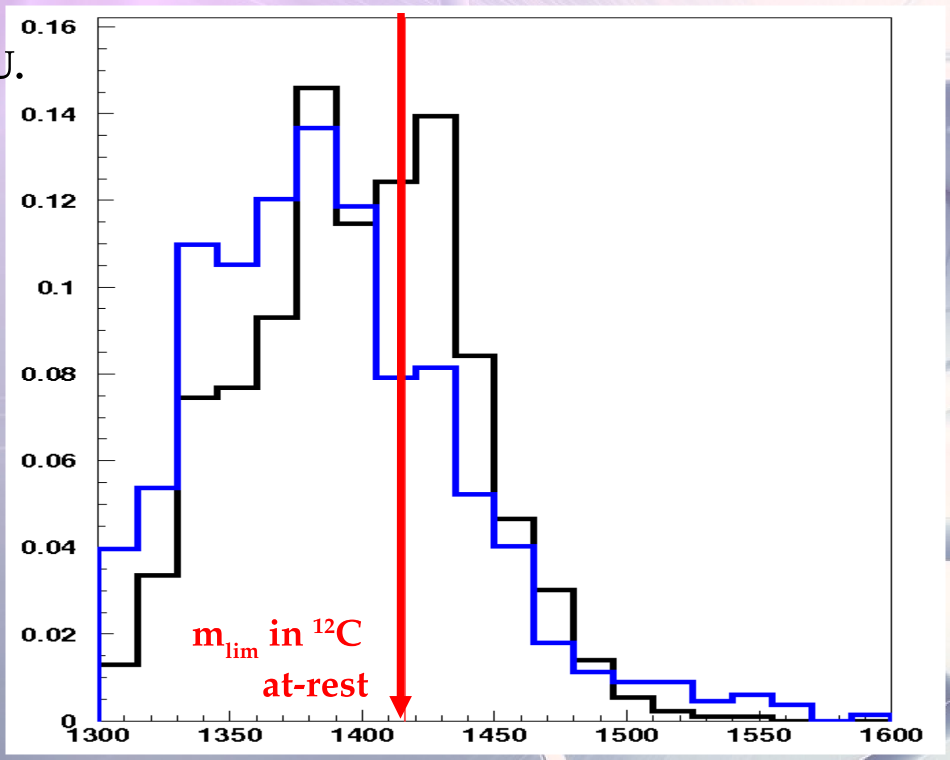

$m_{\Sigma 0 \pi 0}$ (MeV/c²)

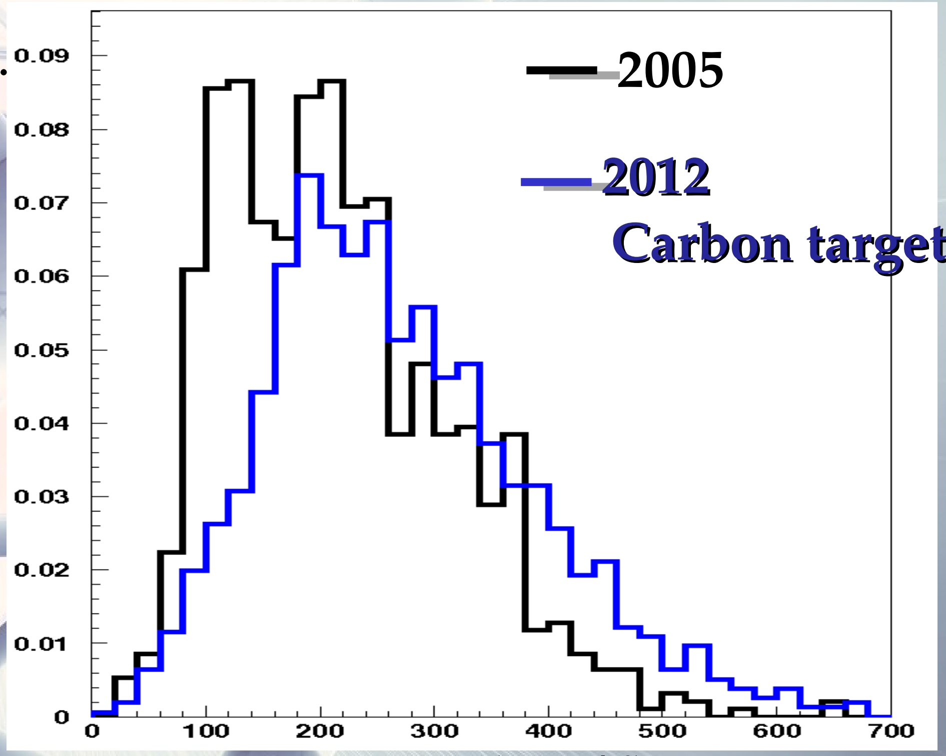

$p_{\Sigma 0 \pi 0}$ (MeV/c²)

$m_{\pi 0 \Sigma 0}$ resolution $\sigma_m \approx 32$ MeV/c² ; $p_{\pi 0 \Sigma 0}$ resolution: $\sigma_p \approx 20$ MeV/c.

Negligible ($\Lambda \pi^0$ + internal conversion) background = (3±1) % → no I=1 contamination

$\Sigma^0 \pi^0$ channel

K⁻ nuclear absorption experiments .. long history .. BUT

K^-

1) $m_{\pi\Sigma}$ spectra always cut at the at-rest limit **2) $(\Sigma\pm\pi\mp)$ spectra suffer $\Sigma(1385)$ contamination**

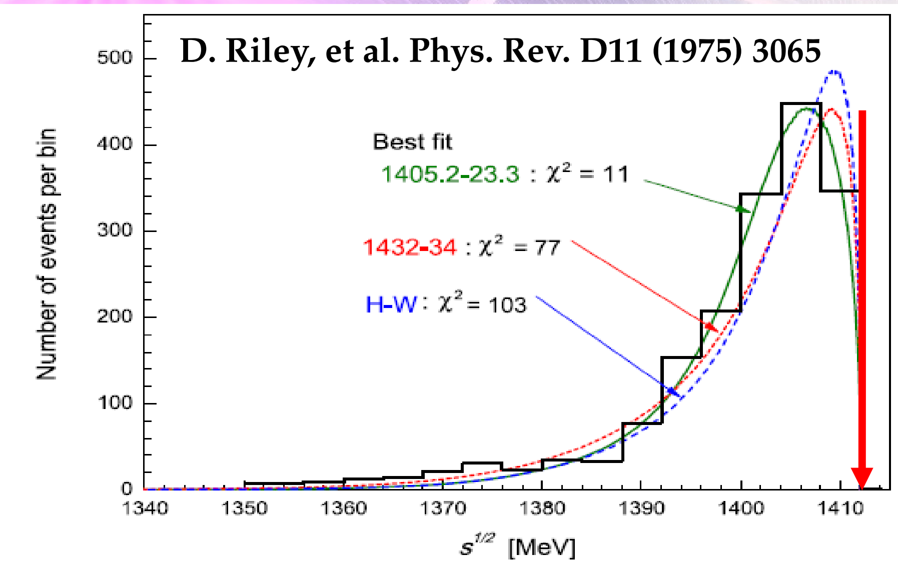

Fig. 6. Detailed differences in $M_{\Sigma\pi}$ spectra among the Hyodo–Weise prediction and the present model predictions.

P. J. Carlson, et al. Nucl. Phys. 74 642

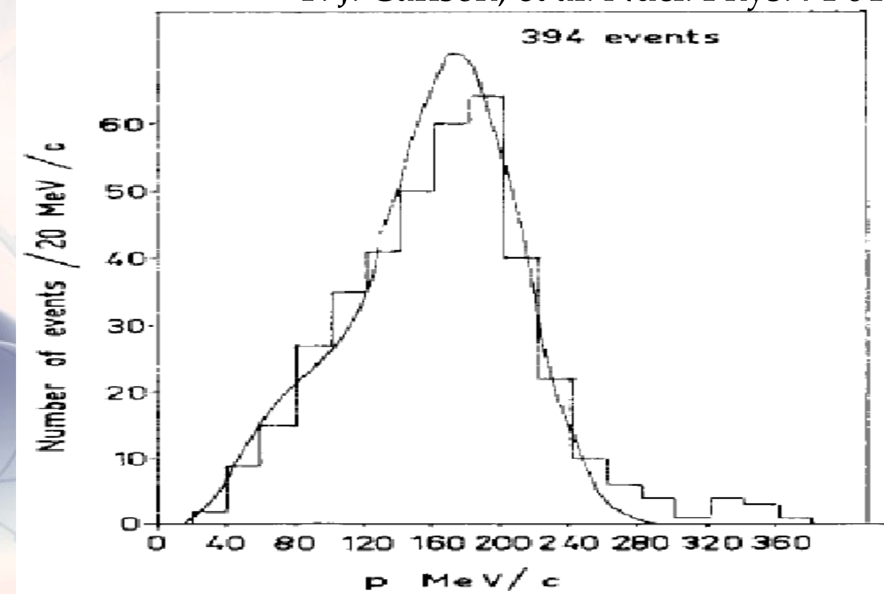

N. U.

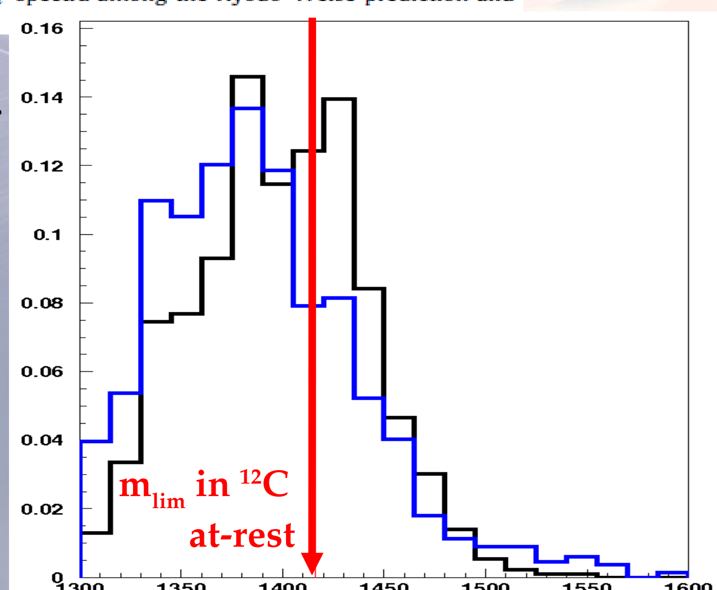

$m_{\Sigma 0 \pi 0}$ (MeV/c²)

N. U.

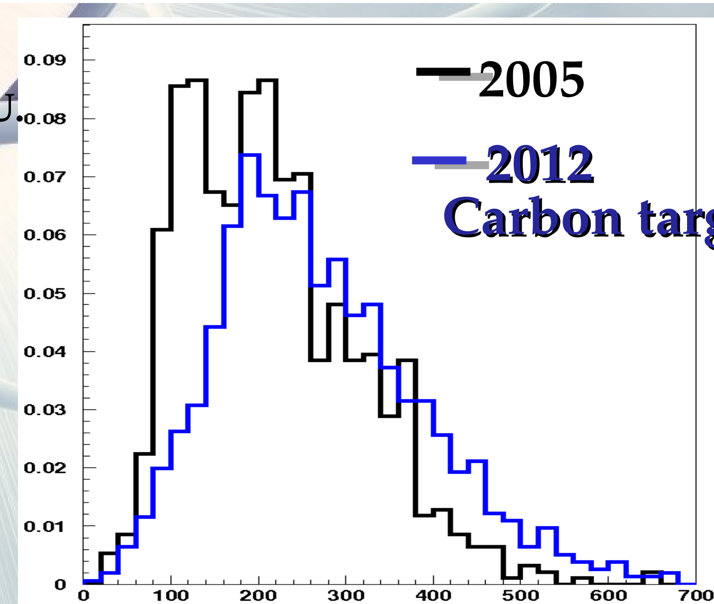

$p_{\Sigma 0 \pi 0}$ (MeV/c²)

$\Sigma^0 \pi^0$ channel

K⁻

Mass momentum correlatation

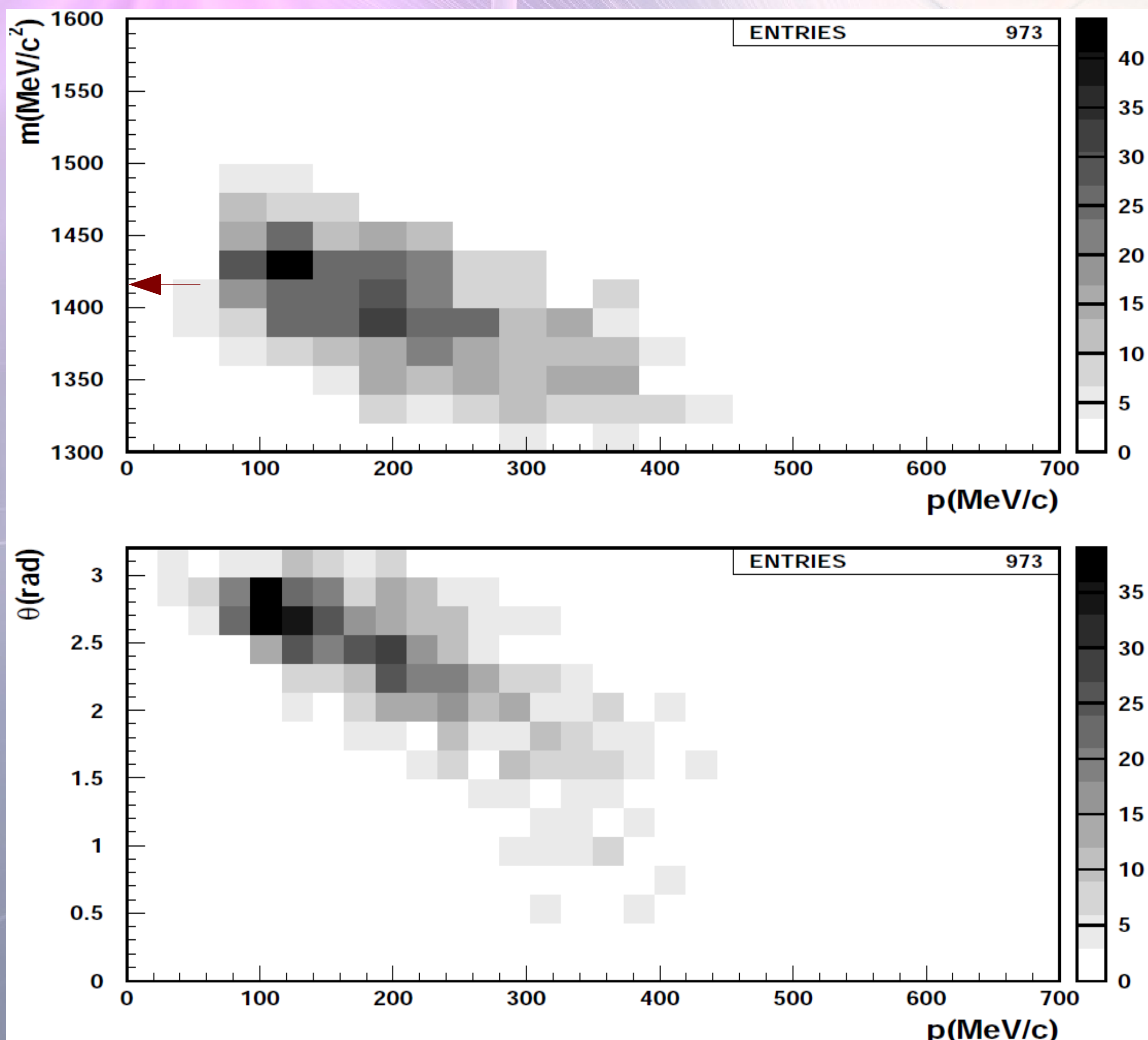

Top $m_{\Sigma^0\pi^0}$ vs $p_{\Sigma^0\pi^0}$, bottom $\theta_{\Sigma^0\pi^0}$ vs $p_{\Sigma^0\pi^0}$.

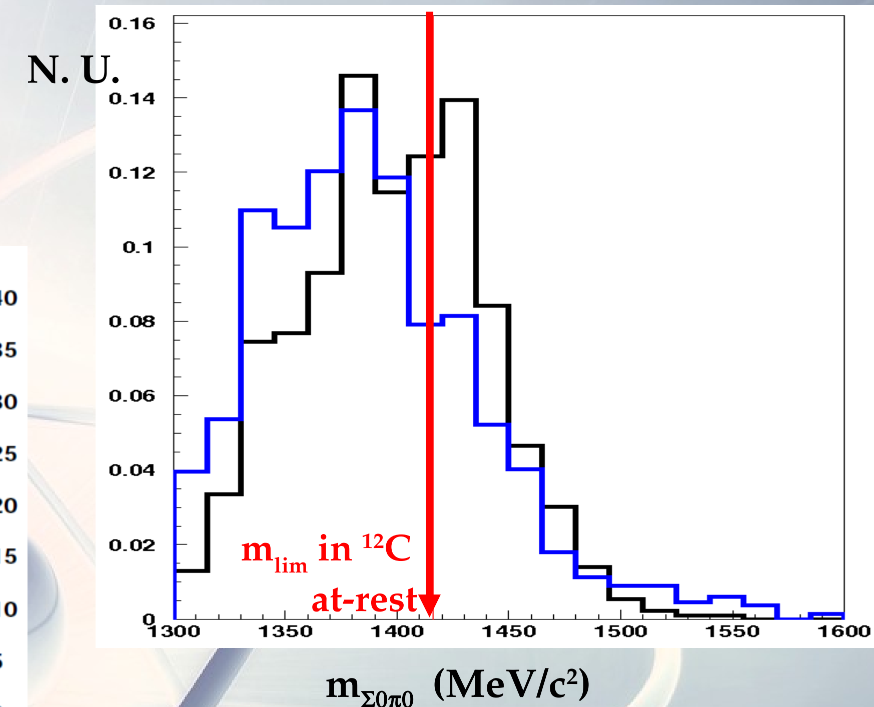

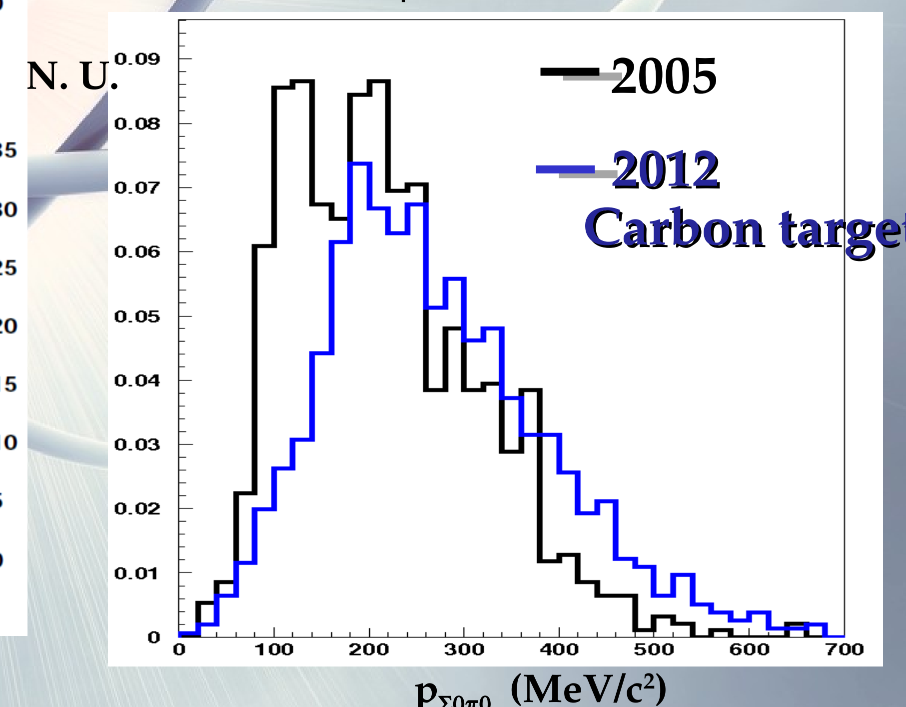

$\Sigma^0 \pi^0$ channel

in-flight component … FIRST EVIDENCE IN K^- ABSORPTION MASS SPECTROSCOPY

open a higher invariant mass region

$p_{\pi 0}$ resolution: $\sigma_p \approx 12$ MeV/c

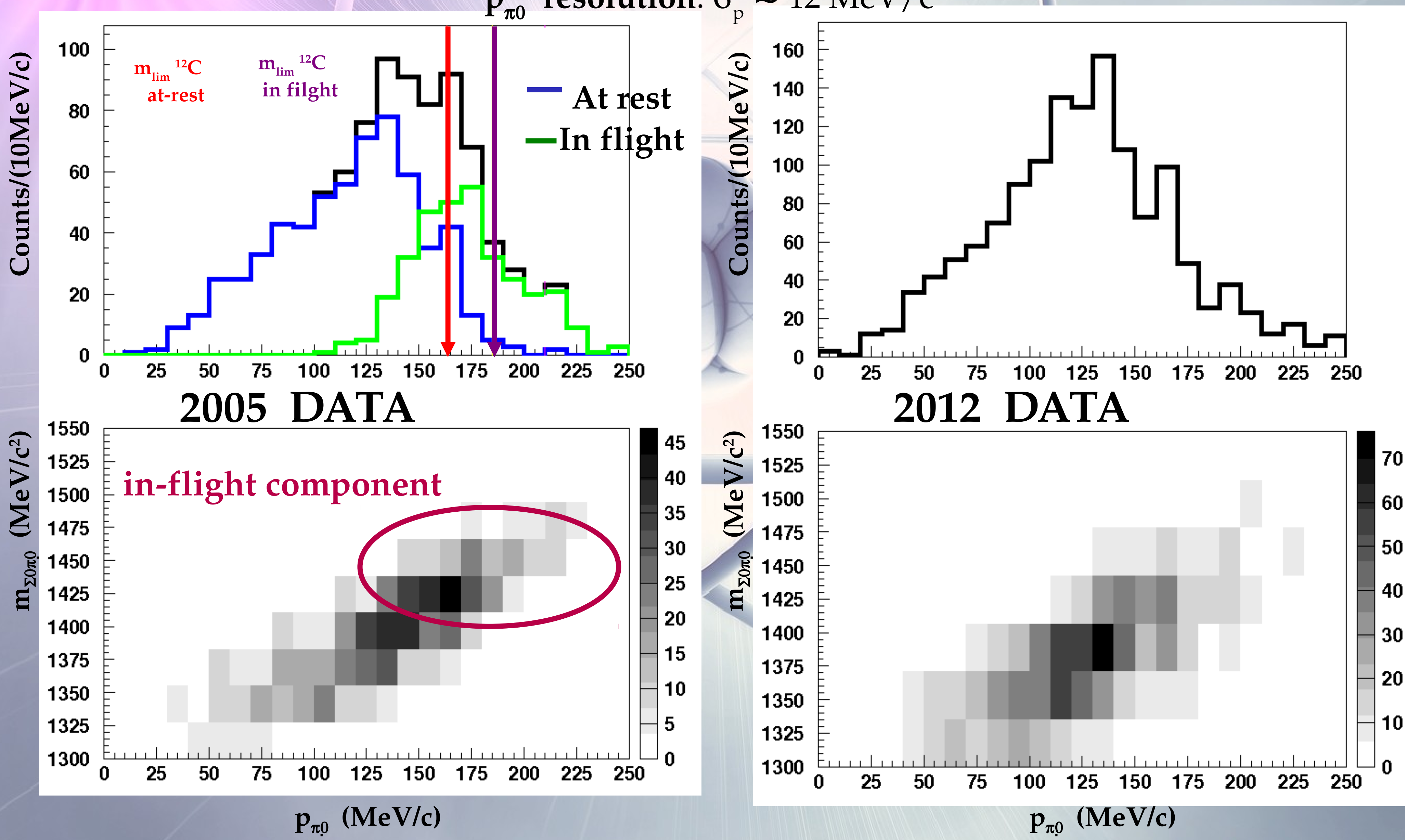

$\Sigma^0 \pi^0$ channel

Invariant mass spectra with mass hypotesis on Σ^0 and π^0 *non resonant misidentification background subtracted (left)*

$\sigma_m \approx 17\ MeV/c^2$ (DC wall) $\sigma_m \approx 15\ MeV/c^2$ (DC gas)

Similar $m_{\pi 0 \Sigma 0}$ shapes due to the similar kinematical thresholds for ^{4}He and ^{12}C.

2005 DATA

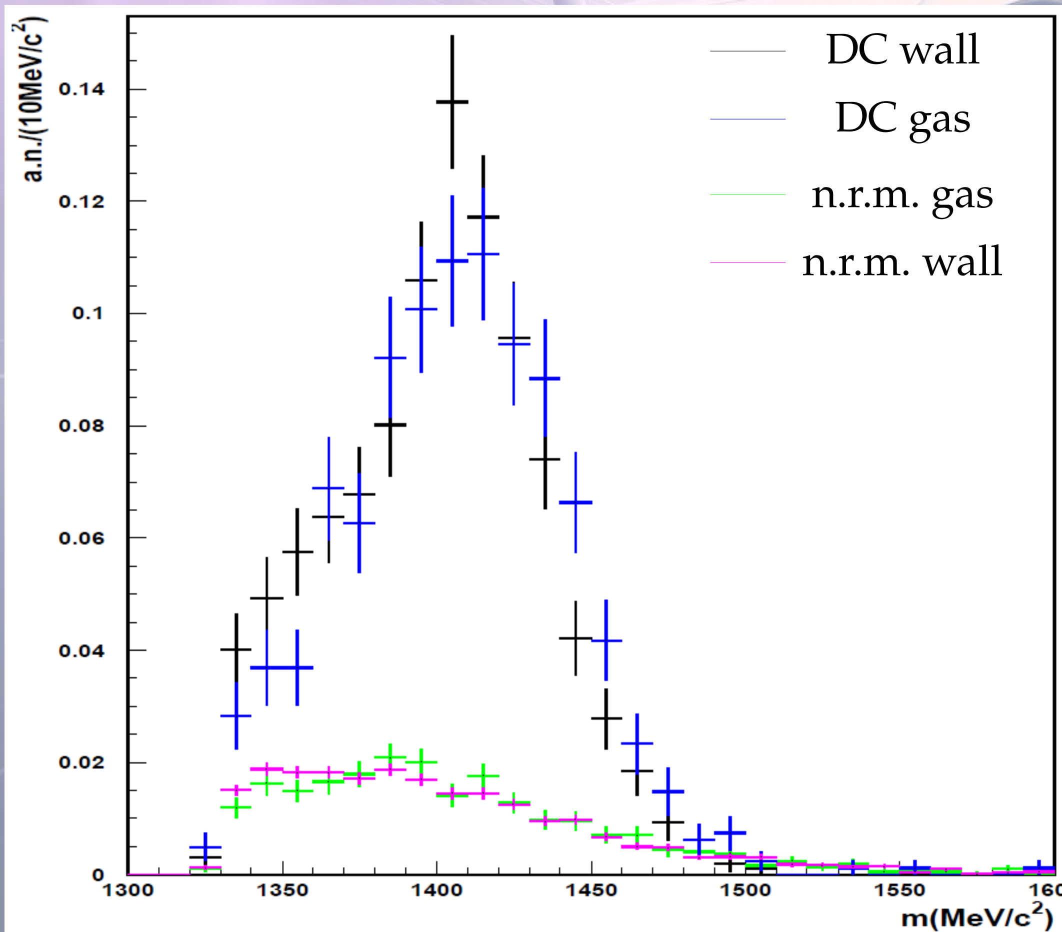

$m_{\Sigma^0\pi^0}$ *spectrum*

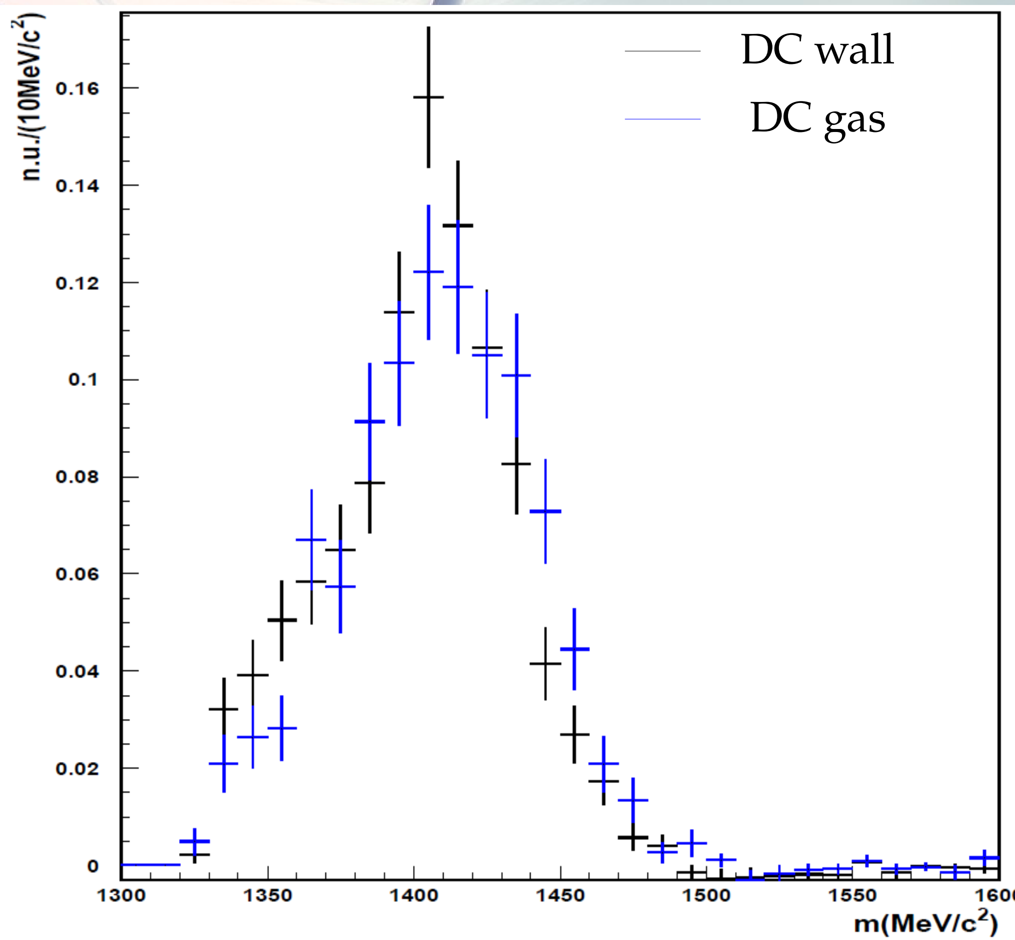

$m_{\Sigma^0\pi^0}$ *spectrum*

$\Sigma^0\ \pi^0$ channel

Acceptance corrected $m_{\pi0\Sigma0}$ spectra, DC wall (left) DC gas (right)

Acceptance function evaluated in 8 intervals of $p_{\pi0\Sigma0}$ (between 0 and 700 MeV/c) 8 intervals of $\theta_{\pi0\Sigma0}$ (between 0 and 3.15 rad) 30 intervals of $m_{\pi0\Sigma0}$ (between 1300 and 1600 MeV/c^2)

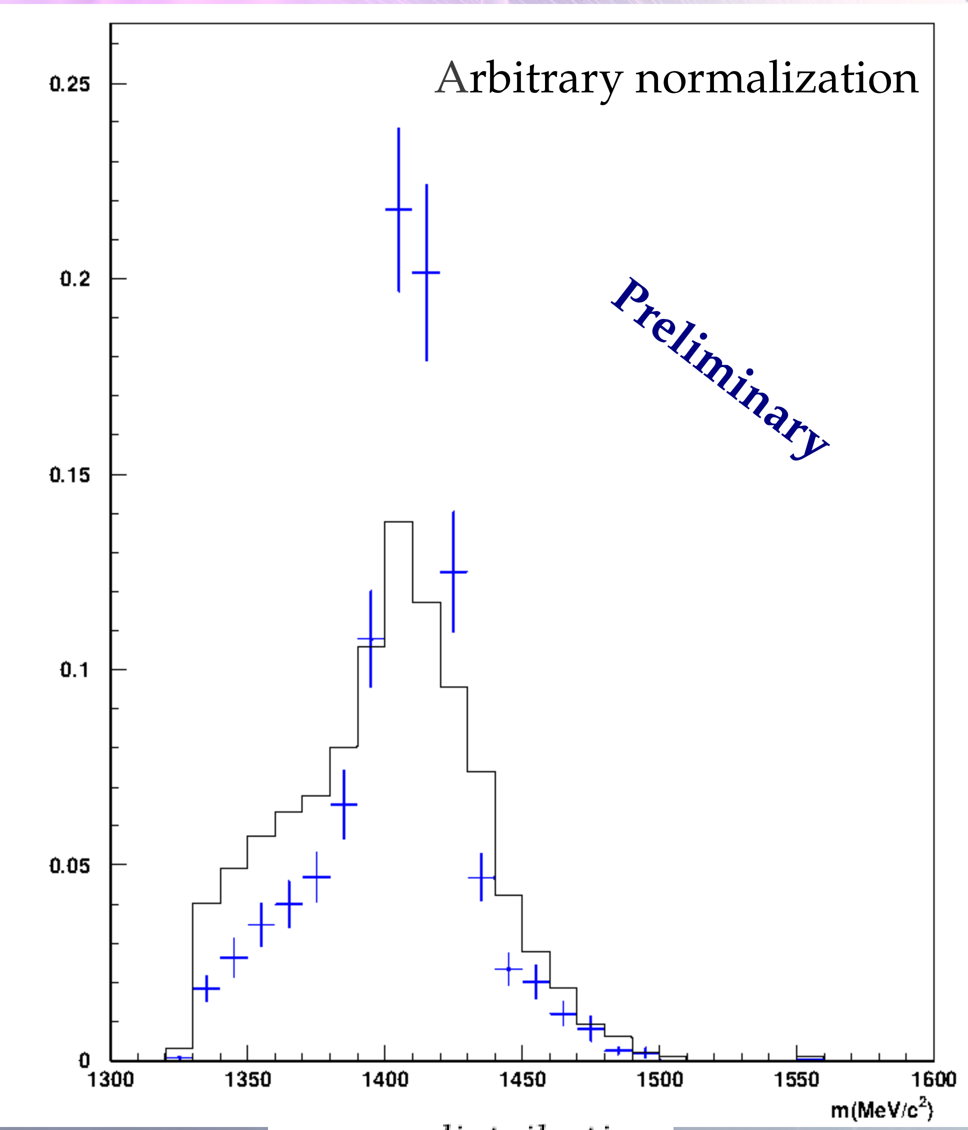

$m_{\Sigma^0\pi^0}$ *distribution*

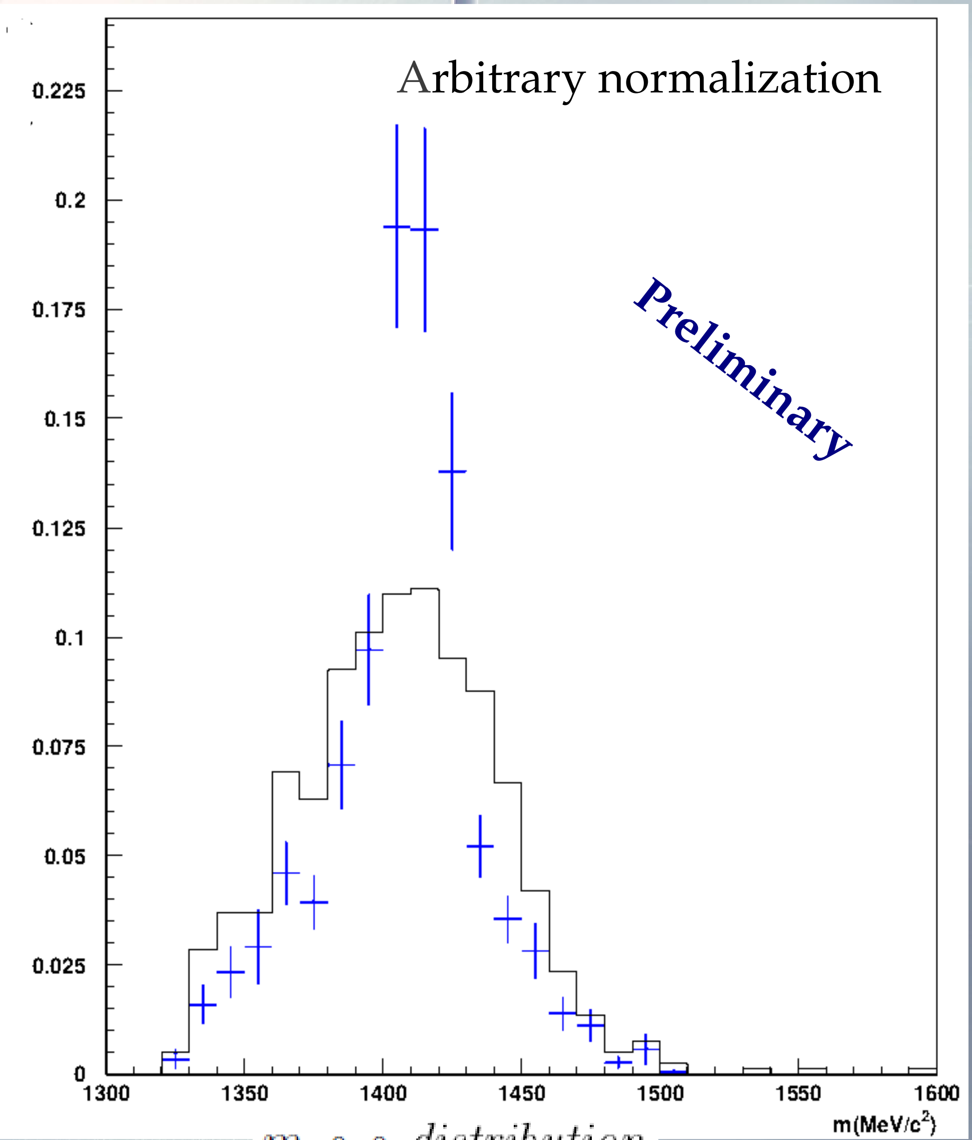

$m_{\Sigma^0\pi^0}$ *distribution*

$\Sigma^+ \pi^-$ channel

$K^- p \rightarrow \Sigma^+ \pi^-$ detected via: $(p\pi^0)\, \pi^-$

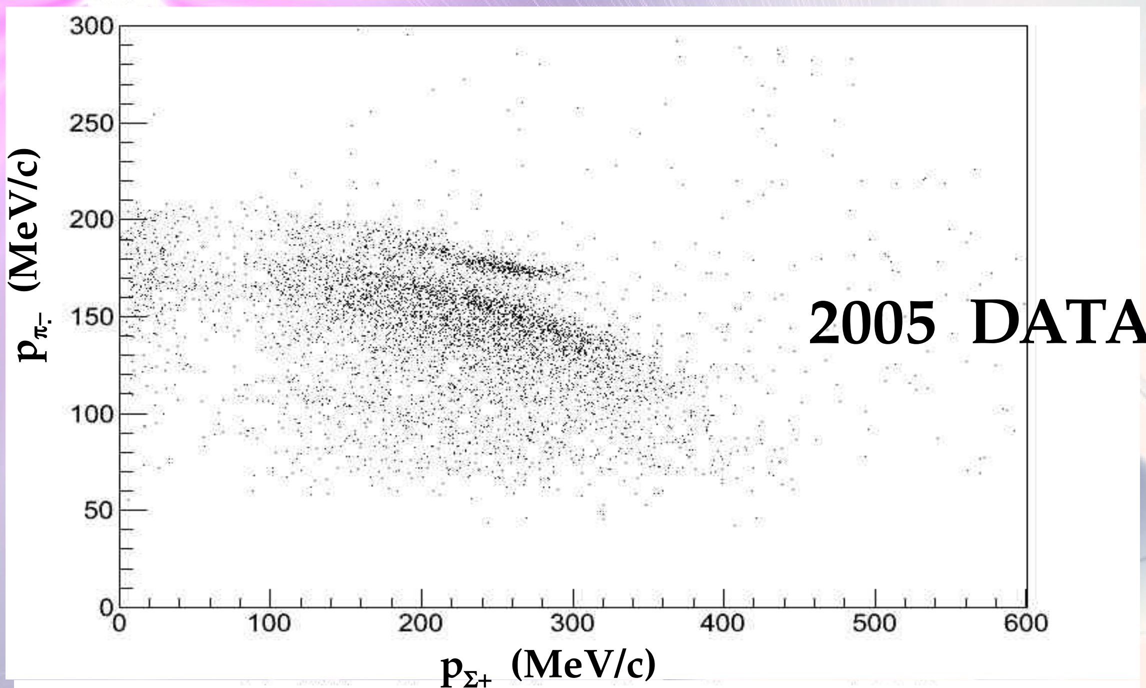

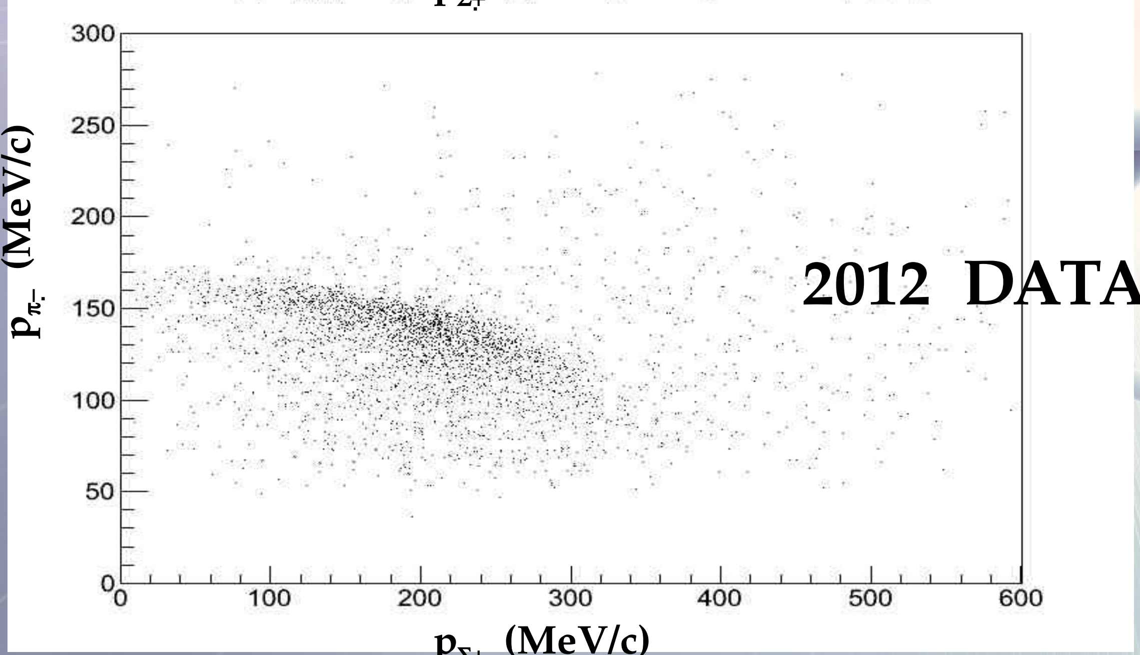

in-flight components clearly evidenced by the excellent p_{π^-} resolution ...

$\Sigma^+ \pi^-$ channel

$K^- p \rightarrow \Sigma^+ \pi^-$ detected via: $(p\pi^0)\, \pi^-$

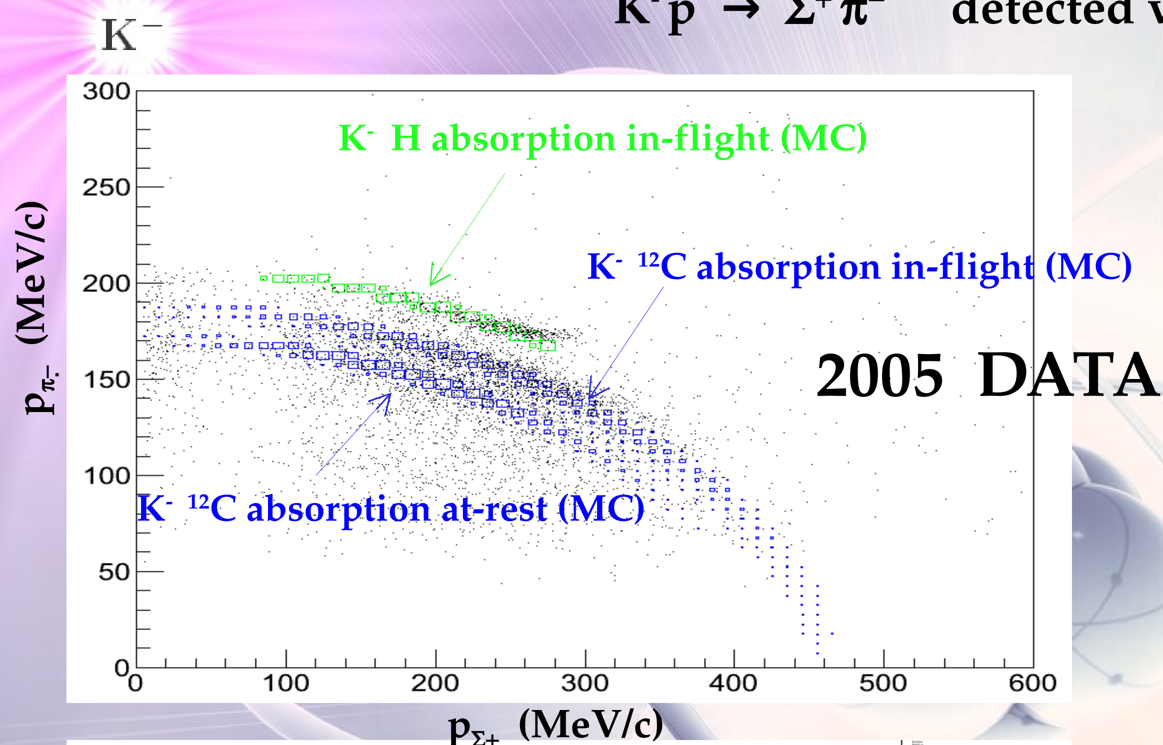

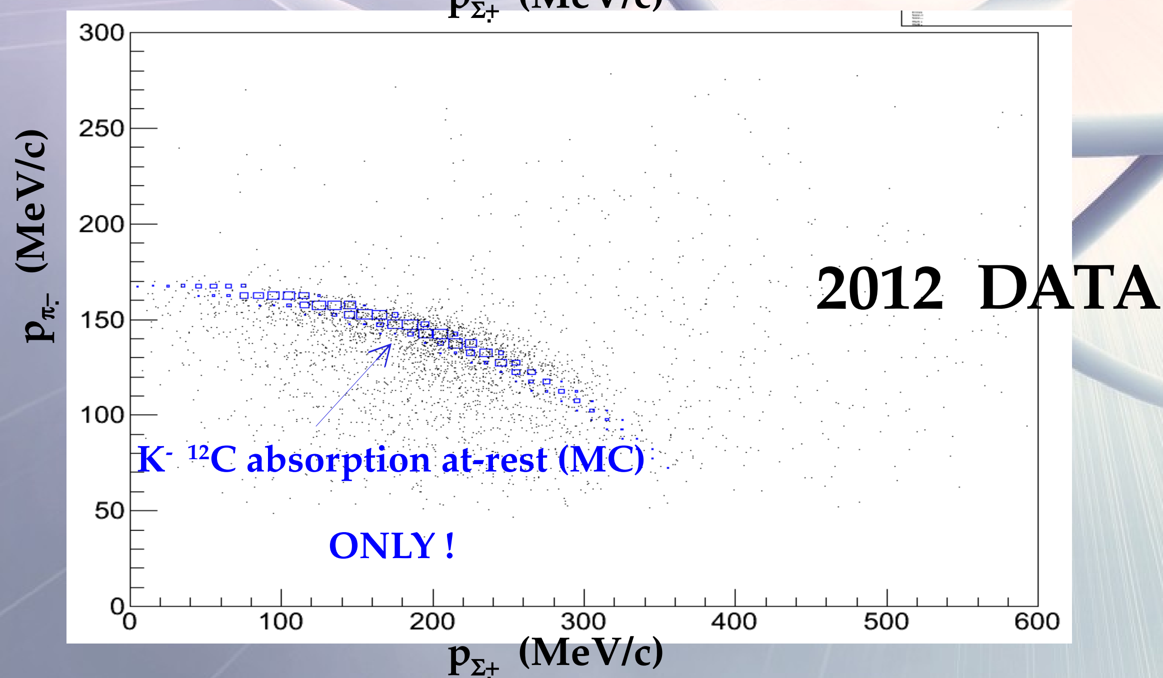

… in-flight components clearly evidenced by the excellent p_{π^-} resolution

$\Sigma^+ \pi^-$ channel

$K^- p \rightarrow \Sigma^+ \pi^-$ detected via: $(p\pi^0)\, \pi^-$

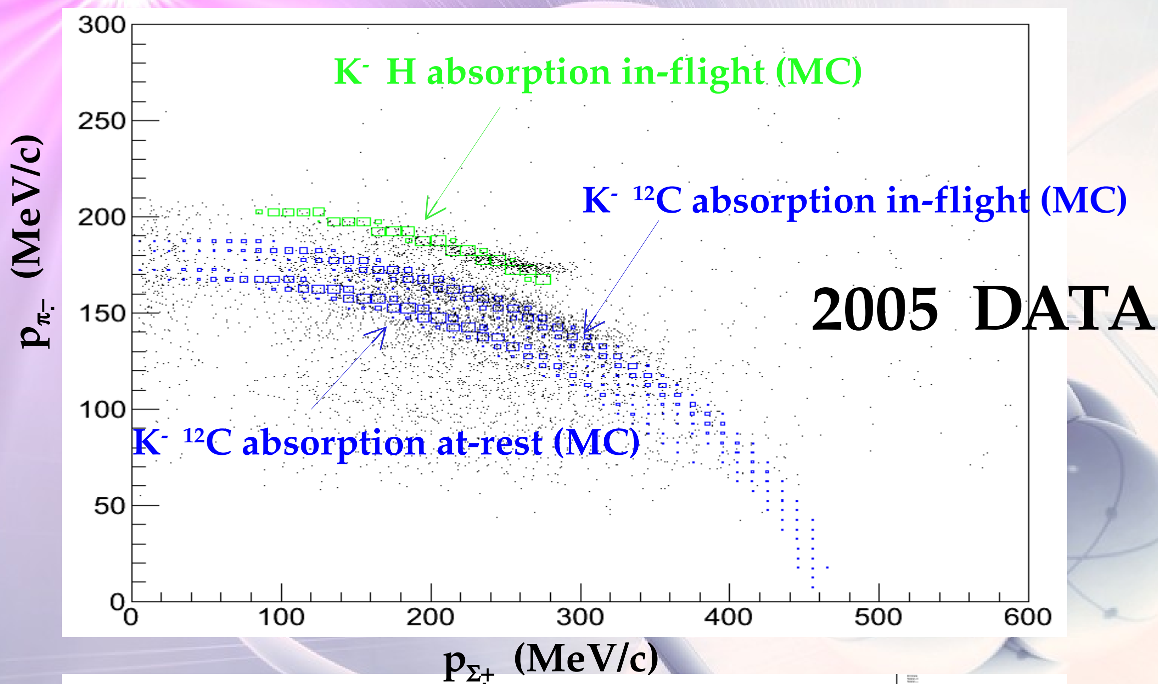

2005 data

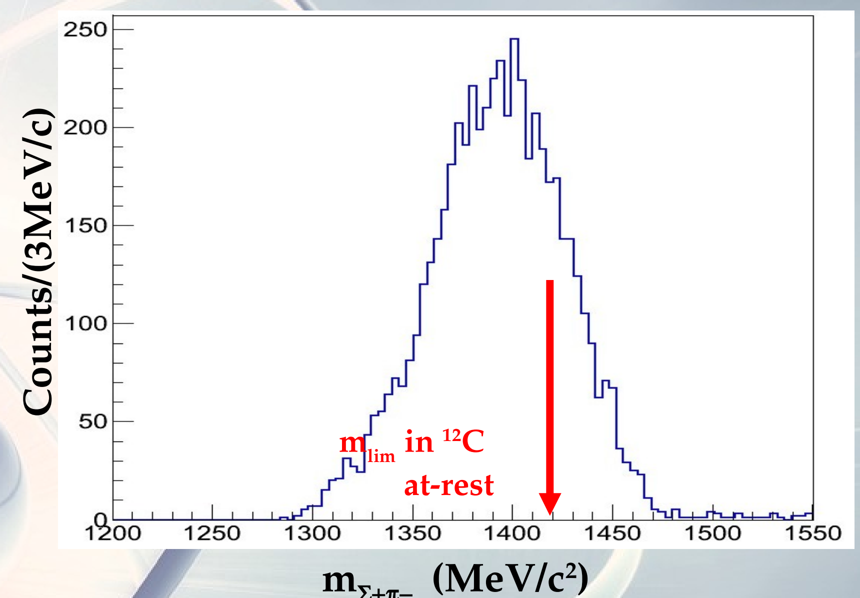

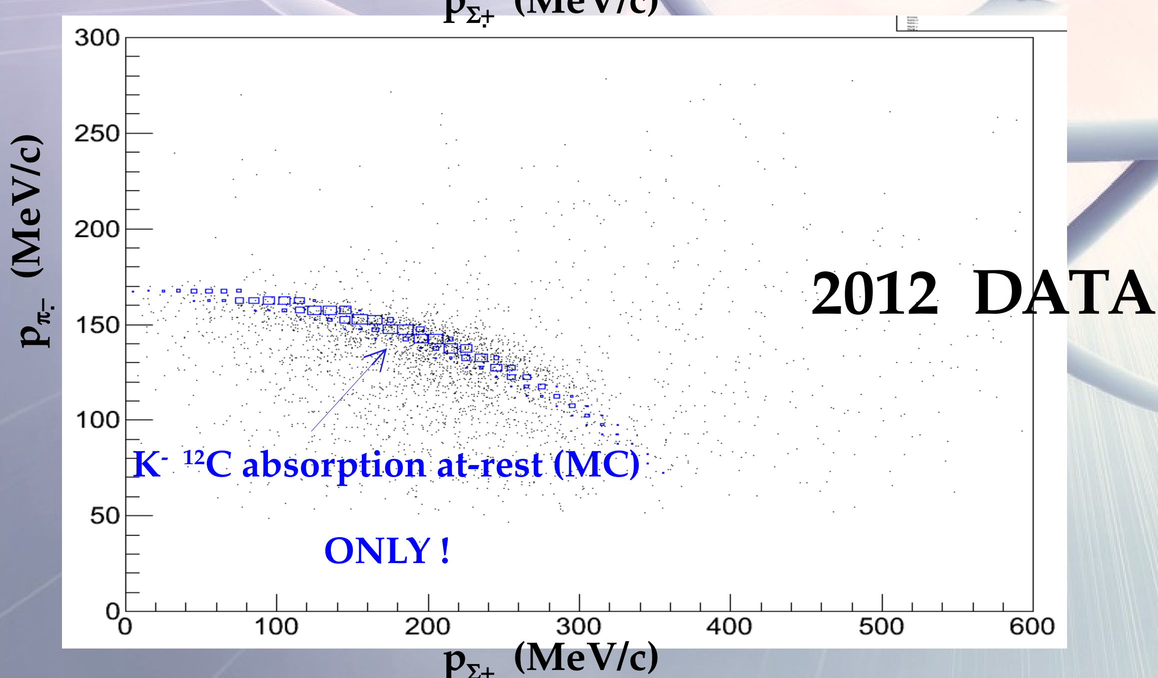

2012 Carbon target

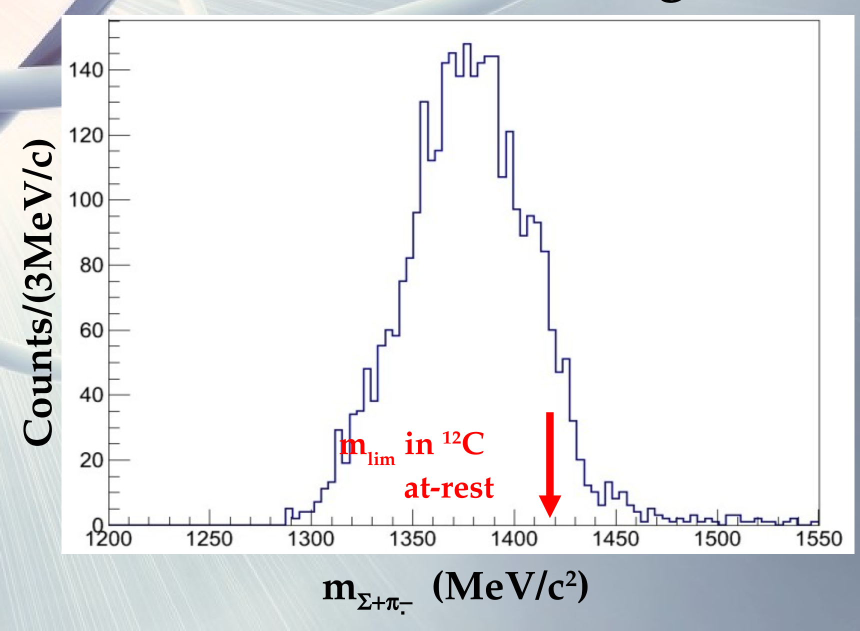

Σ / Λ conversion in nuclear medium

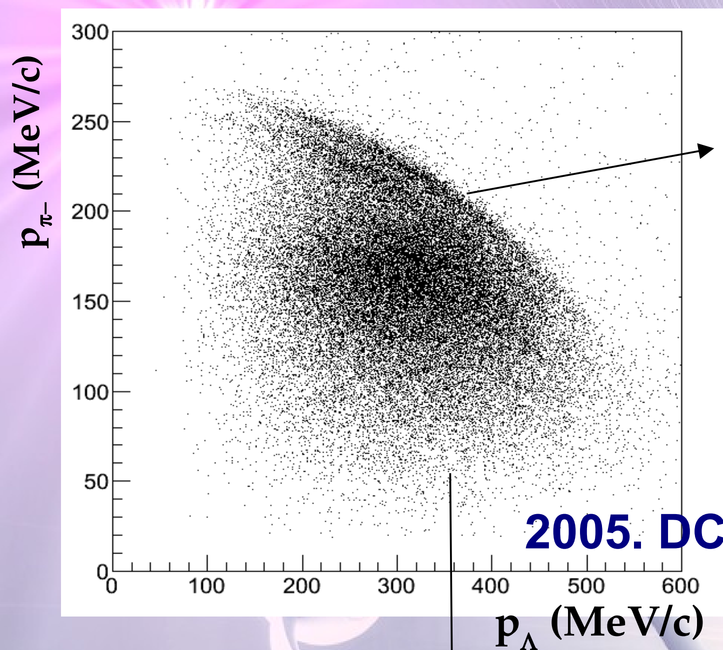

Direct formation $K^- n \rightarrow \Lambda\pi^-$

Clearly visible the 2 bands:

- **in flight**
- **at rest**

(only events at rest in Carbon Target)

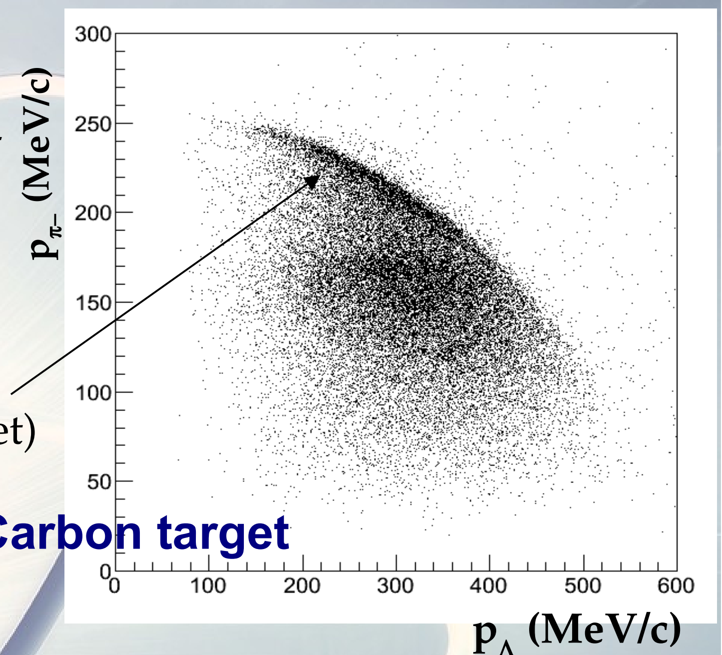

2005. DC-wall carbon

2012 Carbon target

2 step process: $\Lambda\pi^-$ **production follows** Σ^+/Σ^0 **production**
Main contribution from internal conversion

$K^- p \rightarrow \Sigma^+\pi^-$, $\Sigma^+ n \rightarrow \Lambda p$

- The data in this channel is of great value to confirm the predicted branching ratio modifications in medium

- Σ/Λ internal conversion rates can be obtained as well in function of Z

Σ / Λ conversion in nuclear medium

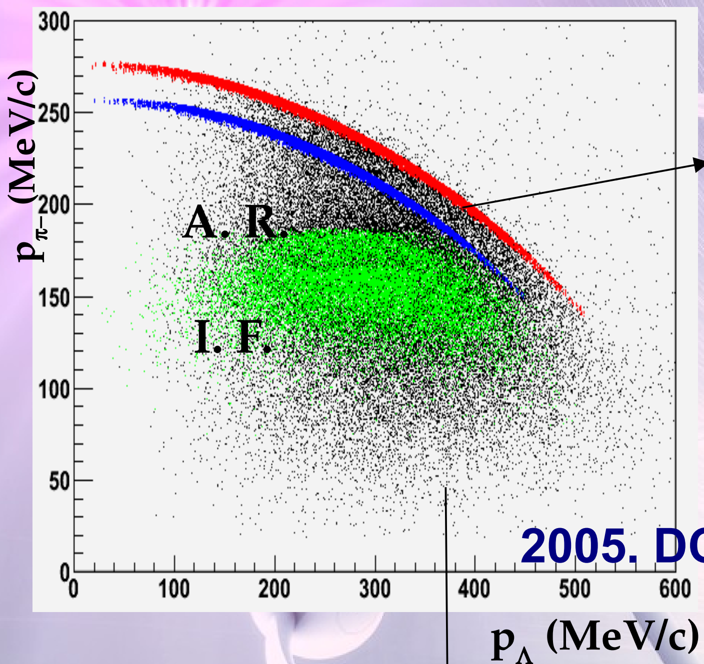

Direct formation $K^- n \rightarrow \Lambda\pi^-$

Clearly visible the 2 bands:

- **in flight**
- **at rest**

(only events at rest in Carbon Target)

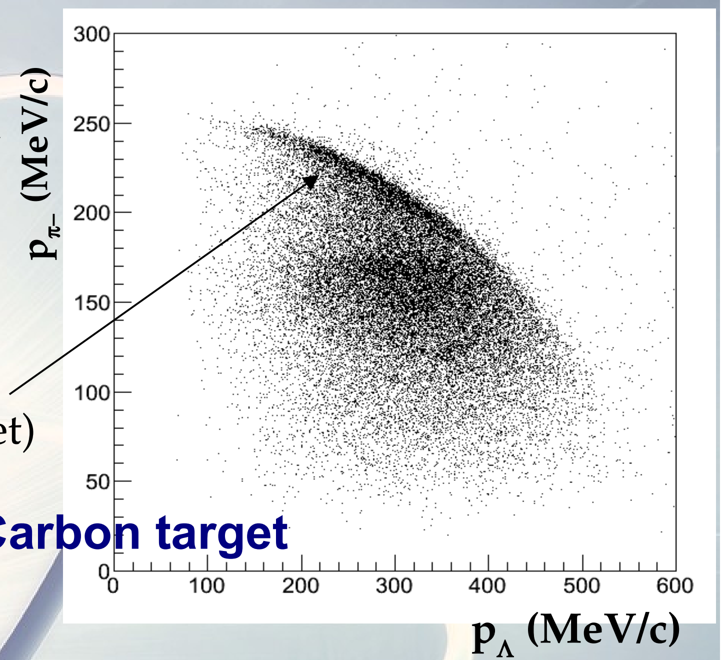

2005. DC-wall carbon

2012 Carbon target

2 step process: $\Lambda\pi^-$ **production follows** Σ^+ / Σ^0 **production**
Main contribution from internal conversion

$$K^- p \rightarrow \Sigma^+\pi^- \quad , \quad \Sigma^+ n \rightarrow \Lambda p$$

- The data in this channel is of great value to confirm the predicted branching ratio modifications in medium

- Σ/Λ internal conversion rates can be obtained as well in function of Z

Concluding $\Sigma^0\pi^0$ / $\Sigma^+\pi^-$ channel

- The $p_{\Sigma 0\pi 0}$ distribution shows a double component structure reflected in the $\theta_{\Sigma 0\pi 0}$ vs $p_{\Sigma 0\pi 0}$ and $m_{\Sigma 0\pi 0}$ vs $p_{\Sigma 0\pi 0}$ correlations. Such correlation is confirmed by the analysis of $p_{\pi 0}$ with similar behaviours in Helium and Carbon.

- The two components are interpreted as due to at-rest and in-flight absorptions of K^-, responsible for masses above the kinematical limit.

- Interepretation is confirmed by the analysis of K^- stop events in pure Carbon target installed in KLOE.

First in flight evidence in $m_{\Sigma\pi}$ from K^- - nuclear absorption!

Interesting future perspectives …

- $\Sigma^+\pi^-$ work in progress .. $\Sigma^-\pi^+$ started work (difficulty of neutrons)

- Branching ratio modifications in different targets (see A. Ohnishi et al., Phys. Rev. C 56 5 (1997) 2767)

- Density dependence of $m_{\Sigma\pi}$ and $p_{\Sigma\pi}$ (see L. R. Staronski, S. Wycech, Nucl. Phys. 13 (1987) 1361 / E. Friedman, A. Gal, arXiv:1211.6336v3 [nucl-th] 2013)

1. Low energy kaon-nuclei interaction studies through the \Sigma^0\pi^0 channel with the KLOE detector, K. Piscicchia, C. Curceanu, A. Scordo, I. Tucakovic, O. Vazquez Doce. Apr 26, 2013. 10 pp. e-Print: arXiv:1304.7165 [nucl-ex]

2. Study of Sigma+pi- Invariant Mass spectrum with the KLOE detector; preliminary results and possible hints for Sigma+n internal conversion, O. Vazquez Doce on behalf of AMADEUS Collaboration (A. Scordo et al.). Apr 26, 2013. e-Print: arXiv:1304.7149 [nucl-ex]

3. A GEM-based Time Projection Chamber for the AMADEUS experiment, M. Poli Lener, M. Bazzi, G. Corradi, C. Curceanu, A. D'Uffizi, C. Paglia, E. Sbardella, A. Scordo, D. Tagnani, A. Romero Vidal et al.. Apr 23, 2013. e-Print: arXiv:1304.6206

4. Kaon-nuclei interaction studies at low energies (the AMADEUS project), AMADEUS Collaboration (K. Piscicchia (INFN, Rome & Rome U.) et al.). Mar, 6, 2013. 3 pp. Published in Nuovo Cim. C36 (2013) DOI: 10.1393/ncc/i2013-11436-3

5. Kaon-nuclei interaction studies at low energies (the AMADEUS project), Kristian Piscicchia (Frascati & Rome III U.), M. Bazzi, C. Berucci, (Frascati), D. Bosnar (Zagreb U.), A.M. Bragadireanu (Frascati & Bucharest U.), M. Cargnelli (Stefan Meyer Inst. Subatomare Phys.), A. Clozza, C. Curceanu, A. D'Uffizi (Frascati), F. Ghio (INFN, Rome) et al., 2012. 4 pp. Published in EPJ Web Conf. 37 (2012) 07002 DOI: 10.1051/epjconf/20123707002

6. Performances of a GEM-based Time Projection Chamber prototype for the AMADEUS experiment, M. Poli Lener, M. Bazzi, G. Corradi, C. Curceanu, A. D'Uffizi, C. Paglia, A. Romero Vidal, E. Sbardella, A. Scordo, D. Tagnani et al.. Feb 13, 2013. e-Print: arXiv:1302.3054

7. Characterization of a scintillating fibers read by MPPC detectors trigger prototype for the AMADEUS experiment, A. Scordo, M. Bazzi, C. Berucci, C. Curceanu, A. D'Uffizi, K. Piscicchia, M.Poli Lener, A.Romero Vidal, E. Sbardella, O.Vazquez Doce. Jan 2013. 9 pp. e-Print: arXiv:1301.7268 [

8. Experimental tests of the trigger prototype for the AMADEUS experiment based on Sci-Fi read by MPPC, M. Bazzi, C. Berucci, G. Corradi, C. Curceanu, A. D'Uffizi, K. Piscicchia, M. Poli Lerner, A. Rizzo, A. Romero Vidal, E. Sbardella (Frascati) et al.. Apr 2012. 4 pp. Published in Nucl.Instrum.Meth. A671 (2012) 125-128

9. Kaon-nuclei interaction studies at low energies (the AMADEUS experiment) Kristian Piscicchia, M. Bazzi, C. Berucci (Frascati), L. Bombelli (Milan Polytechnic), A.M. Bragadireanu (Frascati & Bucharest, IFIN-HH), M. Cargnelli (Stefan Meyer Inst. Subatomare Phys.), A. Clozza, C. Curceanu, A. d'Uffizi (Frascati), F. Ghio (INFN, Rome & Rome, ISS) et al.. 2011. 7 pp. Published in PoS STORI11 (2011) 021

10. Low-energy kaon-nucleon/nuclei interaction studies at DAFNE (SIDDHARTAand AMADEUS experiments), C. Curceanu (Petrascu), M. Bazzi, C. Berucci, A. Clozza, G. Corradi, A. D'Uffizi, C. Fiorini, C. Guaraldo, M. Iliescu, P. Levi Sandri (Frascati) et al.. Oct 2011. 5 pp. Published in Nuovo Cim. C34N6 (2011) 23-27

11. Experimental tests of the trigger prototype for the AMADEUS experiment based on Sci-Fi read by MPPC, M. Bazzi, C. Berucci, G. Corradi, C. Curceanu, A. D'Uffizi, K. Piscicchia, M. Poli Lerner, A. Rizzo, A. Romero Vidal, E. Sbardella (Frascati) et al.. Apr 2012. 4 pp. Published in Nucl.Instrum.Meth. A671 (2012) 125-128

12. Studies of antikaon interactions with nucleons at DAFNE, O. Vazquez Doce, M. Bazzi, C. Berucci, A. Clozza, C. Curceanu, C. Guaraldo, M. Iliescu, P. Levi Sandri, S. Okada, K. Piscicchia (Frascati) et al.. Mar 2011. 4 pp. Published in AIP Conf.Proc. 1388 (2011) 572-575

13. Low-energy kaon-nucleon/nuclei interaction studies at DAFNE (SIDDHARTA and AMADEUS experiments), C. Curceanu (Petrascu), M. Bazzi (Frascati), G. Beer (Victoria U.), L. Bombelli (Milan Polytechnic), A.M. Bragadireanu (Frascati & NILPRP, Bucharest), M. Cargnelli (Stefan Meyer Inst. Subatomare Phys.), G. Corradi, A. d'Uffizi (Frascati), C. Fiorini, T. Frizzi (Milan Polytechnic) et al.. 2011. 3 pp. Published in Few Body Syst. 50 (2011) 447-449

14. Performances of a GEM-based TPC prototype for new high-rate particle experiments, M. Poli Lener, G. Corradi, C. Curceanu, A. Romero Vidal, A. Rizzo, D. Tagnani (Frascati), J. Zmeskal (Stefan Meyer Inst. Subatomare Phys.). 2010. 3 pp. Published in Nucl.Instrum.Meth. A617 (2010) 183-185

15. The AMADEUS experiment: Precision measurements of low-energy antikaon nucleus/nucleon interactions J. Zmeskal (Vienna, OAW), M. Bazzi (Frascati), M. Bragadireanu (Bucharest, IFIN-HH), P. Buhler, M. Cargnelli (Vienna, OAW), C. Curceanu (Frascati), F. Ghio (Rome, ISS), C. Guaraldo, M. Iliescu (Frascati), T. Ishiwatari (Vienna, OAW) et al.. 2010. 4 pp. Published in Nucl.Phys. A835 (2010) 410-413

16. Kaonic atoms / nuclei measurements at DAFNE: SIDDHARTA and AMADEUS SIDDHARTA and AMADEUS Collaborations (C. Curceanu (Frascati) et al.). 2008. 4 pp. Published in Mod.Phys.Lett. A23 (2008) 2524-2527

AMADEUS and SIDDHARTA & DAΦNE

K^-

Completely neutral channel:

$\Lambda \rightarrow n\ \pi^0$

Possibility to detect neutrons!

black MC **red data**

Perspective: $\Sigma^-\pi^+ \rightarrow (n\pi^-)\ \pi^+$

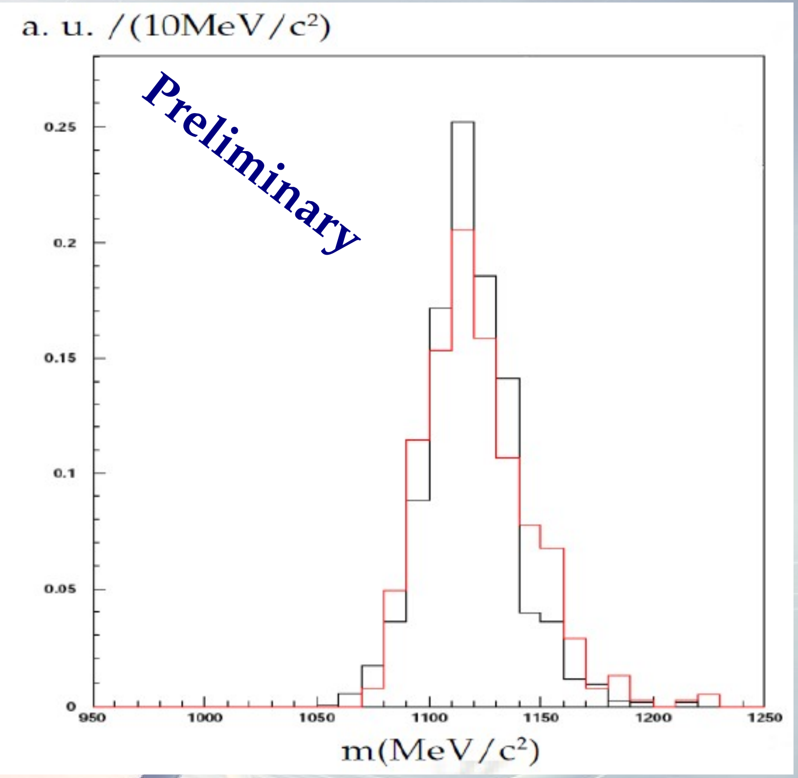

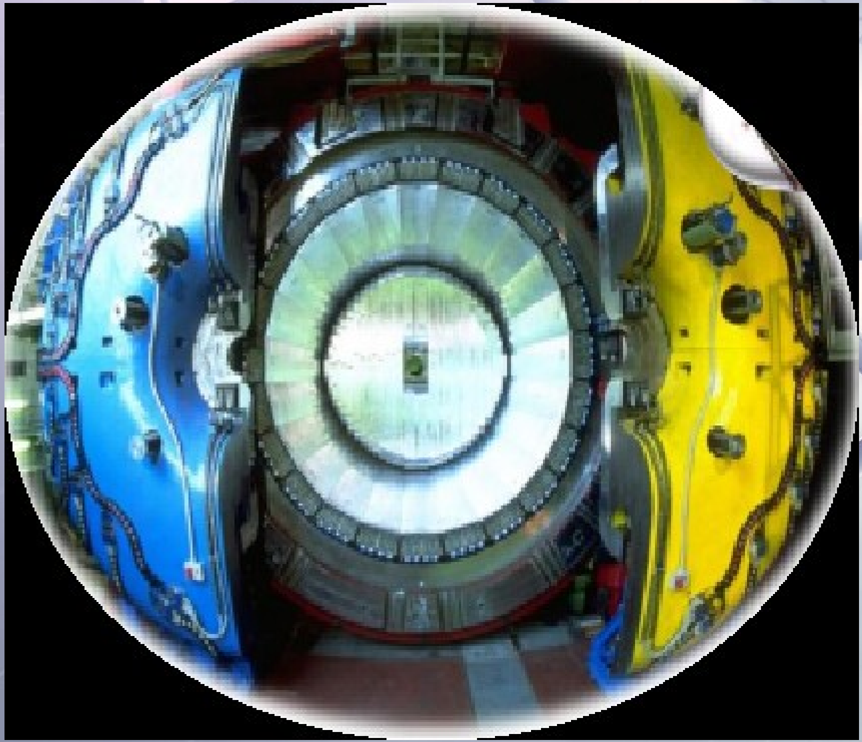

KLOE

- 96% acceptance,
- optimized in the energy range of all charged particles involved
- good performance in detecting photons (and neutrons checked by kloNe group (M. Anelli et al., Nucl Inst. Meth. A 581, 368 (2007)))

Σ / Λ conversion in nuclear medium

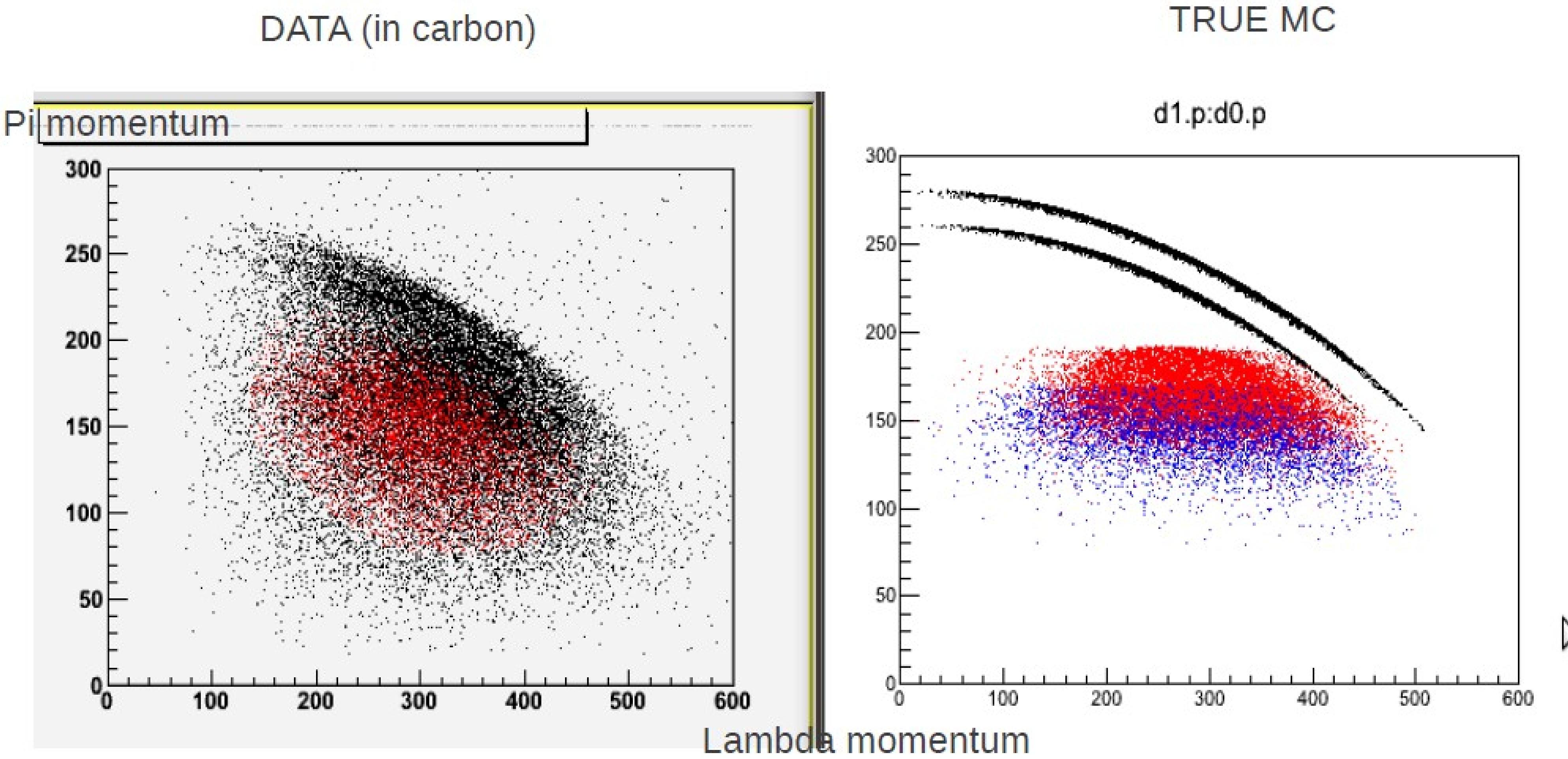

Black-> lambda + pi-
Red-> lambda + pi- **+ proton**

Black-> direct lambda prod
Red-> S+ conversion (in flight)
Blue-> S+ conversion (at rest)

The extra-p indicates nuclear fragmentation → Σ / Λ

K^- nuclear absorption

in the gas filling the DC volume

K^- nuclear absorption in gas

- KLOE DC gas mixture (90% He, 10% C_4H_{10})
  - ratio of absorptions in He and C:

$$\frac{N_{KHe}}{N_{KC}} = \frac{n_{He}\,\sigma_{KHe}\,BR_{KHe}(\Sigma^0\pi^0)}{n_C\,\sigma_{KC}\,BR_{KC}(\Sigma^0\pi^0)}$$

Nuovo Cimento 39 A, 538-547 (1977)

$$\frac{N_{KHe}}{N_{KC}} = 1.6 \pm 0.2$$

- K^-H interaction probability at rest estimated (based on K^- interaction in hydrocarbons mixture data)

Lett. Nuovo Cimento, C, 1099 (1972)

$$\frac{N_{KHe}}{N_{KH}} = 570 \pm 71$$

- ρ_Λ limit set taking into account for Λ decay path and MC simulations

($\sigma_{\rho\Lambda} = 0.13 \pm 0.01$ cm): $\rho_\Lambda > 30$ cm

810 final selected $\Sigma^0\pi^0$ events.

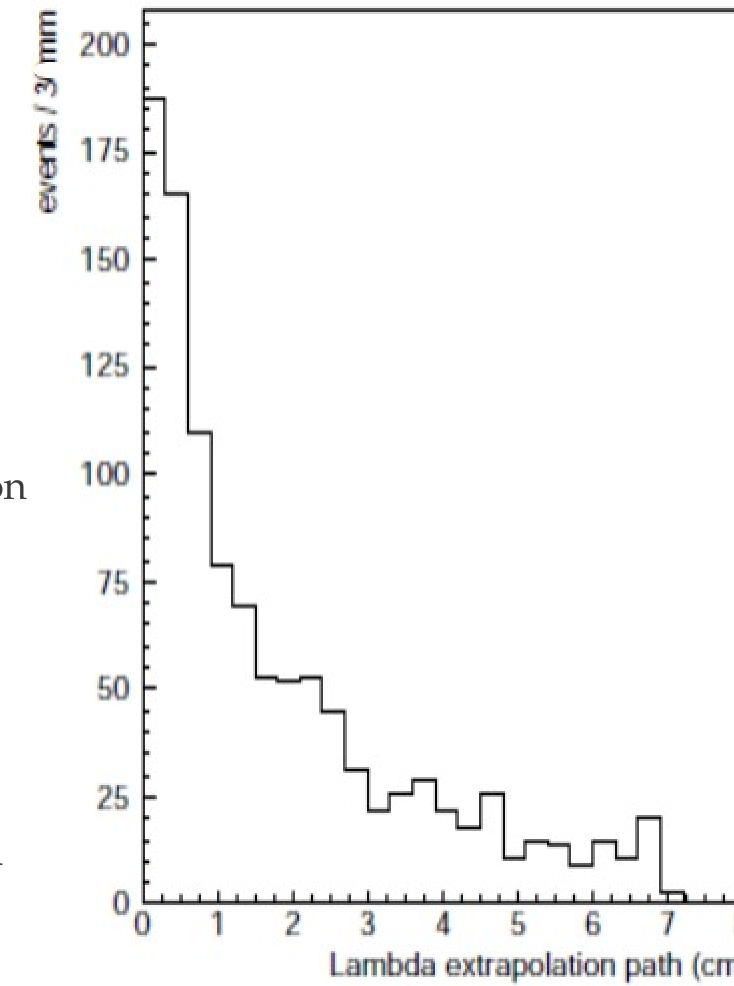

$m_{\pi^0\Sigma^0}$ invariant mass distribution

Invariant mass $m_{\pi 0 \Sigma 0}$ (left) and momentum $p_{\pi 0 \Sigma 0}$ (right) of the reconstructed π^0 - Σ^0 .

Two components in the $p_{\pi 0 \Sigma 0}$ distribution LM ≈ 100 MeV/c , HM ≈ 200 MeV/c

Invariant mass $\mathbf{m_{\pi 0 \Sigma 0}}$ **resolution**: $\sigma_m \approx 30$ MeV/c^2, momentum $\mathbf{p_{\pi 0 \Sigma 0}}$ **resolution**: $\sigma_p \approx 15$ MeV/c.

(true MC information, non resonant, quasi-free K^- C/K^- He, both at-rest/in-flight simulation)

Red arrow shows the kinematical limit for K^- He absorption at-rest.

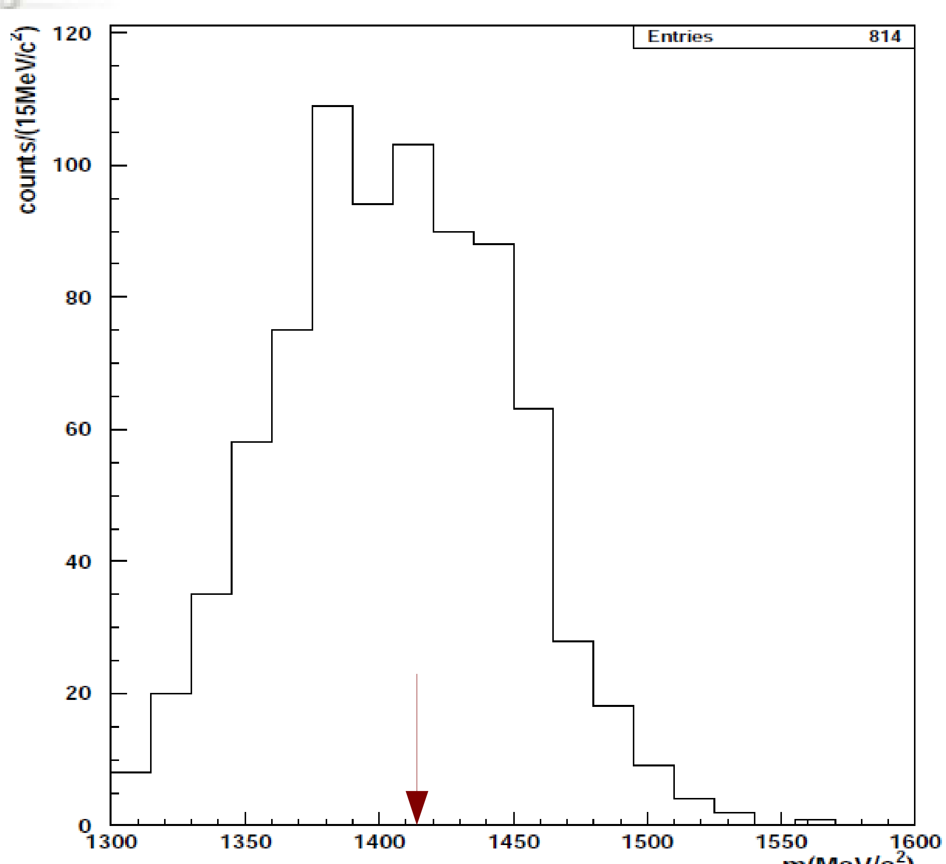

$m_{\Sigma^0\pi^0}$ *distribution*

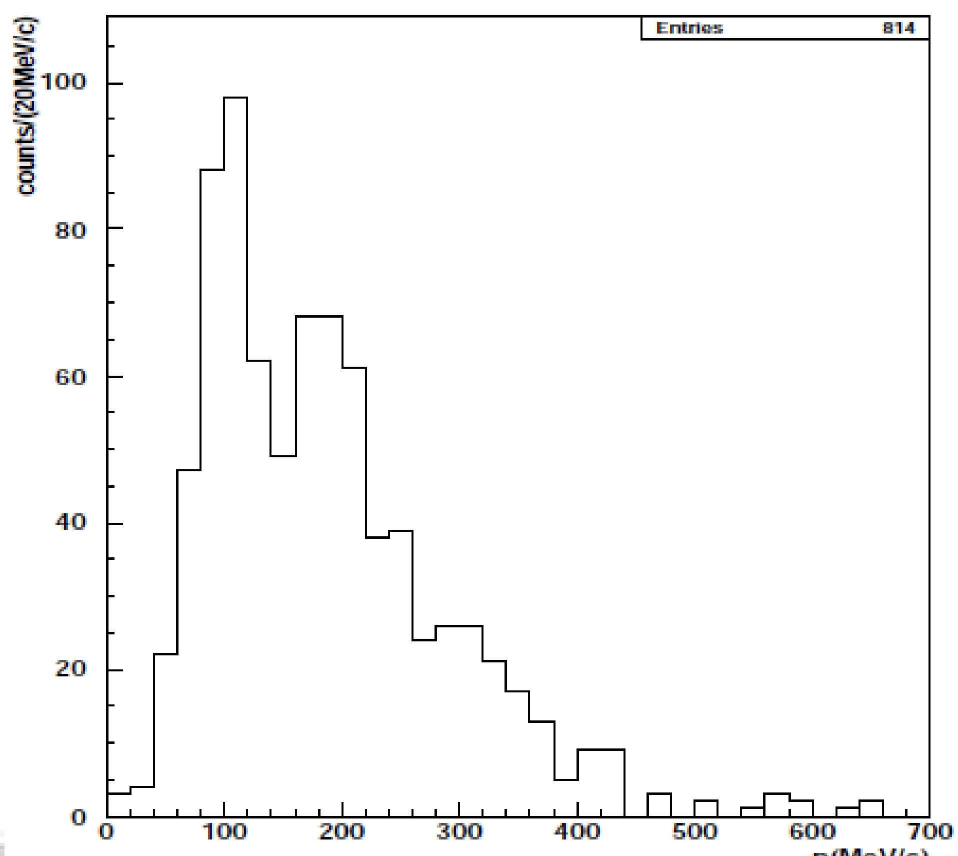

$p_{\Sigma^0\pi^0}$ *distribution*

$\theta_{\pi^0\Sigma^0}$ vs $p_{\pi^0\Sigma^0}$ and $m_{\pi^0\Sigma 0}$ vs $p_{\pi^0\Sigma^0}$ correlation

Correlations of (bottom) the decay angle $\theta_{\pi 0\Sigma 0}$ (angle between π^0 - Σ^0 in the lab. frame) and (top) of $m_{\pi 0\Sigma 0}$ with the momentum $p_{\pi 0\Sigma 0}$. Red arrow corresponds to kinematical limit at-rest in He.

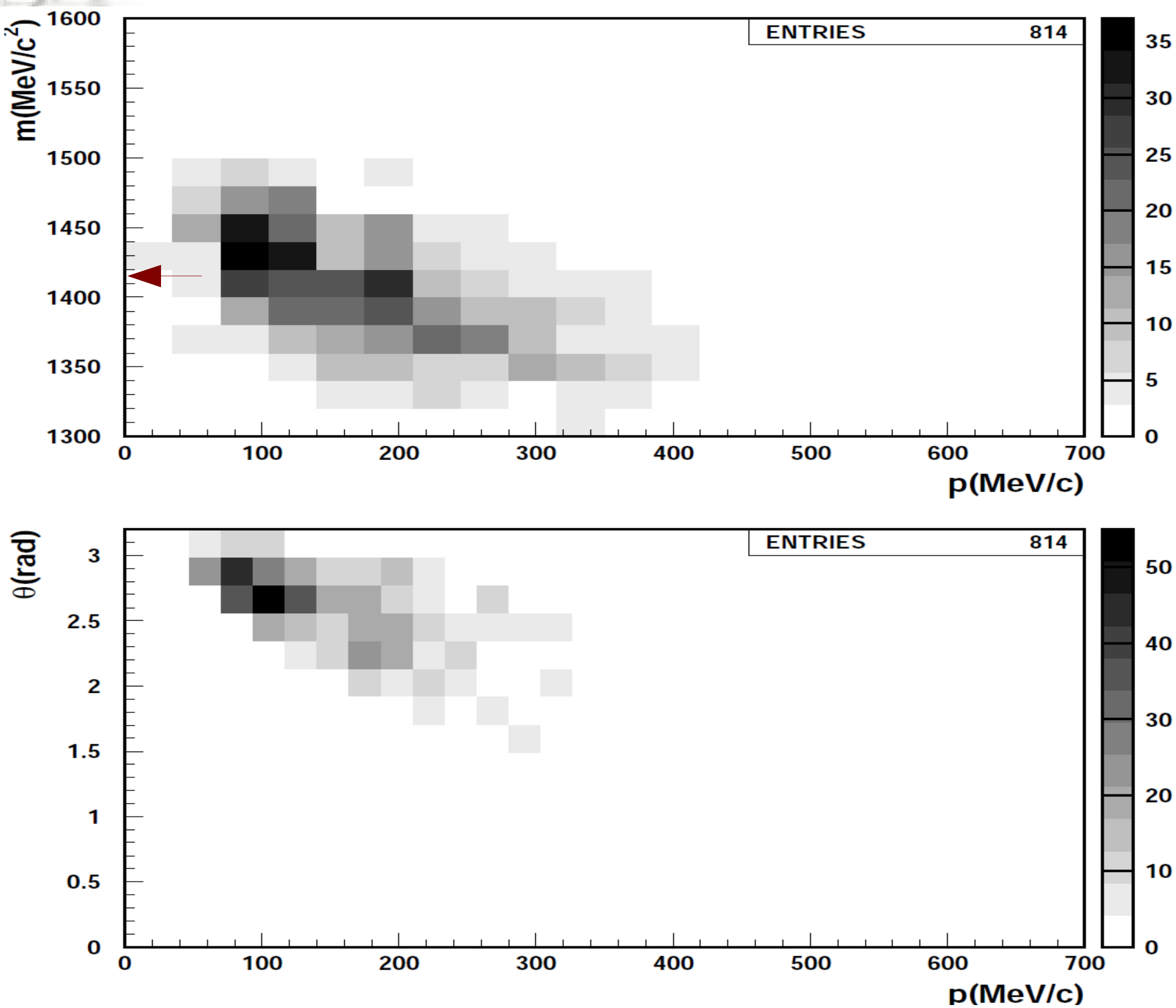

Top $m_{\Sigma^0\pi^0}$ vs $p_{\Sigma^0\pi^0}$, bottom $\theta_{\Sigma^0\pi^0}$ vs $p_{\Sigma^0\pi^0}$.

The LM component ($p_{\pi 0\Sigma 0}$ around 100 MeV/c) is correlated with masses above the k.l. at-rest and larger angles.

Comparison with K^- absorption in bubble chamber

Cutting for $m_{\pi^0\Sigma^0} < m_{lim}$ (kinematical limit for absorption at-rest in He) a lower T_{π^0} component (left) emerge according with T_{π^-} from He bubble chamber experiments AT-REST correlated to the higher $p_{\pi^0\Sigma^0}$ component centered around 190-200 MeV/c ! (reasonable agreement with MC a.r. left / i.f right) (kinetic energy resolution $\sigma_{T\pi^0} = 11.7 \pm 0.2$ MeV)

$n_{>mlim}/n_{<mlim} = 0.82 \pm 0.06$ only indicative due to C contribution.

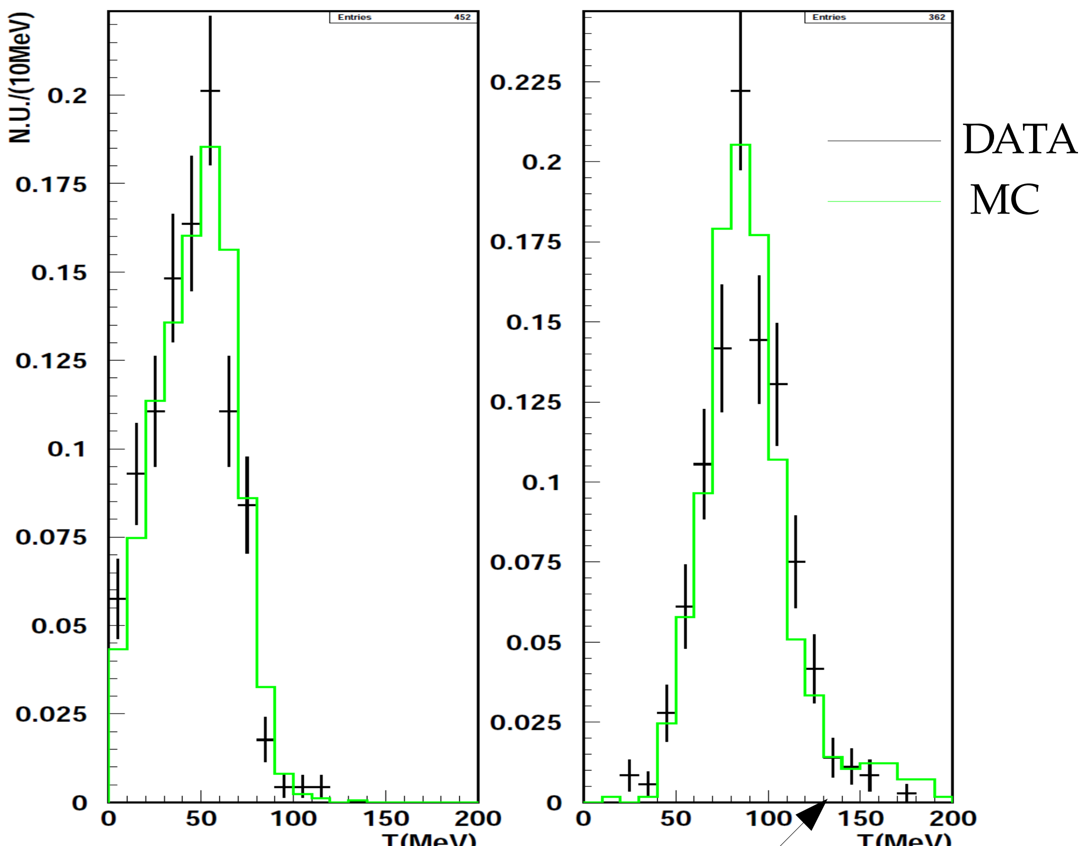

T_{π^0}

no peak around 130 MeV where direct $\Lambda\pi^0$ production is expected !

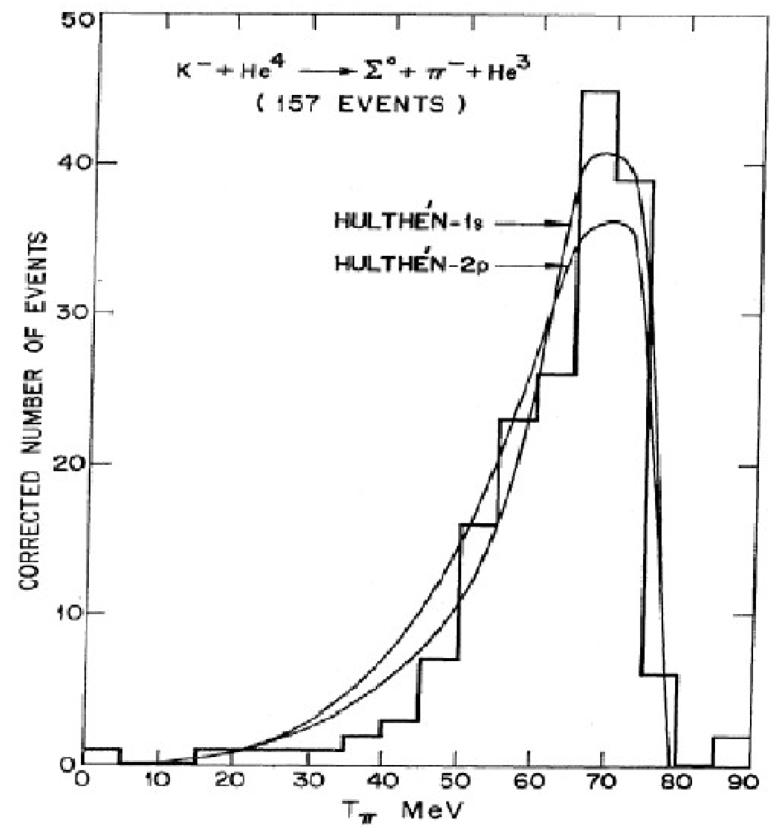

T_{π^-} Bunnel et al 1965.

Study of the background

The main background sources for this channel are (example in ^{12}C):

- $K^- \ ^{12}C \rightarrow \Sigma^0(1385) + {}^{11}B \rightarrow \Lambda\pi^0 + {}^{11}B$

Σ^0(1385) can not decay in $\Sigma^0 \pi^0$ for isospin conservation.

- **Internal conversion** $K^- \ ^{12}C \rightarrow \Lambda(1405) + {}^{11}B \rightarrow \Sigma^0\pi^0 + {}^{11}B$, $\Sigma^0 N \rightarrow \Lambda N$ competes with the decay $\Sigma^0 \rightarrow \Lambda \gamma$.

Both background sources were analized by different methods:

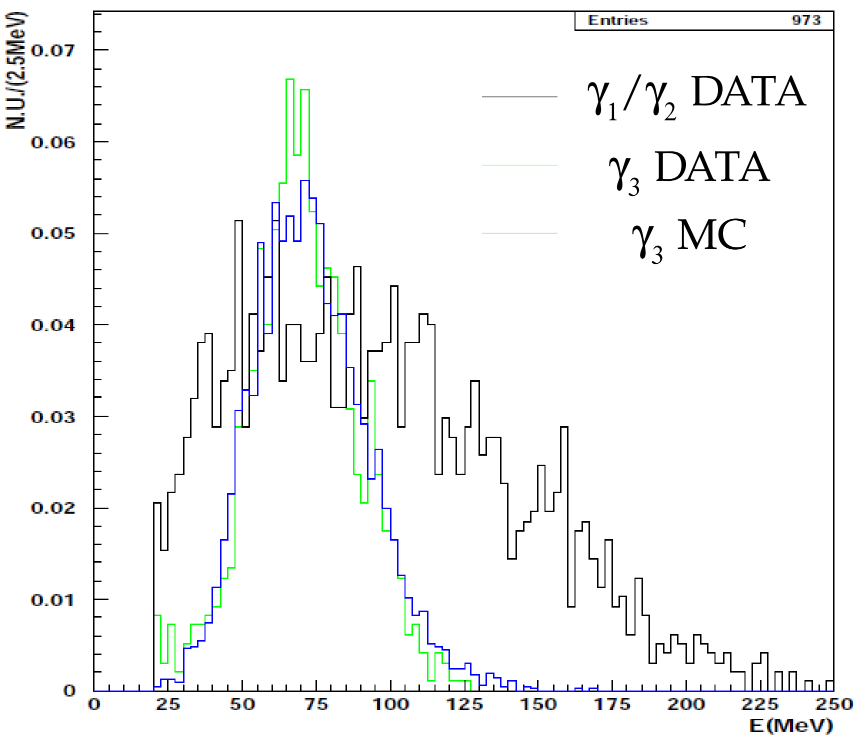

photons energy distribution

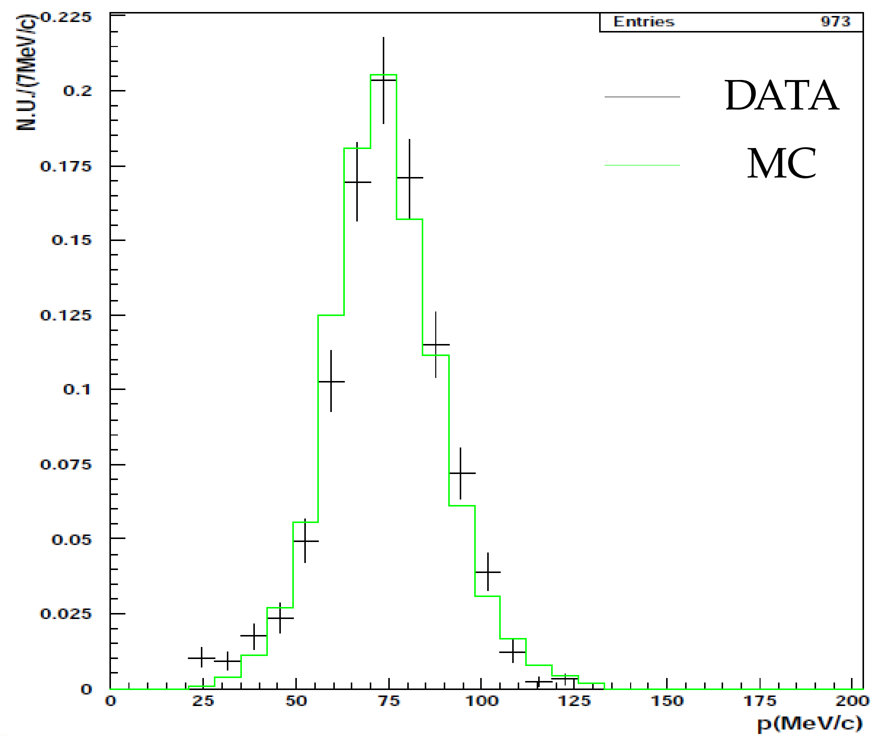

Λ momentum in the Σ^0 rest frame

Study of the background

The numbers of pure background $\Sigma(1385)$ and $\Sigma^0 N \rightarrow \Lambda N$ events passing the analysis cuts are normalized to pure signal $\Lambda(1405)$ events, then weighted to the BRs for $\Lambda\pi^0$ direct production (D), internal conversion (IC) and $\Sigma^0\pi^0$ production due to K^- interaction in ^{4}He and C respectively :

P. A. Katz et al., Phys.Rev. D1 (1970) 1267

C. Vander Velde-Wilquet et al., Nuovo Cimento 39 A, (1977) 538

The percentages of background events entering the final selected samples are:

$$\frac{n_{\Lambda\pi^0\,D\,\mathrm{norm}} + n_{\Lambda\pi^0\,IC\,\mathrm{norm}}}{n_{\Sigma^0\pi^0} + n_{\Lambda\pi^0\,D\,\mathrm{norm}} + n_{\Lambda\pi^0\,IC\,\mathrm{norm}}} = 0.03 \pm 0.01$$

in DC wall (0.03 ± 0.02 in DC gas)

$m_{\pi^0\Sigma^0}$ spectrum with mass hypotesis

$m_{\pi0\Sigma0}$ spectra with mass hypotesis (M.H.) on Σ^0 and π^0 subtracted by *non resonant misidentification (n. r. m.)* (p = 0.22±0.01) the observed $m_{\pi0\Sigma0}$ and $p_{\pi0\Sigma0}$ are used as input for the MC generation of $\Sigma^0\pi^0$. Events in gas (blue), events in DC wall (black) normalized to 1.

$$\sigma_m \approx 17\ \mathrm{MeV/c^2}\ \text{(DC wall)}\quad \sigma_m \approx 15\ \mathrm{MeV/c^2}\ \text{(DC gas)}$$

Similar $m_{\pi0\Sigma0}$ shapes due to the similar kinematical thresholds for ^{4}He and ^{12}C.

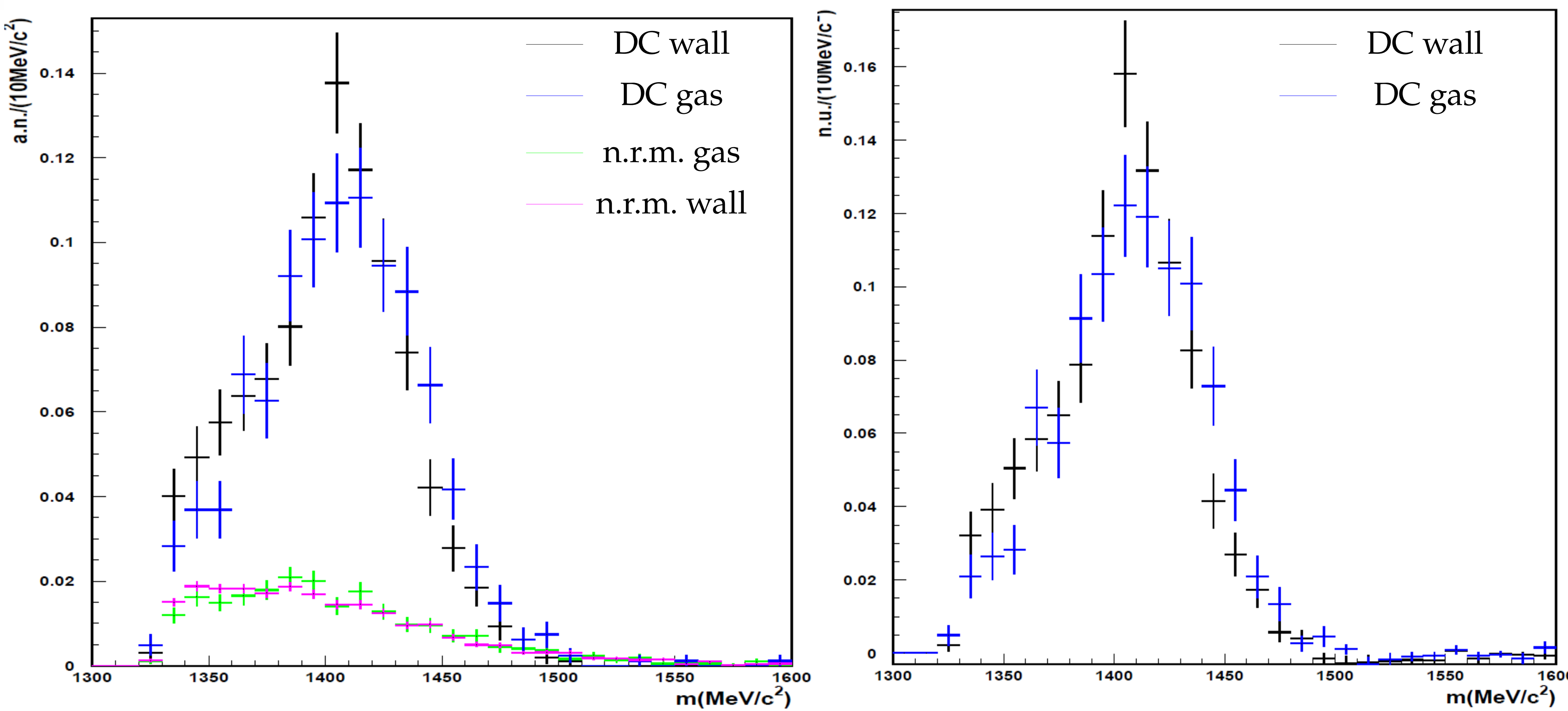

$m_{\Sigma^0\pi^0}$ *spectrum* $m_{\Sigma^0\pi^0}$ *spectrum*

Fit of $\Sigma^0\pi^0$ spectrum in C

A six component fit was performed:

- Resonant component $K^- C$ at-rest/in-flight. (M,Γ) scan from 1381 MeV/c^2 to 1430 MeV/c^2, Breit-Wigner mass distribution
- direct $\Sigma^0\pi^0$ non resonant production at-rest/in-flight
- $\Lambda\pi^0$ background ($\Sigma(1385)$ + I.C.)
- non resonant misidentification (*n.r.m.*) background

$K^- C \rightarrow \Sigma^0\pi^0 + {}^{11}B$ (boron considered as spectator) secondary interactions not taken into account. Then reconstructed in KLOE using standard KLOE MC (fits take into account for acceptance effects, energy loss..).

Fits performed with $m_{\Sigma 0}\, m_{\pi 0}$ hypothesis, employing the better resolution to distinguish the similar shapes of the components.

Fit of $\Sigma^0\pi^0$ spectrum in C

First scan global minimum χ^2_{min} /ndf ~ 1.2 → $(m_{min}, \Gamma_{min}) = (1427, 18) MeV/c^2$

$(M_{min}, \Gamma_{min}) = (1427^{+4}_{-6}, 18^{+15}_{-13})$ MeV/c² cutting for $\chi^2 = \chi^2_{min} + 9$

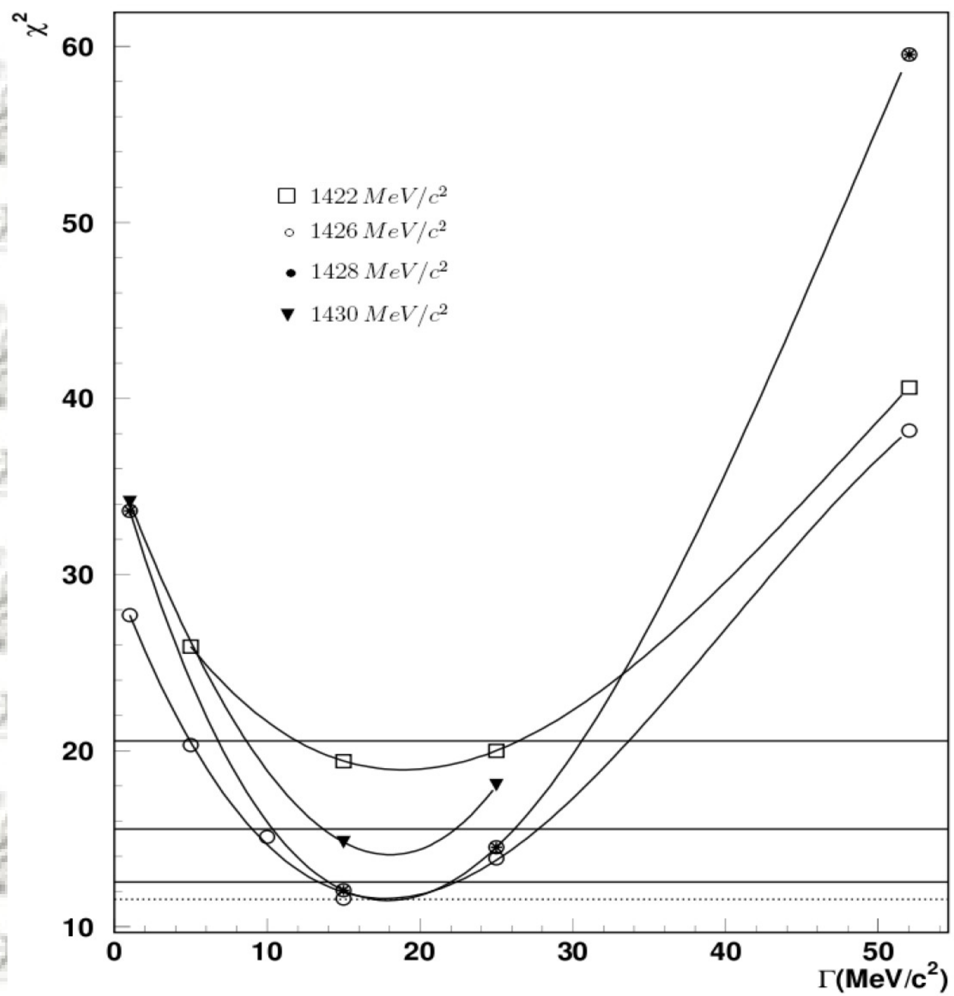

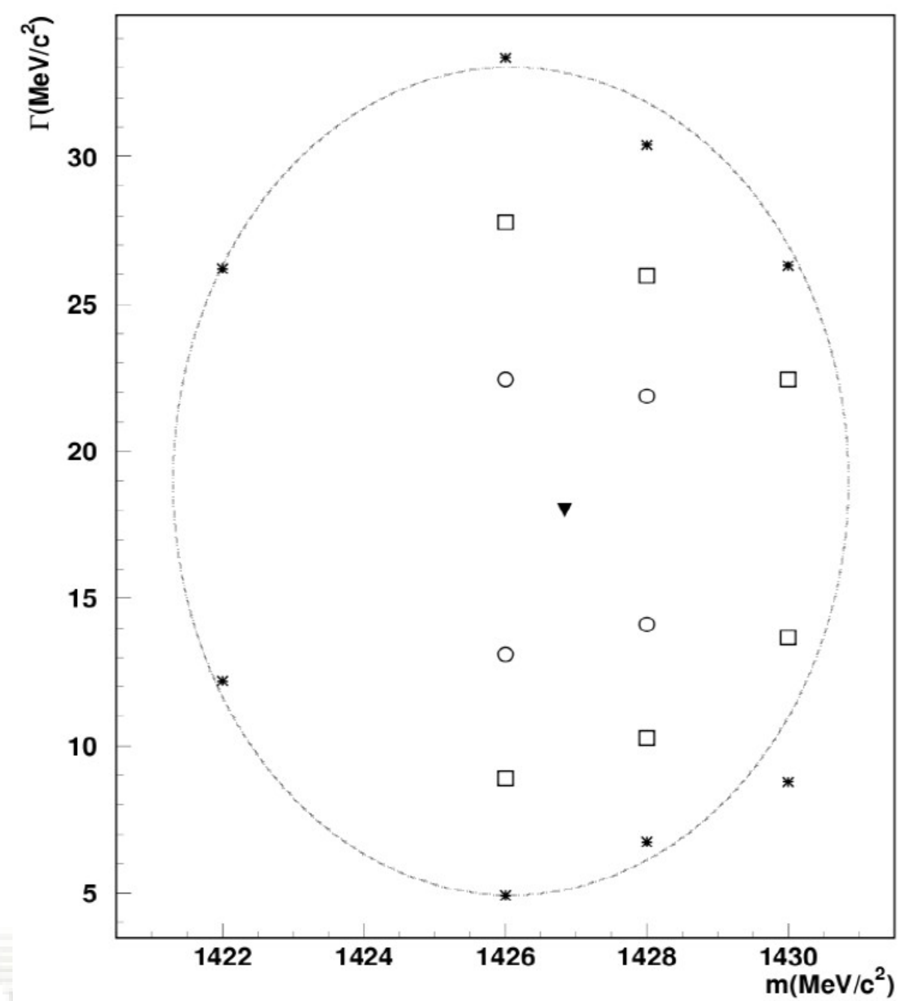

Fit of $\Sigma^0\pi^0$ spectrum in C

χ^2_{min} /ndf ~ 1.2 corresponding to $(M_{min}, \Gamma_{min}) = (1427^{+4}_{-6}, 18^{+15}_{-13})$ MeV/c^2

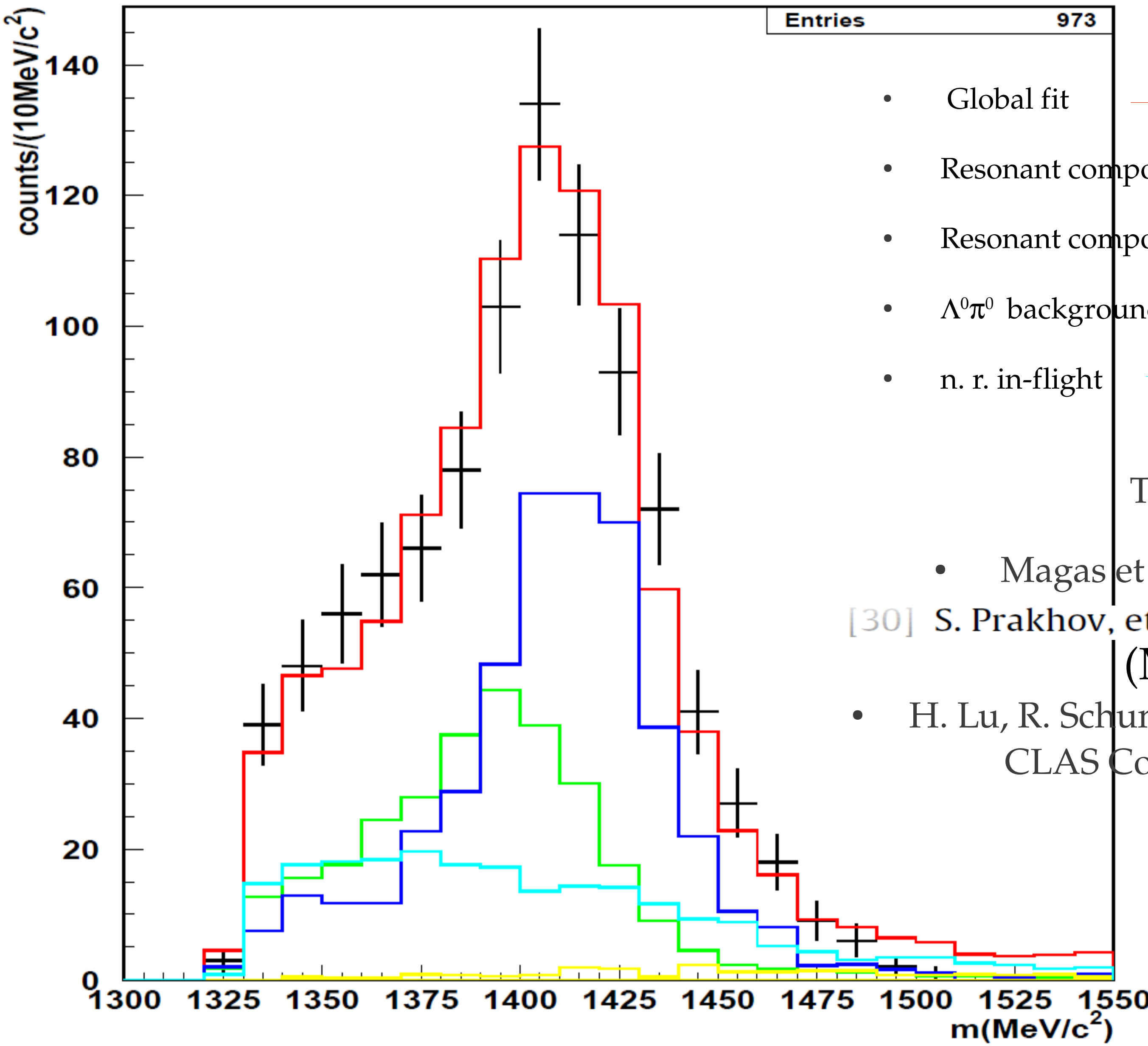

$m_{\Sigma 0\pi 0}$

- Global fit
- Resonant component K^- C at-rest
- Resonant component K^- C in-flight
- $\Lambda^0\pi^0$ background (Σ(1385) + I.C.)
- n. r. in-flight

To be compared with:

- Magas et al. PRL 95, 052301 (2005) **in $\Sigma^0\pi^0$**

[30] S. Prakhov, et al., Phys. Rev. C70 (2004) 034605.

$(M, \Gamma) = (1420, 38)$ MeV/c^2

- H. Lu, R. Schumacher, B. Raue, M. Gabrielyan, and CLAS Collaboration, AIP Conf. Proc. 1432, (2012) 199. **in $\Sigma^+\pi^-$**

$(M,\Gamma) = (1422, 16)$ MeV/c^2

$(M,\Gamma) = (1393, 100)$ MeV/c^2

Kaons momentum distribution

Plot representing the $\boldsymbol{p}_k$ *distribution at the last point of the kaon track*

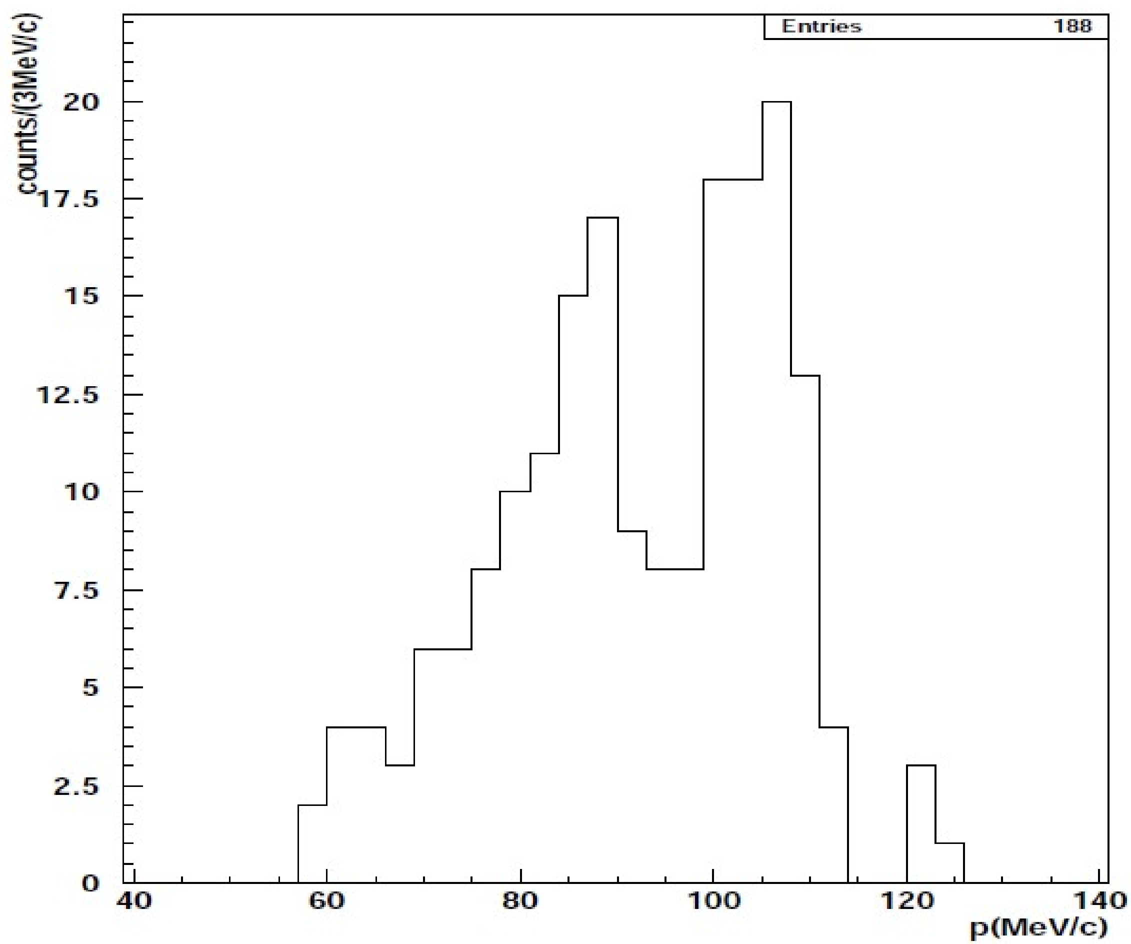

$p_{\pi^0\Sigma^0}$ spectrum for boost and anti-boost events

$p_{\Sigma^0\pi^0}$ distribution for lower (black) and higher (red) p_k values

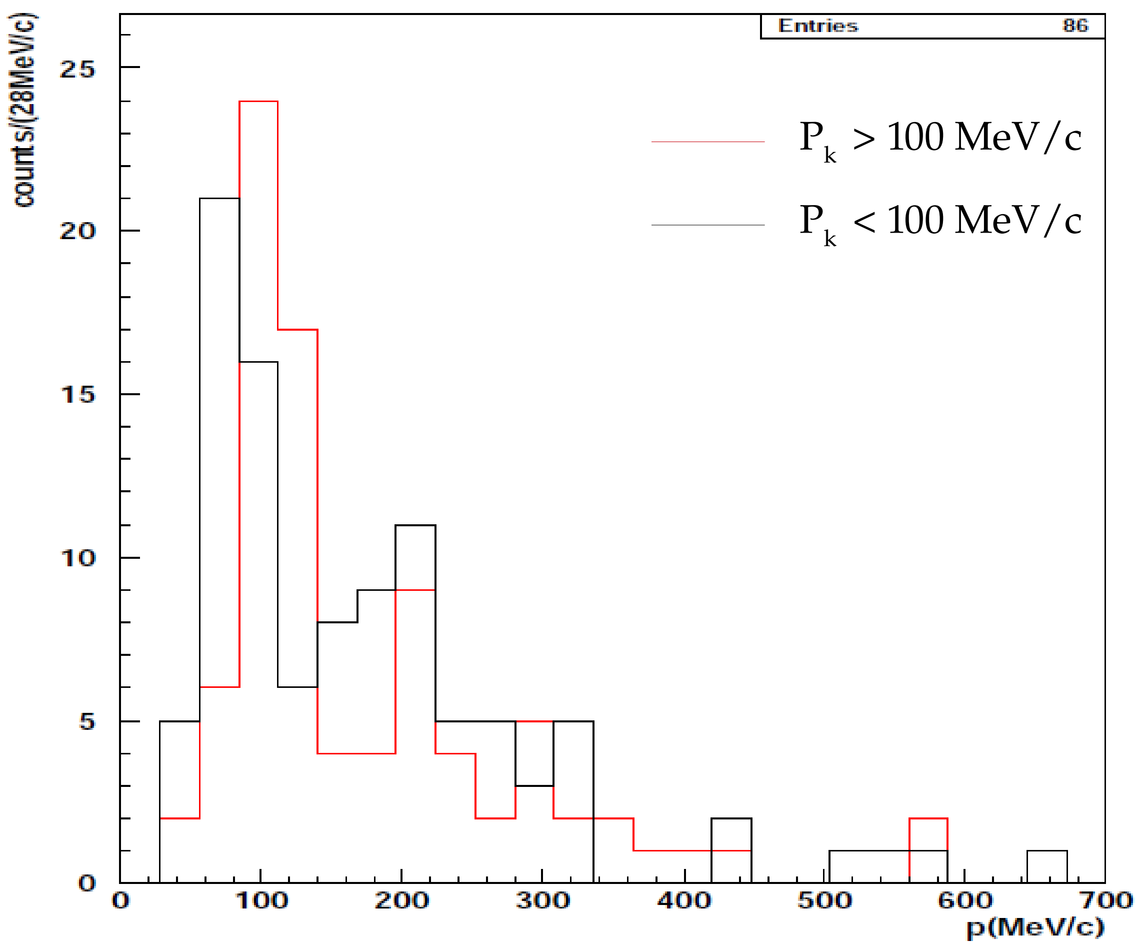

Search for extra-tracks from the hadronic interaction vertex

Positive tracks are searched by dE/dx vs p. Than the Λ path and charged track are extrapolated backwords for the primary interaction vertex. From the extrapolated $\mathbf{p}_{et}$ $\rightarrow$ $\cos(\theta_{\pi 0 \Sigma 0,t})$

$$\cos(\theta_{\pi 0\Sigma 0,t}) = (\mathbf{p}_{\pi 0\Sigma 0} \cdot \mathbf{p}_{et}) / (|\mathbf{p}_{\pi 0\Sigma 0}| \; |\mathbf{p}_{et}|)$$

Back to back recoils correspond to $K^- He \rightarrow \Sigma^0\pi^0 + T$ events at-rest.

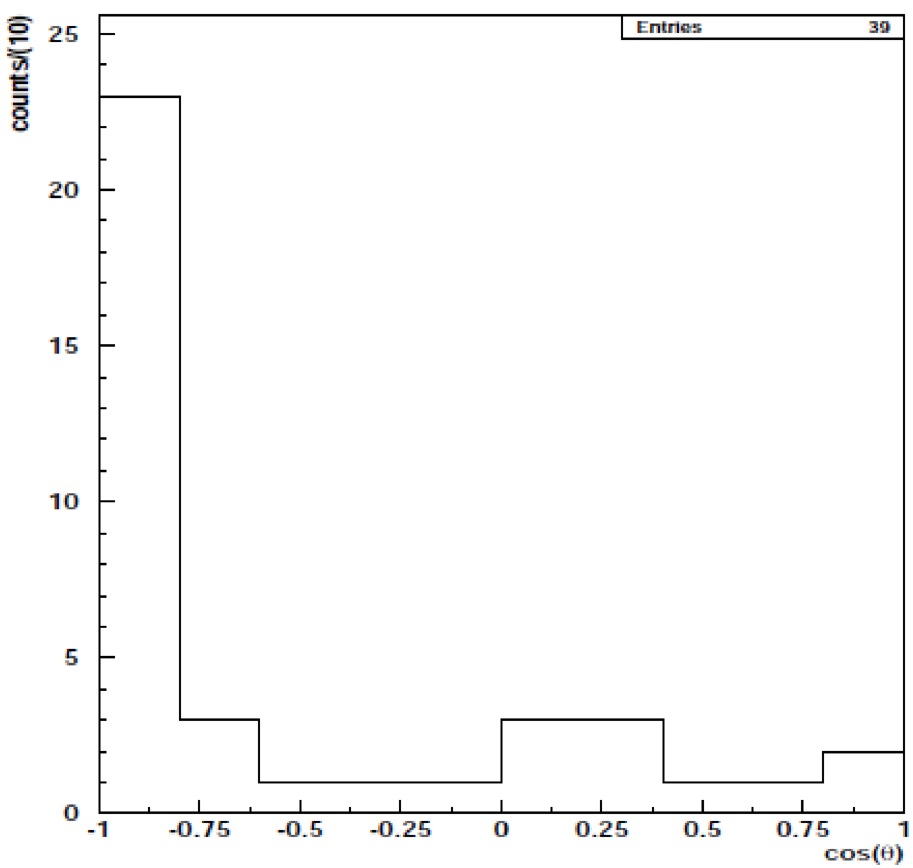

$cos(\theta_{\Sigma^0\pi^0,t})$

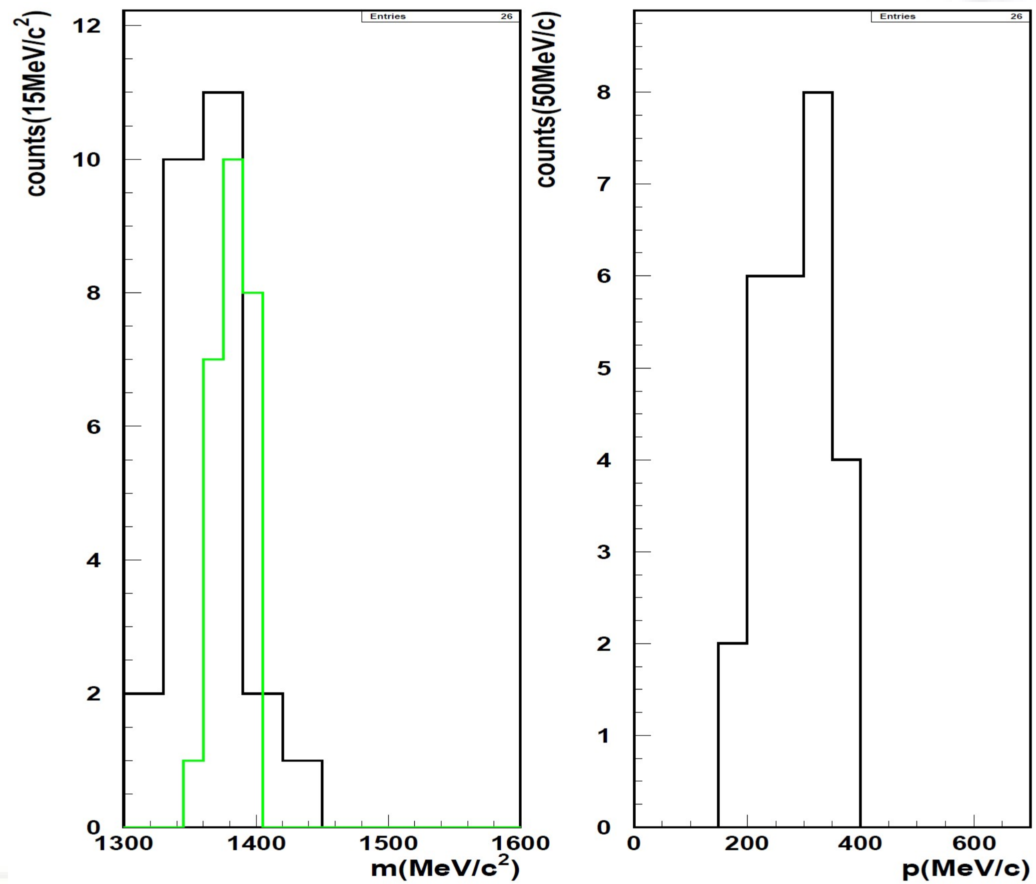

Figure 4.16: $m_{\Sigma^0\pi^0}$ *(left black) (binning: counts/(30MeV/c^2)), mm (left green) (binning: counts/(15MeV/c^2)),* $p_{\Sigma^0\pi^0}$ *(right black).*

Study of the background

In both cases γ_3 is not present, if a contamination is present, the neutral cluster which is associated to γ_3 by reconstruction should show differences.

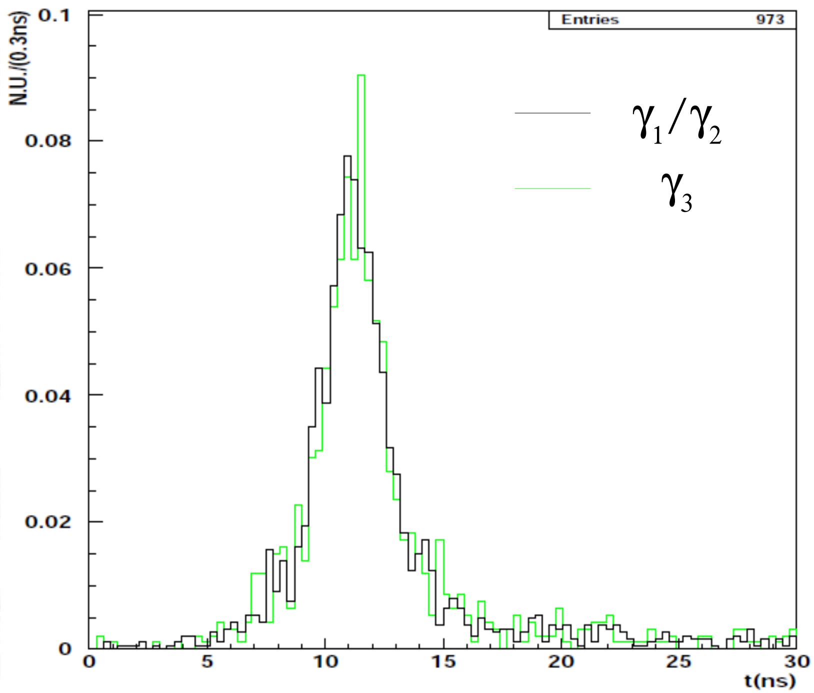

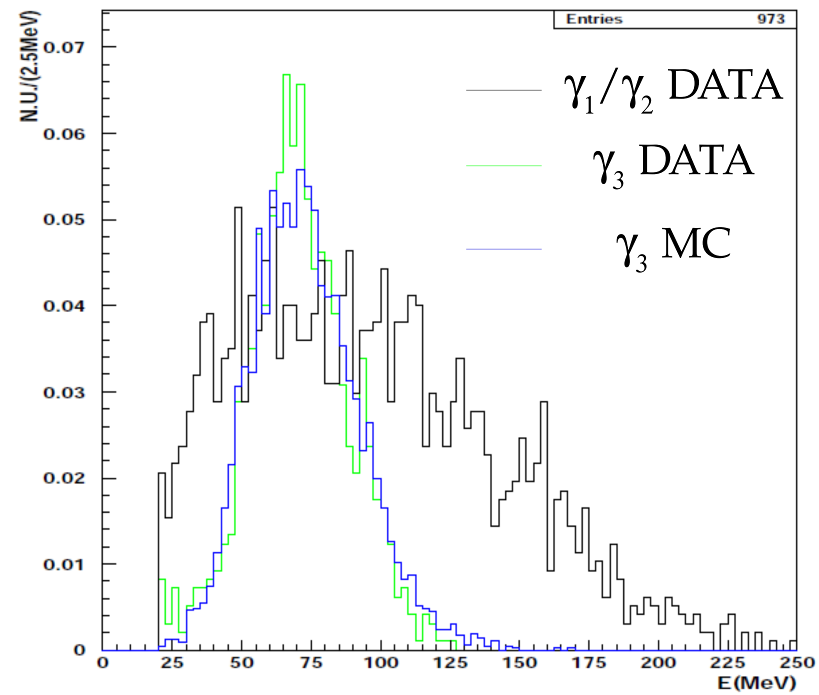

- Right: the energy distribution of γ_3 (green) is in perfect agreement with MC simulations of pure signal events (blue) (energy spectrum of $\gamma_1\gamma_2$ is shown in black).
- Left: the time distribution of γ_3 (green) is in agreement with the time distributions of the two photons coming from π^0 decay (black).

Study of the background

To test the possible contamination of $\Sigma(1385)$, we employed the great mass difference between $\Sigma(1385)$ and Σ^0 (1192 MeV) to distinguish such events. Indeed Σ^0 decays in its rest frame in $\Lambda\gamma$ with momentum of 74 MeV/c, while $\Sigma(1385)$ decays in its rest frame in $\Lambda\pi^0$ with momentum of 208 MeV/c.

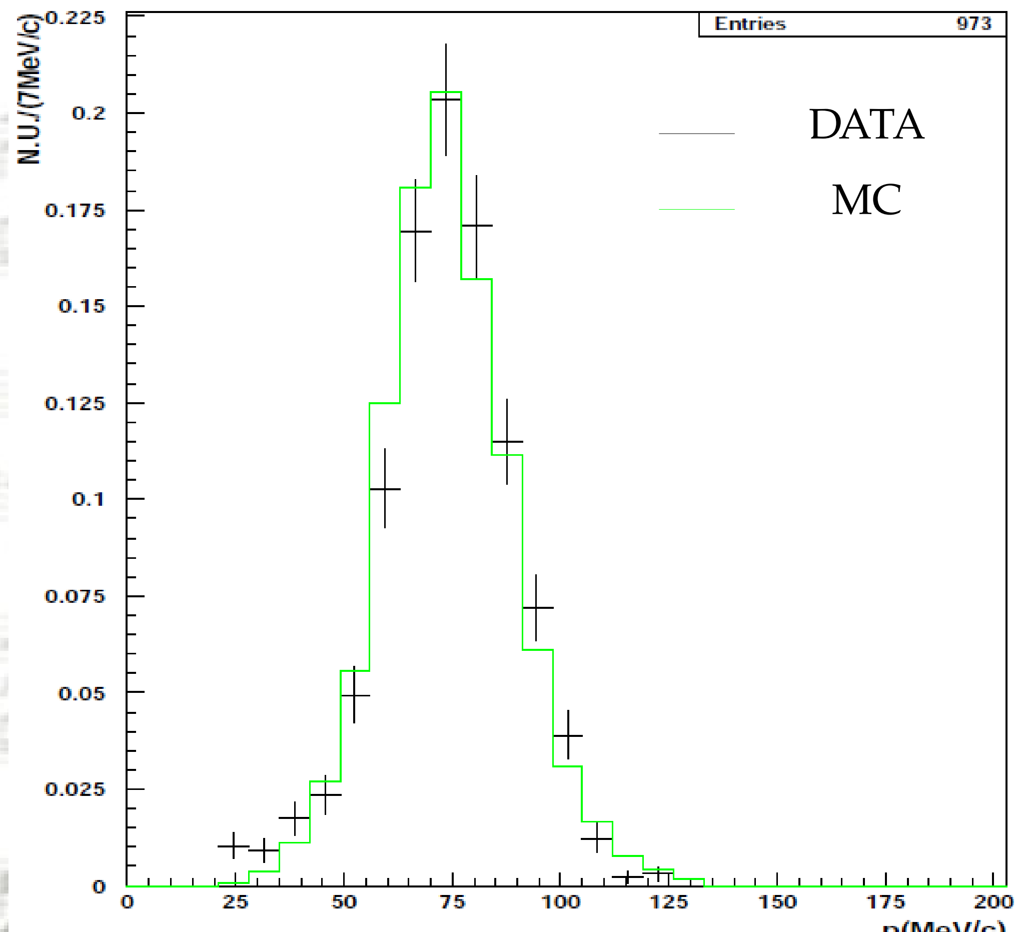

$p_{\Lambda\gamma 3\, CM}$ *distribution*

The **Λ momentum distribution** calculated **in the Σ^0 rest frame (black) agrees with pure signal MC** (green). A Gaussian fit to the green distribution gives a central value:

$$p_{\Lambda\gamma 3\, CM} = 74.5 \pm 0.5.$$

Study of the background

The Λ momentum was then transformed in the $\Lambda\pi^0$ rest frame (black distribution) and compared with $K^- \ {}^{12}C \rightarrow \Sigma^0(1385) + {}^{11}B \rightarrow \Lambda\pi^0 + {}^{11}B$

MC simulated events (green).

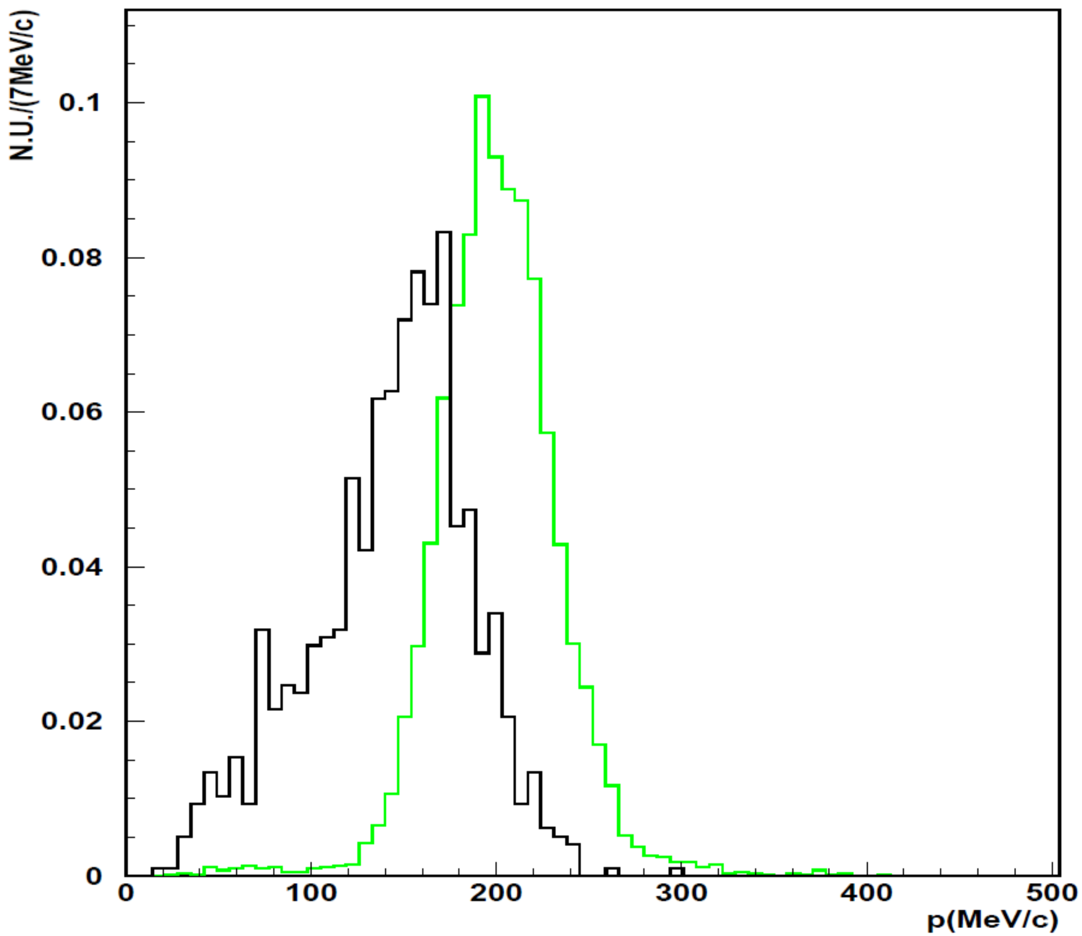

$p_{\Lambda\pi^0\,CM}$ distribution

Analysis of K- interactions in the beryllium beam sphere

K- interactions in the Beryllium-Alluminum sphere (r = 10 cm) surrounding the interaction point. Only **few events** surviving due to geometrical cut (r_Λ < 11.2 cm) to avoid absorptions in air. The invariant mass spectrum with MH is shown.

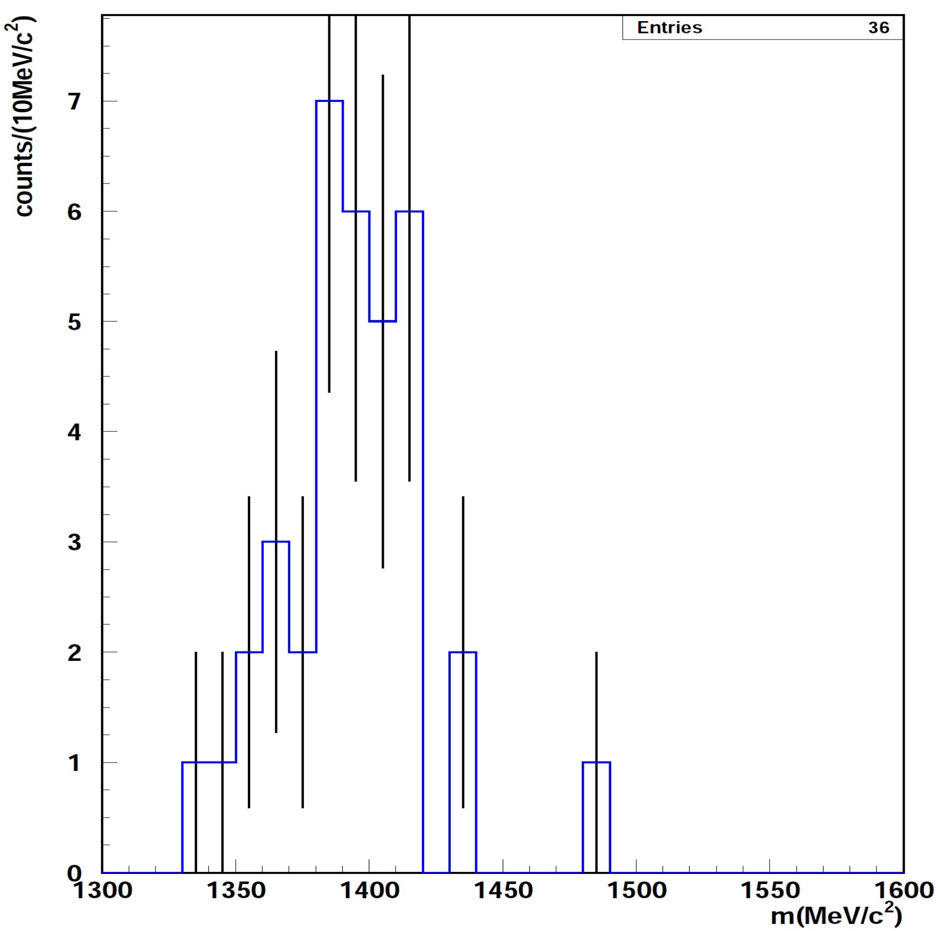

$m_{\pi 0 \Sigma 0}$ invariant mass

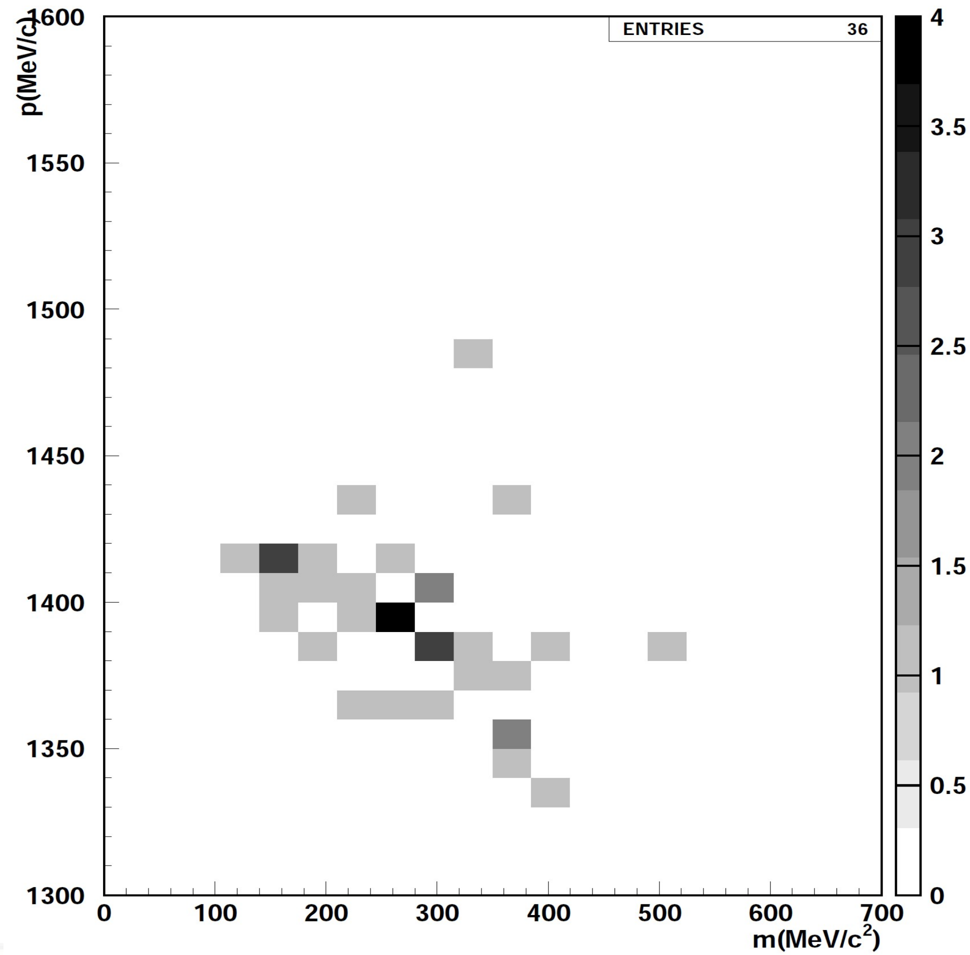

$m_{\pi 0 \Sigma 0}$ vs $p_{\pi 0 \Sigma 0}$

$m_{\pi^0\Sigma^0}$ spectrum

MC $m_{\pi0\Sigma0}$ spectrum for non-resonant, quasi-free $K^- C \rightarrow \Sigma^0\pi^0 + {}^{11}B$.

AT-REST left, IN-FLIGHT right. MC true black, reconstructed red, reconstructed with M.H. green.

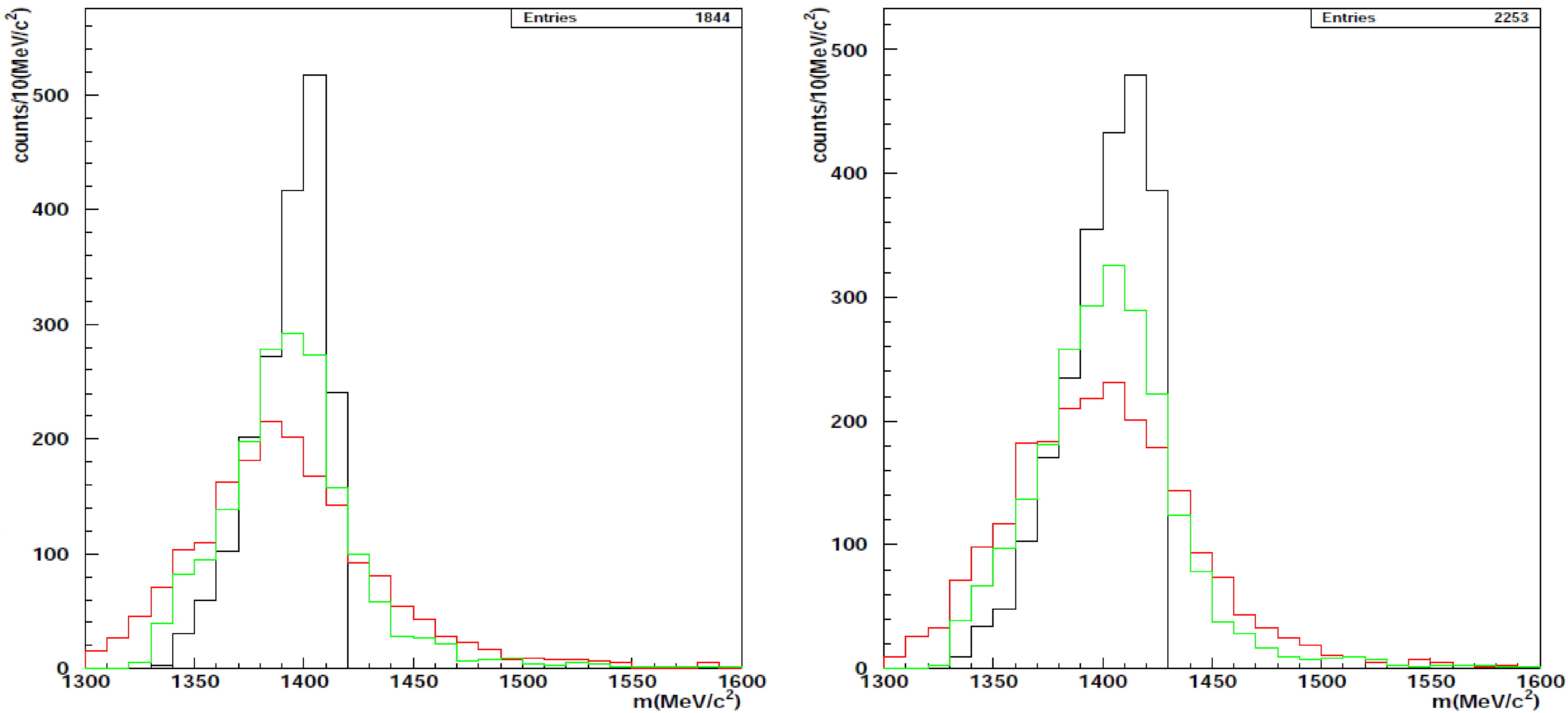

$m_{\Sigma^0\pi^0}$ *spectrum* $m_{\Sigma^0\pi^0}$ *spectrum*

$m_{n\pi^0}$ spectrum

Investigated channels: K^-"p" $\rightarrow \Sigma^0\pi^0$ and K^-"p" $\rightarrow \Lambda\pi^0$

With: $\Sigma^0 \rightarrow \Lambda\gamma$ and $\Lambda \rightarrow n\,\pi^0$ decays

a. u. /(10MeV/c²)

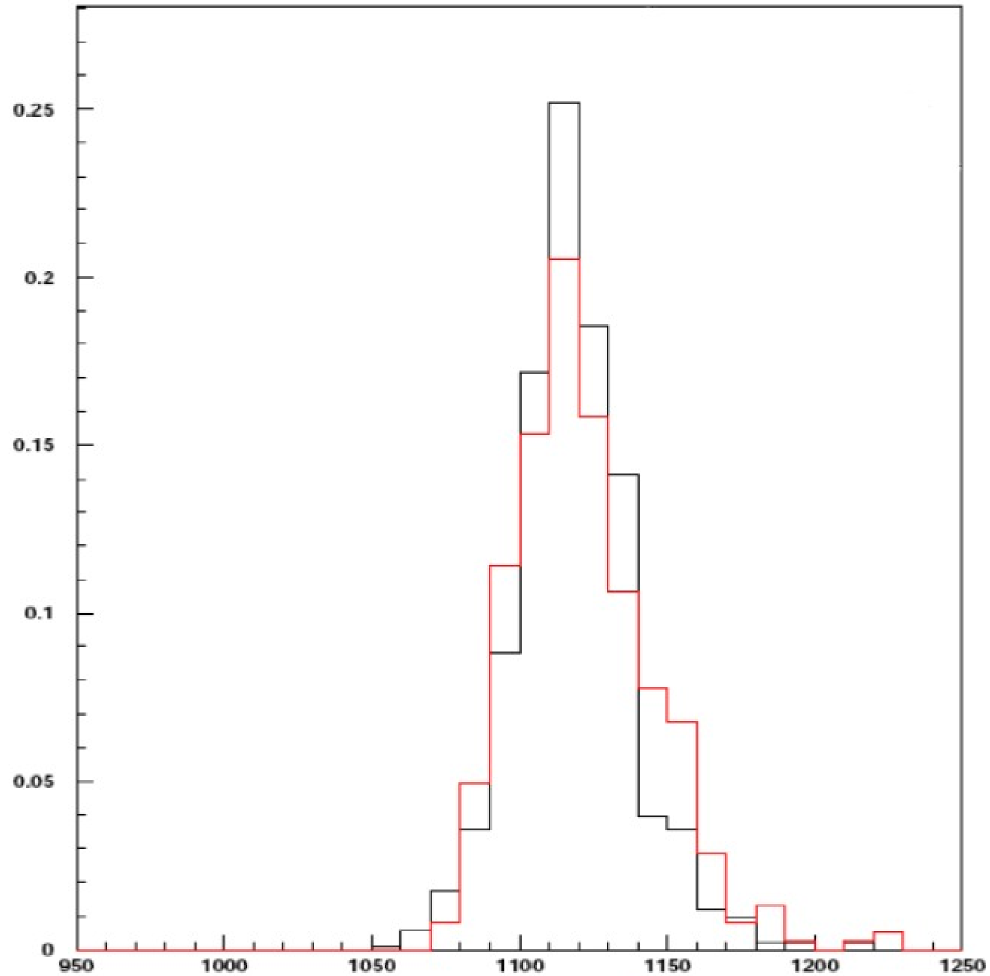

m(MeV/c²)

$m_{n\,\pi^0}$ invariant mass spectrum

K^- "p" → $\Sigma^+\pi^-$ channel

$K^- + p + {}^{11}B \to \Lambda^*(1405) + {}^{11}B \to \Sigma^+ + \pi^- + (5p+6n\ ?)$

$\quad\quad + n$

$n + \pi^0 + p \leftarrow \Lambda(1116) + p$

$\quad \gamma + \gamma$

Similar final states:

$K^- + p + {}^{11}B \to p + \pi^- + \gamma + \gamma + {}^{11}B$ (Signal)

$K^- + p + {}^{11}B \to p + \pi^- + \gamma + \gamma + (5p+6n\ ?)$ (BG)

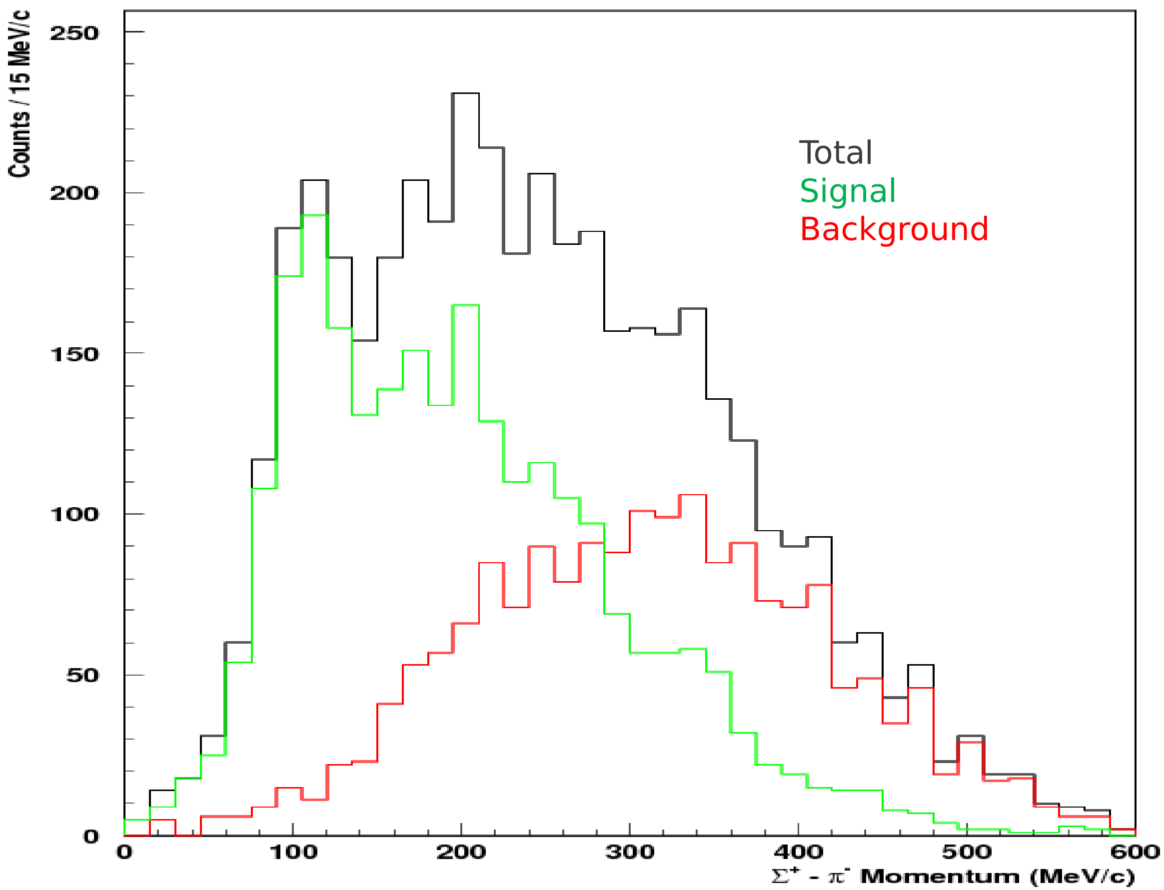

First hint .. missing mass evidences nuclear fragmentation correlated to the possible internal conversion component